

ลักษณะสมบัติและบทบาทของไซโตเคมิคัลที่เอนไซม์ในการทนเค็มของไซยาโนแบคทีเรียทนเค็ม

Aphanothece halophytica

นางสาว กัลย์ธีรา สุนทรารักษ์กุล

วิทยานิพนธ์นี้เป็นส่วนหนึ่งของการศึกษาตามหลักสูตรปริญญาวิทยาศาสตรดุษฎีบัณฑิต

สาขาวิชาชีวเคมี ภาควิชาชีวเคมี

คณะวิทยาศาสตร์ จุฬาลงกรณ์มหาวิทยาลัย

ปีการศึกษา 2553

ลิขสิทธิ์ของจุฬาลงกรณ์มหาวิทยาลัย

CHARACTERIZATION OF Na⁺-ATPase AND ITS ROLE IN
SALINITY TOLERANCE OF A HALOTOLERANT
CYANOBACTERIUM *Aphanothece halophytica*

Miss Kanteera Soontharapirakkul

A Dissertation Submitted in Partial Fulfillment of the Requirements
for the Degree of Doctor of Philosophy Program in Biochemistry

Department of Biochemistry

Faculty of Science


Chulalongkorn University

Academic Year 2010


Copyright of Chulalongkorn University


Thesis Title CHARACTERIZATION OF Na⁺-ATPase AND ITS ROLE
IN SALINITY TOLERANCE OF A HALOTOLERANT
CYANOBACTERIUM *Aphanothece halophytica*
By Miss Kanteera Soontharapirakkul
Field of Study Biochemistry
Thesis Advisor Professor Aran Incharoensakdi, Ph.D.
Thesis Co-Advisor Professor Teruhiro Takabe, Ph.D.


Accepted by the Faculty of Science, Chulalongkorn University in Partial
Fulfillment of the Requirements for the Doctoral Degree



..... Dean of the Faculty of Science
(Professor Supot Hannongbua, Dr.rer.nat.)

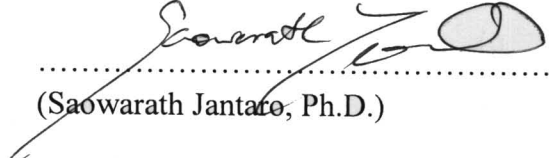
THESIS COMMITTEE

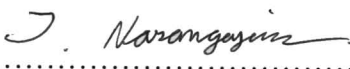

..... Chairman
(Professor Anchalee Tassanakajon, Ph.D.)


..... Thesis Advisor
(Professor Aran Incharoensakdi, Ph.D.)


..... Thesis Co-Advisor
(Professor Teruhiro Takabe, Ph.D.)


..... Examiner
(Associate Professor Teerapong Buaboocha, Ph.D.)


..... Examiner
(Saowarath Jantato, Ph.D.)


..... External Examiner
(Associate Professor Jarunya Narangajavana, Ph.D.)

นางสาวกัลย์ธีรา สุนทรภักษ์กุล : ลักษณะสมบัติและบทบาทของโซเดียมเอทีพีเอสในการทน
เค็มของไซยาโนแบคทีเรียทนเค็ม *Aphanothece halophytica* (CHARACTERIZATION OF Na⁺-
ATPase AND ITS ROLE IN SALINITY TOLERANCE OF A HALOTOLERANT
CYANOBACTERIUM *Aphanothece halophytica*) อ.ที่ปรึกษาวิทยานิพนธ์หลัก: ศ.ดร.อรรณู อิน
เจริญศักดิ์, อ.ที่ปรึกษาวิทยานิพนธ์ร่วม: Prof. Teruhiro Takabe, Ph.D., 205 หน้า

เอทีพีเอสจากเมมเบรนเวสจิกิลของไซยาโนแบคทีเรียทนเค็ม *Aphanothece halophytica* ถูกทำให้บริสุทธิ์
โดยความบริสุทธิ์เพิ่มขึ้น 17.5 เท่าและได้ปริมาณผลผลิต 6.5% การทดสอบแอกทิวิตีของเอนไซม์บริสุทธิ์พบว่าเอทีพี
เอสสามารถเร่งปฏิกิริยาการสลายเอทีพีในสภาวะที่มีโซเดียม การศึกษากลไกทางจลนพลศาสตร์ของโซเดียมเอทีพี
เอสพบว่าค่า K_m ของ Na⁺ และ ATP เท่ากับ 2.0 และ 1.2 มิลลิโมลาร์ ตามลำดับ การศึกษาแถบโปรตีนโดยวิธีโซเดียม
โดเดซิลซัลเฟตพอลิอะคริลาไมด์เจลอิเล็กโตรโฟรีซิสและการศึกษาผลของตัวยับยั้ง พบว่าโซเดียมเอทีพีเอสที่ได้จัด
อยู่ในกลุ่ม F-type ATPase เมื่อทำการศึกษากลไกการขนส่งโซเดียมโดยใช้โพทโทโอลิโพรทที่มีโซเดียมเอทีพีเอสบริ
สุทธิ์ ผลการทดลองพบว่าการขนส่งโซเดียมเข้าสู่โพทโทโอลิโพรทมีความเกี่ยวข้องกับการขนส่งโปรตอนออกสู่
สารละลาย นอกจากนี้ยังพบว่าโซเดียมเอทีพีเอสมีการทำงานเป็นแบบยูนิพอร์ต (uniport) ซึ่งจะขนส่งเฉพาะโซเดียม
เข้าสู่โพทโทโอลิโพรท ต่อจากนั้นโปรตอนจะถูกขนส่งออกสู่สารละลายโดยอาศัยความแตกต่างของศักย์ไฟฟ้า
ระหว่างโพทโทโอลิโพรทซึ่งเกิดขึ้นจากการทำงานของโซเดียมเอทีพีเอส

F-type Na⁺-atp operon ซึ่งประกอบด้วยยีนจำนวนเก้ายีนที่เป็นตัวกำหนดการเรียงตัวของกรดอะมิโนใน
การสังเคราะห์โปรตีน Na⁺-ATP synthase (Na⁺-ATPase) ซับยูนิตต่างๆ ได้แก่ ซับยูนิตบีต้า (β), เอพซีลอน (ε), ไอ
(I), ไฮโปเทติกัล โปรตีน (hypothetical protein), เอ (a), ซี (c), บี (b), แอลฟา (α), และแกมมา (γ) ได้ถูกแยกจากจีโนม
ของ *A. halophytica* โดยมีการสร้าง expression plasmid (pTrcHis2C-*ApNa⁺-atp*) แล้วนำไปใส่ในแบคทีเรีย *E. coli*
mutant DK8 (Δatp) ซึ่งไม่มียีนที่ใช้ในการสังเคราะห์ ATP synthase จากนั้นจึงทำการศึกษาลักษณะสมบัติของ
โปรตีน *ApNa⁺-ATPase* การศึกษาพบว่าแอกทิวิตีของการสลายเอทีพีใน inverted membrane vesicles จาก *E. coli*
DK8 ที่มีการแสดงออกของ *ApNa⁺-ATPase* ขึ้นกับโซเดียมและเอนไซม์แอกทิวิตียังถูกยับยั้งด้วยตัวทำลายโซเดียม
เกรเดียนท์ monensin และตัวยับยั้ง F-type ATPase แอกทิวิตี tributyltin chloride ในขณะที่ carbonyl cyanide m-
chlorophenyl hydrazone (CCCP) ซึ่งเป็นตัวทำลายโปรตอนเกรเดียนท์ไม่สามารถยับยั้งเอนไซม์แอกทิวิตีได้ อีกทั้ง
โซเดียมไอออนยังช่วยป้องกันการยับยั้งแอกทิวิตีของ *ApNa⁺-ATPase* ด้วย N,N'-dicyclohexylcarbodiimide (DCCD)
นอกจากนั้นยังพบแอกทิวิตีของการสร้างเอทีพีใน Na⁺-loaded inverted membrane vesicles จาก *E. coli* DK8 ที่มีการ
แสดงออกของ *ApNa⁺-ATPase* ในการศึกษาเรื่องการแสดงออกของยีน *ApNa⁺-atp* operon ซึ่งเป็นยีนที่สังเคราะห์
ApNa⁺-ATPase พบว่า *ApNa⁺-ATPase* มีการแสดงออกอยู่ในส่วน cytoplasmic membranes ของ *Synechococcus* sp.
PCC 7942 และยังช่วยให้ไซยาโนแบคทีเรียน้ำจืดสายพันธุ์นี้สามารถเจริญได้ในสภาวะความเข้มข้นเกลือสูง จาก
ผลการทดลองข้างต้น เราจึงสามารถสรุปได้ว่า F-type Na⁺-dependent ATPase ใน *A. halophytica* มีบทบาทในการ
ช่วยต้านทานต่อสภาวะเครียดที่เกิดจากความเข้มข้นเกลือสูง

ภาควิชา.....ชีวเคมี.....ลายมือชื่อนิสิต กัลย์ธีรา สุนทรภักษ์กุล.....

สาขาวิชา.....ชีวเคมี.....ลายมือชื่อ อ.ที่ปรึกษาวิทยานิพนธ์หลัก.....

ปีการศึกษา.....2553.....ลายมือชื่อ อ.ที่ปรึกษาวิทยานิพนธ์ร่วม.....

#4873873423: MAJOR BIOCHEMISTRY

KEY WORD: *Aphanothece halophytica* / ATPase / CYANOBACTERIA / SALT TOLERANCE / SODIUM TRANSPORT

KANTEERA SOONTHARAPIRAKKUL: CHARACTERIZATION OF Na^+ -ATPase AND ITS ROLE IN SALINITY TOLERANCE OF A HALOTOLERANT CYANOBACTERIUM *Aphanothece halophytica*.
 THESIS ADVISOR : PROF. ARAN INCHAROENSAKDI, Ph.D.,
 THESIS CO-ADVISOR : PROF. TERUHIRO TAKABE, Ph.D., 205 pp.

ATPase was purified from *Aphanothece halophytica* membrane vesicles with a 17.5-fold purification with 6.5% yield. The purified enzyme catalyzed the hydrolysis of ATP in the presence of Na^+ . The apparent K_m values for Na^+ and ATP were 2.0 and 1.2 mM, respectively. The enzyme is likely the F-type ATPase based on the usual subunit pattern from SDS-PAGE and inhibitors study. The purified enzyme reconstituted into liposomes functions as an electrogenic Na^+ pump which transports Na^+ upon hydrolysis of ATP and then a secondary event, Na^+ - and ATP-dependent H^+ efflux from proteoliposomes, is driven by the electric potential generated by Na^+ -stimulated ATPase.

A putative F-type Na^+ -*atp* operon coding for Na^+ -ATP synthase (Na^+ -ATPase) from *A. halophytica* was isolated. The operon consists of nine genes which encode putative subunits β , ϵ , I, hypothetical protein, a, c, b, α , and γ . The expression plasmid (pTrcHis2C-*ApNa⁺-atp*) was constructed and transformed into *E. coli* mutant DK8 (Δatp) deficient in ATP synthase. The inverted membrane vesicles from *ApNa⁺-ATPase*-expressing *E. coli* DK8 cells exhibited Na^+ -dependent ATP hydrolysis activity, which was inhibited by the sodium gradient dissipator monensin and the F-type ATPase inhibitor tributyltin chloride, but not by the protonophore, carbonyl cyanide m-chlorophenyl hydrazone (CCCP). The Na^+ ion protected the inhibition of *ApNa⁺-ATPase* by N,N'-dicyclohexylcarbodiimide (DCCD). The ATP synthesis activity was also observed using the Na^+ -loaded inverted membrane vesicles from *ApNa⁺-ATPase*-expressing *E. coli* DK8 cells. Expression of *ApNa⁺-atp* operon in a heterologous cyanobacterium *Synechococcus* sp. PCC 7942 showed its localization in the cytoplasmic membrane fractions and increased tolerance to salt stress. These results indicate that *A. halophytica* has additional F-type Na^+ -dependent ATPase playing a potential role of salt-stress tolerance.

Department:.....Biochemistry.....Student's Signature: *Kanteera Soontharapirakkul*
 Field of Study:.....Biochemistry.....Advisor's Signature: *Aran Incharoenesakdi*
 Academic Year:.....2010.....Co-Advisor's Signature: *Teruhiko Takabe*

ACKNOWLEDGEMENTS

I am cordially delighted to express my appreciation to my admirable advisor Professor Dr. Aran Incharoensakdi and my co-advisor, Professor Dr. Teruhiro Takabe, for their great understanding, excellent counselling, encouragements, guidance and supporting throughout this thesis. Without their kindness and understanding, this work could not be accomplished.

My thankfulness is also expressed to my co-advisor in Japan, Professor Dr. Teruhiro Takabe and all members in Research Institute of Meijo University, Meijo University for valuable comments and many chemical reagents and also their friendships I had received.

In addition, I also would like to express my deeply indebted and special appreciation to Professor Dr. Aran Incharoensakdi, Professor Dr. Teruhiro Takabe, Professor Dr. Anchalee Tassanakajorn, Associate Professor Dr. Teerapong Buaboocha, Dr. Saowarath Jantaro and Associate Professor Dr. Jarunya Narangajavana, serving as the members of the defence committee, for their helpful suggestions and valuable comments.

My appreciation is also expressed to Dr. Saowarath Jantaro, Dr. Surachet Burut-archanai, Dr. Wipawee Baebprasert and Dr. Wuttinun Raksajit for advice, comments and interesting discussions.

I would also like to thank all members of the Cyanobacteria and Cyclodextrin groups at Department of Biochemistry, Chulalongkorn University for lending helping hand whenever needed, sharing the great time in laboratory, their assistance and friendship.

Eventually, the extreme gratitude is expressed to my lovely family for their love, understanding, helping, supporting and encouragement with care which have enabled me to carry out this study successfully despite the fact that almost the whole of my time with this thesis rather than with them.

This work was supported in part by the grant from Royal Golden Jubilee (RGJ) Ph. D. program (PHD/0012/2550), the 90th Anniversary of Chulalongkorn University Fund (Ratchadaphiseksomphot Endowment Fund).

CONTENTS

	PAGE
ABSTRACT (THAI).....	iv
ABSTRACT (ENGLISH).....	v
ACKNOWLEDGEMENTS.....	vi
CONTENTS.....	vii
LIST OF TABLES.....	xv
LIST OF FIGURES.....	xvi
LIST OF ABBREVIATIONS.....	xxi
CHAPTER I: INTRODUCTION.....	1
1.1 Statements of problems.....	1
1.2 Objectives.....	5
1.3 Hypothesis.....	5
1.4 Scope of study.....	5
1.5 Organization of the dissertation.....	6
CHAPTER II: THEORETICAL BACKGROUND AND LITERATURE	
REVIEWS.....	7
2.1 Lineage of cyanobacterium.....	7
2.2 Hypersaline environments.....	12
2.2.1 Halophiles.....	12
2.2.2 Adaptations of organisms to high salt concentrations.....	13
2.3 Sodium transport systems.....	13
2.3.1 Na ⁺ -translocating membrane-bound decarboxylase.....	14
2.3.2 Methyltetrahydromethanopterin:coenzyme M methyltransferase.....	17
2.3.3 Na ⁺ -translocating NADH:ubiquinone oxidoreductase	18
2.3.4 Na ⁺ -translocating ATPase.....	20
2.4 Type of ATPases.....	20
2.4.1 P-type ATPases.....	20
2.4.2 V-type ATPases	22
2.4.3 F-type ATPases	22
2.5 Na ⁺ -dependent ATP hydrolysis (Na ⁺ -ATPase).....	24

	PAGE
CHAPTER III: MATERIALS AND METHODS.....	28
3.1 Materials.....	28
3.1.1 Equipments.....	28
3.1.2 Chemicals.....	30
3.1.3 Enzymes.....	34
3.1.4 Antibiotics.....	35
3.1.5 Kits.....	35
3.1.6 Supplies.....	36
3.1.7 Organisms.....	36
3.1.7.1 <i>Aphanothece halophytica</i>	36
3.1.7.2 <i>Escherichia coli</i> strain DH5 α , DK8 and TO114.....	36
3.1.7.3 <i>Synechococcus</i> sp. PCC 7942.....	37
3.1.8 Plasmids.....	37
3.1.8.1 pBluescript SK (+).....	37
3.1.8.2 pTrcHis2C.....	37
3.1.8.3 pUC303.....	37
3.1.9 Oligonucleotides.....	38
3.2 Methods.....	39
3.2.1 Methods for purification, reconstitution and characterization of ATPase from <i>A. halophytica</i>	39
3.2.1.1 Growth condition for <i>A. halophytica</i>	39
3.2.1.2 Preparation of inverted membrane vesicles from <i>A.</i> <i>halophytica</i>	40
3.2.1.3 Solubilization of membrane-bound ATPase.....	40
3.2.1.4 Polyethylene glycol 6000 precipitation.....	40
3.2.1.5 Gel filtration chromatography.....	41
3.2.1.6 Determination of ATP hydrolysis activity.....	41
3.2.1.7 Determination of protein.....	42
3.2.1.8 Sodium dodecyl sulfate polyacrylamide gel electrophoresis (SDS-PAGE).....	42
3.2.1.9 Sample preparation and LC-MS/MS analysis.....	42

	PAGE
3.2.1.10 Preparation of reconstituted proteoliposomes.....	43
3.2.1.11 Determination of Na ⁺ uptake into proteoliposomes..	43
3.2.1.12 Detection of H ⁺ efflux from proteoliposomes.....	44
3.2.1.13 Detection of membrane potential.....	44
3.2.2 Methods for genomic DNA extraction and cloning of <i>ApNa⁺-atp</i> operon from <i>A. halophytica</i>	45
3.2.2.1 <i>A. halophytica</i> genomic DNA extraction.....	45
3.2.2.2 Cloning of <i>ApNa⁺-atp</i> operon.....	46
3.2.3 Methods for construction of expression plasmids containing <i>ApNa⁺-atp</i> operon and IPTG-inducible <i>trc</i> promoter.....	46
3.2.3.1 Construction of pTrcHis2C- <i>ApNa⁺-atp</i>	46
3.2.3.2 Construction of pUC303- <i>ApNa⁺-atp</i>	47
3.2.4 Methods for characterization of biochemical properties and physiological functions of ApNa ⁺ -ATPase expressed in <i>E.</i> <i>coli</i> DK8 and freshwater cyanobacterium <i>Synechococcus</i> <i>sp.</i> PCC 7942 cells	48
3.2.4.1 Complementation test of <i>ApNa⁺-atp</i> operon.....	48
3.2.4.2 Measurement of Na ⁺ contents in Na ⁺ -loaded transformants.....	49
3.2.4.3 Preparation of inverted membrane vesicles from the transformants and determination of ATP hydrolysis activity.....	51
3.2.4.4 Preparation of Na ⁺ -loaded inverted membrane vesicles of from the transformants and determination of ATP synthesis.....	52
3.2.4.5 Isolation of periplasmic, cytoplasmic and membrane fractions from ApNa ⁺ -ATPase-expressing <i>E. coli</i> DK8 cells.....	53
3.2.4.6 Isolation of cytoplasmic and thylakoid membranes from ApNa ⁺ -ATPase-expressing <i>Synechococcus sp.</i> PCC 7942 cells.....	54

	PAGE
3.2.4.7 Western blot analysis of ApNa ⁺ -ATPase expressed in <i>E. coli</i> DK8 and <i>Synechococcus sp.</i> PCC 7942 cell	54
CHAPTER IV: RESULTS.....	56
4.1 Characterization of the growth of <i>A. halophytica</i> and ATP hydrolysis activity of inverted membrane vesicles in the presence of various external NaCl concentrations, pH ranges and ionophores.....	56
4.1.1 Effect of NaCl concentration and pH of the growth medium on the growth of <i>A. halophytica</i>	56
4.1.2 Effect of NaCl concentration and pH of the growth medium on ATP hydrolysis activity of inverted membrane vesicles from <i>A. halophytica</i>	59
4.1.3 Effect of Gramicidin D and CCCP in the growth medium on the growth of <i>A. halophytica</i> and ATP hydrolysis activity of inverted membrane vesicles.....	59
4.2 Optimization of purification conditions for obtaining high ATP hydrolysis activity.....	62
4.2.1 Effect of <i>A. halophytica</i> culture time on ATP hydrolysis activity of inverted membrane vesicles	62
4.2.2 Effect of sodium cholate on ATP hydrolysis activity of solubilized ATPase.....	62
4.2.3 Effect of solubilization time on ATP hydrolysis activity of solubilized ATPase.....	62
4.3 Purification of ATPase from <i>A. halophytica</i>	66
4.5 Preparation of reconstituted proteoliposomes.....	72
4.6 Characterization of purified ATPase and proteoliposomes.....	72
4.6.1 Effect of storage temperature on ATP hydrolysis activity of purified ATPase.....	72
4.6.2 Effect of cations, ATP, Mg ²⁺ and pH on ATP hydrolysis activity of purified ATPase and proteoliposomes.....	72

	PAGE
4.6.3 Effect of Na ⁺ ion concentration on ATP hydrolysis activity of purified ATPase at different pH values.....	73
4.6.4 Effect of inhibitors on ATP hydrolysis activity of purified ATPase and proteoliposomes.....	78
4.6.5 Protection of purified ATPase from DCCD inhibition by Na ⁺ at pH 7.6 and pH 9.0.....	81
4.6.6 Na ⁺ uptake into proteoliposomes at various incubation times	81
4.6.7 Dependence of Na ⁺ and ATP on Na ⁺ uptake into proteoliposomes.....	85
4.6.8 Effect of effectors on Na ⁺ uptake into proteoliposomes.....	85
4.6.9 Detection of H ⁺ efflux from proteoliposomes.....	88
4.6.10 Detection of membrane potential generated by proteoliposomes.....	88
4.7 Gene organization in the <i>ApNa⁺-atp</i> operon.....	91
4.8 Cloning of F-type <i>ApNa⁺-atp</i> operon from <i>A. halophytica</i>	97
4.9 Characterization of <i>ApNa⁺-ATPase</i> expressed in <i>E. coli</i> DK8 cells.....	102
4.9.1 Effect of NaCl on the growth of <i>E. coli</i> DK8 transformants..	102
4.9.2 Effect of NaCl on the growth of <i>E. coli</i> TO114 transformants.....	102
4.9.3 Growth of <i>E. coli</i> DK8 transformants on M13 minimal agar containing glucose or succinate.....	105
4.9.4 Na ⁺ content inside the cells of Na ⁺ -loaded <i>E. coli</i> DK8 transformants.....	105
4.9.5 Effect of NaCl, ATP, Mg ²⁺ and pH on ATP hydrolysis activity of inverted membrane vesicles from <i>E. coli</i> DK8 transformants.....	108
4.9.6 Effect of inhibitors on ATP hydrolysis activity of inverted membrane vesicles from <i>ApNa⁺-ATPase</i> -expressing <i>E. coli</i> DK8 cells.....	111

	PAGE
4.9.7 ATP synthesis by Na ⁺ -loaded inverted membrane vesicles from <i>E. coli</i> DK8 transformants.....	114
4.10 Western blot analysis of ApNa ⁺ -ATPase expressed in <i>E. coli</i> DK8 cells.....	117
4.10.1 Effect of induction time on the expression of ApNa ⁺ -ATPase in <i>E. coli</i> DK8 transformants.....	117
4.10.2 Effect of NaCl in the growth medium on ATP hydrolysis activity of inverted membrane vesicles from <i>E. coli</i> DK8 transformants.....	117
4.10.3 Effect of NaCl in the growth medium on the expression of ApNa ⁺ -ATPase in inverted membrane vesicles from ApNa ⁺ -ATPase-expressing <i>E. coli</i> DK8 cells.....	120
4.10.4 Localization of ApNa ⁺ -ATPase in ApNa ⁺ -ATPase-expressing <i>E. coli</i> DK8 cells.....	120
4.11 Construction of pUC303- <i>ApNa⁺-atp</i> plasmid for the expression of ApNa ⁺ -ATPase in a freshwater cyanobacterium <i>Synechococcus</i> sp. PCC 7942 cells.....	123
4.12 Characterization of ApNa ⁺ -ATPase expressed in <i>Synechococcus</i> sp. PCC 7942 cells.....	126
4.12.1 Effect of NaCl in the growth medium on the growth of <i>Synechococcus</i> sp. PCC 7942 transformants.....	126
4.12.2 Na ⁺ content inside the cells of Na ⁺ -loaded <i>Synechococcus</i> sp. PCC 7942 transformants.....	128
4.12.3 Effect of NaCl, ATP, Mg ²⁺ and pH on ATP hydrolysis activity of inverted membrane vesicles from <i>Synechococcus</i> sp. PCC 7942 transformants.....	130
4.12.4 The effect of inhibitors on ATP hydrolysis activity of inverted membrane vesicles from ApNa ⁺ -ATPase-expressing <i>Synechococcus</i> sp. PCC 7942 cells.....	133
4.12.5 ATP synthesis by Na ⁺ -loaded inverted membrane vesicles from <i>Synechococcus</i> sp. PCC 7942 transformants.....	136

	PAGE
4.13 Western blot analysis of ApNa ⁺ -ATPase expressed in <i>Synechococcus</i> sp. PCC 7942 cells.....	139
4.13.1 Expression and localization of ApNa ⁺ -ATPase in <i>Synechococcus</i> sp. PCC 7942 cells.....	139
4.13.2 Effect of NaCl in the growth medium on ATP hydrolysis activity of inverted membrane vesicles from <i>Synechococcus</i> sp. PCC7942 transformants.....	143
4.13.3 Effect of NaCl in the growth medium on the expression of ApNa ⁺ -ATPase in inverted membrane vesicles from ApNa ⁺ -ATPase-expressing <i>Synechococcus</i> sp. PCC 7942 cells.....	143
CHAPTER V: DISCUSSION.....	146
CHAPTER VI: CONCLUSION.....	155
REFERENCES.....	157
APPENDICES.....	174
APPENDIX A pBluescript SK (+).....	175
APPENDIX B pTrcHis2C.....	176
APPENDIX C pUC303.....	177
APPENDIX D BG11 and BG11 plus Turk Island Salt Solution.....	178
APPENDIX E ATP hydrolysis activity assay.....	180
APPENDIX F Determination of inorganic phosphate (Pi).....	181
APPENDIX G Determination of protein by Bradford's method.....	182
APPENDIX H Preparation for polyacrylamide gel electrophoresis..	183
APPENDIX I In-gel tryptic digestion.....	187
APPENDIX J Sodium-22 and scintillation fluid preparation.....	188
APPENDIX K PCR amplification protocol for <i>ApNa⁺-atp</i> operon...	189
APPENDIX L <i>E. coli</i> transformation by heat shock method.....	190
APPENDIX M LB medium.....	191
APPENDIX N Preparation of <i>E. coli</i> plasmid by alkaline lysis method.....	192
APPENDIX O Agarose gel electrophoresis for DNA.....	194

	PAGE
APPENDIX P LBK medium.....	196
APPENDIX Q ATP calibration curve.....	197
APPENDIX R Buffers for Western blotting.....	198
APPENDIX S Detection reagents for Western blotting.....	199
APPENDIX T Plasmid transformation into <i>Synechococcus</i> sp. PCC 7942.....	200
APPENDIX U Preparation of <i>Synechococcus</i> sp. PCC 7942 plasmid by alkaline lysis method.....	201
APPENDIX V PCR amplification protocol for chloramphenicol resistance gene.....	203
APPENDIX W PCR amplification protocol for <i>atpG</i> encoding γ subunit of ApNa ⁺ -ATPase.....	204
BIOGRAPHY.....	205

LIST OF TABLES

		PAGE
Table 1	PCR primers for PCR amplification of <i>ApNa⁺-atp</i> operon from <i>A. halophytica</i> genomic DNA	38
Table 2	PCR primers for sequencing <i>ApNa⁺-atp</i> operon.....	38
Table 3	PCR primers for PCR amplification of chloramphenicol resistance gene (Cmr) in <i>E. coli/Synechococcus</i> shuttle vector pUC303.....	39
Table 4	PCR primers for PCR amplification of <i>atpG</i> encoding γ subunit of <i>ApNa⁺-atp</i> operon.....	39
Table 5	Purification of ATPase from <i>A. halophytica</i>	67
Table 6	Effect of inhibitors on ATP hydrolysis activity of purified ATPase.....	79
Table 7	Effect of inhibitors on ATP hydrolysis activity of proteoliposomes.....	80
Table 8	Comparison of the protein sequences of nine <i>Na⁺-atp</i> gene from <i>A. halophytica</i> with the corresponding of ATPase subunits from various organisms including Na^+ -ATPase from <i>I. tartaricus</i> (AF522463), <i>P. modestum</i> (X53960), <i>A. woodii</i> (U10505), <i>C. paradoxum</i> (DQ193538) and H^+ -ATPase from <i>E. coli</i> (J01594)....	93

LIST OF FIGURES

		PAGE
Figure 1	<i>Nostoc</i> sp. 86-3 hormogonia responsible for gliding motility, adhesion and aggregation in the nostocacean life cycle. The hormogonia are preferentially stained with dilute methylene blue (x400).....	10
Figure 2	Filamentous cyanobacterium with a nitrogen fixing heterocyst, an akinete, and adjacent photosynthetic vegetative cells.....	10
Figure 3	<i>Aphanothece halophytica</i> grown in Turk Island Salt Solution plus modified BG11 medium.....	11
Figure 4	Schematics of the citrate fermentation pathway in <i>Klebsella pneumonia</i>	15
Figure 5	Schematics of the succinate fermentation pathway of <i>Propionigenium modustum</i>	16
Figure 6	Schematic overview of bioenergetic processes coupled to Na ⁺ circulation.....	19
Figure 7	Mechanism of P-Type ATPase Action.....	21
Figure 8	Structure and evolutionary relationships of F- and V-type ATPases.....	23
Figure 9	Microscopic picture of <i>A. halophytica</i> grown in BG11 medium supplemented with 18 mM NaNO ₃ and Turk Island salt solution containing 0.5 M NaCl at day 14 (x2,250).....	57
Figure 10	Effect of NaCl concentration and pH of the growth medium on the growth of <i>A. halophytica</i>	58
Figure 11	Effect of NaCl concentration and pH of the growth medium on ATP hydrolysis activity of inverted membrane vesicles from <i>A. halophytica</i>	60
Figure 12	Effect of Gramicidin D and CCCP in the growth medium on growth of <i>A. halophytica</i> and ATP hydrolysis activity of inverted membrane vesicles.....	61
Figure 13	Effect of <i>A. halophytica</i> culture time on ATP hydrolysis activity of inverted membrane vesicles.....	63

	PAGE
Figure 14 Effect of sodium cholate on ATP hydrolysis activity of solubilized ATPase.....	64
Figure 15 Effect of solubilization time on ATP hydrolysis activity of solubilized ATPase.....	65
Figure 16 Separation of ATPase from <i>A. halophytica</i> by Superose 6 gel filtration chromatography.....	68
Figure 17 Determination of molecular weight of ATPase from <i>A. halophytica</i> separated by Superose 6 gelfiltration.....	69
Figure 18 SDS-PAGE of ATPase from <i>A. halophytica</i>	70
Figure 19 Determination of molecular weight of ATPase subunits by SDS-PAGE.....	71
Figure 20 Effect of storage temperature on ATP hydrolysis activity of purified ATPase.....	74
Figure 21 Dependence of purified ATPase on cations, ATP, Mg ²⁺ and pH.....	75
Figure 22 Dependence of proteoliposomes on cations, ATP, Mg ²⁺ and pH.....	76
Figure 23 Effect of Na ⁺ ion concentration on ATP hydrolysis activity of purified ATPase at different pH values.....	77
Figure 24 Protection of purified ATPase from DCCD inhibition by Na ⁺ at pH 7.6 and pH 9.0.....	82
Figure 25 Effect of cations on the protection of purified ATPase from DCCD inhibition.....	83
Figure 26 Na ⁺ uptake into proteoliposomes at various incubation times.....	84
Figure 27 Na ⁺ uptake into proteoliposomes at various NaCl and ATP concentrations.....	86
Figure 28 Effect of effectors on Na ⁺ uptake into proteoliposomes	87
Figure 29 Changes in Δ pH of proteoliposome lumen detected with Δ pH probe acridine orange.....	89

	PAGE
Figure 30 Changes in membrane potential across proteoliposome detected with voltage-sensitive probe oxonol VI.....	90
Figure 31 Schematic structures of gene organization of several ATP synthases.....	92
Figure 32 Phylogenetic trees for β subunit of H^+ - and Na^+ -translocating ATPases from several species.....	95
Figure 33 (A) Phylogenetic trees for c subunit of H^+ - and Na^+ -translocating ATPases from several species. (B) Alignment of c subunit sequences of H^+ - and Na^+ -translocating ATPases from several species.....	96
Figure 34 1% agarose gel electrophoresis of the 6.8-kb PCR product of <i>ApNa⁺-atp</i> operon.....	98
Figure 35 Schematics of the construction of recombinant plasmid pBSK+ <i>-ApNa⁺-atp</i>	99
Figure 36 1% agarose gel electrophoresis of the recombinant plasmid pBSK+ <i>-ApNa⁺-atp</i> cut with <i>NcoI</i> , <i>PvuII</i> , <i>BamHI</i> + <i>Sall</i>	100
Figure 37 Schematics of the construction of recombinant plasmid pTrcHis2C- <i>ApNa⁺-atp</i>	101
Figure 38 Effect of NaCl on the growth of <i>E. coli</i> DK8 transformants.....	103
Figure 39 Effect of NaCl on the growth of <i>E. coli</i> TO114 transformants...	104
Figure 40 Complementation test of <i>ApNa⁺-atp</i> operon in <i>E. coli</i> mutant DK8 (Δatp) grown on M13 minimal agar containing 35 mM glucose (A) or succinate (B) for 2 days.....	106
Figure 41 Extrusion of Na^+ from Na^+ -loaded <i>E. coli</i> DK8 transformants...	107
Figure 42 Effect of NaCl on ATP hydrolysis activity of inverted membrane vesicles from <i>E. coli</i> DK8 transformants.....	109
Figure 43 Effect of ATP, Mg^{2+} and pH on ATP hydrolysis activity of inverted membrane vesicles from <i>ApNa⁺-ATPase</i> -expressing <i>E. coli</i> DK8 cells.....	110

Figure 44	Effect of inhibitors on ATP hydrolysis activity of inverted membrane vesicles from ApNa ⁺ -ATPase-expressing <i>E. coli</i> DK8 cells.....	112
Figure 45	Protection of ATPase in inverted membrane vesicles from ApNa ⁺ -ATPase-expressing <i>E. coli</i> DK8 cells from DCCD inhibition by Na ⁺ at pH 7.6 and pH 9.0.....	113
Figure 46	ATP synthesis by Na ⁺ -loaded inverted membrane vesicles from <i>E. coli</i> DK8 transformants.....	115
Figure 47	Dependence of ΔpNa^+ and $\Delta\Psi$ on ATP synthesis by Na ⁺ -loaded inverted membrane vesicles from ApNa ⁺ -ATPase-expressing <i>E. coli</i> DK8 cells.....	116
Figure 48	Effect of induction time on the expression of ApNa ⁺ -ATPase in <i>E. coli</i> DK8 transformants by 1 mM IPTG.....	118
Figure 49	Effect of NaCl in the growth medium on ATP hydrolysis activity of inverted membrane vesicles from <i>E. coli</i> DK8 transformants.....	119
Figure 50	Effect of NaCl in the growth medium on the expression of ApNa ⁺ -ATPase in ApNa ⁺ -ATPase-expressing <i>E. coli</i> DK8 cells	121
Figure 51	Localization of ApNa ⁺ -ATPase in ApNa ⁺ -ATPase-expressing <i>E. coli</i> DK8 cells.....	122
Figure 52	Schematics of the construction of recombinant plasmid pUC303- <i>ApNa⁺-atp</i>	124
Figure 53	The map of pUC303 and pUC303- <i>ApNa⁺-atp</i> and the band of PCR products amplified check with chloramphenicol-specific primers (product size 800 bp) and <i>atpG</i> encoding γ subunit of <i>ApNa⁺-atp</i> -specific primers (product size 520 bp).....	125
Figure 54	Effect of NaCl on the growth of <i>Synechococcus</i> sp. PCC 7942 transformants.....	127
Figure 55	Extrusion of Na ⁺ from Na ⁺ -loaded <i>Synechococcus</i> sp. PCC 7942 transformants.....	129

Figure 56	Effect of NaCl on ATP hydrolysis activity of inverted membrane vesicles from <i>Synechococcus</i> sp. PCC 7942 transformants.....	132
Figure 57	Effect of ATP, MgCl ₂ and pH on ATP hydrolysis activity of inverted membrane vesicles from ApNa ⁺ -ATPase-expressing <i>Synechococcus</i> sp. PCC 7942 cells.....	132
Figure 58	Effect of inhibitors on ATP hydrolysis activity of inverted membrane vesicles from ApNa ⁺ -ATPase-expressing <i>Synechococcus</i> sp. PCC 7942 cells.....	134
Figure 59	Protection of ATPase in inverted membrane vesicles from ApNa ⁺ -ATPase-expressing <i>Synechococcus</i> sp. PCC 7942 cells from DCCD inhibition by Na ⁺ at pH 7.6 and pH 9.0.....	135
Figure 60	ATP synthesis by Na ⁺ -loaded inverted membrane vesicles from <i>Synechococcus</i> sp. PCC 7942 transformants.....	137
Figure 61	Dependence of ΔpNa^+ and $\Delta\Psi$ on ATP synthesis by Na ⁺ -loaded inverted membrane vesicles from ApNa ⁺ -ATPase-expressing <i>Synechococcus</i> sp. PCC 7942 cells.....	138
Figure 62	Immunoblot analysis of ApNa ⁺ -ATPase expressed in cyanobacterium <i>Synechococcus</i> sp. PCC 7942 cells.....	139
Figure 63	Separation of plasma membrane and thylakoid membrane fractions on a sucrose gradient centrifugation.....	141
Figure 64	The localization of ApNa ⁺ -ATPase in ApNa ⁺ -ATPase-expressing <i>Synechococcus</i> sp. PCC 7942 cells.....	142
Figure 65	Effect of NaCl in the growth medium on ATP hydrolysis activity of inverted membrane vesicles from <i>Synechococcus</i> sp. PCC 7942 transformants.....	144
Figure 66	Effect of NaCl in the growth medium on ApNa ⁺ -ATPase expression in ApNa ⁺ -ATPase-expressing <i>synechococcus</i> sp. PCC 7942 cells.....	145

LIST OF ABBREVIATIONS

Amp	Ampicillin
ATP	Adenosine-5'-triphosphate
bp	Base pair
BSA	Bovine serum albumin
CCCP	Carbonyl cyanide <i>m</i> -chlorophenylhydrazone
Ci	Curie
Cm	Chloramphenicol
cpm	Count per minute
Δ pH	pH gradient or proton gradient
$\Delta\psi$	Membrane potential
Δ pNa	Sodium gradient
DCCD	<i>N, N'</i> -dicyclohexylcarbodiimide
DMSO	Dimethyl sulfoxide
°C	Degree Celsius
DNA	Deoxyribonucleic acid
EDTA	Ethylenediaminetetraacetic acid
<i>et al.</i>	Et. Alii (latin), and others
FPLC	Fast performance liquid chromatography
g	Gram
hr	Hour
IPTG	Isopropyl- β -D-thiogalactoside
kb	Kilobase

kDa	KiloDalton
Km	Kanamycin
l	Liter
M	Molar
μl	Microliter
μM	Micromolar
mA	Milliampere
mg	Milligram
min	Minute
ml	Milliliter
mM	Millimolar
MW	Molecular weight
NBT	<i>p</i> -Nitro blue tetrazolium chloride
NEM	<i>N</i> -ethylmaleimide
ng	Nanogram
nm	Nanometer
OD	Optical density
ORF	Open reading frame
PAGE	Polyacrylamide gel electrophoresis
PCR	Polymerase chain reaction
PMF	Proton motive force
rpm	Revolution per minute
SDS	Sodium dodecyl sulphate
Str	Streptomycin sulfate

TBE	Tris-borate-EDTA
TEMED	N,N,N',N'-tetramethylene ethylene diamine
V	Volt
v/v	Volume by volume
w/v	Weight by volume
X-gal	5-bromo-4-chloro-3-indolyl-b-D-galactopyranoside

ABBREVIATION OF GENE, PLASMIDS AND PROTEIN

<i>ApNa⁺-atp</i>	Na ⁺ -ATPase gene from <i>Aphanothece halophytica</i>
pBSK+ <i>-ApNa⁺-atp</i>	pBluescript SK (+) harboring <i>ApNa⁺-atp</i>
pTrcHis2C <i>-ApNa⁺-atp</i>	pTrcHis2C harboring <i>ApNa⁺-atp</i>
pUC303 <i>-ApNa⁺-atp</i>	pUC303 harboring <i>ApNa⁺-atp</i>
ApNa ⁺ -ATPase	Na ⁺ -ATPase protein from <i>Aphanothece halophytica</i>

CHAPTER I

INTRODUCTION

1.1 Statements of problems

One of the physical parameters to determine the ability of living organisms to survive in their environment is an accumulation of salts in aquatic habitats. Evaporation posed difficulties to the survival of aquatic organisms due to the reduction in volume of aquatic environments, an increase of ionic concentrations and mineral precipitation. High salinity causes both osmotic (water) and ionic (NaCl) stress effects in microorganisms and etc (Ueda *et al.*, 2003).

Generally, the responses to salt can be classified into “osmotic” and “ionic” stresses. The osmotic stress induced by salt stress causes the water loss and turgor pressure onto cytoplasm (Cayley *et al.*, 1991, 1992). As cell growth depends on turgor-driven stretching of the cell wall, the defense against osmotic stress requires osmotic adjustment by synthesizing and/or accumulating low molecular weight compatible solutes (osmolytes or osmoprotectants) which counteract the outflow of water under hypertonic growth condition. These compatible solutes include sugars such as sucrose; polyols such as trehalose and glycerol; amino acids such as glutamate and proline; and amino acid derivatives such as betaines, glycine betaines and ectoines (Yancey, 1982; McCue and Hanson, 1990). Accumulation of compatible solutes is a particular response. It serves a dual function as osmoregulator cells and stabilizer of the native of proteins, lipids and cells components against the deleterious effects of high ionic strength (Kempf and Bremer, 1998). Moreover, these compatible solutes are not inhibitory to most cellular processes even at near molar concentrations.

The type of compatible solutes is varied depending on organisms, for example, ectoine in *Chromohalobacter israelensis* (formerly *Bacterium* Ba1) (Regev *et al.*, 1990), glycine betaine in a halotolerant cyanobacterium *Aphanothece halophytica* (Incharoensakdi and Wutipraditkul, 1999), glucosylglycerol in *Synechocystis* sp. PCC 6803 (Hagemann and Erdmann, 1994), glycerol in *Saccharomyces cerevisiae* (Edgley and Brown, 1983), and trehalose in *Desulfovibrio halophilus* (Welsh *et al.*, 1996).

In addition to osmotic stress, salinity creates the specific problem of ion toxicity (ionic stress) because high intracellular Na^+ is harmful to several metabolic events, particularly nitrogen fixation, protein synthesis, respiration, photosynthesis, and consequently inhibits the growth of cyanobacteria (Apte *et al.*, 1987; Thomas *et al.*, 1988; Fernandes *et al.*, 1993; Joset *et al.*, 1996). In contrast, NaCl, in trace quantities, is essential for some crucial metabolic functions in cyanobacteria, such as nitrate/nitrite reductase (Brownell and Nicholas, 1967) and nitrogenase (Apte and Thomas, 1980, 1983a, 1984) activities. In addition, NaCl is also necessary for the uptake of bicarbonate (Reinhold *et al.*, 1984; Sanchez-Maeso *et al.*, 1987) and phosphate (Apte and Thomas, 1985) and regulates nitrogen fixation/assimilation and photosynthetic efficiency in cyanobacteria (Thomas and Apte, 1984; Garcia-Gonzalez *et al.*, 1987; Thomas *et al.*, 1988). At high salt concentrations (>0.4 M), most enzymes were inhibited because the hydrophobic-electrostatic balance between the forces maintaining the protein structure was perturbed (Wyn Jones and Pollard, 1983). However, toxic effects on cells occur at much lower concentrations (about 0.1 M), pointing to specific salt toxicity targets (Serrano, 1996).

When organisms are subjected to a sudden salt stress condition, they usually respond with an adaptation reaction. There occurs a passive flux of Na^+ into the cells (Richie, 1992). This Na^+ influx increases the cytoplasmic Na^+ concentration above a

critical level. To survive, cells must reduce or eliminate Na^+ concentration in the cytoplasm by extrusion of Na^+ out of the cells or by transporting Na^+ into the vacuoles of plant cells. One obvious possibility of Na^+ extrusion is the well-known Na^+/H^+ antiporter. Na^+/H^+ antiporter is membrane protein which located in the cytoplasmic membranes of cells and organellar membranes of the prokaryotic and eukaryotic kingdoms (Padan and Schuldiner, 1992, 1994; Padan, 1998; Padan and Krulwich, 2000). Na^+/H^+ antiporter plays a variety of function such as (i) exchanging internal Na^+ (Li^+) for external H^+ (secondary energized Na^+ export) by using a proton motive force provided by H^+ -ATPase as the driving force for this process (Padan and Schuldinger, 1993), this being the driving force for Na^+ -coupled processes such as Na^+ /solute symport and Na^+ -driven flagellar rotation (Vimont and Borch, 2000). (ii) extrusion of Na^+ and Li^+ , which are toxic if they accumulate to high concentrations in cells (Dover and Padan, 2001). (iii) regulation of intracellular pH under alkaline conditions. (iv) regulation of morphogenesis (Soong *et al.*, 2000) and (iv) regulation of cell volume (Padan and Schuldiner, 1996). In addition, it has been reported that Na^+/H^+ antiporters from *A. halophytica* can make *E. coli* and a freshwater cyanobacterium *Synechococcus* sp. PCC 7942 tolerant to high salinity (Waditee *et al.*, 2002).

The second mechanism for Na^+ extrusion is by means of primary Na^+ pumps which is the Na^+ -ATPase (primary energized Na^+ export) (Benito *et al.*, 1997). Na^+ -ATPase is a membrane-bound protein which maintains Na^+ ion concentrations inside the cells by coupling the hydrolysis of ATP to the translocation of Na^+ ions across the cell membrane. Na^+ -ATPase was found in a number of organisms including bacteria, fungi, yeast, algae, and halophytic higher plants (Glynn and Karlsh, 1975; Heefner and Harold, 1982; Haro *et al.*, 1991; Balnokin and Popova, 1994; Shono *et al.*, 1996;

Kaieda *et al.*, 1998). However, the information on the ATPase involved in Na⁺ transport is scarce in cyanobacteria.

Our group has been studying the mechanism of salt tolerance in the alkaliphilic halotolerant cyanobacterium *Aphanothece halophytica* during the last 10 years. We have shown the accumulation of large amounts of glycine betaine as an osmolyte under salt stress (Incharoensakdi and Wutipraditkul, 1999; Waditee *et al.*, 2003). In addition, we have also demonstrated that *E. coli* as well as a freshwater cyanobacterium *Synechococcus* sp. PCC 7942 transformed with Na⁺/H⁺ antiporter gene from *A. halophytica* could tolerate high salinity (Waditee *et al.*, 2002). In the past 5 years more attention has been focused on the study of Na⁺-homeostasis with respect to the function of Na⁺/H⁺ antiporter (Padan *et al.*, 2001; Apse and Blumwald, 2002; Shi *et al.*, 2003). In contrast, the other aspect of Na⁺-homeostasis via the operation of Na⁺-ATPase has received much less attention.

In the present work, we propose to investigate the involvement of ATPase in Na⁺ transport in the alkaliphilic halotolerant cyanobacterium *Aphanothece halophytica*. This may represent another mechanism for adaptation to changing salinity. *A. halophytica* is a good model organism for the study of salt tolerance due to its ability to grow under a wide range of NaCl concentrations up to 3 M as well as in an alkaline pH up to pH 11.0 (Takabe *et al.*, 1988; Incharoensakdi and Wutipraditkul, 1999). The information obtained from this study will certainly enhance our understanding of the regulation of Na⁺-homeostasis, and hence salt tolerance in this cyanobacterium.

1.2 Objectives

This research work focuses on four objectives, as follows:

1.2.1 To purify and characterize an ATPase from the alkaliphilic halotolerant cyanobacterium *A. halophytica*

1.2.2 To prepare and characterize the proteoliposomes reconstituted with the purified ATPase

1.2.3 To clone F-type Na^+ -*atp* operon encoding Na^+ -ATPase from *A. halophytica* genome

1.2.4 To characterize biochemical properties and physiological functions of $ApNa^+$ -ATPase

1.3 Hypothesis

Na^+ -stimulated ATPase from *A. holophytica* can uptake Na^+ into reconstituted proteoliposomes and confer salt tolerance to both *E. coli* mutant DK8 deficient in ATP synthase (Δatp) and a freshwater cyanobacterium *Synechococcus* sp. PCC 7942. This implies that Na^+ -stimulated ATPase from *A. halophytica* might play an important role in Na^+ transport across cell membrane for Na^+ homeostasis which made microorganisms increase their tolerance to salt stress.

1.4 Scope of study

1.4.1 Purification and characterization of an ATPase from the alkaliphilic halotolerant cyanobacterium *A. halophytica*

1.4.2 Preparation and characterization of the proteoliposomes reconstituted with the purified ATPase

1.4.3 Cloning of F-type Na^+ -*atp* operon encoding Na^+ -ATPase from *A. halophytica* genome

1.4.4 Construction of expression plasmids (pTrcHis2C-*ApNa⁺-atp* and pUC303-*ApNa⁺-atp*) containing IPTG-inducible *trc* promoter for transformation into *E. coli* mutant DK8 (Δatp) and a freshwater cyanobacterium *Synechococcus* sp. PCC 7942

1.4.5 Characterization of biochemical properties and physiological functions of $ApNa^+$ -ATPase expressed in *E. coli* DK8 and a freshwater cyanobacterium *Synechococcus* sp. PCC 7942

1.5 Organization of the dissertation

This dissertation is comprised of six chapters. Chapter I provides the introduction part of this research. Chapter II describes the theoretical background and literature review. Chapter III describes the research methodology. Chapter IV describes the results of the experiment. Chapter V and VI describe the discussion and the conclusion of this research, respectively.

CHAPTER II

THEORETICAL BACKGROUND AND LITERATURE REVIEWS

2.1 Lineage of cyanobacterium

The algae are the simplest members of the plant kingdom. Blue-green algae are not true algae but they are actually bacteria which photosynthesize like algae. Moreover, they do not have nucleus and chloroplast. The name “cyanobacteria” comes from “Cyan” which means the blue color of the bacteria (Echlin, 1966). Blue-greens can be found in lakes, oceans, ponds, soil and tidal flats. Their fossils have been identified as over three billion years old. They were probably the chief primary producers of organic matter and the first organisms to produce O₂, into the primitive atmosphere (Wilmotte, 1994). Thus, Blue-greens were probably evolved in water when the atmosphere is free from O₂. Then, blue-greens lead to the evolution of aerobic metabolism and to the subsequent rise of higher plant and animal forms. In the literature, blue-greens are referred to by various names, for example, Cyanophyta, Myxophyta, Cyanochloronta, Cyanobacteria, blue-green algae, blue-green bacteria.

The majority of blue-greens are aerobic photoautotrophs which require only oxygen, light and inorganic substances for life processes. The glucose produced by photosynthesis of cyanobacteria is stored in formed starch which is similar to glycogen in animal. Some blue-green species use sulfide as electron donor for switching to the typical bacterial an oxygenic photosynthesis (Cohen *et al.*, 1986). A species of *Oscillatoria* that is found in mud at the bottom of the Thames, are able to live anaerobically. They can live in the extremes temperatures -60°C to 85°C, and a

few species are halophilic or salt tolerant (as high as 27%, for comparison with the percentage of salt in seawater is 3%). Blue-greens can grow in full sunlight and in almost complete darkness. They are often the first phototrophic organism to colonize bare areas of rock and soil, as an example subsequent to cataclysmic volcanic explosion (at Krakatoa, Indonesia in 1883). Under nitrogen limitation during bloom conditions, certain cells in *Anabaena* and *Aphanizomenon* evolve into heterocysts, which convert nitrogen gas into ammonium, which is then distributed to the neighboring cells of a filament. In addition, blue-greens that form symbiotic relationships with a wide range of other life forms, can convert nitrogen gas into ammonium.

Blue-greens mostly include unicellular and colonial species. Colonies may form filaments, sheets or even hollow balls. The ability of some filamentous colonies to differentiate was classified into four different cell types; 1) Vegetative cells, the normal photosynthetic cells that are formed under favorable growing conditions. 2) Hormogonia are nongrowing filaments which motile by gliding mechanism (Duggan *et al.*, 2007; Hoiczky and Baumeister, 1998). The motile filaments of cells that are formed during asexual reproduction involved in symbiosis between nitrogen-fixing cyanobacteria in the genus *Nostoc* and their host (Figure 1). Furthermore, the differentiation of cyanobacteria into hormogonia occurs when the cells exposed to salt stress. Hormogonia are distinguished from vegetative cells by their gliding motility and the small size of their cells (Meeks and Elhai, 2002). 3) Akinetes, the climate-resistant spore-like cell that may form when environmental conditions become harsh. Akinetes contain large reserves of carbohydrates, and owing to their density and lack of gas vesicles, eventually settle to the lake bottom (Figure 2). They can tolerate adverse conditions such as the complete drying of a pond or the cold winter

temperatures, and as a consequence, akinetes serve as “seeds” for the growth of juvenile filaments when favorable conditions return (Meeks *et al.*, 2002). 4) Heterocysts, the nitrogen-fixing cells have a thick cell wall with contain the enzyme nitrogenase, vital for nitrogen fixation. Their role is to fix nitrogen from atmosphere to form useful products such as amino acids and nitrogen-containing molecules. Vegetative cells provided the reduced carbon compounds to the heterocyst, in turn, get the fixed nitrogen from them.

Among prokaryotes, cyanobacteria are the only organisms capable of oxygenic photosynthesis. According to endosymbiotic theory, chloroplast in plant and eukaryotic algae have evolved from cyanobacteria via endosymbiosis. Although analysis of ancient genes has indicated a genetic relationship with Gram-positive bacteria. Their phylogenetic position in the bacterial kingdom is still obscure. (Hansmann and Martin, 2000; Xiong *et al.*, 2000).

Aphanothece halophytica is the unicellular alkaliphilic halotolerant cyanobacterium. This cyanobacterium has a short cylindrical shape covered with mucous membrane and the cell multiply by an asexual reproductive process called “binary fission”. This organism is classified into Chroococcales order, Chroococcacean cyanobacteria subgroup (Geitler, 1932; Stanier *et al.*, 1971). Furthermore, *A. halophytica* has the ability to grow under a wide range of salinity concentrations from 0.25-3.0 M NaCl as well as in an alkaline pH up to pH 11.0 (Figure 3) (Takabe *et al.*, 1988; Incharoensakdi and Wutipraditkul, 1999).

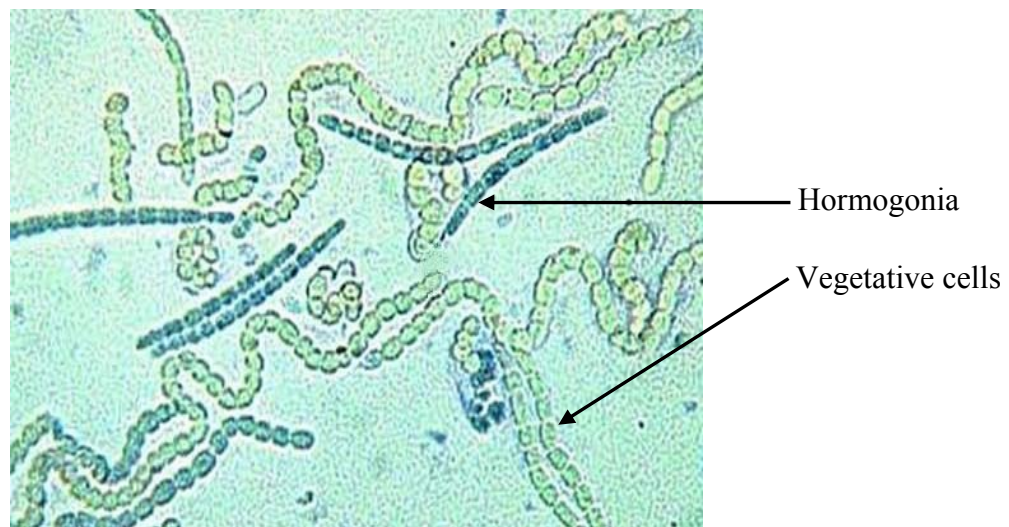


Figure 1 *Nostoc* sp. 86-3 hormogonia responsible for gliding motility, adhesion and aggregation in the nostocacean life cycle. The hormogonia are preferentially stained with dilute methylene blue (x400).

Available from: <http://www.microscopy.org/education/projectmicro/camera.cfm>

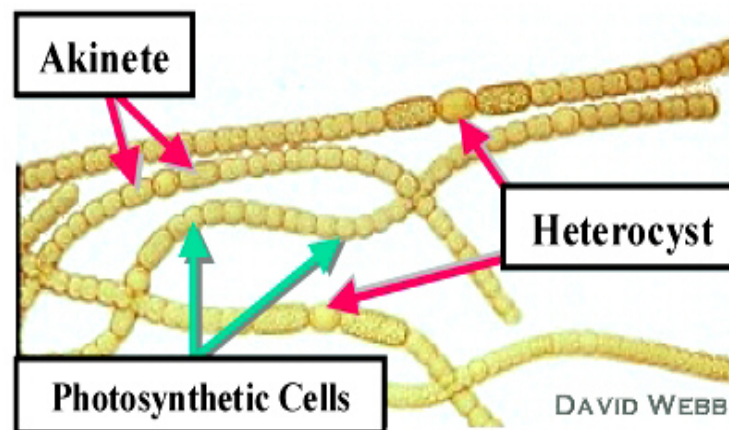


Figure 2 Filamentous cyanobacterium with a nitrogen fixing heterocyst, an akinete, and adjacent photosynthetic vegetative cells (Illustration by David Webb).

Available from: <http://www.biologie.uni-hamburg.de/b-online/library/webb/BOT311/Cyanobacteria/Cyanobacteria.htm>



Figure 3 *Aphanothece halophytica* grown in Turk Island Salt Solution plus modified BG11 medium.

2.2 Hypersaline environments

Salinity is an important ecological factor that influences the types of living organisms. Salinities in hypersaline environments which are greater than the normal seawater salinities, generally originated by evaporation of seawater. Such environments are inhabited by halophiles, the salt loving organisms. Halophiles are distributed in hypersaline environments all over the world, mainly in natural hypersaline brines in arid, coastal and deep sea locations as well as in artificial salterns. Halophiles include prokaryotes and eukaryotes which survive extreme saline conditions and have the capacity to regulate the osmotic pressure, thereby resisting the denaturing effects of salt in their environment.

2.2.1 Halophiles

Halophiles are microorganisms that inhabit hypersaline environments. The Greek name refer to “salt-loving”. They include mainly prokaryotic and eukaryotic microorganisms with the capacity to balance the osmotic pressure of the environmental and resist the denaturing effect of salts. Example of well-adapted and widely distributed extremely halophilic microorganisms, cyanobacteria such as *Aphanothece halophytica*, and the green algae *Dunaliella salina* (Casamayor *et al.*, 2002). For the characterization of microorganism type, the determination of saline spectrum is very important. According to the salt concentration required for their optimum growth, the organisms were classified as nonhalophiles (optimal growth in media containing less than 0.2 M NaCl), slight halophiles (grow best in media containing 0.2 to 0.5 M NaCl), moderate halophiles (grow optimally in media containing 0.5 to 2.5 M NaCl, borderline extreme halophiles (grow best in media with 1.5 to 4.0 M NaCl) and extreme halophiles (grow best in media containing 2.5 to 5.2

M (saturated) NaCl) (Nieto *et al.*, 1989). Beside, halotolerance describes the ability or adaptation of organisms to grow at a salt concentration condition.

2.2.2 Adaptations of organisms to high salt concentrations

To be able to live at high salt concentrations, halophilic and halotolerant organisms must maintain their cytoplasm at least osmotic pressure against the extracellular environments. The critical demands of cyanobacteria exposed to high salinity are accumulation of osmoprotectants and extrusion of sodium ions. These mechanisms are met through immediate activation and/or long term (protein synthesis-dependent) adaptation of various processes (Joset *et al.*, 1996): (i) uptake and endogenous biosynthesis of osmoprotectants. (ii) probable modifications of membrane lipid composition. (iii) increased energetic capacity, at the level of cyclic electron flow around photosystem I (through routes induced under these conditions) and cytochrome c oxidase, and (iv) enhancement of H⁺-ATPase, Na⁺-ATPase, Na⁺/H⁺ antiporter activity and active extrusion of sodium ions.

2.3 Sodium transport systems

Not only the chemiosmotic of proton circulation provides the unifying framework for bacterial energetics, but also a sodium gradient which plays a significant supporting role. The significance of the sodium gradient in bacteria is well known; the sodium current is frequently linked with cotransport systems for extrusion of sodium ions and maintenance of the electrochemical concentration gradient of sodium directed inward (Kakinuma and Unemoto, 1985). In addition, the driving force for flagellar movement can be served by the sodium current (Hirota and Imae, 1983). The maintenance of a constant internal ion composition is required to all living

cells. Bacteria tend to maintain the cytoplasmic pH within a narrow range and to establish gradients of K^+ and Na^+ ions between their cytoplasm and the surrounding medium such that the cytoplasmic K^+ concentration is higher than and the Na^+ concentration is lower than that of the environment. It is accepted that the secondary transport systems coupled to H^+ mediate the movements of K^+ and Na^+ ions. Proton movement across the membrane is the primary event not only for energy metabolism but also for performing this homeostasis work. Microorganisms living in aquatic habitats are directly exposed to the outside world through a cell surface layer. Their habitats commonly encompass a wide range of physical conditions: oxygen, pH, salinity, temperature, light, etc. Bacteria have evolved a variety of ancillary energy conversion mechanisms when they cannot cope with and survive in severe environments by depending on their H^+ -linked machinery alone. Now, the supplement of Na^+ ions to the role of H^+ ions in energy transduction across the bacterial membrane is recognized (Lanyi, 1979). There are diverse primary sodium ion translocating enzymes such as:

2.3.1 Na^+ -translocating membrane-bound decarboxylase

In *Klebsiella pneumonia* and *Salmonella typhimurium*, oxaloacetate decarboxylase was found in the citrate fermentation pathway (Figure 4) (Schwarz, 1988; Wifling and Dimroth, 1989; Dimroth and Thomer, 1993; Woehlke and Dimroth, 1994). Oxaloacetate produced in the pathway is decarboxylated to pyruvate by oxaloacetate decarboxylase.

In *Veillonella alcalescens* and *Propionigenium modestum*, Methylmalonyl-CoA decarboxylase takes part in the fermentation of lactate and succinate, respectively (Figure 5). Methylmalonyl-CoA decarboxylase catalyzed

methylmalonyl-CoA to propionyl-CoA (Hilpert and Dimroth, 1983, 1984; Hilpert *et al.*, 1984; Hoffmann *et al.*, 1989; Bott *et al.*, 1997).

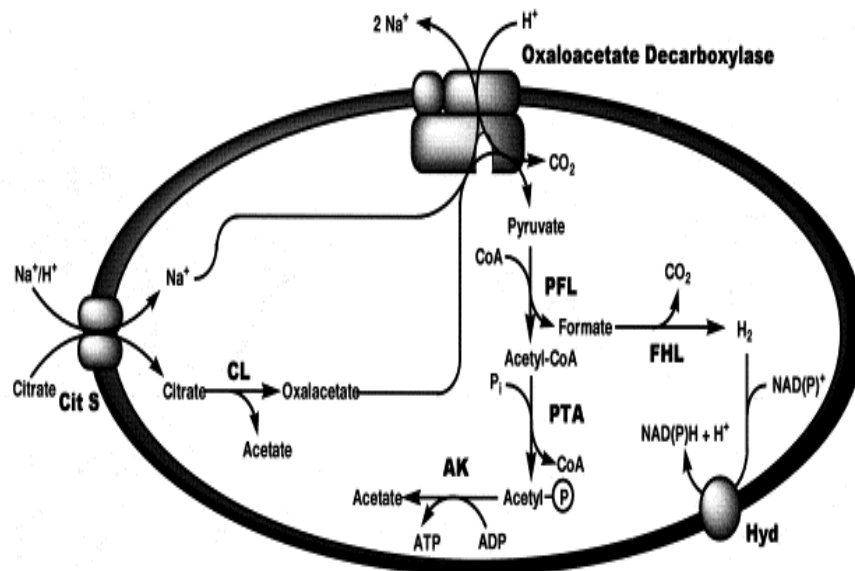


Figure 4 Schematics of the citrate fermentation pathway in *K. pneumoniae* (Dimroth *et al.*, 2001). Citrate is transported into the cell by the Na^+ -specific transporter CitS. Internal citrate is cleaved by citrate lyase (CL) to acetate and oxaloacetate. The latter is decarboxylated to pyruvate by the oxaloacetate decarboxylase. Na^+ pump and the free energy of the decarboxylation reaction is utilized for Na^+ ion pumping out of the cell. Pyruvate formate lyase (PFL) forms formate and acetyl-CoA from pyruvate. Acetyl-CoA is converted to acetyl-phosphate by phosphotransacetylase (PTA) and further to acetate with ATP generation by the acetate kinase (AK) reaction. Formate is split into CO_2 and H_2 by formate hydrogen lyase (FHL) and the H_2 is utilized for NAD(P) reduction by a membrane-bound hydrogenase (Hyd).

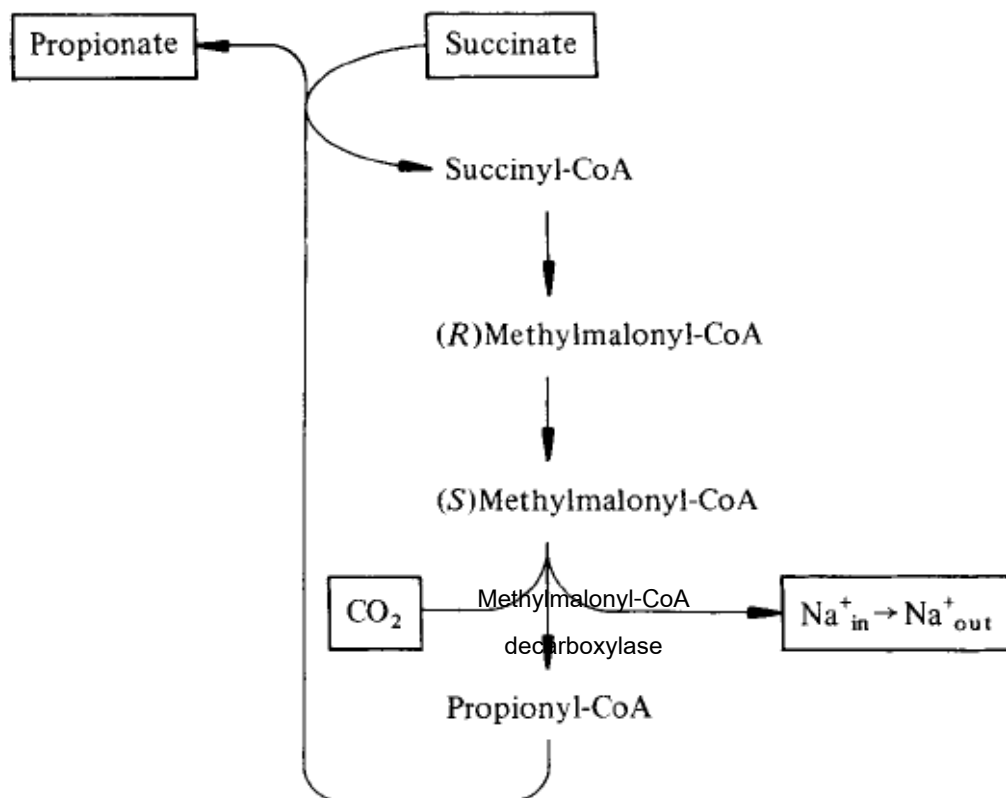


Figure 5 Schematics of the succinate fermentation pathway of *Propionigenium modustum* (Laubinger and Dimroth, 1987). Methylmalonyl-CoA decarboxylase catalyzed methylmalonyl-CoA to propionyl-CoA and the decarboxylation energy is used to drive Na⁺ transport from the inside to the outside of the cells.

In *Acidaminococcus fermentans* and *Fusobacterium nucleatum*, Glutaconyl-CoA decarboxylase is an essential enzyme in several glutamate degrading anaerobic bacteria. This enzyme catalyzed the decarboxylation of glutaconyl-CoA to crotonyl-CoA (Buckel and Semmler, 1982; Buckel and Liedtke, 1986).

In *Malonomonas rubra*, Malonate decarboxylase is responsible for the decarboxylation of malonate to acetate (Hilbi *et al.*, 1992, 1993; Hilbi and Dimroth, 1994).

All four different decarboxylases mentioned belong to the family of Na⁺ translocating decarboxylases that couple the exergonic chemical reaction to an active Na⁺ transport from the inside to the outside of the cell while the H⁺ which is required for decarboxylation mostly come from the outside. These enzymes are biotin enzymes, and the biotin prosthetic group is essential for the catalysis of each specific decarboxylation reaction.

2.3.2 Methyltetrahydromethanopterin:coenzyme M methyltransferase

Methanogenesis from CO₂ and acetate proceeds via methyltetrahydromethanopterin and methyl-coenzyme M as intermediates. The formation of methyl-coenzyme M from methyltetrahydromethanopterin (CH₃-H₄MPT) and coenzyme M (H-S-CoM) is catalyzed by a methyltetrahydromethanopterin:coenzyme M methyltransferase, which is membrane associated, corrinoid-containing protein and which couples the exergonic methyl transfer reaction with the electrogenic translocation of sodium ions across the cytoplasmic membrane (Becher *et al.*, 1992a). A reductant such as titanium (III) citrate and ATP are required for full activity (Kengen *et al.*, 1988, 1992; Becher *et al.*,

1992b; Gartner *et al.*, 1993). The methyltransferase reaction is thus coupled with energy conservation (Figure 6).

In *Methanosarcina mazei* Gö1, the methyltetrahydromethanopterin:coenzyme M methyltransferase was purified and then the reconstituted proteoliposomes were constructed for determination of Na⁺ transport. It was shown that the methyltransferase catalyzed the translocation of sodium ions across the membrane (Lienard *et al.*, 1996).

2.3.3 Na⁺-translocating NADH:ubiquinone oxidoreductase

Two different NADH:ubiquinone oxidoreductases have also been found in the membrane of the marine bacterium *Vibrio alginolyticus*. One of these, termed NQR-2 is of the nonenergy-conserving type, whereas the other one, termed NQR-1, is believed to be coupled to Na⁺ ion pumping. The report on NADH:ubiquinone oxidoreductase of *V. alginolyticus* showed that the Na⁺-dependent step in the electron transfer catalyzed by NADH:ubiquinone oxidoreductase is the reduction of ubisemiquinone to ubiquinol. After reconstitution of the purified NADH:ubiquinone oxidoreductase-1 into proteoliposomes, NADH oxidation by ubiquinone-1 was coupled to Na⁺ transport with an apparent stoichiometry of 0.5 Na⁺ per NADH oxidized. The transport was stimulated by valinomycin (in the presence of K⁺) or by the uncoupler carbonyl cyanide *m*-chlorophenylhydrazone (CCCP). The transport of Na⁺ is therefore a primary event and does not involve the intermediate formation of a proton gradient (Pfenninger-Li *et al.*, 1996).

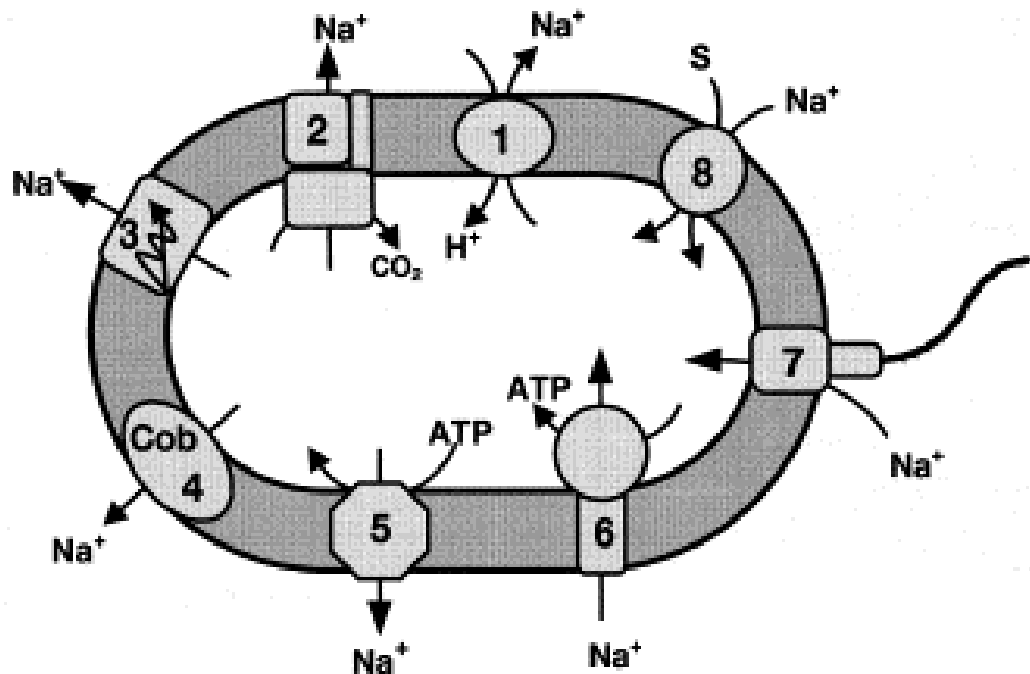


Figure 6 Schematic overview of bioenergetic processes coupled to Na⁺ circulation (Dimroth *et al.*, 2001). The electrochemical sodium ion gradient is generated either by a proton-driven Na⁺/H⁺ antiporter (1), by a decarboxylase (2), respiratory enzymes (3), *N*⁵-methyltetrahydromethanopterin:coenzyme M methyltransferase (4), or a V-type ATPase (5). The established sodium motive force then provides the energy for ATP synthesis by an F₁F₀ ATP synthase (6), for movement of flagellar motors (7), or for solute uptake (8). Please note that the systems depicted here are from different bacteria.

2.3.4 Na⁺-translocating ATPase

The Na⁺-translocating ATPase plays an important role in the maintenance of the Na⁺ ion concentration of cells by coupling the hydrolysis of ATP to the translocation of Na⁺ ions across the cell membrane. This enzyme is found in bacteria, fungi, yeast, algae, and halophytic higher plants (Glynn and Karlsh, 1975; Heefener and Harold, 1982; Balnokin and Popova, 1994; Shono *et al.*, 1996; Kaieda *et al.*, 1998). P-type ATPases were found in *Anabaena* sp. PCC 7120 (Neisser *et al.*, 1994), *Exiguobacterium aurantiacum* (Ueno *et al.*, 2000), *Heterosigma akashiwo* (Shono *et al.*, 1996) and *Tetraselmis viridis* (Popova *et al.*, 1998). V-type ATPases were found in *Caloramator fervidus* (Ubbink-Kok *et al.*, 2000) and *Enterococcus hirae* (Murata *et al.*, 2001). F-type ATPases were found in *Acetobacterium woodii* (Reidlinger and Muller, 1994), *Clostridium paradoxum* (Ferguson *et al.*, 2006); *Ilyobacter tartaricus* (Neumann *et al.*, 1998) and *Propionigenium modestum* (Laubinger and Dimroth, 1987).

2.4 Type of ATPases

There are at least three general types of transport ATPase. Several distinct types of ATP-dependent active transports have arisen, differing in structure, mechanism and localization in specific tissues and intracellular compartments (Nelson and Cox, 2000).

2.4.1 **P-type ATPases** are ATP-driven cation transporters that are reversibly phosphorylated by ATP as part of the transport cycle (Figure 7). All P-type transport ATPases have similarities in amino acid sequence, especially near the Asp residue that undergoes phosphorylation, and all are sensitive to inhibition by phosphate analog vanadate. Each is an integral protein with multiple membrane-spanning

regions in a single polypeptide. Bacteria use P-type ATPase to pump out toxic heavy metal ions such as Ca^{2+} , Cd^{2+} and Cu^{2+} (Kakinuma and Unemoto, 1985).

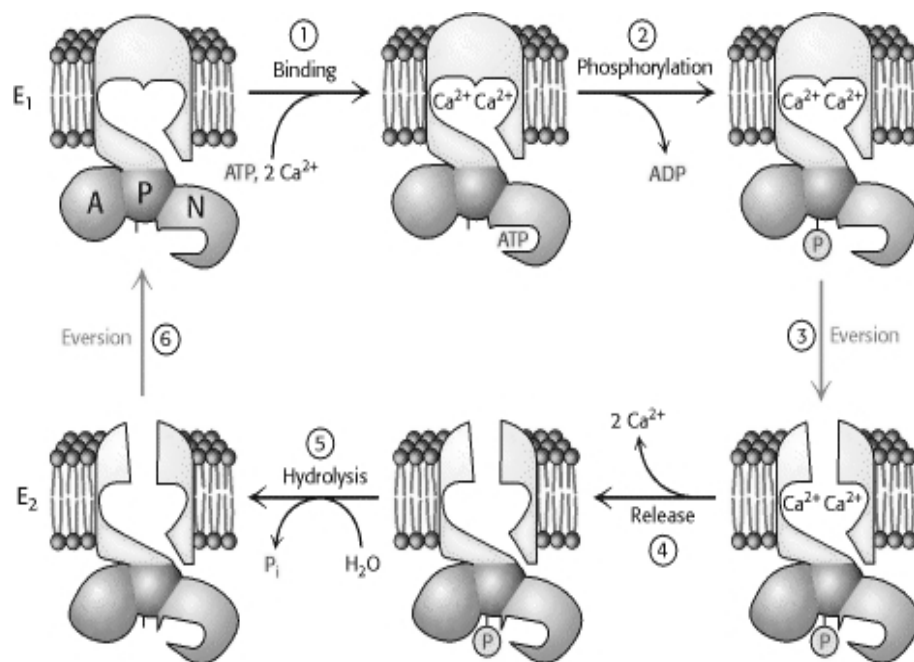


Figure 7 Mechanism of P-Type ATPase Action. The binding of Ca^{2+} and the phosphorylation of the ATPase (steps 1 and 2), illustrated here for the Ca^{2+} ATPase, lead to the eversion of the binding sites (step 3) and the release of Ca^{2+} to the luminal side of the membrane (step 4). Hydrolysis of phosphoaspartate (step 5) and eversion (step 6) reset the enzyme to its initial state (Berg *et al.*, 2002).

2.4.2 **V-type ATPases** (V for vacuolar) are also responsible for the acidification of intracellular compartments such as the golgi complex, lysosomes, endosomes, and secretory vesicles in many organisms. Structurally unrelated to P-type ATPase, the V-type ATPase are not inhibited by vanadate and do not undergo cyclic phosphorylation and dephosphorylation. All V-type ATPases contain 2 domains which have a similar complex structure. An integral (membrane-embedded) domain (V_0) translocates H^+ or Na^+ across the membrane. A peripheral domain (V_1) contains the ATP binding site and the catalytic site of ATPases which mediates the hydrolysis of ATP (Figure 8A). V-type ATPases are related in structure, function and mechanism, to a third family of F-type ATPase (Hilpert *et al.*, 1984; Kakinuma and Unemoto, 1985; Nishi and Forgac, 2002).

2.4.3 **F-type ATPases** play a crucial role in energy-conserving reactions in bacteria, chloroplasts and mitochondria. When the free energy of ATP hydrolysis is greater than the ionic electrochemical potential, F-type ATPases catalyze the uphill transmembrane transport of proton or sodium driven by ATP hydrolysis. In the reverse reaction, when the ionic electrochemical potential is greater than the free energy of ATP hydrolysis, the downhill proton or sodium transport drives ATP synthesis. In the second case, F-type ATPases are more appropriately named ATP synthases. The proton or sodium gradient in oxidative phosphorylation and photophosphorylation is established by others types of proton or sodium pumps powered by substrate oxidation or sunlight. F-type ATPases are multisubunit complexes that provide an interconnected integral membrane F_0 domain and an extra-membranous catalytic F_1 domain (Figure 8B). The integral membrane F_0 domain consists of three different polypeptides (a, b, and c) and mediates the transfer of protons or sodium across the membrane. The number of c subunits shows substantial

variation in different organisms. The hydrophilic F_1 domain consists of five different polypeptides with a stoichiometry of $\alpha_3\beta_3\gamma\delta\varepsilon$.

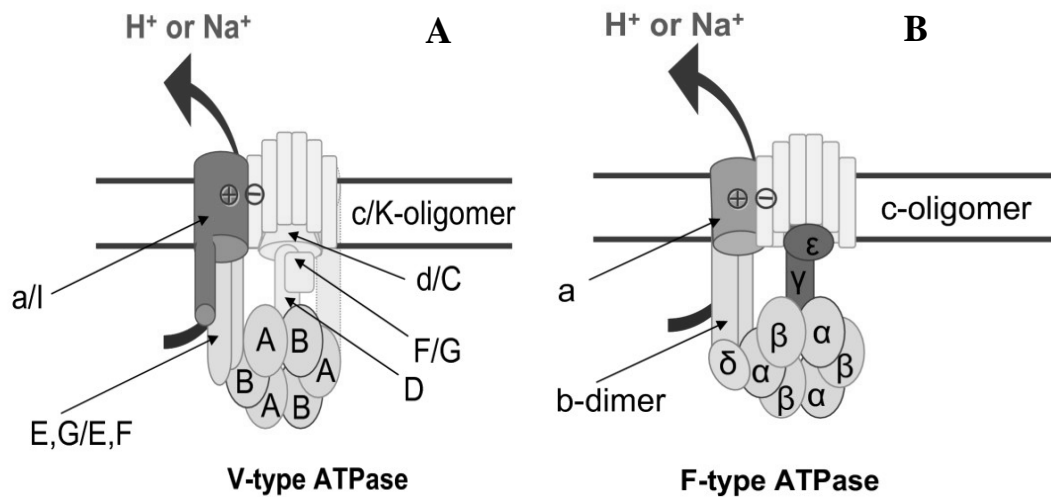


Figure 8 Structure and evolutionary relationships of F- and V-type ATPases (Mulikidjanian *et al.*, 2008). Orthologous subunits are shown by the same color and shape, and unrelated but functionally analogous subunits of the central stalk are shown by different colors and shapes. The subunits that show structural analogy but might not be homologous are shown by different but similar colors. The minimal, prokaryotic sets of subunits are depicted both for the F- and V-type ATPases. In the case of those V-ATPase subunits that are denoted by different letters in prokaryotes and eukaryotes, double notation is used: eukaryotic/prokaryotic.

2.5 Na⁺-dependent ATP hydrolysis (Na⁺-ATPase)

The previous report showed that a facultatively anaerobic alkaliphile, *Exiguobacterium aurantiacum*, possesses a P-type Na⁺-stimulated ATPase in the membrane (Ueno *et al.*, 2000). The purified ATPase exhibited an optimum pH for activity at around 9 and the enzyme activity was strongly inhibited by vanadate (50% inhibition observed at 3 μM) and forms an acylphosphate intermediate, suggesting a P-type ATPase. When the purified ATPase was reconstituted into soybean phospholipid vesicles, it exhibited ATP-dependent ²²Na⁺ uptake, which was completely inhibited by gramicidin. The reconstituted vesicles exhibited a generation of membrane potential (positive, inside). Therefore, the purified ATPase of *E. aurantiacum* is likely to be involved in an electrogenic transport of Na⁺.

Na⁺-activated ATPase was found in the plasma membrane of *Heterosigma akashiwo* (Wada *et al.*, 1989). Moreover, two phosphorylated intermediate forms of ATPase with molecular weight of 150 and 90 kDa were detected in the plasma membrane of *Heterosigma akashiwo* in the presence of both Mg²⁺ and Na⁺. ATP-dependent ²²Na⁺ transport into liposomes reconstituted with plasma membrane proteins from *Heterosigma akashiwo* was examined by Shono *et al.* (1996). The apparent K_m values for Na⁺ transport were 400 μM for ATP and 7 mM for Na⁺ and the transport of ²²Na⁺ was inhibited by an inhibitor of P-type ATPases.

Popova *et al.* (1998) showed that a primary Na⁺-pump has been demonstrated to operate in the plasma membrane (PM) of the marine unicellular alga *Tetraselmis (Platymonas) viridis*. ATP-driven ²²Na⁺ accumulation by the PM vesicles isolated from this alga occurred in the presence of the protonophore, CCCP, thus indicating a proton motive force (pmf)-independent fashion of Na⁺-pumping. The mechanism of

Na^+ transport across the plasma membrane of the marine microalga *Tetraselmis viridis* by Na^+ -ATPase is suggested to operate as an Na^+/H^+ exchanger which catalyzes an exchange of Na^+ for H^+ (Balnokin *et al.*, 2004) while Na^+ -ATPase in the halotolerant microalga *Dunaliella maritima* is suggested to operate as Na^+ uniport (Popova *et al.*, 2005).

V-type Na^+ -ATPase from *Enterococcus hirae* was purified and reconstituted into liposomes (Murata *et al.*, 2001). The reconstituted proteoliposomes exhibited ATP-driven $^{22}\text{Na}^+$ uptake. Inhibition by *N,N'*-dicyclohexylcarbodiimide (DCCD) of the Na^+ -ATPase activity and $\Delta\Psi$ -driven Na^+ uptake was prevented by the presence of Na^+ , suggesting that the Na^+ binding site overlaps with the DCCD-reactive site. The purified ATPase from *Acetobacterium woodii* is not inhibited by vanadate but is inhibited by nitrate, azide and *N,N'*-dicyclohexylcarbodiimide; indicating that the enzyme is of the F-type ATPase (Reidlinger and Muller, 1994). The enzyme activity is dependent on both MgATP and Na^+ with a K_m for Mg^{2+} and Na^+ of 0.4 mM. In addition, the enzyme has a pH optimum of pH 7-9 for their activity. The Na^+ transport into the lumen of proteoliposomes reconstituted with the purified ATPase from *A. woodii* was determined in the presence of ATP. The experiments demonstrate that the ATPase of *A. woodii* is a Na^+ -translocating F-type ATPase.

An anaerobic thermoalkaliphilic bacterium *Clostridium paradoxum* grows rapidly at pH 9.8 and 56°C. Under these conditions, growth is sensitive to the F-type ATP synthase inhibitor *N,N'*-dicyclohexylcarbodiimide (DCCD), suggesting an important role for this enzyme in the physiology of *C. paradoxum* (Ferguson *et al.*, 2006). The purified enzyme (30-fold purification) displayed the typical subunit pattern for an F-type ATP synthase but also included the presence of a stable

oligomeric *c*-ring that could be dissociated by trichloroacetic acid treatment into its monomeric *c* subunits. Na⁺ stimulated activity of the purified ATPase and provided protection against inhibition by DCCD that was pH dependent. An artificially imposed chemical gradient of sodium ions drove ATP synthesis in inverted membrane vesicles in the presence of a transmembrane electrical potential that was sensitive to monensin.

The ATPase of *Ilyobacter tartaricus* was solubilized from the bacterial membranes and purified (Neumann *et al.*, 1998). *N,N'*-dicyclohexylcarbodiimide (DCCD) inhibited the ATPase activity while Na⁺ ions protected the enzyme from this inhibition. The ATPase was specifically activated by Na⁺ or Li⁺ ions, markedly at high pH. The proteoliposomes reconstituted with the purified enzyme catalyzed the ATP-dependent transport of Na⁺, Li⁺, or H⁺. Proton (H⁺) transport was specifically inhibited by Na⁺ or Li⁺ ions, suggesting a competition between these alkali ions and protons for binding and translocation across the membrane. From the above results, *I. tartaricus* ATPase was characterized as a new member of the family of F-type ATPases, which use Na⁺ as the physiological coupling ion for ATP synthesis.

The ATPase of *Propionigenium modestum* was extracted from the membranes with Triton X-100 or by incubation with EDTA at low ionic strength (Laubinger and Dimroth, 1987). The ATPase in the Triton extract was highly sensitive to *N,N'*-dicyclohexylcarbodiimide (DCCD) but not to vanadate. These properties are characteristics for enzymes of the F-type ATPase. Sodium ion specifically activated the ATPase activity about 15-fold. The proteoliposomes reconstituted with the purified ATPase catalyzed an ATP-dependent Na⁺ accumulation that was stimulated to the same extent by dissipating the membrane potential with valinomycin or with the uncoupler carbonylcyanide-*m*-chloro phenylhydrazone. These results indicating

that the transport of Na^+ is a primary event, not a secondary event involving the intermediate formation of a proton gradient (Dimroth, 1992).

The Na^+ -ATPase of *Streptococcus faecalis* is an inducible enzyme that is produced only when the cells are grown in medium rich in Na^+ . Cells grown in medium lacking sodium ion would then be unable to expel sodium. *S. faecalis* was proposed to produce two systems for Na^+ extrusion: a secondary Na^+/H^+ antiporter, which appears to be constitutive, and an inducible primary sodium pump (Na^+ -ATPase) (Kakinuma, 1987). Moreover, *S. faecalis* lives in an environment of fluctuating pH (pH 6 to 10). At acidic pH, the generation of a proton motive force is large enough to drive a Na^+/H^+ antiporter and other proton-linked transport systems. The proton motive force is drastically decreased at pH above 8 (Kobayashi, 1982). At pH 10, the Na^+/H^+ antiporters cannot operate under these conditions, and the induction of the sodium ATPase is required for the growth, presumably because under these conditions the antiporter is not sufficient to exclude Na^+ from the cytoplasm. Thus, the existence of two systems for sodium extrusion allows the organism to cope with an environment subject to fluctuations in both ionic composition and pH.

CHAPTER III

MATERIALS AND METHODS

3.1 Materials

3.1.1 Equipments

Autoclave:

- Model HA-30, Hirayama Manufacturing Cooperation, Japan
- Model MLS-3020, Sanyo Electric Co. Ltd., Japan

Autopipette: Pipetman, Gilson, France

Balances:

- Model AB204-S, Mettler Toledo, Switzerland
- Model LC 620S, Sartorius, USA

Bead-beater: Model 1107900, Biospec Products, USA

Centrifugal concentrator: Model VC-12S, TaiTec, Japan

Centrifuge, refrigerated centrifuge: Model J-21C, Beckman Instrument Inc, USA

DNA electrophoresis chamber: Gelmate 2000, Toyobo, Japan

Fluorescence spectrophotometer: Model LS55, Perkin Elmer, USA

FPLC AKLA Amersham Pharmacia Biotech unit: GE Healthcare, USA

Column: Amersham Biosciences HR 10/30

Detector: UPC-900

Pump: P-920

Fraction collector: Frac-900

FPLC packing column: Superose 6, GE Healthcare, USA

French press cell disrupter: Thermo Electron Corporation, USA

Gel documentation system: ImageMaster VDS, Pharmacia Biotech, USA

GeneAmpPCR system: Model 2400, Perkin Elmer, USA

Genetic analyzer: ABI PRISM 3100-Avant, Hitachi, Japan

Hot air oven: Isotemp oven, Fisher Scientific, USA

Hot plate/stirrer: PMC, PMC Industries, Singapore

Incubator shaker: Model 1H-100, Gallenkamp, UK

Ion analyzer: Model PIA-1000, Shimadzu, Japan

Laminar flow: Model BVT-124, International Scientific Supply Co. Ltd., Thailand

Light microscope: Seek, Seek Inter Co. Ltd., Thailand

Luminometer: Model GloMaxTM 20/20, Promega, USA

Microcentrifuge, refrigerated centrifuge:

- Model 5417C, Eppendorf, Germany
- Hettich Zentrifugen Mikro 22 R, Hettich Laborapparate, Germany

Minicentrifuge: Qualitron DW-41, Qualitron Corporation, Pakistan

Microwave: Model edition I, Daewoo Electronics America, USA

pH meter: SevenEasy, Mettler Toledo, Switzerland

Platform rocker: Model SSL4, Stuart, Barloworld Scientific Ltd., UK

Power supply: Model EC135-90, E-C Apparatus Corporation, USA

Protein electrophoresis unit:

- Mini-protein II cell, Bio-Rad, USA
- Vertical electrophoresis systems, Cleaver Scientific, UK

Pump (vacuum dry): Model DOA-V112-BN, GAST, GAST Manufacturing Inc., USA

Scintillation counters: LS6500 Multi-Purpose Scintillation Counter, Beckman Coulter, USA

Spectrophotometer:

- Model DU800, Beckman Coulter, USA
- NanoVue, GE Healthcare, USA

Ultracentrifuge: OPTIMA™ L-100 XP, Beckman Coulter, USA

Vortex: Touch mixer model 232, Fisher Scientific, USA

Water bath:

- Model G-76, New Brunswick Scientific Co. Inc., USA
- Model WB29, Memmert, Germany

3.1.2 Chemicals

Acetic acid: BDH, England

Acetone: Merck, Germany

Acridine orange: BDH Chemicals Ltd., England

Acrylamide: Merck, Germany

Adenosine-5'-diphosphate (monopotassium salt): Sigma, USA

Adenosine-5'-triphosphate (Tris salt): Sigma, USA

Agar: Scharlau Microbiology, Spain

Agarose: Seakem, USA

Amiloride: Sigma, USA

Ammonium chloride: Sigma, USA

Ammonium molybdate: Sigma, USA

Ammonium sulfate: Ajax Finechem, Australia

Ammonium persulfate: Merck, Germany

Ascorbic acid: Sigma, USA

Bacto tryptone: Difco, USA

Benzamidine: Sigma, USA

1,4-bis(5-phenyl-2-oxazolyl) benzene (POPOP): BDH, England

Bovine serum albumin (BSA): Sigma, USA

5-bromo-4-chloro-3-indolyl-b-D-galactopyranoside (X-gal): Fermentas, USA

5-Bromo-4-chloro-3-indolyl phosphate (BCIP): Sigma, USA

Bromophenol blue: Sigma, USA

Calcium chloride: BDH, England

Carbonyl cyanide *m*-chlorophenylhydrazone: Sigma, USA

Chloroform: Wako, Japan

Citric acid: Ajax Finechem, Australia

Cobalt nitrate: Ajax Finechem, Australia

Coomassie brilliant blue G-250: Sigma, USA

Coomassie brilliant blue R-250: Sigma, USA

Copper acetate: BDH, England

Copper (II) sulfate: Ajax Finechem, Australia

N, N'- dicyclohexylcarbodiimide: Sigma, USA

Dimethylformamide (DMF): Sigma, USA

Dimethyl sulfoxide (DMSO): Sigma, USA

2,5-Diphenyloxazole (PPO): BDH, England

Dipotassium hydrogen phosphate: Scharlau Chemie S.A., Spain

Dithiothreitol (DTT): Sigma, USA

Ethanol: Scharlau Chemie S.A., Spain

Ethidium bromide: Sigma, USA

Ethylamine: Sigma, USA

Ethylenediaminetetraacetic acid (EDTA): Fluka, Switzerland

Ferric sulfate: BDH, England

Folin-Ciocalteu's reagent: Carlo Erba Reagenti, France

Fructose: Sigma, USA

Glucose: Fluka, Switzerland

Glycerol: Scharlau Chemie S.A., Spain

Gramicidine D: Sigma, USA

N-2-hydroxyethylpiperazine-*N'*-2-ethanesulfonic acid (HEPES): Sigma, USA

Isoamylalcohol: Sigma, USA

Isopropanol: Sigma, USA

Isopropyl- β -D-thiogalactopyranoside (IPTG): Sigma, USA

Lithium chloride: Ajax Finechem, Australia

Manganese chloride: Ajax Finechem, Australia

Magnesium sulfate: Scharlau Chemie S.A., Spain

Magnesium chloride: Ajax finechem, Australia

Mercaptoethanol: Sigma, USA

Methanol: Scharlau Chemie S.A., Spain

Monensin: Sigma, USA

p-Nitro blue tetrazolium chloride (NBT): Wako, Japan

N-Ethylmaleimide (NEM): Sigma, USA

N,N,N',N'-tetramethylene ethylene diamine (TEMED): BDH, England

o-Nitrophenyl-beta-galactopyranoside: Wako, Japan

Ouabain: Sigma, USA

Oxonol VI: Fluka, Switzerland

Phenazine methosulfate (PMS): Wako, Japan

Phenol: Merck, Germany

Piperacillin: MP Biomedicals Inc., France

Phenol: BDH, England

Phosphatidylcholine (Sigma; Type II S): Sigma, USA

Phosphoric acid: Scharlau Chemie S.A, Spain

Polyethylene glycol 6000: Fluka, Switzerland

Potassium chloride: Ajax Finechem, Australia

Potassium cyanide: Sigma, USA

Potassium dihydrogen phosphate: Scharlau Chemie S.A., Spain

Potassium ferricyanide: Sigma-Aldrich, USA

Potassium nitrate: BDH, England

Potassium thiocyanate: Sigma, USA

Sodium acetate: BDH, England

Sodium azide: Sigma, USA

Sodium bicarbonate: BDH, England

Sodium carbonate: BDH, England

Sodium chloride: Carlo Erba, France

Sodium cholate: Sigma, USA

Sodium citrate: Sigma, USA

Sodium dodecyl sulfate: Sigma, USA

Sodium fluoride : Sigma, USA

Sodium ionophore: Fluka, Switzerland

Sodium nitrate: BDH, England

Sodium nitrite: BDH, England

Sodium orthovanadate: Sigma, USA

Sodium thiosulfate: Sigma, USA

Sodium-22: Amersham Biosciences, USA

Sorbitol: Ajax Finechem, Australia

Succinate: Sigma, USA

Sucrose: Sigma, USA

Sulfuric acid: BDH, England

Toluene: BDH, England

Tributyltin chloride: Wako, Japan

Tris (hydroxymethyl) aminomethane: USB, USA

Triton X-100: Packard, USA

Tween-20: BIO-RAD, USA

Urea: Sigma, USA

Valinomycin : Sigma, USA

Xylene cyanol FF : Sigma, USA

Yeast extract: Scharlau Microbiology, Spain

Zinc sulfate: Ajax Finechem, Australia

3.1.3 Enzymes

Adenosine-5'-triphosphatase (ATPase): Sigma, USA

Alkaline phosphatase (calf intestine): Takara, Japan

AmpliTaq Gold: Roache, USA

KOD plus: Toyobo, Japan

Lysozyme: Sigma, USA

LA Taq: TaKaRa, Japan

Restriction enzymes: TaKaRa, Japan

RNase A: US Biological, USA

3.1.4 Antibiotics

Ampicillin: Sigma, USA

Chloramphenicol: Sigma, USA

Streptomycin: Sigma, USA

3.1.5 Kits

Anti-6X-histidine purified mouse monoclonal IgG₁: R&D Systems, Japan

Anti-mouse IgG (H&L) (AP-linked antibody): Cell Signaling Technology, USA

BigDye terminator v3.1 cycle sequencing kit: Applied Biosystems, USA

Blunting kination ligation kit: Takara, Japan

DNA ligation kit: TaKaRa, Japan

DNA marker: 1 kb GeneRuler™ (#SM 0311), Fermentas, USA

DNA marker: 100 bp GeneRuler™ (#SM 0241), Fermentas, USA

ENLITEN rLuciferas/Luciferin reagent: Promega, USA

Fast Plasmid Mini Kit: Eppendorf, USA

GeneAmp dNTP mix: Roache, USA.

Lamda DNA: Takara, Japan

Ligation high: Toyobo, Japan

LMW calibration kit for SDS electrophoresis: Amersham Biosciences, England

Monoclonal anti-polyhistidine antibody: R & D systems, Japan

Precision plus protein dual color standards, Bio-Rad, USA

TA cloning kit: Invitrogen, USA

3.1.6 Supplies

Cellulose acetate membrane: Whatman International, England

Micropure-EZ: Millipore Corporation, USA

Midisart 2000 vent filter: Sartorius, Germany

Polyvinylidene Fluoride membrane (PVDF): Whatman International, England

SuprecTM-01: Takara, Japan

Whatman No.1 filter paper: Whatman International, England

X-ray film: X-Omat XK-1, Eastman Kodak, USA

3.1.7 Organisms

The three organisms, namely *Aphanothece halophytica*, *Escherichia coli* and *Synechococcus* sp. PCC 7942 were used in this study.

3.1.7.1 *Aphanothece halophytica* was originally isolated from solar lake in Israel (Geitler, 1932; Stainer *et al.*, 1971). The organism was kindly provided by Professor. Dr. Teruhiro Takabe of the Research Institute of Meijo University, Japan.

3.1.7.2 *Escherichia coli* strains were obtained from Professor Dr. Teruhiro Takabe of the Research Institute of Meijo University, Japan.

Strain DH5 α (Woodcock *et al.*, 1989), genotype (F⁻, ϕ 80dlacZ Δ M15, Δ (lacZYA-argF)U169, *deoR*, *recA1*, *endA1*, *hsdR17*(rk⁻, mk⁺), *phoA*, *supE44*, λ^- , *thi-1*, *gyrA96*, *relA1*) was used as a host for plasmid propagation.

Strain DK8 (Moriyama *et al.*, 1991), a *unc* gene-defective mutant (deficient in ATP synthase), genotype (1100 Δ [*uncB-uncC*] *ilv::Tn10*) was used a host for expression of *ApNa⁺-atp* operon.

Strain TO114 ($\Delta nhaA$, $\Delta nhaB$, $\Delta chaA$), a salt-sensitive mutant, was used as a host for expression of *ApNa⁺-atp* operon.

3.1.7.3 *Synechococcus* sp. PCC 7942 (wild type strain) is a freshwater cyanobacterium, and was obtained from Professor Dr. Teruhiro Takabe of the Research Institute of Meijo University, Japan.

3.1.8 Plasmids

The three plasmids, namely pBluescript® SK (+), pTrcHis2C and pUC303 vectors were used in this study. Circle maps are shown in APPENDIX A, B and C, respectively.

3.1.8.1 pBluescript® SK (+) (Toyobo, Japan): vector for cloning; β -galactosidase α -fragment coding sequence (*lacZ'*) is present in this phagemid but the coding sequence is interrupted by the large polylinker. Phagemid having no inserts in the polylinker will produce blue colonies in *E. coli* while phagemid that have inserts will produce white colonies using the same strain, because the inserts disrupt the coding region of the *lacZ* gene fragment.

3.1.8.2 pTrcHis2C (Invitrogen, USA): vector for expression of recombinant proteins containing C-terminal 6xHis tags in *E. coli*. Moreover, this vector contains ampicillin resistance gene which allows selection of the plasmid in *E. coli*.

3.1.8.3 pUC303 (obtained from Professor Dr. Teruhiro Takabe of the Research Institute of Meijo University, Japan: *E. coli/Synechococcus* shuttle vector for expression of recombinant proteins; this vector contains chloramphenicol resistance gene which allows selection of the plasmid in cyanobacterium *Synechococcus* sp. PCC 7942.

3.1.9 Oligonucleotides

Table 1 PCR primers for PCR amplification of *ApNa⁺-atp* operon from *A. halophytica* genomic DNA

Primer name	Primer sequences	Amplified fragment length (bp)
ApATPase BamHI-F	5'-GGATCCGGAGTTAGGGGCGATGGTACAAT-3'	6,854
ApATPase Sall-R	5'-GTCGACGGATGAAGGATGATCACTC-3'	

Table 2 PCR primers for sequencing *ApNa⁺-atp* operon

Primer name	Primer sequences
M13-F	5'-GTAAAACGACGGCCAGT-3'
400-F1	5'-GCAACATACGACCTCATCAG-3'
940-F2	5'-GTATGTGCCTGCGGATGATT-3'
1522-F3	5'-GTCCTGTTACCGCAACACAT-3'
2113-F4	5'-CAACCGAAGAAGAGTCAGAG-3'
2740-F5	5'-GGCGTATCGAATGTGTTGAC-3'
3243-R	5'-ATCGCGCCTAAGCCAATGGT-3'
3783-R0	5'-AAGCCTCCTGCCATTGTTCC-3'
4308-R1	5'-GTGACCAGTTACCAGTTACC-3'
4826-R2	5'-CTCGTGCTGGACGTTCTGTG-3'
5328-R3	5'-GTTGCTCGCTCTAGCAATCG-3'
5923-R4	5'-CAGTTGCGTGGTTGTGTTCT-3'
6500-R5	5'-ATAGGTGGTTCCGGTACTGG-3'
M13-R	5'-CCTTTGTCGATACTGGTACT-3'

Table 3 PCR primers for PCR amplification of chloramphenicol resistance gene (Cmr) in *E. coli/Synechococcus* shuttle vector pUC303

Primer name	Primer sequences	Amplified fragment length (bp)
pACYCcm1-F	5'-ATCGGCACGTAAGAGGTTCCAAC-3'	800
pACYCcm1-R	5'-GCTTTCGAATTTCTGCCATTCATC-3'	

Table 4 PCR primers for PCR amplification of *atpG* encoding γ subunit of *ApNa⁺-atp* operon

Primer name	Primer sequences	Amplified fragment length (bp)
gammaXbaI-F	5'-TTATTAACGCCTCTAGAAAGTGAA-3'	520
gammaSalI-R	5'-GTCGACGGATGAAGGATGATCACTC-3'	

3.2 Methods

3.2.1 Methods for purification, reconstitution and characterization of ATPase from *A. halophytica*

3.2.1.1 Growth condition for *A. halophytica*

A. halophytica cells were grown photoautotrophically in BG11 medium supplemented with 18 mM NaNO₃ and Turk Island salt solution as described previously (Incharoensakdi and Waditee, 2000) (Appendix D) except that the NaCl concentration of the culture medium was adjusted to the desired concentration. Cells were grown in cotton-plugged 250-ml Erlenmeyer flasks containing 100 ml of medium on a rotary shaker with 160 rpm at 30 °C under continuous illumination by cool white fluorescence tubes of 25 $\mu\text{mol photon m}^{-2} \text{s}^{-1}$. For large scale cultivation, a

2-L Erlenmeyer flask containing 1 L of medium was used and the aeration of the culture was provided in the form of filtered air bubbles by an air pump.

3.2.1.2 Preparation of inverted membrane vesicles from *A. halophytica*

Cells at exponential growth phase were harvested by centrifugation at 9,800 g for 20 min and washed three times with 20 mM Tris-HCl pH 7.6 containing 1.0 M sucrose. The collected cells were resuspended in extraction buffer (20 mM Tris-HCl pH 7.6, 1 mM DTT, 4 mM benzamidine and 5 mM MgCl₂) with ratio (g ml⁻¹) of 1.0-2.0. After homogenization, the cells were disrupted by two passages through a French pressure at 400 kPa. Unbroken cells and large debris were removed by centrifugation at 9,800 g for 15 min. The inverted membrane vesicles were sedimented by centrifugation at 100,000 g for 30 min and resuspended in 50 mM HEPES-KOH pH 7.0 to a final protein concentration of 1 mg ml⁻¹.

3.2.1.3 Solubilization of membrane-bound ATPase

ATPase in inverted membrane vesicles prepared as described in section 3.2.1.2 was solubilized by incubation of the membrane vesicles with sodium cholate at a final concentration of 7 mM. After 30 min with occasional mixing at 0 °C, the solubilized membrane proteins were isolated by centrifugation at 100,000 g for 1 h. The solubilized ATPase was supplied with MgCl₂ to a final concentration of 50 mM.

3.2.1.4 Polyethylene glycol 6000 precipitation

Contaminating proteins were precipitated with PEG 6000 (2% w/v). The precipitate was removed by centrifugation at 40,000 g for 15 min. After that, PEG 6000 (7% w/v) was added into the supernatant to precipitate the ATPase. The pellet

was collected by centrifugation at 40,000 g for 15 min and dissolved in 1 ml of 50 mM Tris-HCl pH 7.6 containing 1 mM DTT and 0.1 mM benzamidine. Insoluble material was removed by centrifugation at 3,800 g for 10 min.

3.2.1.5 Gel filtration chromatography

Two hundred microliter of supernatant containing ATPase (0.4 to 0.5 mg protein) was subjected to gel chromatography with a superose 6 HR10/30 column pre-equilibrated with 50 mM Tris-HCl pH 7.6, 150 mM KCl, 5 mM MgCl₂ and 0.4 mM sodium cholate. Each two ml of collecting fraction was collected and measured for ATP hydrolysis activity. The active ATPase fractions were pooled, dialyzed by 12,000-14,000 MW cut-off dialysis bag, concentrated by aquasorb and kept at - 20 °C.

3.2.1.6 Determination of ATP hydrolysis activity

The ATP hydrolysis activity was assayed by measuring the release of inorganic phosphate resulting from the hydrolysis of ATP according to the method of Koyama (1983) with slight modification (Appendix E). The reaction mixture (1 ml) contained 20 mM Tris-HCl pH 7.6, 5 mM MgCl₂, 10 mM NaCl, and ATPase (30 µg protein). The reaction was started by addition of 4 mM ATP (Tris salt). After incubation at 37 °C for 15 min, proteins were precipitated with 5% TCA and centrifuged 3,800 g for 10 min. The supernatant was used for the determination of inorganic phosphate as described by Lebel (1978) with slight modification. To 1.0 ml of the supernatant, 3.0 ml of solution A, 0.1 ml of solution B and 0.01 ml of solution C were added and mixed. Twenty minutes later, the absorbance was read at 850 nm

using a spectrophotometer Beckman DU 800 and the Pi content was calculated by comparison to the standard curve of Pi (Appendix F).

3.2.1.7 Determination of protein

Protein contents were determined by the protein-dye binding method of Bradford (1976) using bovine serum albumin as standard (Appendix G). The sample (10 μ l) was diluted with deionized water to 90 μ l and 1.0 ml of Bradford's reagent was added and rapidly mixed. The mixture was incubated at 30°C for 10 minutes.

Finally, the absorbance was measured at 595 nm.

3.2.1.8 Sodium dodecyl sulfate polyacrylamide gel electrophoresis (SDS-PAGE)

Sodium-dodecyl-sulfate polyacrylamide gel electrophoresis (SDS-PAGE) was performed as described by Laemmli (1970) (Appendix H). Samples (30 μ g protein) were resuspended in sample buffer at a 4:1 ratio. The mixture was heated for 5 minutes in boiling water before loading on a 12% separating gel. The electrophoresis buffer was used for gel running at constant current 40 mA. Electrophoresis was run continuously until the dye front reaching the bottom of the gel. The gel was stained with staining solution for 3 hrs and, then destained with destaining solution at room temperature overnight.

3.2.1.9 Sample preparation and LC-MS/MS analysis

Prior to gel slicing, the gels were washed twice in water. After washing, the subunit c band on SDS-PAGE (Lane 5) was cut with clean scalpel and digested in-gel with trypsin (Appendix I) before analysis by liquid chromatography mass

spectrometry (LC-MS/MS) which performed as a service at Proteomics Laboratory (BIOTEC, Pathumthani, Thailand). The ion spectra were recorded on an ESI-Q-TOF mass spectrometer (Waters Corporation) and determined peptide molecular mass and amino acid sequences by using Mascot program (www.matrixscience.com). Sequence-similarity of peptide was searched via the National Center for Biotechnology Information (NCBI) database.

3.2.1.10 Preparation of reconstituted proteoliposomes

Reconstituted proteoliposomes were prepared as described by Neumann *et al.* (1998) with slight modification. A suspension of 60 mg phosphatidylcholine (Sigma; Type II S) in 1.9 ml of 50 mM Tris-HCl pH 7.6, 1 mM MgCl₂, 1 mM DTT and 5 mM sodium cholate was sonicated until the suspension was clear. The detergent was used as a disaggregating agent to aid membrane protein reconstitution. Purified ATPase (0.1 ml; 0.3 mg protein) was added to the suspension and the mixture was incubated at 25 °C for 10 min with occasional shaking, then frozen in liquid nitrogen and thawed at 0 °C. The proteoliposomes were sonicated twice for 5 s each and diluted 200-fold with 50 mM Tris-HCl pH 7.6. The proteoliposomes were collected by centrifugation at 100,000 g for 60 min and resuspended in 0.3 ml of 5 mM Tris-HCl pH 7.6 containing 1 mM MgCl₂.

3.2.1.11 Determination of Na⁺ uptake into proteoliposomes

The ²²Na tracer was used for Na⁺ uptake measurement. The proteoliposomes (30 µg protein) were suspended in 60 µl of 20 mM Tris-HCl pH 7.6 containing 5 mM MgCl₂ and 5.7 mM ²²NaCl (80 µCi mmol⁻¹). The uptake reaction was started by the addition of 4 mM ATP (Tris salt). After equilibration for 30 min, 50 µl of the reaction

mixture was filtered through a 0.2 μm cellulose acetate membrane. The membrane filter was washed once with 1 ml of 20 mM Tris-HCl pH 7.6 and then kept in 1.5 ml eppendorf tube. A 1-ml aliquot of Scintillation fluid was added before measuring the radioactivity with a liquid scintillation counter (Appendix J). Ionophores and inhibitors were added 10 min before starting the reaction with ATP.

3.2.1.12 Detection of H⁺ efflux from proteoliposomes

Proton (H⁺) efflux from proteoliposomes was determined as ATP-dependent alkalization of the proteoliposome lumen. The assay was performed at room temperature by monitoring the changes in fluorescence intensity of the ΔpH probe acridine orange with a fluorescence spectrophotometer set at 493 nm (excitation) and 525 nm (emission) (Blumwald *et al.*, 1984; Allakhverdiev *et al.*, 2000). The assay was performed in 1 ml of a reaction mixture containing 0.5 M sorbitol, 10 mM Hepes-Tris buffer pH 7.6, 1 μM acridine orange, 100 mM NaCl, and proteoliposomes (25 μg protein). After 15 min incubation of proteoliposomes in the medium, the reaction was initiated by the addition of ATP (Tris salt) at 4 mM.

3.2.1.13 Detection of membrane potential

ATP-dependent formation of the membrane potential across proteoliposomes was detected by monitoring the differential absorbance changes (621/582 nm) of the membrane potential probe oxonol VI using a dual wavelength spectrophotometer as described by Popova *et al.* (2005) with slight modification. The reaction mixture (1 ml) contained 0.4 M sucrose, 20 mM Hepes-Tris buffer pH 7.6, 1 mM MgSO₄, 3 μM oxonol VI and proteoliposomes (25 μg of protein). The reaction mixture was incubated for 15 min at room temperature. The generation of membrane potential was

initiated by supplementing the reaction mixture with ATP (Tris salt) and NaCl at final concentrations of 4 and 100 mM, respectively.

3.2.2 Methods for genomic DNA extraction and cloning of *ApNa⁺-atp* operon from *A. halophytica*

3.2.2.1 *A. halophytica* genomic DNA extraction

A. halophytica grown in modified BG11 medium (Appendix D) plus 0.5 M NaCl under continuous fluorescent white light was used for chromosomal DNA extraction. Cells at exponential growth phase were harvested by centrifugation at 8,000 g for 15 min at 4 °C, washed twice with SET buffer (20% sucrose, 50 mM EDTA and 50 mM Tris-HCl, pH 7.6). Pellet was frozen at -20 °C for 2 hours, thawed at 65 °C for 10 min and resuspended in SET buffer. Cells were lysed by using lysozyme (final concentration of 0.5 mg ml⁻¹), incubated at 37 °C for 30 min with gentle shaking. Subsequently, SDS and RNase were added at final concentration of 0.5% and 0.25 mg ml⁻¹, respectively. After an incubation at 37 °C for 3 hrs, proteinase K was added at final concentration of 0.25 mg ml⁻¹ and further incubated for 30 min. The mixture was extracted once with equal volume of phenol:chloroform:isoamylalcohol (25:24:1), mixed gently and centrifuged at 12,000 g for 5 min at 25 °C. The aqueous layer was collected and re-extracted at least 3 times with equal volume of phenol:chloroform:isoamylalcohol. High molecular weight DNA was precipitated by adding 2 volumes of absolute ethanol and chilled at -20 °C for 1-2 hr. Chromosomal DNA was collected by centrifugating at 12,000 g for 5 min at 4 °C and washed once with 70% ethanol. Chromosomal DNA was allowed to dry under vacuum and resuspended with TE buffer, pH 8.0 (10 mM Tris-HCl, pH 8.0 and

1 mM EDTA). This DNA solution was then stored at -20 °C until use. To determine concentration and purity of chromosomal DNA, sample was diluted with TE buffer and checked by measuring the ratio of OD₂₆₀/OD₂₈₀.

3.2.2.2 Cloning of *ApNa⁺-atp* operon

A. halophytica genomic DNA prepared from section 3.2.2.1 was used as a template DNA for isolating *ApNa⁺-atp* operon. The coding region of *ApNa⁺-atp* was amplified by PCR using a primer set (Table 1). The forward primer, ApATPaseBamHI-F, contains *Bam*HI site. The reverse primer, ApATPaseSalI-R, contains *Sal*I restriction site. The PCR amplification was performed as follows: 35 cycles of 30 s at 94 °C, 30 s at 52 °C and 7 min at 68 °C (Appendix K). The 6,854-bp PCR product containing 6,832-bp coding region obtained from PCR reaction was concentrated and primers were eliminated by SuprecTm-O2 followed by ligation into cloning vector, pBluescript[®] II SK (+) digested at *EcoRV* site, by ligation kit. The resulting plasmid, pBSK+*-ApNa⁺-atp*, was transformed firstly into *E. coli* DH5 α cells by heat shock method (Appendix L). The positive clones were selected on LB agar (Appendix M) containing 100 μ g ml⁻¹ ampicillin, allowed to grow in LB medium at 37 °C for 16 hrs and the plasmids were extracted by alkaline lysis method (Appendix N). Insert fragment of an expected size 6,854 kb was sequenced with 14 primers as shown in Table 2.

3.2.3 Methods for construction of expression plasmids containing *ApNa⁺-atp* operon and IPTG-inducible *trc* promoter

3.2.3.1 Construction of pTrcHis2C-*ApNa⁺-atp*

The pBSK⁺-*ApNa⁺-atp* was double digested with *Bam*HI and *Sal*I. The cohesive end fragment was ligated into *Bam*HI and *Sal*I site of the digested pTrcHis2C expression vector. The resulting plasmid, pTrcHis2C-*ApNa⁺-atp*, encoding *ApNa⁺-ATPase* fused in frame to six histidine residues, was transformed firstly into *E. coli* DH5 α cells by heat shock method (Appendix L). The positive clones were selected on LB agar (Appendix M) containing 100 $\mu\text{g ml}^{-1}$ ampicillin, allowed to grow in LB medium at 37 °C for 16 hrs and the plasmids were extracted by alkaline lysis method (Appendix N).

pTrcHis2C-*ApNa⁺-atp*, which was double digestion with *Bam*HI and *Sal*I, was confirmed from the mobility on agarose electrophoresis of DNA fragments (Appendix O). The recombinant plasmid was re-extracted and then transformed to the *unc* deletion mutant, *E. coli* DK8 and the salt-sensitive mutant, *E. coli* TO114 cells.

3.2.3.2 Construction of pUC303-*ApNa⁺-atp*

For the construction of expression plasmid pUC303-*ApNa⁺-atp*, pTrcHis2C-*ApNa⁺-atp* which contains *trc* promoter was digested with *Sca*I and then ligated into the *E. coli*/*Synechococcus* shuttle vector pUC303 at *Sal*I-digested and blunt-ended site. The resulting plasmid, designated as pUC303-*ApNa⁺-atp*, was transformed firstly into *E. coli* DH5 α cells by heat shock method (Appendix L). The positive transformants were selected on LB agar (Appendix M) containing 10 $\mu\text{g ml}^{-1}$ chloramphenicol and 100 $\mu\text{g ml}^{-1}$ streptomycin and allowed to grow in LB medium at

37 °C for 16 hrs and the plasmids were extracted by alkaline lysis method (Appendix N).

The plasmid, pUC303-*ApNa⁺-atp*, extracted from *E. coli* DH5 α cells was then transformed into the salt-sensitive mutant, cyanobacterium *Synechococcus* sp. PCC 7942 cells (Appendix T). The transformants were grown in BG11 medium (Appendix D) at 30 °C for 24 hrs and after that the cells were spread on BG11 agar containing 50 $\mu\text{g ml}^{-1}$ streptomycin until green colonies appear. The positive clone was picked up and grown in BG11 liquid medium containing 50 $\mu\text{g ml}^{-1}$ streptomycin with air bubble at 30 °C for 7 days and the plasmid was extracted by alkaline lysis method with slightly modification (Appendix U). The obtained plasmid was amplified and checked by PCR technique with the chloramphenicol resistance- and *atpG* (encoding γ subunit of *ApNa⁺-atp* operon)-specific primers as shown in table 3 and 4, respectively. The PCR amplification for chloramphenicol resistance gene was performed in reaction mixture (Appendix V) as follows: 35 cycles of 30 s at 94 °C, 30 s at 55 °C and 1 min at 72 °C. The obtained fragment size was approximately 800 bp. The PCR amplification for *atpG* was performed in reaction mixture (Appendix W) as follows: 35 cycles of 30 s at 94 °C, 30 s at 51 °C and 40 s at 72 °C. The obtained fragment size was approximately 520 bp.

3.2.4 Methods for characterization of biochemical properties and physiological functions of ApNa⁺-ATPase expressed in *E. coli* DK8 and freshwater cyanobacterium *Synechococcus* sp. PCC 7942 cells

3.2.4.1 Complementation test of ApNa⁺-atp operon

In *E. coli* DK8 (Δatp) and *E. coli* TO114 (salt-sensitive) mutants

E. coli DK8 and *E. coli* TO114 cells transformed with pTrcHis2C (empty vector transformants) and pTrcHis2C-ApNa⁺-atp (ApNa⁺-ATPase-expressing cells) were grown in LB medium containing 100 $\mu\text{g ml}^{-1}$ ampicillin at 37 °C for 16 hrs. *E. coli* DK8 transformants were tested for the ability to grow in LB medium (Appendix M), LB medium plus 0.2 M NaCl, LB medium plus 0.5 M NaCl. *E. coli* TO114 transformants were tested for the ability to grow in LBK medium (Appendix P), LBK plus 0.1 M NaCl, LBK plus 0.2 M NaCl. The IPTG (1 mM) was used to induce the ApNa⁺-atp expression under the *trc* promoter. The growth rate of both *E. coli* DK8 and TO114 were measured at various time intervals by spectrophotometer at 620 nm.

For complementation studies on agar plate, *E. coli* DK8 transformants were grown in LB medium containing 100 $\mu\text{g ml}^{-1}$ ampicillin at 37 °C for 16 hrs. Cells were plated onto a 1.5% M13 minimal agar plate (pH 7.0), containing 42 mM Na₂HPO₄, 22 mM KH₂PO₄, 8.5 mM NaCl, 2 mM MgSO₄, 15 μM thiamine, 0.1 mM CaCl₂, 50 $\mu\text{g ml}^{-1}$ each of isoleucine, leucine and valine, a carbon source (35 mM glucose or succinate), 100 $\mu\text{g ml}^{-1}$ ampicillin, and 1 mM IPTG. Plates were incubated at 37 °C for 2 days.

In a freshwater cyanobacterium *Synechococcus* sp. PCC 7942

Synechococcus sp. PCC 7942 cells transformed with pUC303 (empty vector transformants) and pUC303-*ApNa⁺-atp* (*ApNa⁺-ATPase*-expressing cells) were grown in BG11 medium (Appendix D) supplemented with 50 $\mu\text{g ml}^{-1}$ streptomycin at 30 °C for 7 days. The transformants were transferred into fresh BG11 medium containing various concentrations of NaCl (0–0.5 M) and seawater. The IPTG (0.5 mM) was used to induce the *ApNa⁺-atp* expression under the *trc* promoter. The growth rate was measured at various time intervals by spectrophotometer at 730 nm.

3.2.4.2 Measurement of Na⁺ contents in Na⁺-loaded transformants

In Na⁺-loaded *E. coli* DK8 transformants

E. coli DK8 cells transformed with pTrcHis2C (empty vector transformants) and pTrcHis2C-*ApNa⁺-atp* (*ApNa⁺-ATPase*-expressing cells) were grown in LB medium containing 100 $\mu\text{g ml}^{-1}$ ampicillin at 37 °C until the optical density at 620 nm reached 0.6 and then the cells were transferred into fresh medium containing 0.15 M NaCl. After incubation on ice for 1 hr, the cells were collected and transferred into Na⁺-free medium in the presence of 1 mM IPTG. Ten mM of glucose was added for 10 min prior to start the extrusion of Na⁺. At the appropriate time, a 1-ml sample was collected by filtration and the filter was placed in 1.5 ml eppendorf tube. The cells trapped on the filter were suspended in 1 ml of distilled water and boiled for 5 min. After removal of cell debris by centrifugation, Na⁺ content in the supernatant was determined using a Shimadzu Personal Ion Analyzer PIA-1000.

In Na⁺-loaded *Synechococcus* sp. PCC 7942 transformants

Synechococcus sp. PCC 7942 cells transformed with pUC303 (empty vector transformants) and pUC303-*ApNa⁺-atp* (*ApNa⁺-ATPase*-expressing cells) were grown in BG11 medium containing 50 µg ml⁻¹ streptomycin at 30 °C for 7 days and then the transformants were transferred into fresh medium containing 0.15 M NaCl. After incubation for 1 day, the cells were collected and transferred into Na⁺-free medium in the presence of 0.5 mM IPTG. Ten mM of glucose was added for 10 min prior to start the extrusion of Na⁺. At the appropriate time, a 1-ml sample was collected by filtration and the filter was placed in 1.5 ml eppendorf tube. The cells trapped on the filter were suspended in 1 ml of distilled water and boiled for 5 min. After removal of cell debris by centrifugation, Na⁺ content in the supernatant was determined using a Shimadzu Personal Ion Analyzer PIA-1000.

3.2.4.3 Preparation of inverted membrane vesicles from the transformants and determination of ATP hydrolysis activity

From *E. coli* DK8 transformants

E. coli DK8 cells transformed with pTrcHis2C (empty vector transformants) and pTrcHis2C-*ApNa⁺-atp* (*ApNa⁺-ATPase*-expressing cells) were grown in LB medium containing 100 µg ml⁻¹ Ampicillin at 37 °C until the optical density at 620 nm reached 0.6 and then IPTG was added to final conc. of 1 mM. At appropriate time, the cells were harvested by centrifugation at 9,800 g for 20 min and washed three times with 20 mM Tris-HCl pH 7.6 containing 1.0 M sucrose. The collected cells were resuspended in extraction buffer (20 mM Tris-HCl pH 7.6, 1 mM DTT, 1 mM PMSF and 5 mM MgCl₂) with ratio (g ml⁻¹) of 1.0-2.0. After homogenization, the cells were disrupted by two passages through a French pressure cell at 400 kPa.

Unbroken cells and large debris were removed by centrifugating at 4,000 g for 15 min. The inverted membrane vesicles were sedimented by centrifugating at 100,000 g for 30 min and resuspended in 50 mM Hepes-KOH pH 7.0 to a final protein concentration of 1 mg ml⁻¹. Inverted membrane vesicles were used for determining ATP hydrolysis activity as previously described in section 3.2.1.6.

From *Synechococcus* sp. PCC 7942 transformants

Synechococcus sp. PCC 7942 cells transformed with pUC303 (empty vector transformants) and pUC303-*ApNa⁺-atp* (*ApNa⁺-ATPase*-expressing cells) were grown in BG11 medium containing 50 µg ml⁻¹ streptomycin at 30 °C for 7 days and then IPTG was added to final conc. of 1 mM. At appropriate time, the cells were harvested by centrifugating at 9,800 g for 20 min and washed three times with 20 mM Tris-HCl pH 7.6 containing 1.0 M sucrose. The collected cells were resuspended in extraction buffer (20 mM Tris-HCl pH 7.6, 1 mM DTT, 1 mM PMSF and 5 mM MgCl₂) with ratio (g ml⁻¹) of 1.0-2.0. After homogenization, the cells were disrupted by two passages through a French pressure cell at 400 kPa. Unbroken cells and large debris were removed by centrifugating at 9,800 g for 15 min. The membrane vesicles were sedimented by centrifugating at 100,000 g for 30 min and resuspended in 50 mM Hepes-KOH pH 7.0 to a final protein concentration of 1 mg ml⁻¹. Inverted membrane vesicles were used for determining ATP hydrolysis activity as previously described in section 3.2.1.6.

3.2.4.4 Preparation of Na⁺-loaded inverted membrane vesicles of from the transformants and determination of ATP synthesis

Inverted membrane vesicles from *E. coli* DK8 and *Synechococcus* sp. PCC 7942 were suspended in 5 mM potassium phosphate pH 7.5 containing 0.25 mM

EDTA and 0.2 M NaCl. After incubation for 1 hr (in *E. coli* DK8) and 1 day (in *Synechococcus* sp. PCC 7942), Na⁺-loaded inverted membrane vesicles were collected by centrifugating at 100,000 g for 30 min and then resuspended in 5 mM potassium phosphate pH 7.5 containing 0.25 mM EDTA.

ATP synthesis was measured in the reaction medium (0.5 ml) containing 5 mM potassium phosphate pH 7.5, 5 mM MgCl₂, 0.2 M KCl, 0.1 mM ADP, 1 μM valinomycin and Na⁺-loaded inverted membrane vesicles (30 μg protein). At different time intervals, 50-μl samples were taken and immediately added to 5 μl of 20% TCA. The samples were briefly centrifuged at 13,000 g for 5 min. A 1-μl aliquot of the supernatant was diluted with 99 μl of distilled water and the ATP content was measured by ENLITEN rLuciferase/Luciferin reagent. The ATP content was calculated by comparing to the standard curve of ATP (Appendix Q).

3.2.4.5 Isolation of periplasmic, cytoplasmic and membrane fractions from ApNa⁺-ATPase-expressing *E. coli* DK8 cells

E. coli DK8 cells transformed with pTrcHis2C-*ApNa⁺-atp* (ApNa⁺-ATPase-expressing cells) were grown in LB medium containing 100 μg ml⁻¹ ampicillin at 37 °C until the optical density at 620 nm reached 0.6 and then IPTG was added to final conc. of 1 mM. At appropriate time, cells were harvested by centrifugating at 9,800 g for 20 min and washed three times with 20 mM Tris-HCl pH 7.6 containing 1.0 M sucrose. The collected cells were resuspended in periplasting buffer (20% sucrose, 1 mM EDTA). The sample was incubated on ice for 5 min and gently mixed by slow pipetting. The sample was again incubated on ice for another 5 min. The sample was centrifuges at 12,000 g for 2 min to recover the supernatant as the periplasmic fraction and the pellet contained spheroplasted. Spheroplasts are lysed using a lysis buffer (10

mM Tris-HCl pH 7.5, 50 mM KCl, 1 mM EDTA, and 0.1% Deoxycholate). The sample was allowed to sit at room temperature for 5 min to cause spheroplast swelling and lysis. The sample was then sonicated with a micro-tip at approximately 30-40% full power in 2 second bursts. Spheroplasmic fraction in the supernatant obtained by centrifugating at 12,000 g for 15 min. The spheroplasmic fraction was further fractionated by ultra-centrifugating to separate the membranes from the cytoplasmic fraction. The spheroplasmic fraction was centrifuged at 138,000 g for 1 hr. The supernatant was reserved as the cytoplasmic fraction and the pellet was reserved as membrane fraction.

3.2.4.6 Isolation of cytoplasmic and thylakoid membranes from ApNa⁺-ATPase-expressing *Synechococcus* sp. PCC 7942 cells

The membrane vesicles (total membrane fraction) prepared from *Synechococcus* sp. PCC 7942 cells transformed with pUC303-*ApNa⁺-atp* (ApNa⁺-ATPase-expressing cells) as described in section 3.2.4.3 were used for the separation of cytoplasmic and thylakoid membranes by sucrose gradient ultra-centrifugating at 110,000 g for 16 hrs (Berger *et al.*, 1991). The gradient consisted of four layers: 5.5 ml of 58% sucrose, 4.5 ml of 40% sucrose, 4.5 ml of 30% sucrose, and 4 ml of 10% sucrose layer. Each collected fraction was diluted with 5 mM Tris-HCl pH 7.6 to a final sucrose concentration of about 10 % and centrifuged at 110,000 g for 1 hr. The pelleted membranes were homogenized in a small volume of 5 mM Tris-HCl pH 7.6.

3.2.4.7 Western blot analysis of ApNa⁺-ATPase expressed in *E. coli* DK8 and *Synechococcus sp.* PCC 7942 cells

Fifty micrograms of sample prepared as described in section 3.2.4.3, 3.2.4.5 and 3.2.4.6 were separated by 12.0% sodium dodecyl polyacrylamide gel electrophoresis (SDS-PAGE) (Appendix H) and transferred to PVDF membrane by blotting transfer buffer (Appendix R). Blotting was done at 150 mA/in² for 1 hr followed by blocking in blocking solution (Appendix R) for 2 hrs. The PVDF membrane was incubated with primary antibody (an antibody raised against 6-histidine, 6xHis tag) for 1 hr and washed with 100 ml of PBS plus 5% skim milk solution for 15 min, 3 times. After washing with PBS buffer plus 0.5% skim milk, the membrane was immediately incubated with secondary antibody (an antibody raised against mouse) for 1 hr and washed with 100 ml of PBS plus 5% skim milk buffer for 15 min, 3 times. The PVDF membrane was visualized after incubation with the detection reagent (Appendix S) for 30 min.

CHAPTER IV

RESULTS

4.1 Characterization of the growth of *A. halophytica* and ATP hydrolysis activity of inverted membrane vesicles in the presence of various external NaCl concentrations, pH ranges and ionophores

4.1.1 Effect of NaCl concentration and pH of the growth medium on *A. halophytica* growth

A. halophytica is a short cylindrical shape cyanobacterium surrounded with mucous membrane as shown in Figure 9, and the cells multiply by binary fission. The cells were grown photoautotrophically in BG11 medium supplemented with 18 mM NaNO₃ and Turk Island salt solution. The pH range of the growth medium were adjusted to 5.0, 7.6, 9.0, 10.0 at different NaCl concentrations, i.e. 0.5 M NaCl for normal condition and 2.0 M NaCl for salt stress condition. The growth rate was monitored every day for 14 days by spectrophotometer at 730 nm. Figure 10A shows the effect of NaCl concentration in the growth medium on cell growth. The growth rate increased with increasing NaCl concentration up to 0.5 M, and then a reduction of growth was observed at 1 and 2 M NaCl. No growth was observed when 0.5 M NaCl was replaced by 0.5 M KCl in the medium. Figure 10B shows the effect of varying pH range of the growth medium on cell growth. The maximum growth was observed when cell grown in the growth medium at pH 9.0. Increasing an alkalinity of the medium to pH 10.0 retarded cell growth. At pH 5.0, the cells showed a low growth rate.



Figure 9 Microscopic picture of *A. halophytica* grown in BG11 medium supplemented with 18 mM NaNO₃ and Turk Island salt solution containing 0.5 M NaCl at day 14th (x2,250).

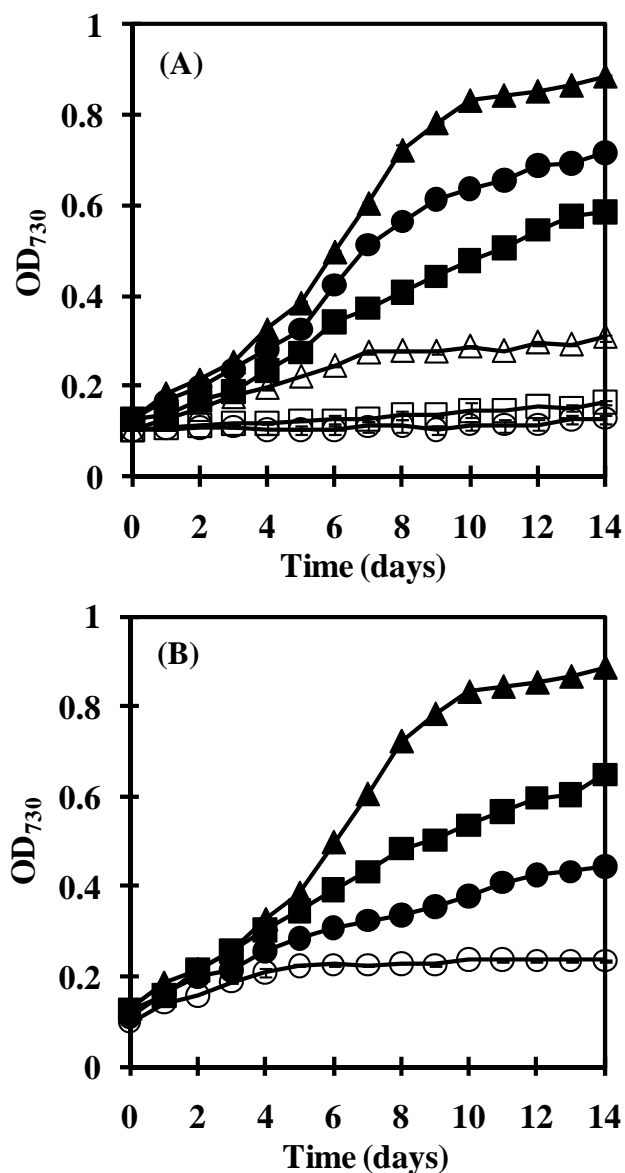


Figure 10 Effect of NaCl concentration and pH of the growth medium on *A. halophytica* growth. (A) Growth of *A. halophytica* grown in the growth medium containing various NaCl concentrations. 0 M NaCl (○), 0.25 M NaCl (■), 0.5 M NaCl (▲), 1.0 M NaCl (●), 2.0 M NaCl (△) and 0.5 M KCl (□) at pH 9.0. (B) Growth of *A. halophytica* grown in the growth medium containing 0.5 M NaCl at pH 5.0 (○), pH 7.6 (■), pH 9.0 (▲) and pH 10.0 (●). Each value shows the average of three independent measurements.

4.1.2 Effect of NaCl concentration and pH of the growth medium on ATP hydrolysis activity of inverted membrane vesicles from *A. halophytica*

Since *A. halophytica* is a halotolerant and alkaliphilic cyanobacterium, it is of interest to investigate the changes of ATP hydrolysis activity in response to changes of NaCl concentration and pH of the growth medium. Figure 11A shows that increasing NaCl concentration in the growth medium up to 2 M led to a progressive increase of ATP hydrolysis activity of inverted membrane vesicles. Higher ATP hydrolysis activity was observed in cells grown at high pH than at low pH at all four concentrations of NaCl tested. When the cells were grown at different pH values, ATP hydrolysis activity of inverted membrane vesicles was slightly increased upon increasing the pH from 5.0 to 7.6 (Figure 11B). A marked increase of enzyme activity was evident at pH higher than 7.6. Cells grown at 2 M NaCl showed higher enzyme activity than those grown at 0.5 M NaCl at all four pH values tested.

4.1.3 Effect of Gramicidin and CCCP in the growth medium on the growth of *A. halophytica* and ATP hydrolysis activity of inverted membrane vesicles

The presence of gramicidin D, an ionophore that dissipates Na⁺-gradients, in the growth medium resulted in the cessation of cell growth and the reduction in the ATP hydrolysis activity of inverted membrane vesicles (Figure 12A, B). In contrary, CCCP, a H⁺-gradient dissipator, had no effect on both cell growth and ATP hydrolysis activity of inverted membrane vesicles (Figure 12A, B).

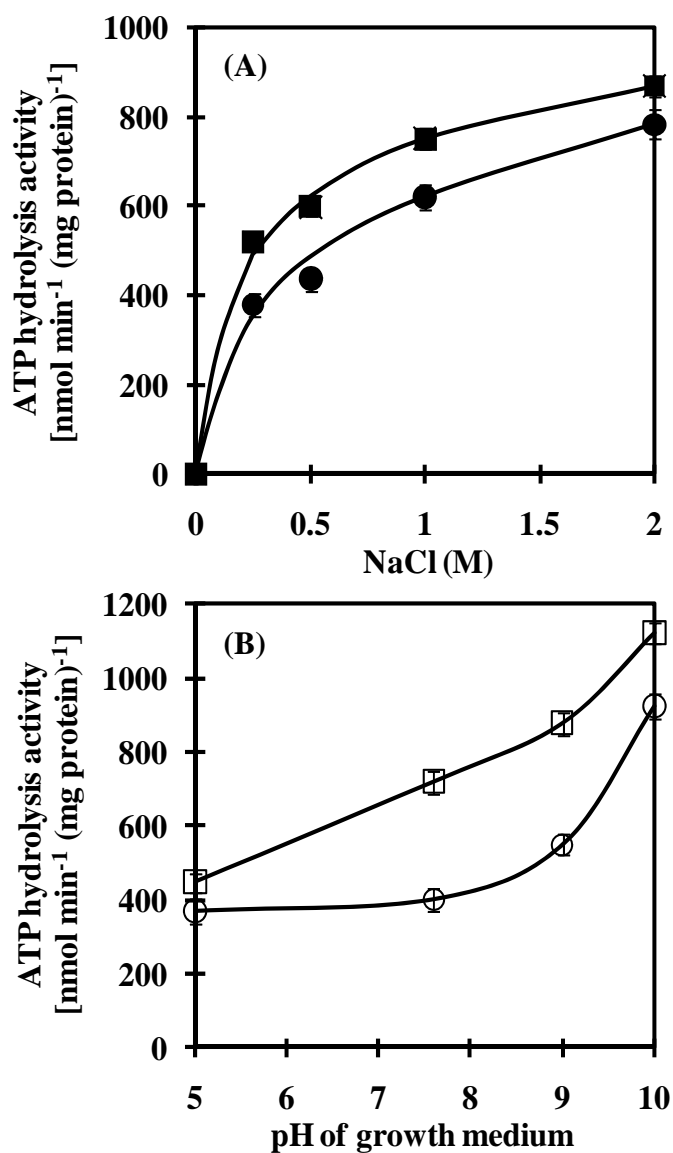


Figure 11 Effect of NaCl concentration and pH in the growth medium on ATP hydrolysis activity of inverted membrane vesicles from *A. halophytica*. Membrane vesicles were prepared from cells grown in the growth medium at different NaCl concentrations (A) at pH 7.6 (●) or pH 9.0 (■), and at different pHs (B) at 0.5 M NaCl (○) or 2.0 M NaCl (□). ATP hydrolysis activity was assayed in the mixture containing 20 mM Tris-HCl pH 7.6, 5 mM MgCl₂, 10 mM NaCl and inverted membrane vesicles (30 μg protein). The reaction was started by addition of 4 mM ATP (Tris salt). Each value shows the average of three independent measurements.

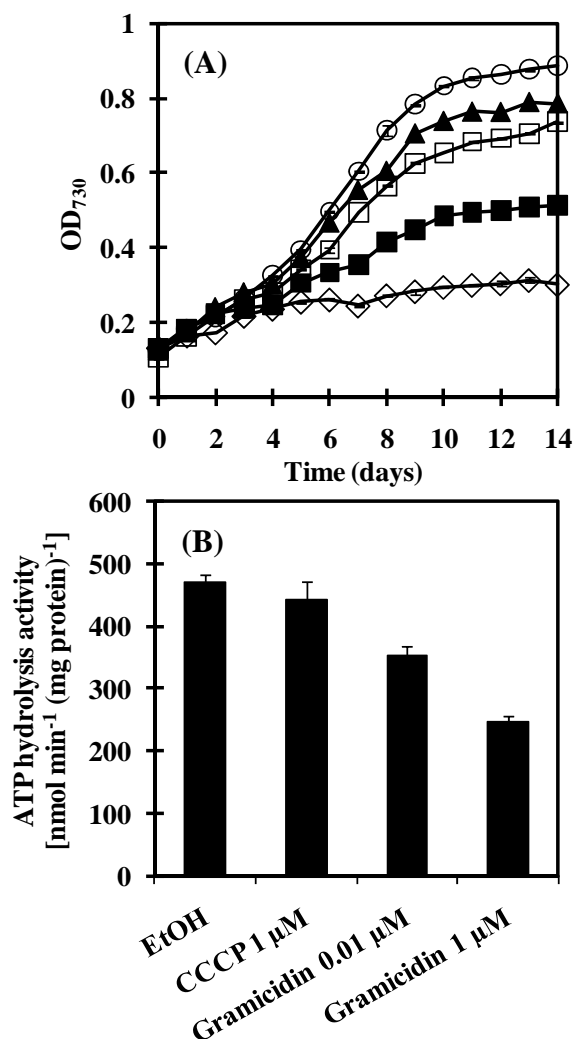


Figure 12 Effect of Gramicidin and CCCP in the growth medium on growth of *A. halophytica* and ATP hydrolysis activity of inverted membrane vesicles. (A) Growth of *A. halophytica* grown in the growth medium containing 0.5 M NaCl in the presence of CCCP/gramicidin. Control (○), 0.01 μM CCCP (▲), 1 μM CCCP (□), 0.01 μM gramicidin (■), 1 μM gramicidin (◇). (B) ATP hydrolysis activity of inverted membrane vesicles prepared from cells grown in the growth medium containing 0.5 M NaCl in the presence of CCCP/gramicidin. ATP hydrolysis activity was assayed in the mixture containing 20 mM Tris-HCl pH 7.6, 5 mM MgCl₂, 10 mM NaCl and inverted membrane vesicles (30 μg protein). The reaction was started by addition of 4 mM ATP (Tris salt). Each value shows the average of three independent measurements.

4.2 Optimization of purification conditions for obtaining high ATP hydrolysis activity

4.2.1 Dependence of *A. halophytica* culture time on ATP hydrolysis activity of inverted membrane vesicles

ATP hydrolysis activity of inverted membrane vesicles increased when *A. halophytica* culture time increased until the 7th day (Figure 13). Cells grown for 7 days (mid-log phase) shows the highest ATP hydrolysis activity and the activity decreased when cells grown for 12 and 15 days (stationary growth phase).

4.2.2 Effect of sodium cholate on ATP hydrolysis activity of solubilized ATPase

Na⁺-ATPase is a membrane protein, hence it is necessary to find optimum conditions for solubilize Na⁺-ATPase from the membranes. After subjecting inverted membrane vesicles to treatments with various concentrations of sodium cholate, it was found that the highest ATP hydrolysis activity was obtained with 7 mM sodium cholate (Figure 14).

4.2.3 Effect of solubilization time on ATP hydrolysis activity of solubilized ATPase

After the ATPase was solubilized by incubating the inverted membrane vesicles with 7 mM sodium cholate at various incubation times. The result showed that ATP hydrolysis activity was highest when ATPase was solubilized with sodium cholate for 30 min (Figure 15). The solubilization time that is higher or lower than 30 min caused a reduction of ATP hydrolysis activity.

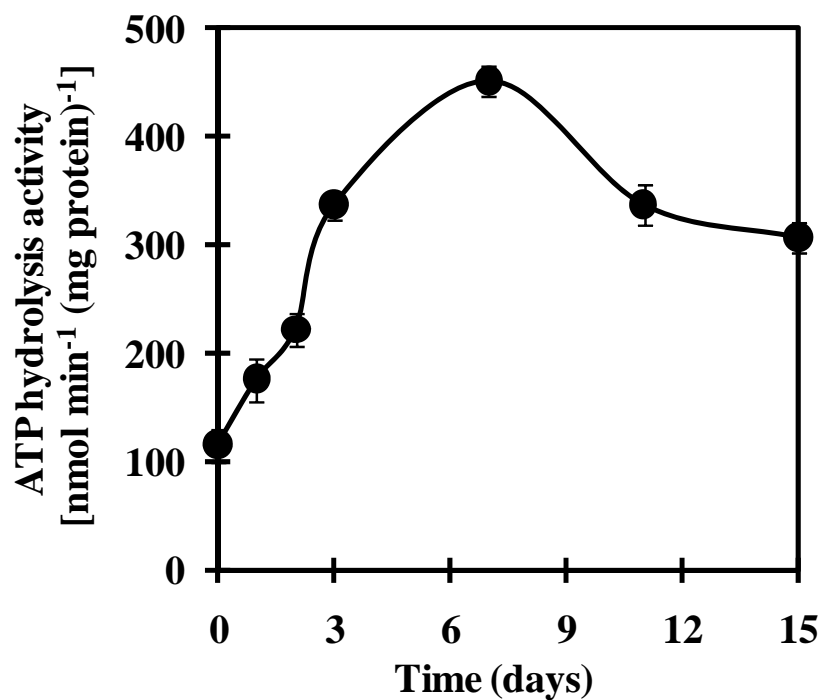


Figure 13 Effect of *A. halophytica* culture time on ATP hydrolysis activity of inverted membrane vesicles. Inverted membrane vesicles were prepared at various culture times from cells grown in the growth medium containing 0.5 M NaCl at pH 9.0. ATP hydrolysis activity was assayed in the mixture containing 20 mM Tris-HCl pH 7.6, 5 mM MgCl₂, 10 mM NaCl and inverted membrane vesicles (30 μg protein). The reaction was started by adding of 4 mM ATP (Tris salt) into the reaction mixture. Each value shows the average of three independent measurements.

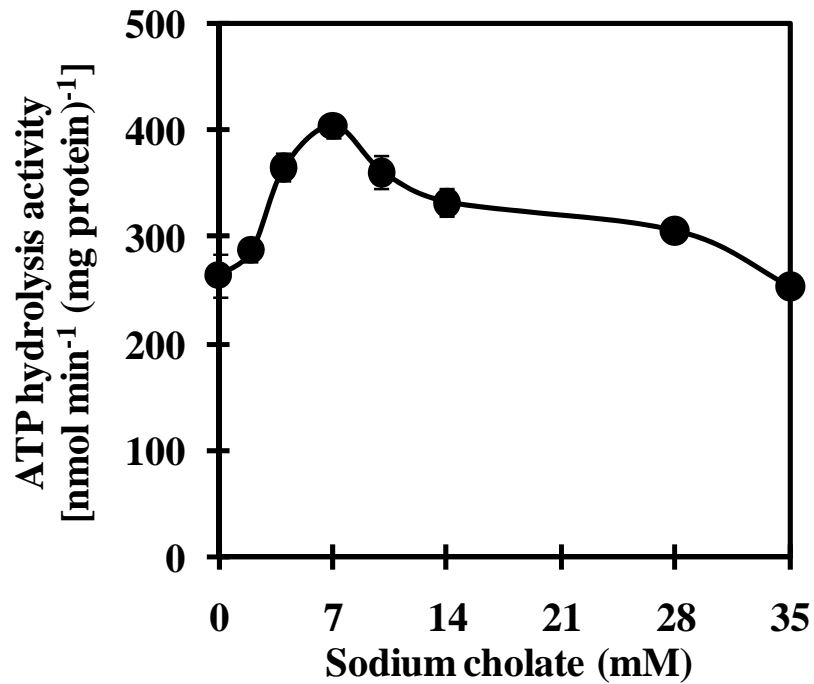


Figure 14 Effect of sodium cholate on ATP hydrolysis activity of solubilized ATPase. The ATPase was solubilized by incubating the inverted membrane vesicles (protein concentration 1 mg ml⁻¹) with sodium cholate at various final concentrations. After 30 min, the solubilized ATPase was isolated by ultracentrifugation at 100,000 g for 1 hr. The supernatant containing ATPase was assayed by incubating the supernatant (30 µg protein) in the mixture containing 20 mM Tris-HCl pH 7.6, 5 mM MgCl₂, 10 mM NaCl. The reaction was then started by adding of 4 mM ATP (Tris salt) into the reaction mixture. Each value shows the average of three independent measurements.

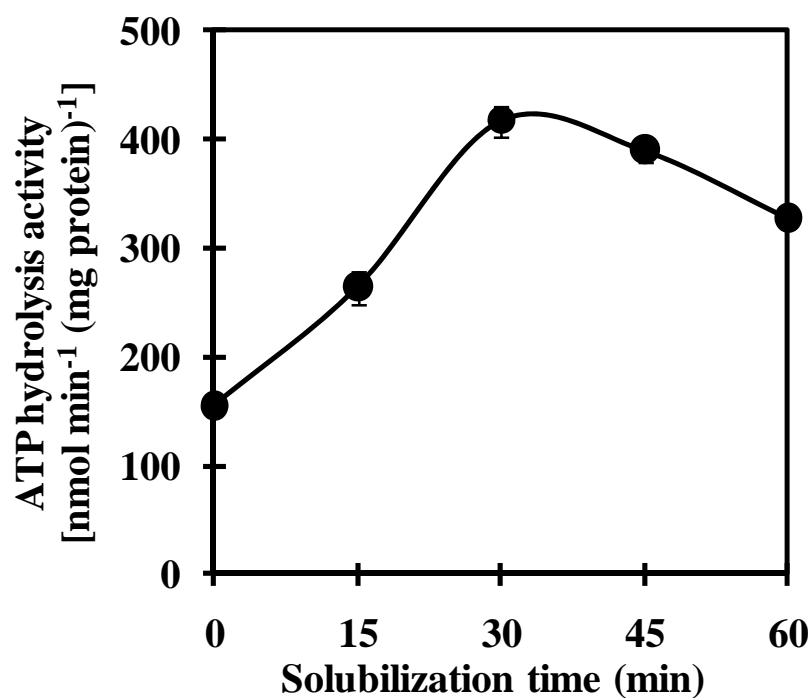


Figure 15 Effect of solubilization time on ATP hydrolysis activity of solubilized ATPase. The ATPase was solubilized by incubation of inverted membrane vesicles (protein concentration 1 mg ml⁻¹) with 7 mM sodium cholate. At indicated times, the solubilized membrane proteins were isolated by ultracentrifugation at 100,000 g for 1 hr. The supernatant containing ATPase was assayed activity by incubating the supernatant in (30 µg protein) in the mixture containing 20 mM Tris-HCl pH 7.6, 5 mM MgCl₂, 10 mM NaCl. The reaction was started by addition of 4 mM ATP (Tris salt). Each value shows the average of three independent measurements.

4.3 Purification of ATPase from *A. halophytica*

After solubilized ATPase from the membranes, a 2.5-fold increase in the purity of Na⁺-ATPase and 86.2 % recovery of the activity of Na⁺-ATPase was observed (Table 5). It is noteworthy that more than 85% Na⁺-ATPase activity was recovered in the solubilized membrane protein suggesting that nearly all Na⁺-ATPase proteins were solubilized in their native forms. After that the two-step purification namely PEG 6000 precipitation and Superose 6 gel filtration were performed. Approximately 9.1-fold increase on the purity of Na⁺-ATPase and 24.6 % recovery of the activity of Na⁺-ATPase were achieved by PEG 6000 precipitation. The ATPase was further separated by Superose 6 gel filtration. The chromatogram showed the dominant protein peak which corresponded to the Na⁺-ATPase activity peak (Figure 16). The apparent molecular weight (M_r) of F-type ATPase determined by gel filtration chromatography was about 528 kDa (Figure 17). Moreover, a 17.5-fold purified enzyme with 6.5% yield was obtained from this step. SDS-PAGE analysis (Figure 18) revealed some polypeptide bands which could tentatively be identified as ATPase subunits of an F-type ATPase, namely α (56 kDa), β (52 kDa), γ (35 kDa), δ (25 kDa), ϵ (22 kDa), δ (22 kDa), ϵ (16.5 kDa) and c (6.5 kDa) based on the comparison with the typical mobilities, band pattern of an F-type ATPase subunits from both *Ilyobacter tartaricus* (Neumann *et al.*, 1998) and thermoalkaliphilic *Bacillus* sp. strain TA2.A1 (Cook *et al.*, 2003) and the determination of molecular weight of ATPase subunits by SDS-PAGE (Figure 19). The calculated molecular weight of the ATPase complex determined by SDS-PAGE (suggested to be $\alpha_3\beta_3\gamma\delta\epsilon abc_{8,9}$) (~500 kDa) is in close agreement with the molecular weight of ATPase complex determined by gel filtration (528 kDa). The subunit c was further characterized by cutting the band on SDS-PAGE (Lane 5) and digesting with trypsin

before analysis by liquid chromatography mass spectrometry (LC-MS/MS). The spectra were recorded on an ESI-Q-TOF mass spectrometer (Waters Corporation). The amino acid sequences of the peptides were obtained using Mascot program (<http://www.matrixscience.com>). One resultant tryptic peptide “ISSGAEGIAR” with the molecular mass of 959.5036, by searching the National Center for Biotechnology Information (NCBI) database, was highly identical to the sequence of F-type ATPase subunit c of *Synechococcus* sp. WH 8102 (UniProtKB Q7U8W9), *Synechococcus* sp. PCC 9902 (UniProtKB Q3AZM5), *Synechococcus* sp. PCC 7002 (UniProtKB B1XHZ2) and *Gloeobacter violaceus* (UniProtKB Q7NCR9) with % identity of 90, 90, 80 and 60%, respectively.

Table 5 Purification of ATPase from *Aphanothece halophytica*

Step	Total protein (mg)	Total activity (unit) ^a	Specific activity (unit mg ⁻¹)	Purification (fold)	Yield (%)
Membrane vesicles	162.0	4315	26.6	1.0	100.0
Solubilized protein	55.5	3720	67.0	2.5	86.2
PEG 6000 precipitation	4.4	1062	241.4	9.1	24.6
Superose 6	0.6	280	466.7	17.5	6.5

^a One unit corresponded to 1 nmol of inorganic phosphate produced per min.

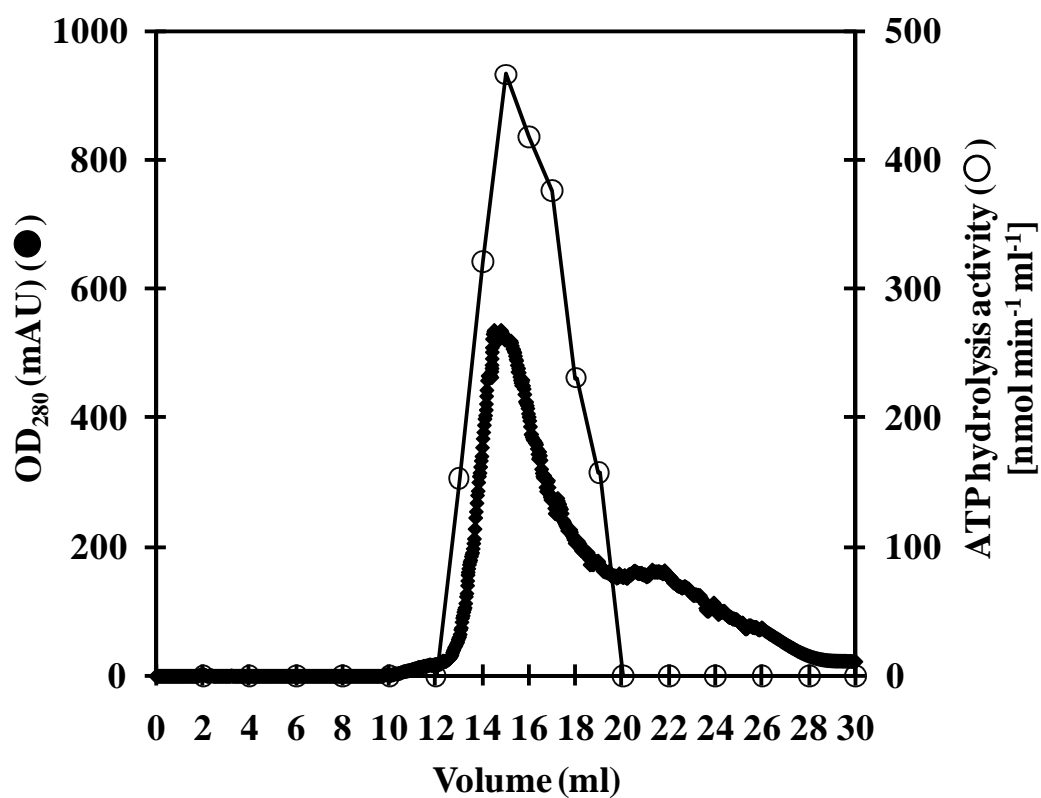


Figure 16 Separation of ATPase from *A. halophytica* by Superose 6 gel filtration chromatography.

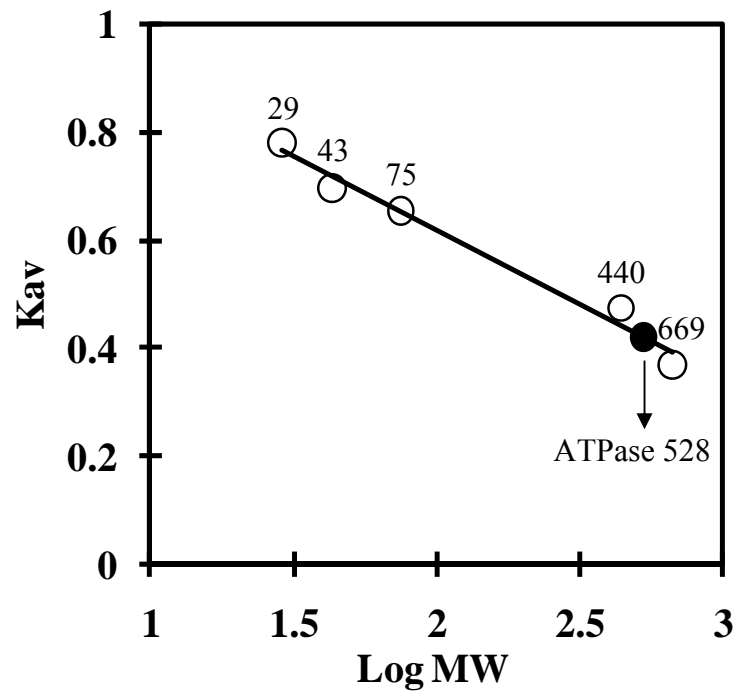


Figure 17 Determination of molecular weight of ATPase from *A. halophitica* separated by Superose 6 gel filtration. The molecular weight marker containing carbonic anhydrase 29 kDa, ovalbumin 43 kDa, conalbumin 75 kDa, ferritin 440 kDa, thyroglobulin 669 kDa.

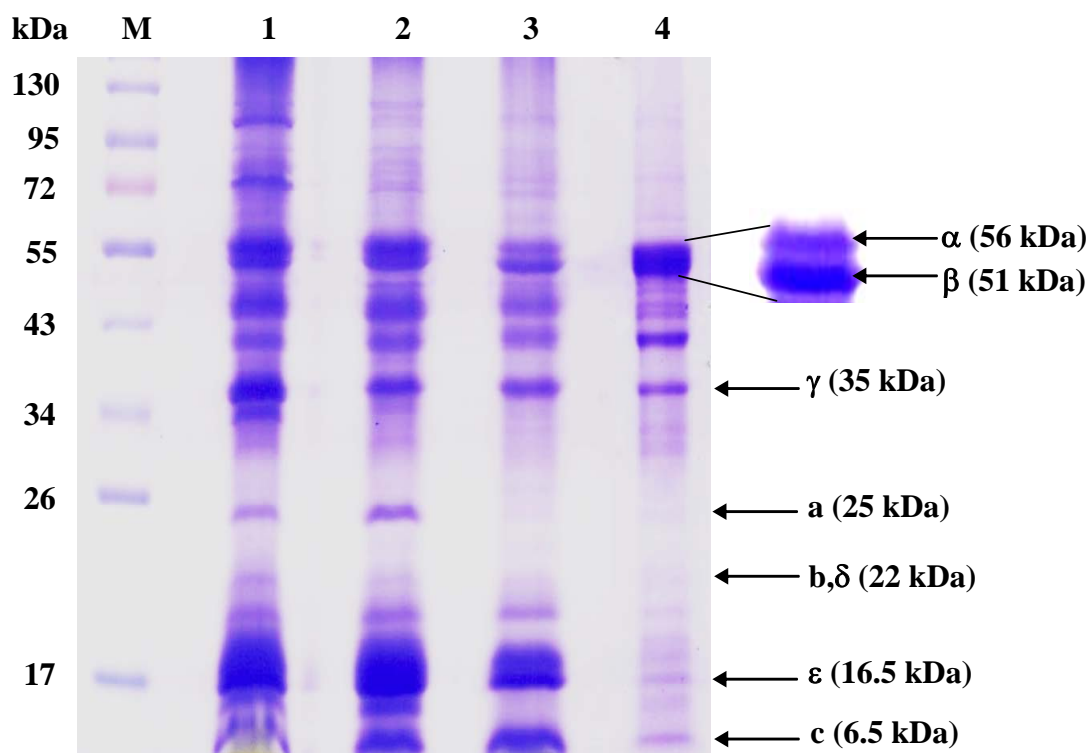


Figure 18 SDS-PAGE of ATPase from *A. halophytica*. Samples (30 μ g protein) were resolved on 12% polyacrylamide gel which stained with Coomassie brilliant blue. Lane M, PageRuler Prestained Protein Ladder (Fermentas); Lane 1, membrane vesicles; Lane 2, solubilized protein; Lane 3, protein from polyethylene glycol 6000 precipitation; Lane 4, purified ATPase from Superose 6. All F-type ATPase subunits were identified with reference to the previously reported F-type ATPases in *Ilyobacter tartaricus* (Neumann et al., 1998) and *Bacillus* sp. strain TA2.A1 (Cook et al., 2003). Samples in all lanes except lane M were precipitated with 10% TCA before performing SDS-PAGE. The contaminated bands were therefore unlikely due to a SDS-stable c ring.

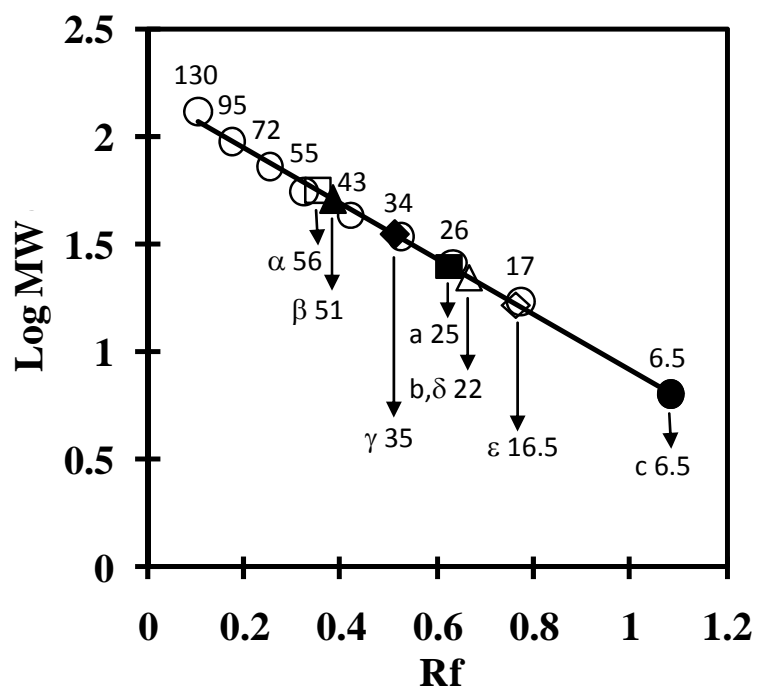


Figure 19 Determination of molecular weight of ATPase subunits by SDS-PAGE. The calculated molecular weight of each ATPase subunit was presented in kDa. ATPase subunits are represented as α (\square), β (\blacktriangle), γ (\blacklozenge), ϵ (\diamond), a (\blacksquare), b and δ (\triangle), c (\bullet).

4.5 Preparation of reconstituted proteoliposomes

The purified ATPase from *A. halophytica* was reconstituted into liposomes by a freeze-thaw/dilution method as described in materials and methods section 3.2.1.10 and then the proteoliposomes were characterized for biochemical properties and Na⁺ transport.

4.6 Characterization of purified ATPase and proteoliposomes

4.6.1 Effect of storage temperature on ATP hydrolysis activity of purified ATPase

The purified ATPase was stored at 4 and -20 °C at indicated time and ATP hydrolysis activity was measured as shown in Figure 20. The enzyme was stable up to one month when kept at -20 °C while the enzyme kept at 4 °C was stable up to 5-7 days. Therefore, the purified ATPase should be kept at -20 °C to avoid the lost of enzyme activity.

4.6.2 Effect of cations, ATP, Mg²⁺ and pH on ATP hydrolysis activity of purified ATPase and proteoliposomes

The ATP hydrolysis activity of the purified ATPase and the reconstituted proteoliposomes as influenced by various cations were tested and the results are shown in Figure 21A and 22A, respectively. Increasing Na⁺ concentration up to 10 mM caused a progressive increase in enzyme activity. In contrast, K⁺, Li⁺, and Ca²⁺ had no stimulatory effect on enzyme activity. The apparent K_m value of ATPase activity of the purified ATPase and the proteoliposomes for Na⁺ as determined from the Lineweaver-Burk plot was 2 and 3.17 mM, respectively (Figure 21A, 22A, inset).

It is noteworthy that only marginal activity was detected in the absence of Na^+ accounting for about 10% of the maximum activity. Figure 21B and 22B show that ATPase activity increased as ATP increased and the activity was saturated at about 6 mM ATP. The apparent K_m value of ATPase activity of the purified ATPase and the proteoliposomes for ATP was 1.2 and 2.98 mM, respectively (Figure 21B, 22B, inset).

The dependence of ATPase on Mg^{2+} was also tested. Figure 21C and 22C show that maximal ATP hydrolysis activity was observed at 5 mM Mg^{2+} . The enzyme activity was slightly decreased when the Mg^{2+} concentration was higher than 5 mM. The pH of the assay medium also influenced on the enzyme activity. When the pH was increased from pH 6.0 to pH 9.0, the enzyme activity was increased progressively (Figure 21D, 22D). Increasing the pH further to pH 11.0 resulted in a slightly declined enzyme activity.

4.6.3 Effect of Na^+ ion concentration on ATP hydrolysis activity of purified ATPase at different pH values

The observation that high activity of ATPase occurred at alkaline pH as high as pH 11.0 prompted us to investigate further the effect of Na^+ on the stimulation of ATP hydrolysis activity at different pH values. Maximal stimulation of ATP hydrolysis activity occurred at 10 mM NaCl when assayed at pH 7.6, 9.0 and 11.0 (Figure 23). The enzyme was stimulated about 9-fold at pH 7.6 and about 11-fold at both pH 9.0 and 11.0 in the presence of 10 mM NaCl as compared to the absence of NaCl.

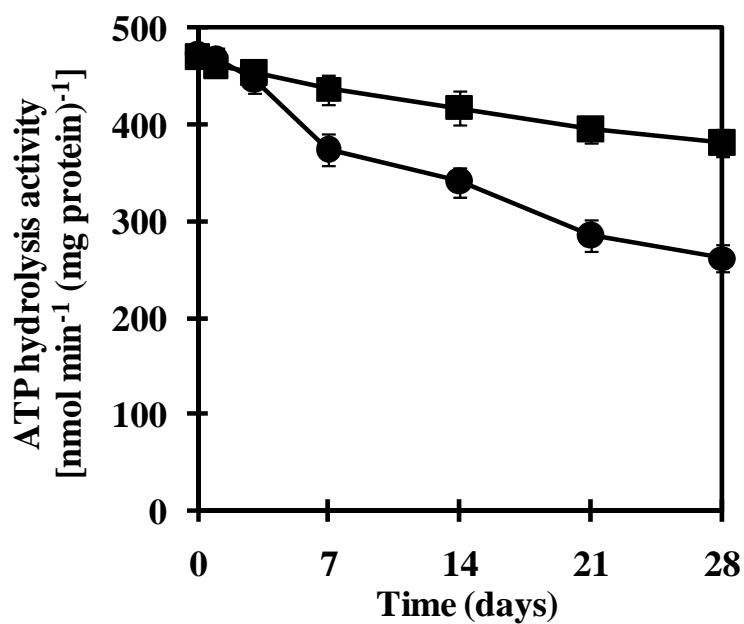


Figure 20 Effect of storage temperature on ATP hydrolysis activity of purified ATPase. The purified ATPase were stored at $4\text{ }^{\circ}\text{C}$ (●) and $-20\text{ }^{\circ}\text{C}$ (■) at indicated time and used for ATP hydrolysis activity assay. The purified ATPase ($30\text{ }\mu\text{g}$ proteins) was incubated in 20 mM Tris-HCl buffer pH 7.6 containing 5 mM MgCl_2 and 10 mM NaCl. The reaction was started by addition of 4 mM ATP (Tris salt). Each value shows the average of three independent measurements.

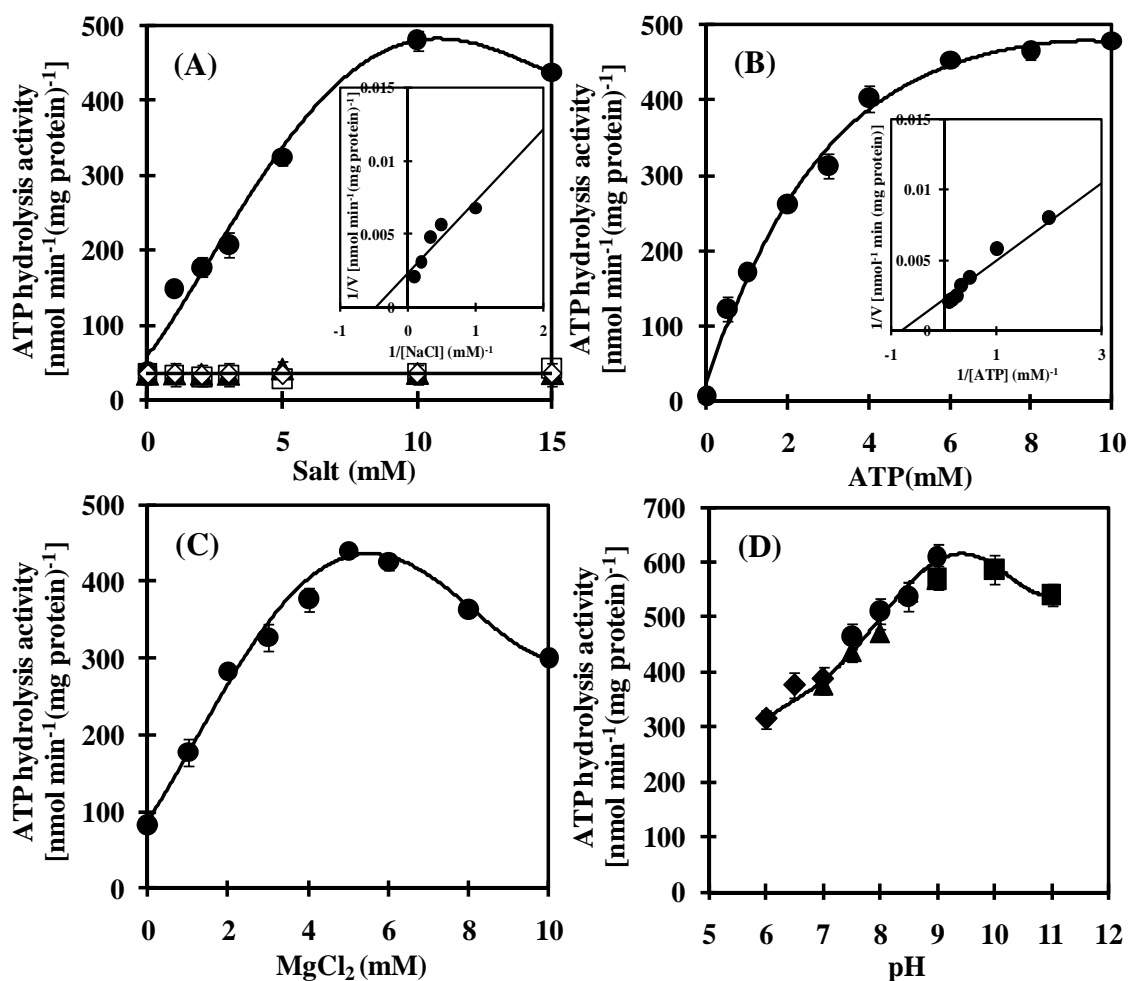


Figure 21 Dependence of purified ATPase on cations, ATP, Mg^{2+} and pH. In (A), the enzyme activity was measured in the presence of various concentrations of NaCl (●), KCl (□), LiCl (◇) and CaCl_2 (▲). Inset shows a double-reciprocal plot of activity versus NaCl concentration. In (B) and (C), the enzyme activity was measured in the presence of various concentrations of ATP and MgCl_2 , respectively. Inset in (B) shows a double-reciprocal plot of activity versus ATP concentration. In (D), the enzyme activity was measured at various pH values using 20 mM Mes-KOH for pH 6.0-7.0 (◆), 20 mM HEPES-KOH for pH 7.0-8.5 (▲), 20 mM Tris-HCl for pH 7.5-9.0 (●) and 20 mM Glycine-KOH for pH 9.0-11.0 (■). Each value shows the average of three independent measurements.

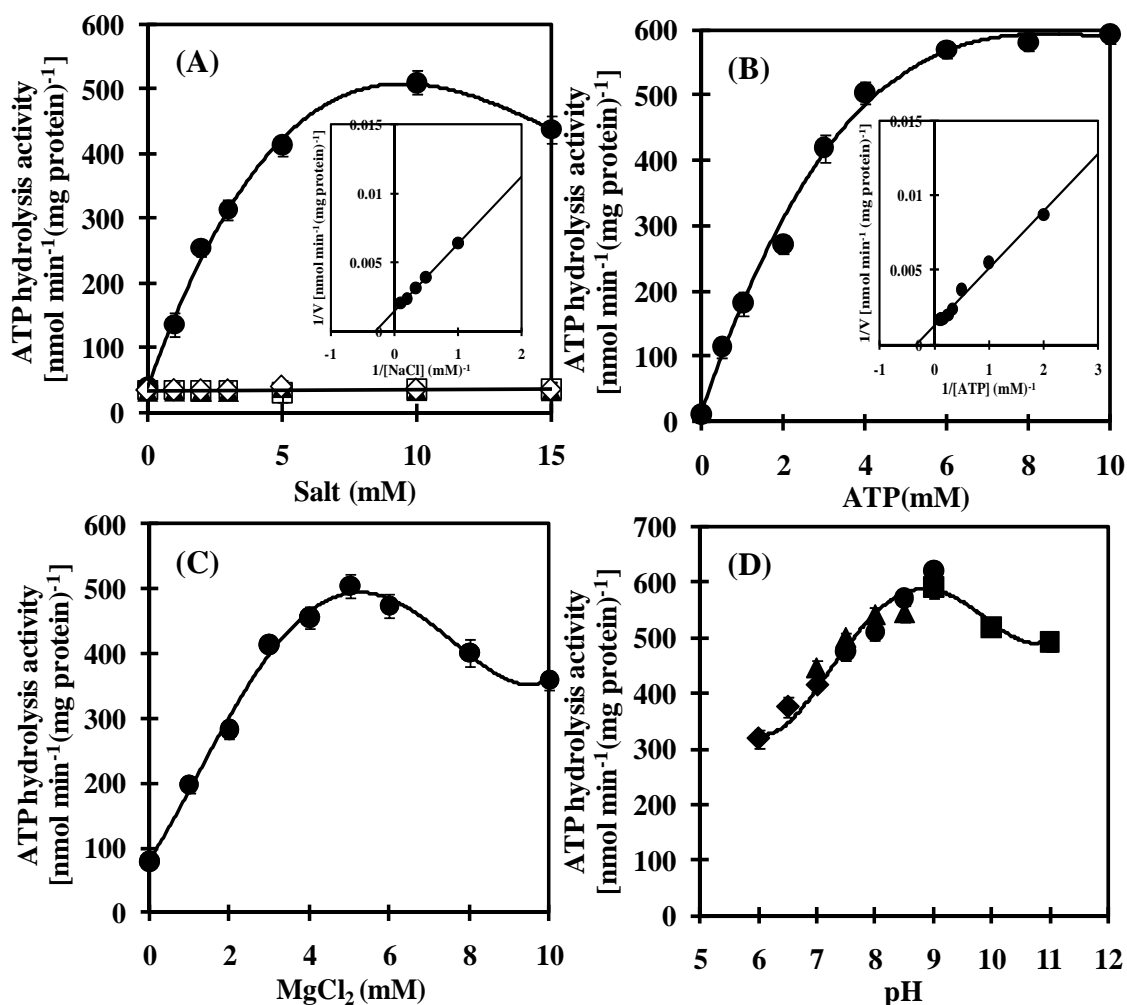


Figure 22 Dependence of proteoliposomes on cations, ATP, Mg^{2+} and pH. In (A), the enzyme activity was measured in the presence of various concentrations of NaCl (●), KCl (□), LiCl (◇) and CaCl_2 (▲). Inset shows a double-reciprocal plot of activity versus NaCl concentration. In (B) and (C), the enzyme activity was measured in the presence of various concentrations of ATP and MgCl_2 , respectively. Inset in (B) shows a double-reciprocal plot of activity versus ATP concentration. In (D), the enzyme activity was measured at various pH values using 20 mM Mes-KOH for pH 6.0-7.0 (◆), 20 mM Hepes-KOH for pH 7.0-8.5 (▲), 20 mM Tris-HCl for pH 7.5-9.0 (●) and 20 mM Glycine-KOH for pH 9.0-11.0 (■). Each value shows the average of three independent measurements.

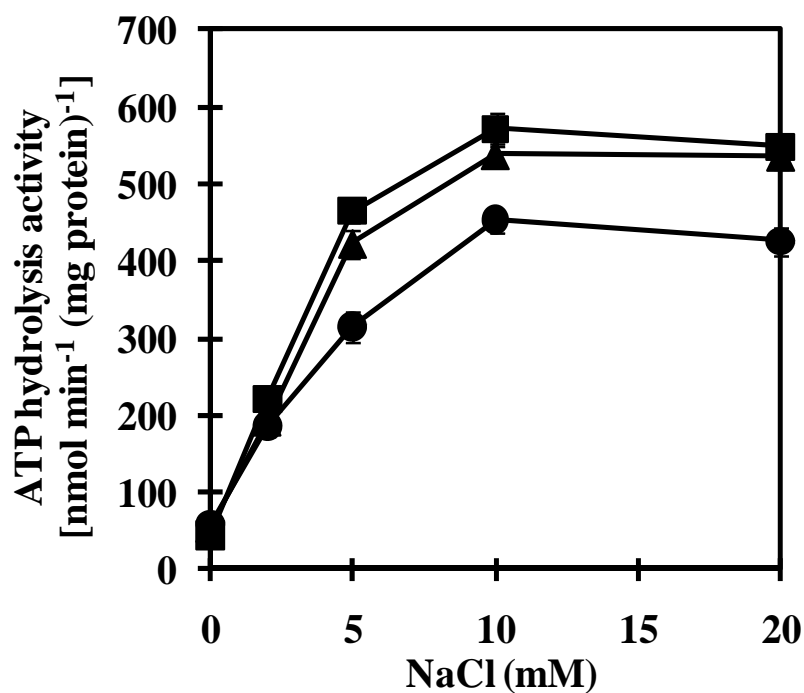


Figure 23 Effect of Na⁺ ion concentration on ATP hydrolysis activity of purified ATPase at different pH values. The ATPase activity was determined in the reaction mixture containing the purified ATPase (30 μ g protein), 5 mM MgCl₂ with either 20 mM Tris-HCl, pH 7.6 (●), 20 mM Tricine-KOH, pH 9.0 (■) or 20 mM Glycine-KOH, pH 11.0 (▲) and NaCl concentrations as indicated. The reaction was started by addition of 4 mM ATP (Tris salt). Each value shows the average of three independent measurements.

4.6.4 Effect of inhibitors on ATP hydrolysis activity of purified ATPase and proteoliposomes

The protonophore carbonyl cyanide *m*-chlorophenylhydrazone (CCCP), the V-type ATPase inhibitors *N*-ethylmaleimide (NEM), KNO₃ and KSCN, had no inhibitory effect on ATP hydrolysis activity of the purified ATPase and the proteoliposomes (Table 6, 7). Ouabain, an animal Na⁺/K⁺-ATPase inhibitor and orthovanadate, an inhibitor of P-type ATPase also did not inhibit ATP hydrolysis activity. Amiloride, a potent inhibitor of many Na⁺-coupled transport systems including Na⁺/H⁺ antiporters had no effect on ATP hydrolysis activity.

Sodium azide, an F₁ inhibitor, and *N,N'*-dicyclohexylcarbodiimide (DCCD), an F₀ inhibitor, inhibited ATP hydrolysis activity of the purified ATPase by about 36 and 22%, respectively (Table 6).

In the proteoliposomes, gramicidin D and monensin, Na⁺-gradient dissipators, inhibited ATPase activity by about 43 and 39%, respectively. Sodium azide, an F₁ inhibitor, and *N,N'*-dicyclohexylcarbodiimide (DCCD), an F₀ inhibitor, inhibited ATP hydrolysis activity by about 40 and 67%, respectively (Table 7).

Table 6 Effect of inhibitors on ATP hydrolysis activity of purified ATPase

Inhibitors	Residual ATPase activity (%)
None	100
1 mM CCCP	107
0.5 mM NEM	102
50 mM KNO ₃	103
20 mM KSCN	101
1 mM Ouabain	115
0.01 mM Orthovanadate	100
0.2 mM Amiloride	98
5 mM Sodium azide	64
1 mM DCCD	78

ATP hydrolysis activity was assayed in the reaction mixture containing 20 mM Tris-HCl pH 7.6, 5 mM MgCl₂, 10 mM NaCl and purified ATPase (30 µg protein). The reaction was started by addition of 4 mM ATP (Tris salt). Each inhibitor was added to the reaction mixture 10 min before the start of the reaction. One hundred percent activity corresponded to 450 nmol min⁻¹ (mg protein)⁻¹.

Table 7 Effect of inhibitors on ATP hydrolysis activity of proteoliposomes

Inhibitors	Residual ATPase activity (%)
None	100
1 mM CCCP	112
0.5 mM NEM	105
50 mM KNO ₃	98
20 mM KSCN	104
1 mM Ouabain	109
0.01 mM Orthovanadate	97
0.2 mM Amiloride	95
0.001 mM Gramicidin D	57
0.001 mM Monensin	61
5 mM Sodium azide	60
1 mM DCCD	33

ATP hydrolysis activity was assayed in the reaction mixture containing 20 mM Tris-HCl pH 7.6, 5 mM MgCl₂, 10 mM NaCl and proteoliposomes (30 µg protein). The reaction was started by addition of 4 mM ATP (Tris salt). Each inhibitor was added to the reaction mixture 10 min before the start of the reaction. One hundred percent activity corresponded to 431 nmol min⁻¹ (mg protein)⁻¹.

4.6.5 Protection of purified ATPase from DCCD inhibition by Na⁺ at pH

7.6 and pH 9.0

The weak inhibition of ATP hydrolysis activity by DCCD was due to the presence of 10 mM NaCl during the assay of ATP hydrolysis activity. Indeed, strong inhibition by DCCD in the absence of NaCl occurred after 20 min yielding 80 and 70% inhibition at pH 7.6 and pH 9.0, respectively (Figure 24A, B). The presence of 1 mM NaCl during incubation with DCCD had no (at pH 7.6) or little (at pH 9.0) protection against DCCD inhibition. However, increasing the concentration of NaCl led to the reduction of the inhibition by DCCD on ATP hydrolysis activity for both conditions at pH 7.6 and 9.0. Stronger protection was observed at pH 9.0 than at pH 7.6. Treatment with DCCD for 20 min in the presence of 50 mM NaCl resulted in approximately 30 and 50% inhibition at pH 9.0 and 7.6, respectively. The presence of 20 mM LiCl or KCl during incubation with DCCD afforded no protection against DCCD inhibition (Figure 25).

4.6.6 Na⁺ uptake into proteoliposomes at various incubation times

The transport of Na⁺ into proteoliposomes reconstituted with ATPase increased with increasing incubation time of proteoliposomes and Na⁺ up to 120 min (Figure 26).

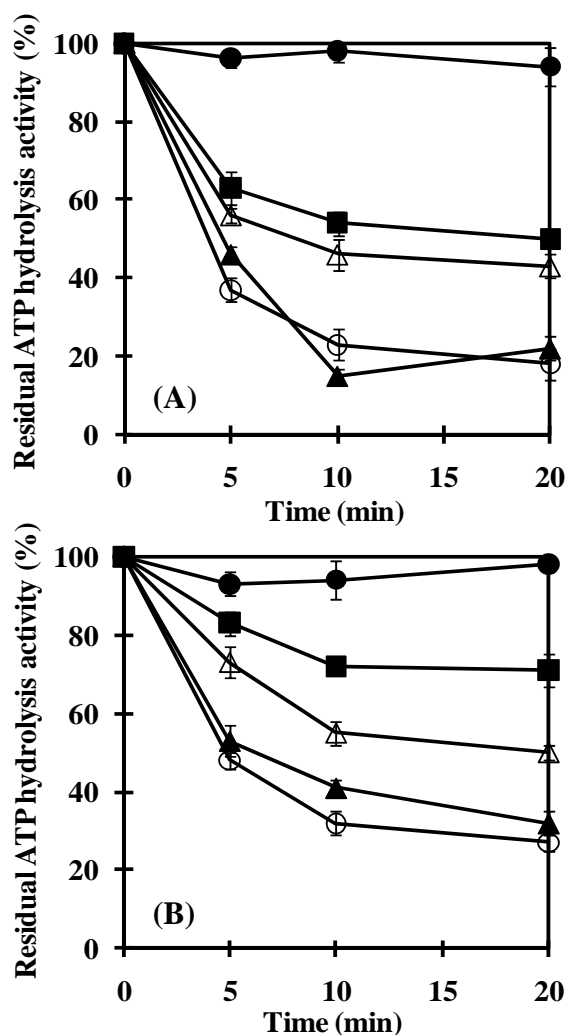


Figure 24 Protection of purified ATPase from DCCD inhibition by Na^+ at pH 7.6 and pH 9.0. The purified ATPase was incubated with 200 μM DCCD in either 20 mM Tris-HCl, pH 7.6 (A) or 20 mM Tricine-KOH, pH 9.0 (B). The individual mixtures contained the following additions of NaCl: no NaCl added (O), 1 mM NaCl (\blacktriangle), 10 mM NaCl (\triangle) and 50 mM NaCl (\blacksquare). The residual ATP hydrolysis activity of purified ATPase (30 μg protein) taken at the indicated times was determined in the reaction mixture containing 20 mM Tris-HCl pH 7.6, 5 mM MgCl_2 . The reaction was started by addition of 4 mM ATP (Tris salt). One hundred percent activity corresponded to 437 $\text{nmol min}^{-1} (\text{mg protein})^{-1}$. Control without DCCD (\bullet). Each value shows the average of three independent measurements.

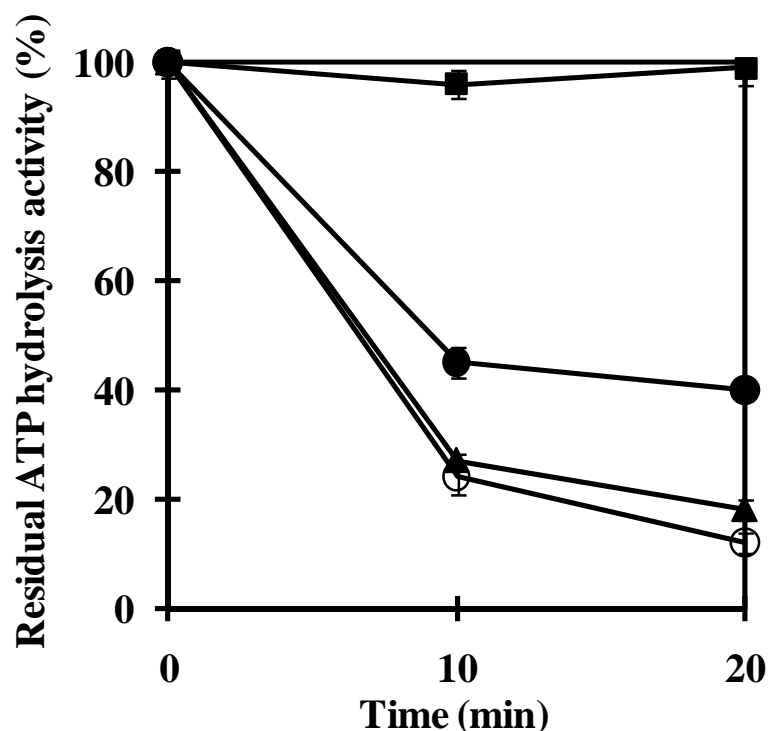


Figure 25 Effect of cations on the protection of purified ATPase from DCCD inhibition. The purified ATPase was incubated with 200 mM DCCD. The individual mixtures contained 10 mM NaCl (●), 20 mM LiCl (○), or 20 mM KCl (▲). The residual ATP hydrolysis activity of purified ATPase (30 ug protein) taken at the indicated times was determined in the reaction mixture containing 20 mM Tris-HCl pH 7.6, 5 mM MgCl₂. The reaction was started by addition of 4 mM ATP (Tris salt). One hundred percent activity corresponded to 462 nmol min⁻¹ (mg protein)⁻¹. Control without DCCD (■). Each value shows the average of three independent measurements.

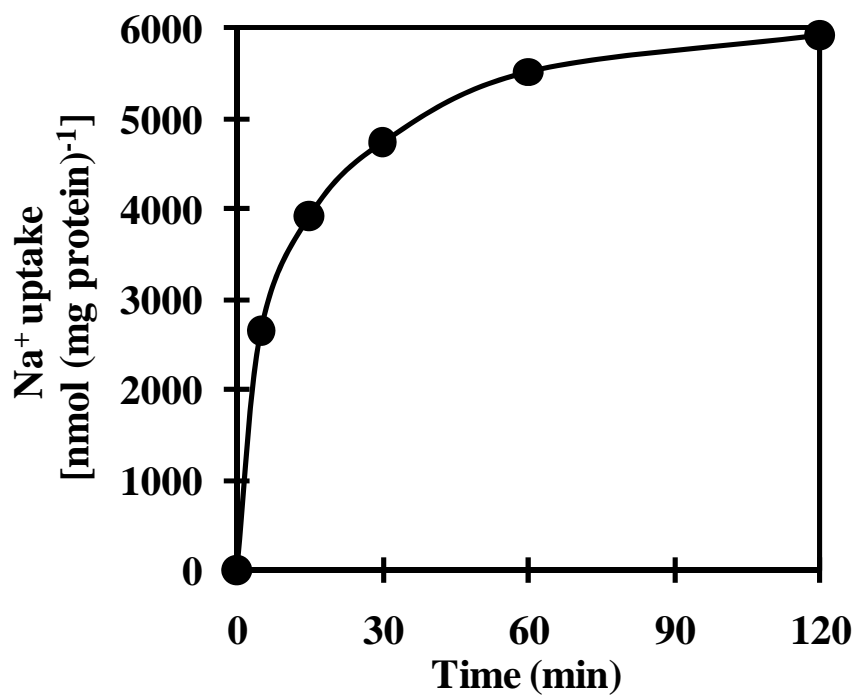


Figure 26 Na^+ uptake into proteoliposomes at various incubation times. The proteoliposomes 0.03 mg were incubated in 20 mM Tris-HCl, pH 7.6, 5.7 mM $^{22}\text{NaCl}$ ($0.0789 \mu\text{Ci } \mu\text{mol}^{-1}$) for 5, 30, 60, 120 min. The uptake reaction was started by the addition of 4 mM ATP (Tris salt).

4.6.7 Dependence of Na⁺ and ATP on Na⁺ uptake into proteoliposomes

The transport of Na⁺ into proteoliposomes reconstituted with ATPase increased with increasing concentration of NaCl with an apparent saturation at about 10 mM NaCl (Figure 27A) and the apparent K_m value for Na⁺ of 3.3 mM (Figure 27A, inset). Moreover, Na⁺ accumulated in proteoliposomes after the addition of ATP while no significant uptake of Na⁺ was detected in the absence of ATP (Figure 27B). An increase in ATP concentration resulted in an increase of Na⁺ transport reaching saturation at about 4 mM ATP. The apparent K_m value for ATP was estimated to be 0.5 mM (Figure 27B, inset).

4.6.8 Effect of effectors on Na⁺ uptake into proteoliposomes

The time course of Na⁺ uptake into proteoliposomes reconstituted with purified ATPase is shown in Figure 28. In the absence of ATP, Na⁺ uptake was very low but upon the addition of ATP the uptake was significantly accelerated. The ATP-dependent Na⁺ uptake was strongly inhibited by gramicidin D and monensin while a protonophore CCCP and the permeant anion nitrate stimulated the uptake of Na⁺.

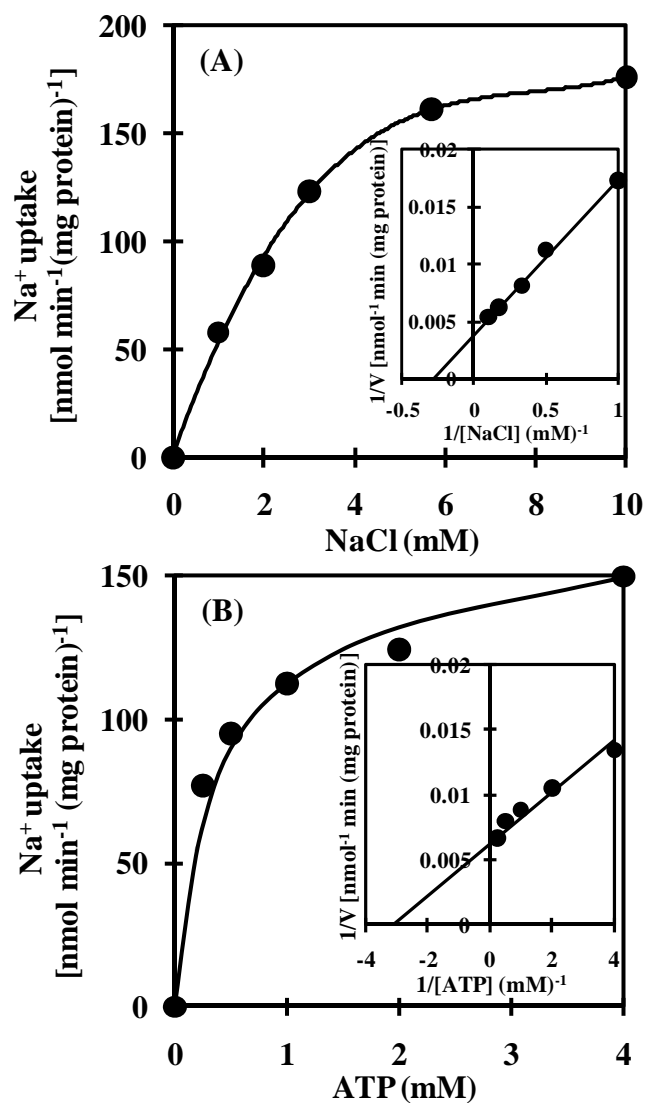


Figure 27 Na⁺ uptake into proteoliposomes at various NaCl and ATP concentrations. Na⁺ uptake was measured in 20 mM Tris-HCl pH 7.6 containing 5 mM MgCl₂ and various concentrations of ²²NaCl (80 μCi mmol⁻¹) (A) and ATP (B). The uptake reaction was started by the addition of 4 mM ATP (Tris salt). Insets in (A) and (B) show double-reciprocal plots of Na⁺ uptake versus NaCl and ATP concentration, respectively.

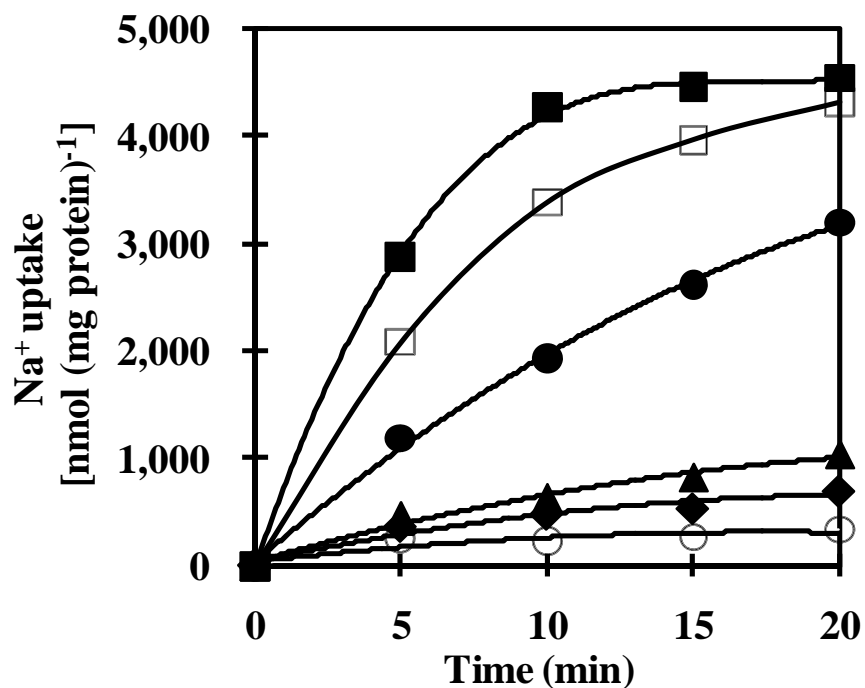


Figure 28 Time course of Na⁺ uptake into proteoliposomes in the presence of effectors. Na⁺ uptake into proteoliposomes was measured in 20 mM Tris-HCl pH 7.6 containing 5 mM MgCl₂ and 5.7 mM ²²NaCl (80 μCi mmol⁻¹) at times indicated in the presence (●) and absence (○) of 4 mM ATP and in the presence of 4 mM ATP with 0.05 mM CCCP (■), 100 mM KNO₃ (□), 0.1 mM monensin (◆), 0.01 mM gramicidin D (▲). Effectors were added at 10 min before starting the reaction with ATP.

4.6.9 Detection of H⁺ efflux from proteoliposomes

In order to investigate whether Na⁺ uptake into proteoliposomes is accompanied with H⁺ efflux from proteoliposomes, alkalization of the proteoliposome lumen was detected using the Δ pH probe acridine orange with a pK_a of 10.45. Addition of ATP to the reaction medium containing NaCl at 100 mM initiated H⁺ efflux from proteoliposome lumen to the outer medium (Figure 29A). This H⁺ efflux was ATP concentration-dependent. The protonophore CCCP induced ATP-dependent lumen alkalization while the permeant anion nitrate suppressed ATP-dependent lumen alkalization. When Na⁺ in the reaction medium was replaced with K⁺, Li⁺ and Ca²⁺, the ATP-dependent alkalization of proteoliposome lumen was not observed (Figure 29B).

4.6.10 Detection of membrane potential generated by proteoliposomes

To investigate the nature of coupling of Na⁺ and H⁺ fluxes upon the addition of ATP to proteoliposomes reconstituted with the purified ATPase, the role of membrane potential in the ATP-dependent H⁺ translocation was studied with a voltage-sensitive probe oxonol VI. Figure 30A shows the generation of membrane potential (positive inside the proteoliposome lumen) upon the addition of ATP to the reaction medium containing 8 mM NaCl. The generation of membrane potential was further enhanced when 100 mM NaCl was added. These results indicated that the membrane potential was built up by the operation of a Na⁺-stimulated ATPase. On the contrary, both the protonophore CCCP and the permeant anion nitrate collapsed the membrane potential built up by Na⁺-stimulated ATPase. Figure 30B shows that the increase in membrane potential generation was Na⁺ concentration-dependent.

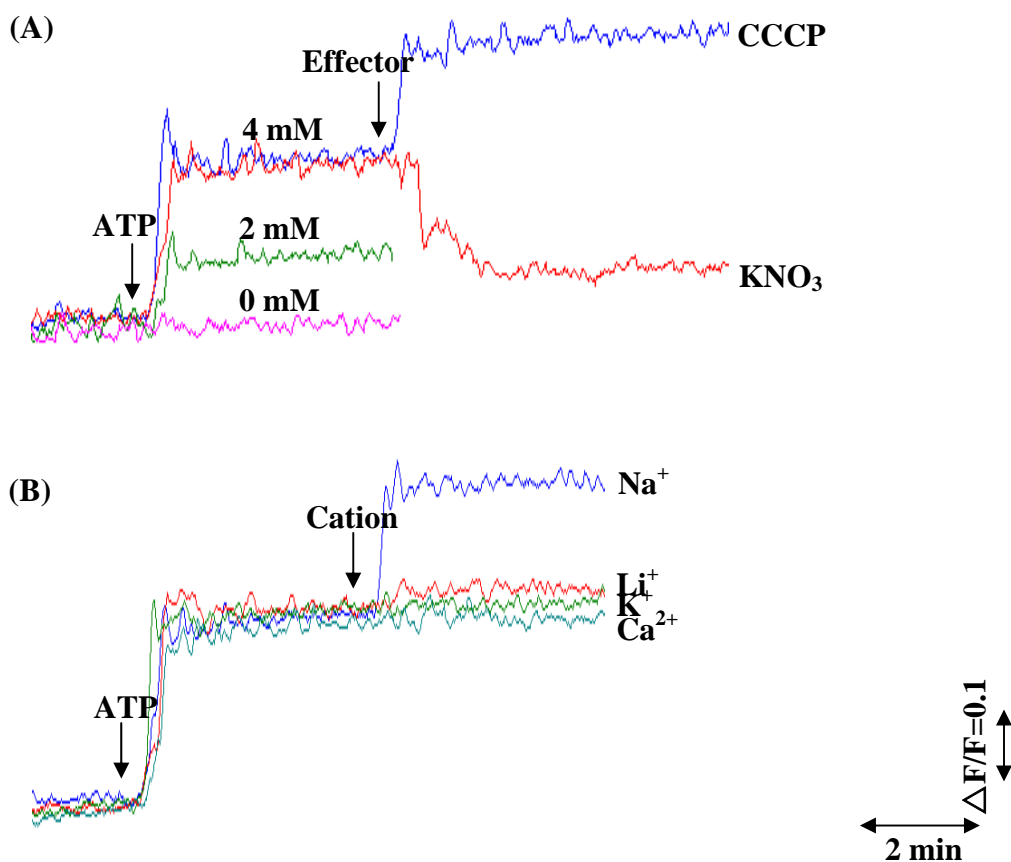


Figure 29 Changes in ΔpH of proteoliposome lumen detected with ΔpH probe acridine orange. (A) Effect of NaCl, ATP and effectors (CCCP and permeant anion NO_3^-) on alkalization of proteoliposome lumen. Proteoliposomes were incubated in the reaction mixture containing 0.5 M sorbitol, 10 mM Hepes-Tris buffer pH 7.6, 1 μM acridine orange and proteoliposomes (25 μg protein). After 15 min incubation of proteoliposomes in the mixture, the reaction was run by the addition of NaCl, ATP at various concentrations and effectors (CCCP at 12 μM or KNO_3 at 100 mM) as shown by the arrows. (B) Effect of cations on alkalization of proteoliposome lumen. NaCl was initially present in the reaction mixture at the concentration of 8 mM. The reaction was run by the addition of ATP at 4 mM and cations (chloride salts) at 100 mM as shown by the arrows.

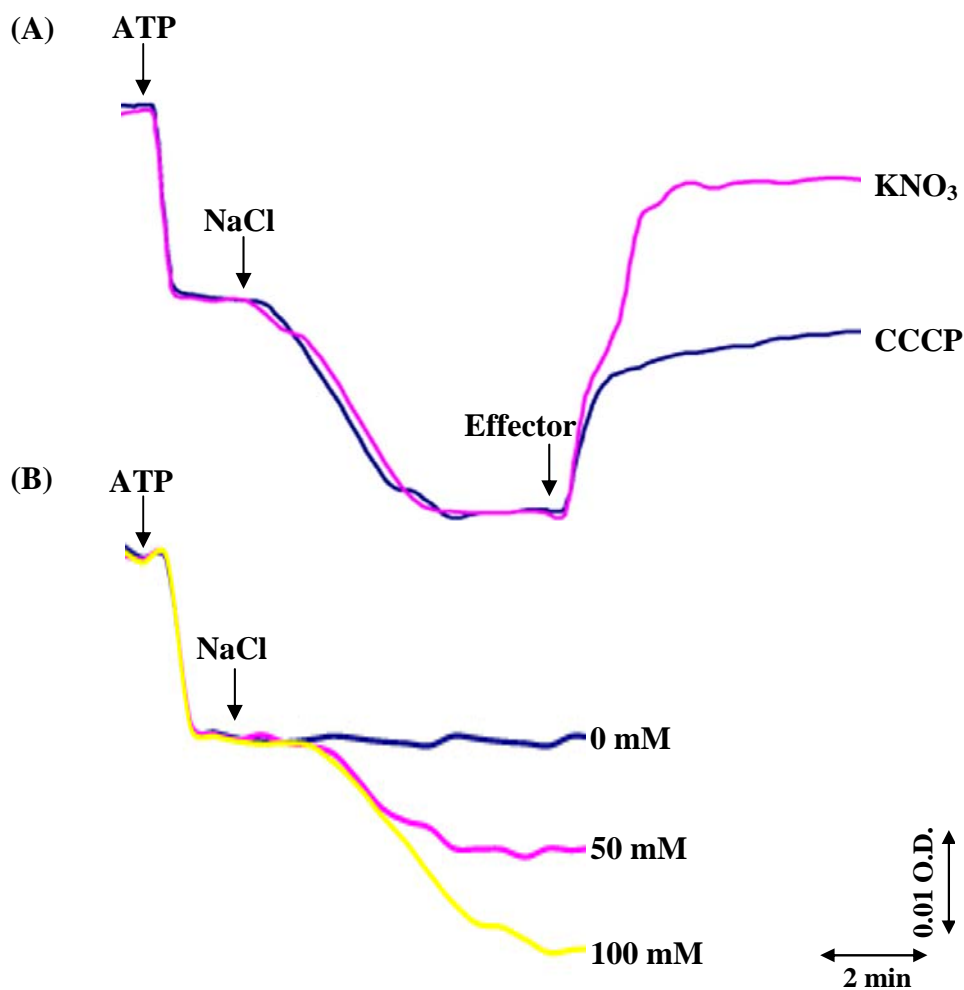


Figure 30 Changes in membrane potential across proteoliposome detected with voltage-sensitive probe oxonol VI. (A) Effect of CCCP and the permeant anion NO_3^- on the membrane potential across proteoliposome built up in the presence of ATP and Na^+ . The solution of 8 mM NaCl was initially present in the reaction mixture containing 0.4 M sucrose, 20 mM HEPES-Tris buffer pH 7.6, 1 mM MgSO_4 , 3 μM oxonol VI and proteoliposomes (25 μg of protein). The reaction was initiated by adding ATP at 4 mM, NaCl at 100 mM, CCCP at 12 μM or KNO_3 at 100 mM as shown by the arrows. (B) Effect of NaCl concentration on the membrane potential across proteoliposome. NaCl was initially present in the reaction mixture at the concentration of 8 mM. The reaction was initiated by adding ATP at 4 mM and NaCl at various concentrations as shown by the arrows.

4.7 Gene organization in the *ApNa⁺-atp* operon

From the shotgun sequence analysis of the *A. halophytica* genome, we found a putative F-type *ApNa⁺-atp* operon in addition to the typical H⁺-ATPase (*ApH⁺-ATPase*) operon (*ApH⁺-atp*). The *ApNa⁺-atp* operon had nine open reading frames (ORFs), each having a putative start codon. These genes were organized in the order *atpD* (β), *atpC* (ϵ), *atpI* (I), hypothetical gene (hypothetical protein), *atpB* (a), *atpE* (c), *atp F* (b), *atpA* (α), and *atp G* (γ) (Figure 31A). By contrast, gene organization of *ApH⁺-atp* splits into two clusters, encoding $Iacbb'\delta\alpha\gamma$ and $\beta\epsilon$ (Figure 31B). The gene organization of *ApNa⁺-atp* is similar to those of the *atp* operons in *E. coli* (*EcH⁺-atp*) (Moriyama *et al.*, 1991; Walker *et al.*, 1982) and *Ilyobacter tartaricus* (*ItNa⁺-atp*) (Walker *et al.*, 1982) that encode F-type H⁺- and Na⁺-ATPases, respectively. On the contrary, *EcH⁺-atp* and *ItNa⁺-atp*, the operon starts from gene I and does not contain the hypothetical gene (Figure 31C, D). Blast search revealed the presence of a similar operon in some cyanobacteria, such as *Synechococcus* sp. PCC 7002, *Acaryochloris marina* MBIC11017, and *Cyanothece* sp. ATCC 51142 (Figure 31E). Among them, *Synechococcus* sp. PCC 7002 had the same gene organization to that of *ApNa⁺-atp*, whereas in *A. marina* MBIC 11017 and *Cyanothece* sp. ATCC 51142 additional gene(s) were found. The deduced protein sequences of the nine genes, except the gene encoding hypothetical protein, were compared with the corresponding sequences of ATPase subunits from different species (Table 8). The protein encoded by *ApNa⁺-atpI* showed the least homologous (4-7% identity) compared with the corresponding subunit of H⁺-transporting ATPase from *E. coli* and Na⁺-transporting ATPase from *Ilyobacter tartaricus*, *Propionigenium modestum*, *Acetobacterium woodii*, and *Clostridium paradoxum*. The α and β subunits of *ApNa⁺-ATPase* showed greater

similarity to the corresponding subunits from other species (40-51% identity) than the remaining subunits which showed about 15-39% identity.

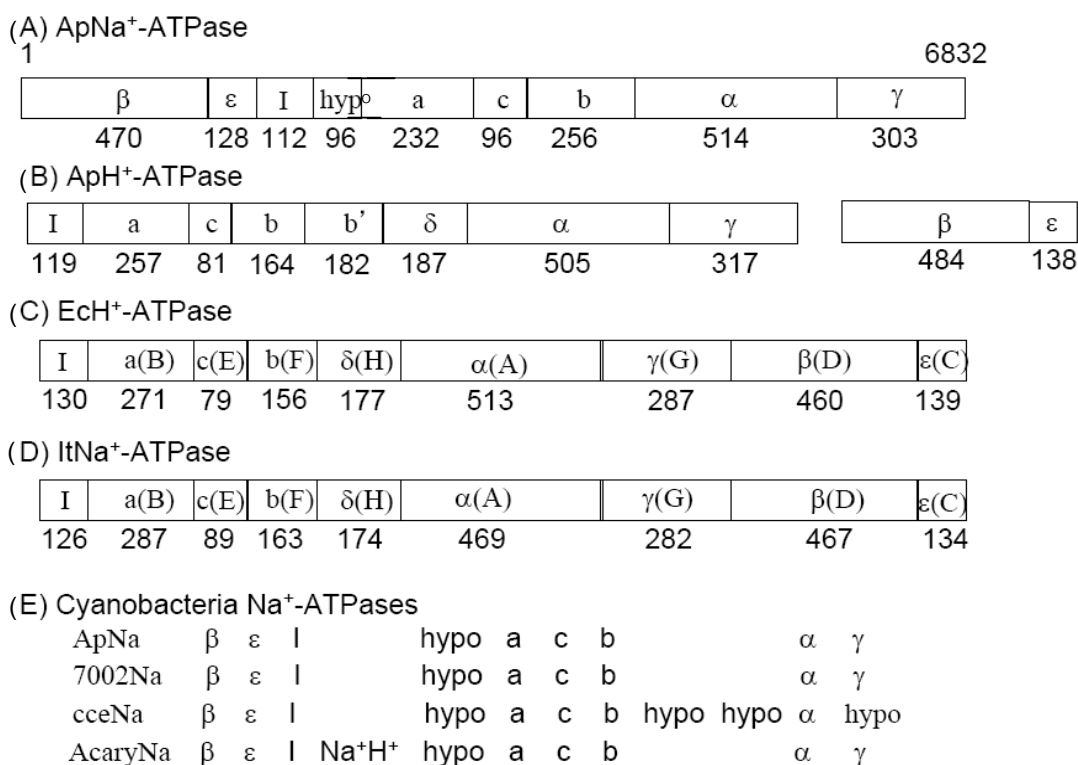


Figure 31 Schematic structures of gene organization of several ATP synthases. (A) ApNa⁺-ATPase (*A. halophytica*, AB602793); (B) ApH⁺-ATPase (*A. halophytica*, AB602794, AB602795); (C) EcH⁺-ATPase (*E. coli*, J01594); (D) ItNa⁺-ATPase (*I. tartaricus*, AF522463); and (E) four kinds of cyanobacterial Na⁺-ATPases. In (A), (B), and (E), names of encoded proteins are shown. In (C) and (D), both genes and encoded-proteins are shown. In (E), ApNa, 7002Na, cceNa, and AcaryNa show the putative Na⁺-ATPases from *A. halophytica* (AB602793), *Synechococcus* sp. PCC7002 (SYNPCC7002_G0144-0152), *Cyanothece* sp. ATCC 51142 (cce_1502-1512), and *Acaryochloris marina* (AM1_D0157-0167), respectively. The numbers of amino acid residues in each subunit are shown below boxes. “Hypo” in (A, E) and “Na⁺H⁺” in (E) represent “hypothetical protein” and Na⁺/H⁺ antiporter, respectively.

Table 8 Comparison of the protein sequences encoded by nine Na^+ -*atp* gene from *A. halophytica* with the corresponding of ATPase subunits from various organisms including Na^+ -ATPase from *I. tartaricus* (AF522463), *P. modestum* (X58461), *A. woodii* (U10505), *C. paradoxum* (DQ193538) and H^+ -ATPase from *E. coli* (J01594).

Gene	Subunit	Amino acids	Calculated Mol wt	% Identity				
				<i>I. tartaricus</i>	<i>P. modestum</i>	<i>A. woodii</i>	<i>C. paradoxum</i>	<i>E. coli</i>
<i>atpD</i>	β	470	54,050	51	51	49	51	51
<i>atpC</i>	ϵ	128	14,720	15	17	18	21	15
<i>atpI</i>	I	112	12,880	4	5	7	6	7
hypothetical gene	hypothetical protein	96	11,040	ND	ND	ND	ND	ND
<i>atpB</i>	a	232	26,680	24	25	23	27	19
<i>atpE</i>	c	96	11,040	30	30	39	33	25
<i>atpF</i>	b	256	29,440	15	15	15	17	18
<i>atpA</i>	α	514	59,110	49	52	40	50	41
<i>atpG</i>	γ	303	34,845	24	26	21	22	24

Figure 32 shows the phylogenetic tree of β subunit of H^+ - and Na^+ -translocating ATPases from several species. It was found that β subunit of ApH^+ -ATPase exhibited high homology to the cyanobacterial H^+ -ATPases from *Synechococcus* sp. PCC 7002, *A. marina* MBIC 11017, and *Cyanothece* sp. ATCC 51142. It also exhibited high homology to that of spinach chloroplast H^+ -ATPase, supporting the view that the plant chloroplast originated through endosymbiosis from a cyanobacterium. The β subunit of $ApNa^+$ -ATPase exhibited high homology to the Na^+ -ATPases from *Synechococcus* sp. PCC 7002, *Acaryochloris marina* MBIC 11017, and *Cyanothece* sp. ATCC 51142, but relatively low homology to subunit B of A-type ATPase from *Methanosarcina mazei* Go1 and V-type ATPase from *Enterococcus hirae*. This result suggests that F-type cyanobacterial Na^+ -ATPases evolved earlier than the separation between cyanobacteria, *E. coli*, and *I. tartaricus*.

ApNa⁺-ATPase has putative Na⁺-binding site in subunit *c*. The membrane-spanning helices of the multiple copies of subunit *c* in the F₀ complex are the rotor ring of H⁺ (or Na⁺)-translocating ATP synthases (von Ballmoos *et al.*, 2009). Figure 33A shows the phylogenetic tree of subunit *c* in several ATPases. Subunit *c* of ApH⁺-ATPase exhibited high homology to that of cyanobacterial H⁺-ATPase and spinach H⁺-ATPase, but was considerably different from that of ApNa⁺-ATPase, which is similar to the phylogenetic tree of β subunit. Figure 33B shows the alignment of subunit *c* of several F-type ATPases. Based on the x-ray crystallography, cryo-electron microscopy, and atomic force microscopy studies, the binding sites for H⁺ and Na⁺ have been identified (von Ballmoos *et al.*, 2009; Meier *et al.*, 2003). The H⁺-binding site (Q34, E67, T70, and Y72) was conserved in all cyanobacterial H⁺-translocating ATPases (Figure 33B). Furthermore, the Phe (F65) seems to be conserved in all cyanobacterial H⁺-translocating ATPases. For Na⁺ binding site, E67, S68, T69 and Y72 were conserved in all cyanobacterial Na⁺-translocating ATPases. However, the Gln (Q34) changed to Glu (E34) in all cyanobacterial Na⁺-ATPases except Na⁺-ATPase in bacteria *I. tartaricus* and *P. modestum*. These results indicate that ApH⁺-ATPase presumably H⁺-translocating ATPases, although ion specificity of ApNa⁺-ATPase need to be tested experimentally.

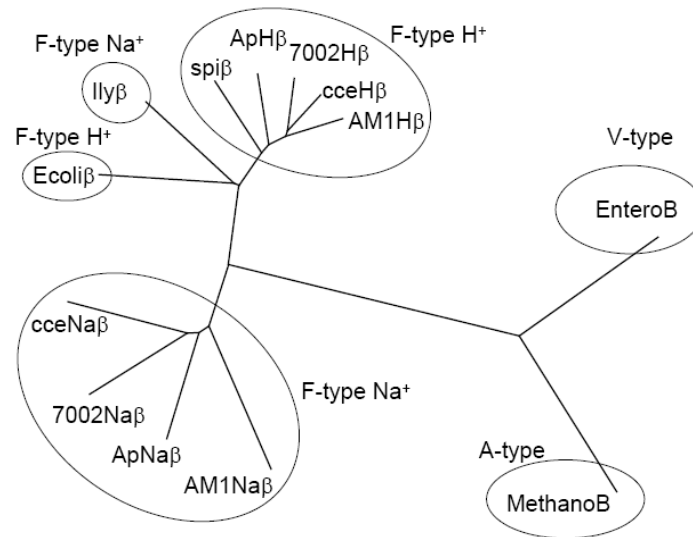


Figure 32 Phylogenetic trees for β subunit of H^+ - and Na^+ -translocating ATPases from several species. F-type Na^+ translocating β -subunits, ApNa β (*A. halophytica*, AB602793), cceNa β (*Cyanothece* sp. ATCC 51142, cce_1512), 7002Na β (*Synechococcus* sp. PCC7002, SYNPPCC7002_G0144), AM1Na β (*Acaryochloris marina*, AM1_D0157), and IlyNa β (*Ilyobacter tartaricus*, AF522463). F-type H^+ translocating β -subunits, ApH β (*A. halophytica*, AB602795), cceH β (*Cyanothece* sp. ATCC 51142, cce_2813), 7002H β (*Synechococcus* sp. PCC7002, SYNPPCC7002_A0749), AM1H β (*Acaryochloris marina*, AM1_5328), and spi β (spinach, NP_054943). A-type β -subunit of *Methanosarcina mazei*, MethanoB (NP_632803.1) and V-type β -subunit of *Enterococcus faecalis*, Entero B (NP_815220.1).

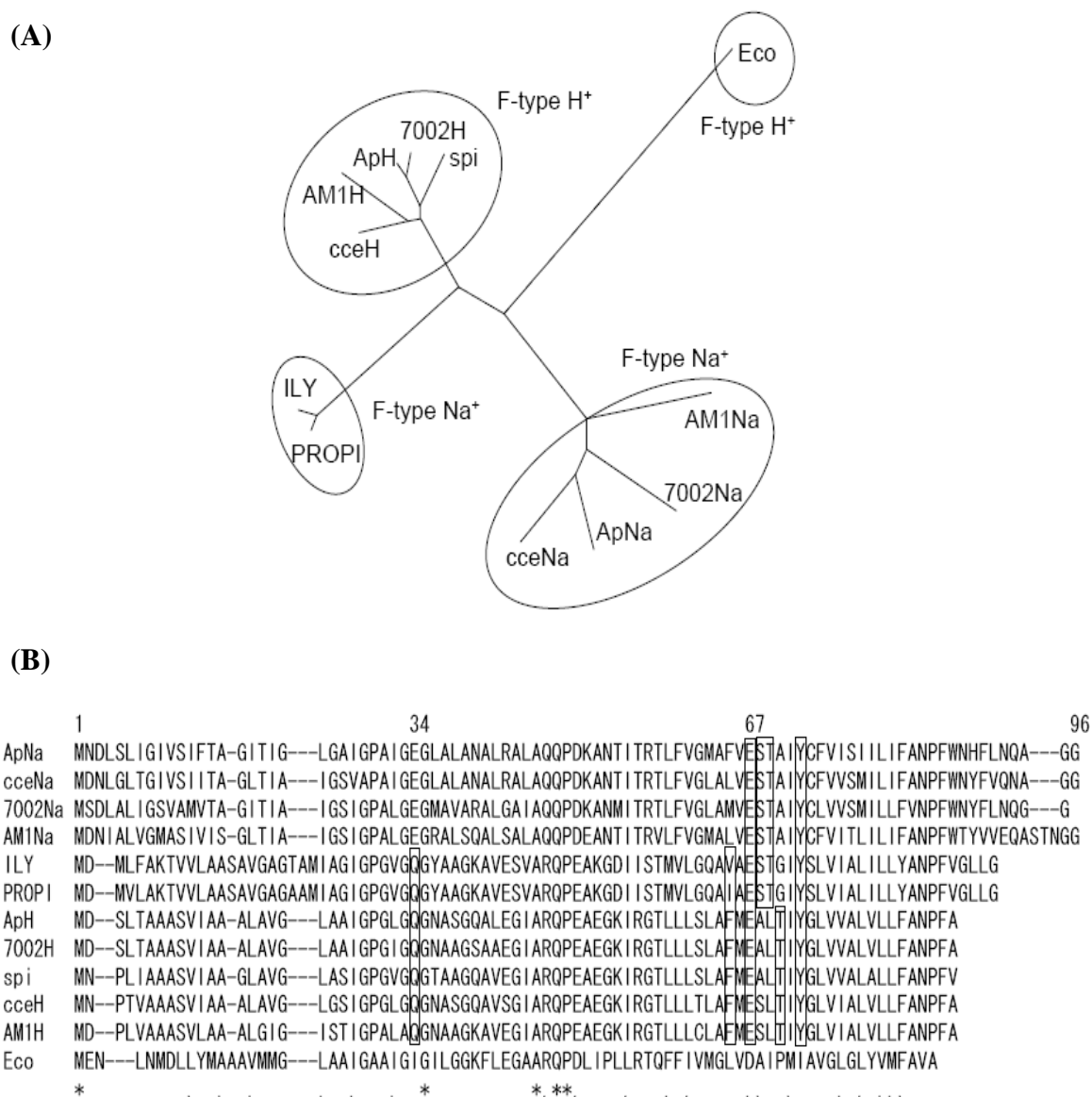


Figure 33 (A) Phylogenetic trees for c subunit of H^+ - and Na^+ -translocating ATPases from several species. PROPI shows the Na^+ -ATPases from *Propionigenium modestum* (X53960). (B) Alignment of c subunit sequences of H^+ - and Na^+ -translocating ATPases from several species.

4.8 Cloning of F-type *ApNa⁺-atp* operon from *A. halophytica*

To clone the *ApNa⁺-atp* operon, primers ApATPaseBamHI-F and ApATPaseSalI-R (Table 1) were used for amplification. The PCR amplification was performed as follows: 35 cycles of 30 s at 94 °C, 30 s at 52 °C and 7 min at 68 °C. The obtained PCR product of 6,854 bp containing 6,832-bp coding region in which GTG start codon in *atpD* was changed to ATG for improving the expression efficiency in *E. coli* (Figure 34). The PCR product was cloned into the *EcoRV* restriction site of pBSK+ vector (Figure 35) and sequenced. Although one nucleotide change from GAG (Glu41) to GAT (Asp41) was found in beta subunit, this clone was used for further experiments. Moreover, the recombinant plasmid was cut check with *BamHI+SalI*, *PvuII*, *NcoI* and digestion pattern were shown in Figure 36. For construction of the expression plasmid of pTrcHis2C-*ApNa⁺-atp*, the recombinant plasmid pBSK+-*ApNa⁺-atp* was digested with *BamHI* and *SalI* to obtain a 6854-bp *ApNa⁺-atp* operon fragment and then this fragment was run and eluted from the gel. After that *ApNa⁺-atp* operon fragment was subcloned into the *BamHI/SalI* sites of pTrcHis2C expression vector (Figure 37). The last gene, *atpG* encoding γ subunit, was fused in frame with 6xHis-tag.

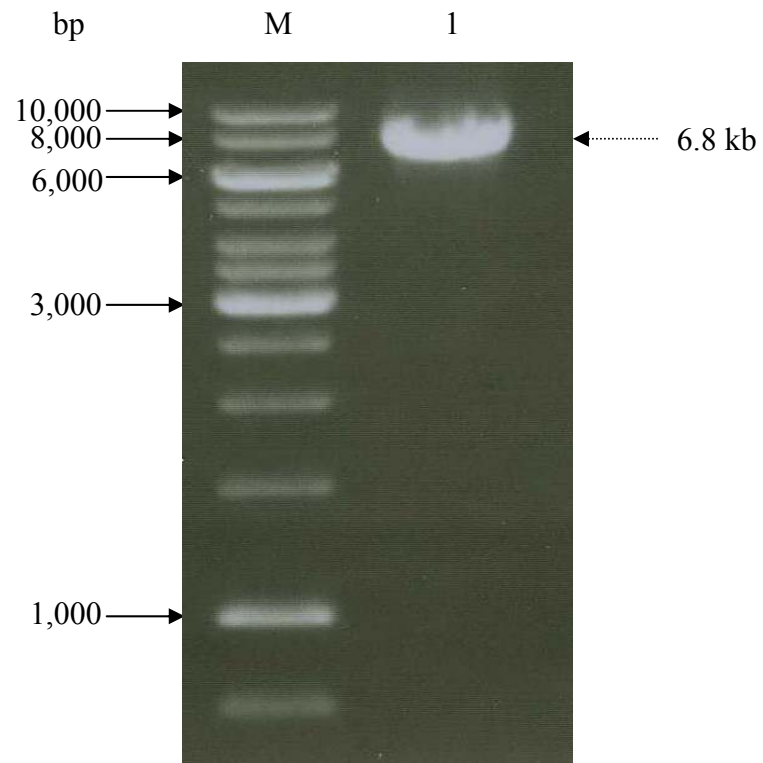


Figure 34 1% agarose gel electrophoresis of the 6.8-kb PCR product of *ApNa⁺-atp* operon (lane 1) and DNA marker (lane M).

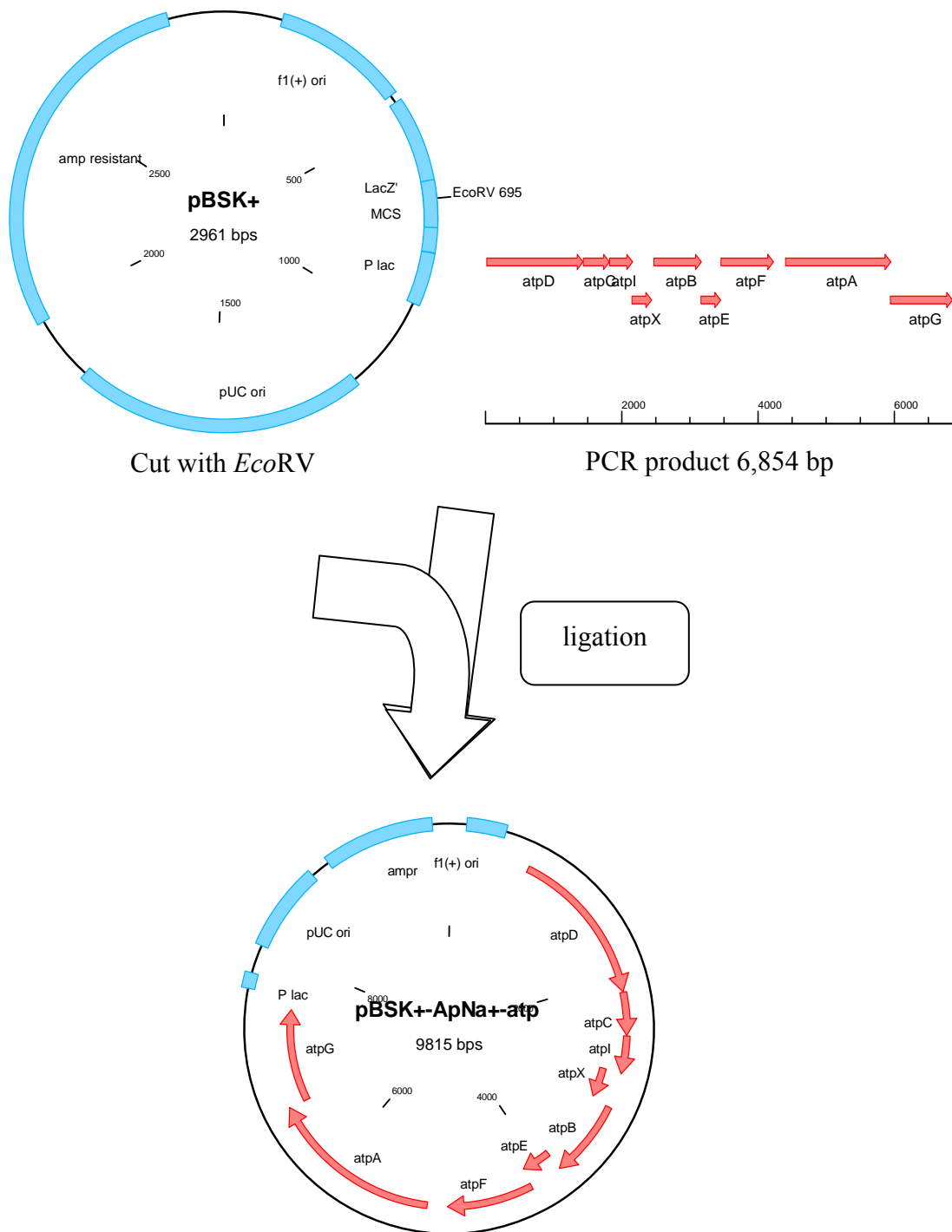


Figure 35 Schematics of the construction of recombinant plasmid **pBSK+-*ApNa*⁺-*atp***. The 6.8-kb PCR product was ligated into the *EcoRV* site of pBSK+ plasmid and then transformed into *E. coli* DH5 α .

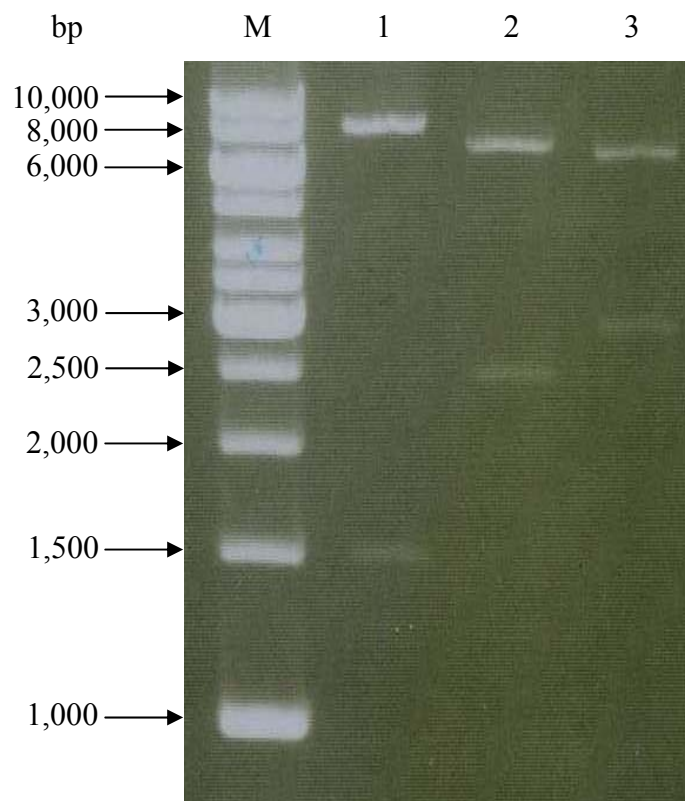


Figure 36 1% agarose gel electrophoresis of the recombinant plasmid pBSK⁺-ApNa⁺-atp cut with *Nco*I (product size 1,522+8,293) (lane 1), *Pvu*II (product size 7,302+2,513) (lane 2), *Bam*HI+*Sal*I (product size 6,848+2,916+27+24) (lane 3) and DNA marker (lane M).

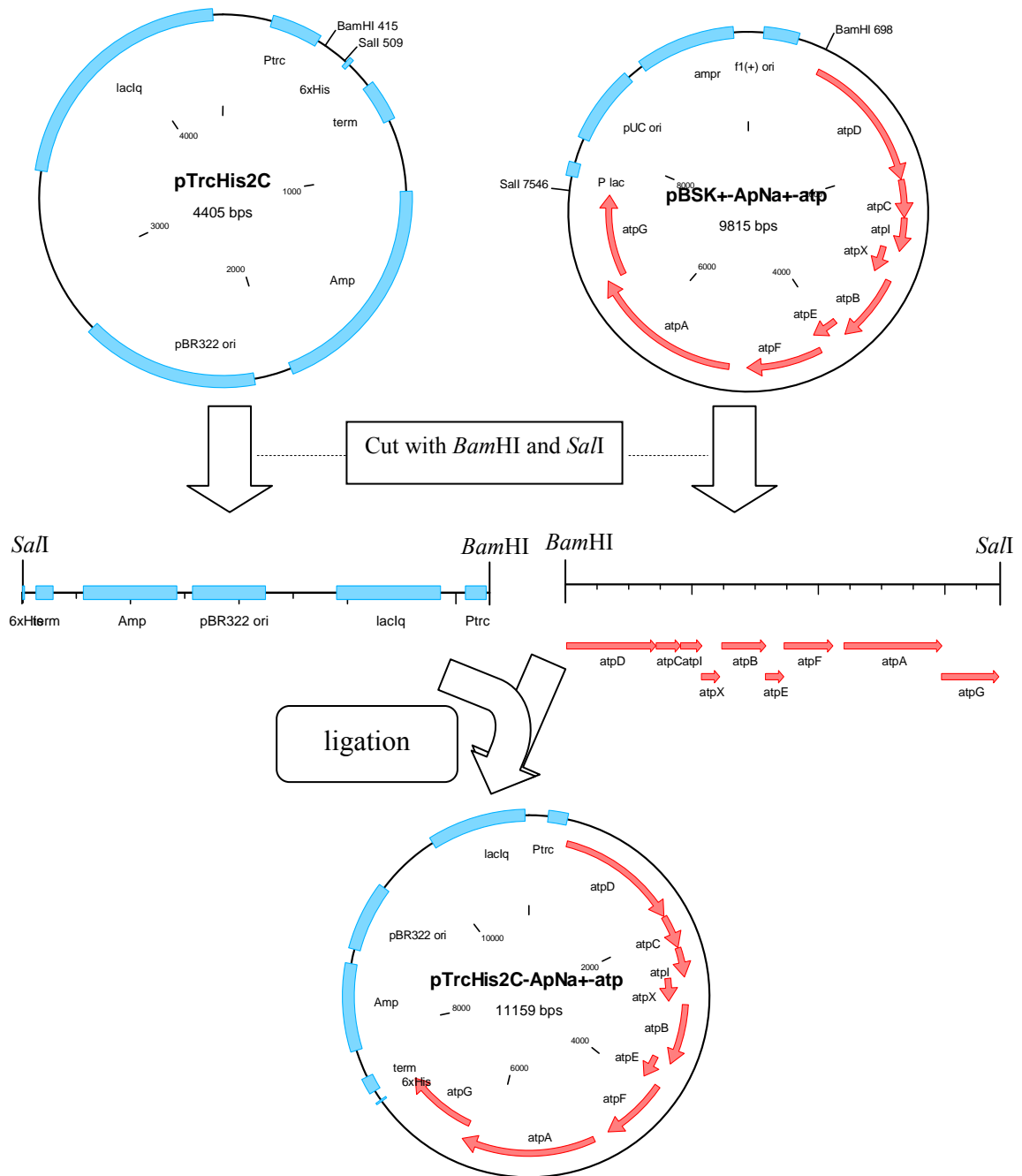


Figure 37 Schematics of the construction of recombinant plasmid *pTrcHis2C-ApNa⁺-atp*. The recombinant plasmid *pBSK⁺-ApNa⁺-atp* was digested with *Bam*HI and *Sal*I. The cohesive end fragment was ligated into *Bam*HI and *Sal*I site of the digested *pTrcHis2C* expression vector. The obtained recombinant plasmid, *pTrcHis2C-ApNa⁺-atp*, was then transformed into *E. coli* DH5 α , *E. coli* DK8 (Δatp) and *E. coli* TO114 (salt-sensitive mutant).

4.9 Characterization of ApNa⁺-ATPase expressed in *E. coli* DK8 and *Synechococcus* sp. PCC 7942 cells

4.9.1 Effect of NaCl on the growth of *E. coli* DK8 transformants

The physiological role of ApNa⁺-ATPase, namely the NaCl-stress tolerance in *E. coli* DK8 transformants was investigated. As shown in Figure 38, *E. coli* DK8 cells transformed with pTrcHis2C (empty vector transformants) and pTrcHis2C-ApNa⁺-atp (ApNa⁺-ATPase-expressing cells) exhibited similar growth patterns in LB medium in the absence of NaCl. An increase in the NaCl concentration up to 0.2 M and 0.5 M NaCl resulted in slow growth of all cells. However, the growth rate of ApNa⁺-ATPase-expressing cells was higher than that of empty vector transformants.

4.9.2 Effect of NaCl on the growth of *E. coli* TO114 transformants

The effect of NaCl on growth of a salt-sensitive mutant *E. coli* TO114, in which *nhaA*, *nhaB* and *chaA* genes were deleted, was determined. The *E. coli* TO114 cells transformed with pTrcHis2C-ApNa⁺-atp (ApNa⁺-ATPase-expressing cells) grew in LBK medium containing 0.2 M NaCl, whereas the *E. coli* TO114 cells transformed with pTrcHis2C (empty vector transformants) did not (Figure 39).

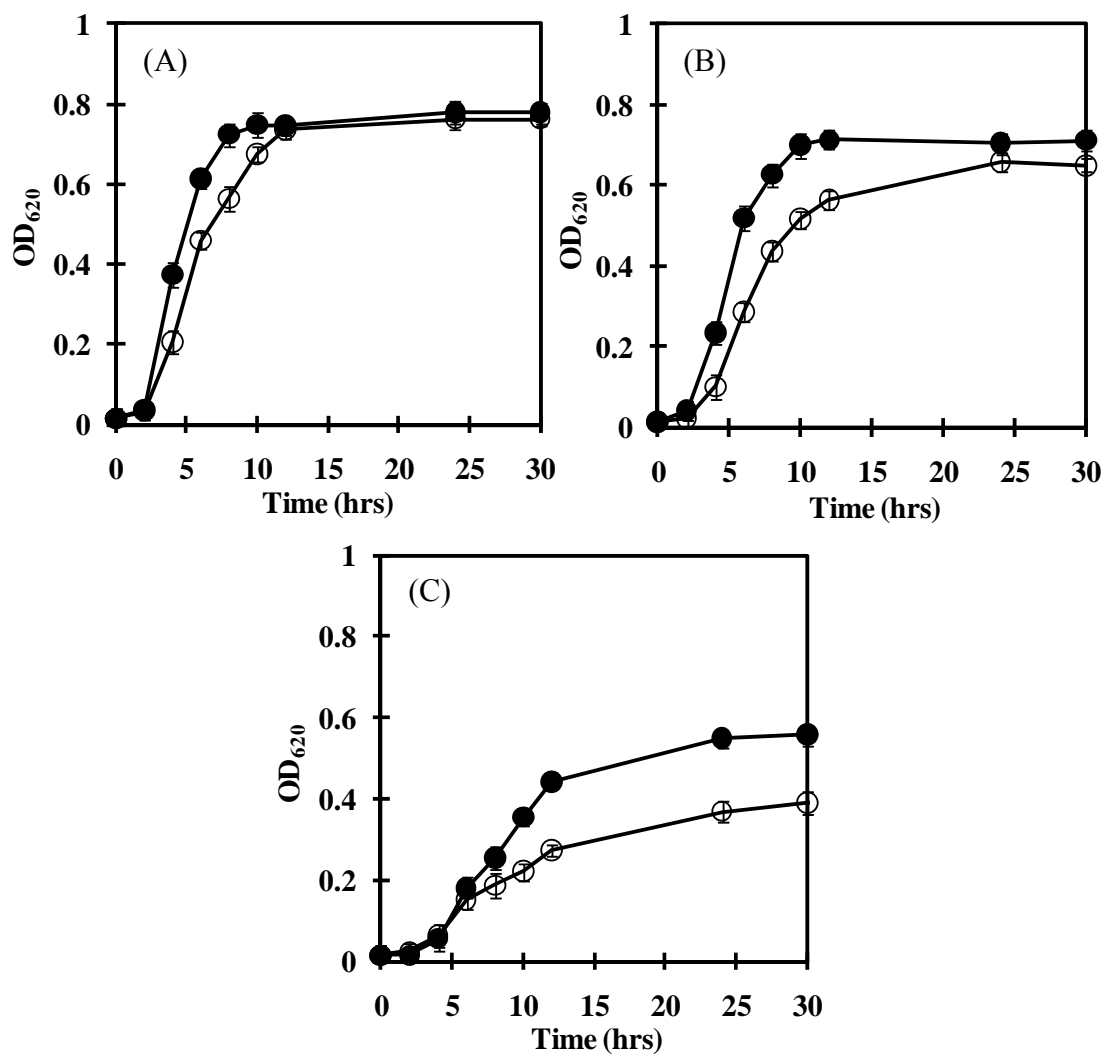


Figure 38 Effect of NaCl on the growth of *E. coli* DK8 transformants. *E. coli* DK8 transformants were grown in LB medium containing 0.0 M NaCl (A), 0.2 M NaCl (B) or 0.5 M NaCl (C). (○) represent the empty vector transformants, whereas (●) represent the ApNa⁺-ATPase-expressing cells. Each value shows the average of three independent measurements.

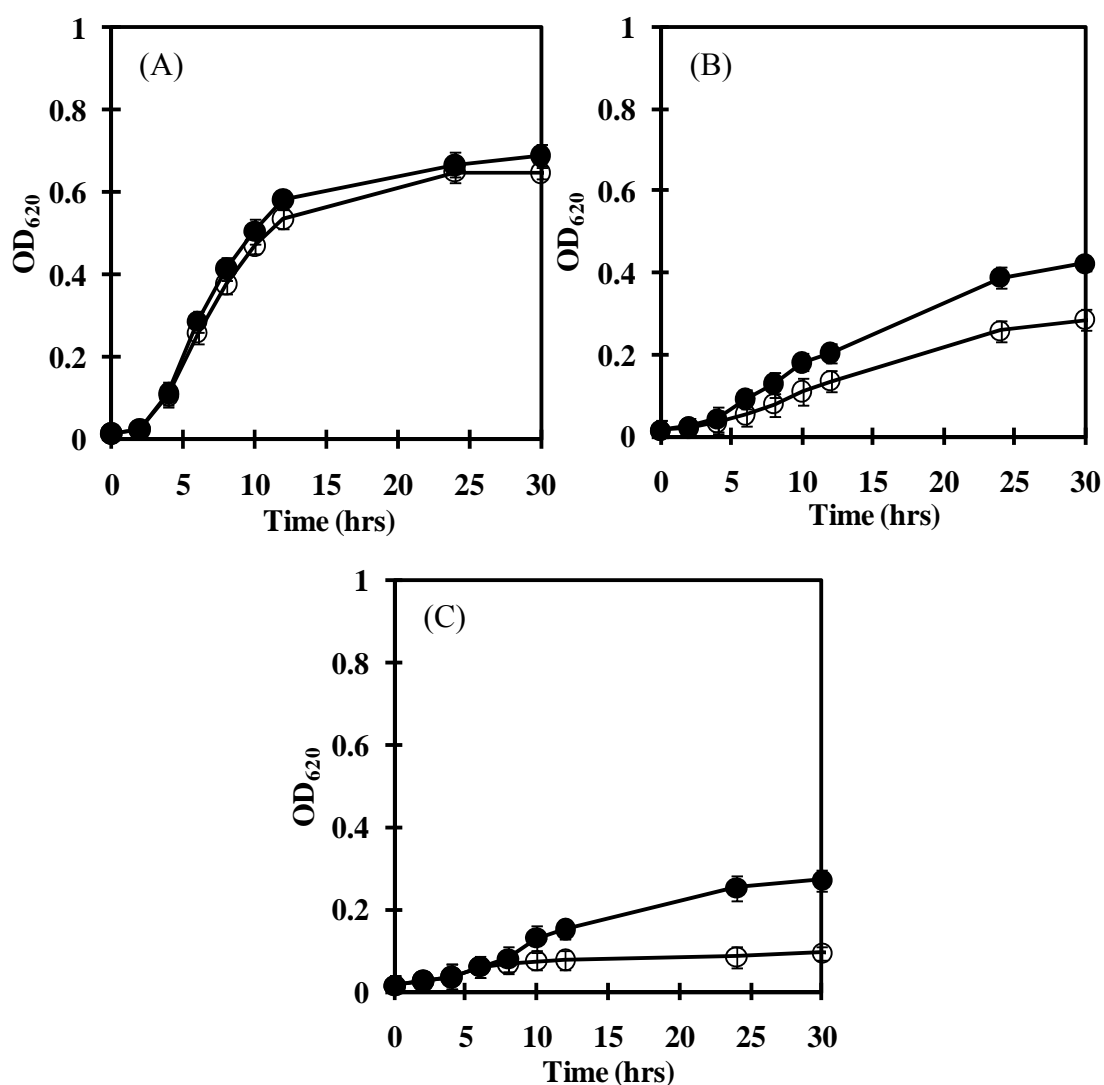


Figure 39 Effect of NaCl on the growth of *E. coli* TO114 transformants. *E. coli* TO114 transformants were grown in LBK medium containing 0.0 M NaCl (A), 0.1 M NaCl (B) or 0.2 M NaCl (C). (○) represent the empty vector transformants, whereas (●) represent the ApNa⁺-ATPase-expressing cells. Each value shows the average of three independent measurements.

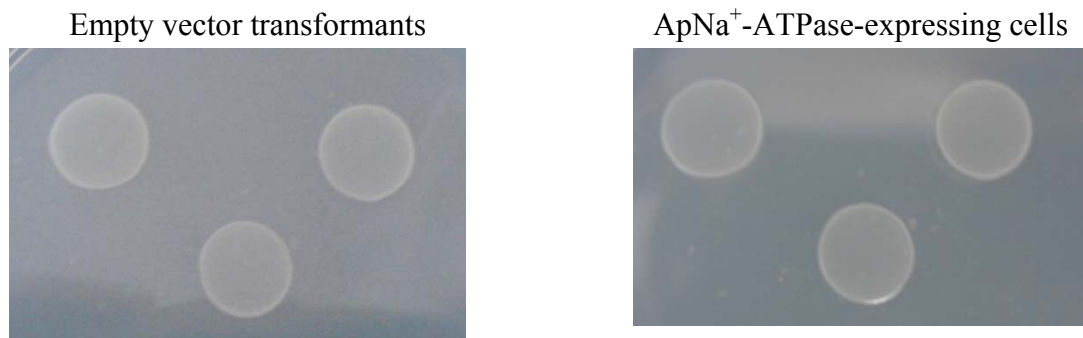
4.9.3 Growth of *E. coli* DK8 transformants on M13 minimal agar containing glucose or succinate

To determine whether *ApNa⁺-atp* could complement *E. coli* mutant DK8 (Δatp), *E. coli* DK8 cells transformed with pTrcHis2C (empty vector transformants) and pTrcHis2C-*ApNa⁺-atp* (*ApNa⁺-ATPase*-expressing cells) were plated onto M13 minimal agar containing succinate as the sole carbon and energy source. Control plates contained glucose in the same amount as succinate. Results showed that empty vector transformants could grow only on glucose while *ApNa⁺-ATPase*-expressing cells could grow on both glucose and succinate (Figure 40). Hence, the *ApNa⁺-atp* operon encoding F-type *ApNa⁺-ATPase* was able to produce *ApNa⁺-ATPase* in the host cells, supporting the growth of *E. coli* DK8 transformants on a non-fermentable carbon source.

4.9.4 Na⁺ content inside the cells of Na⁺-loaded *E. coli* DK8 transformants

To determine whether Na⁺-loaded *E. coli* DK8 transformants could extrude Na⁺ from inside to outside the cells, the Na⁺ content inside the cells of Na⁺-loaded *E. coli* DK8 transformed with pTrcHis2C (empty vector transformants) and pTrcHis2C-*ApNa⁺-atp* (*ApNa⁺-ATPase*-expressing cells) was measured. It was found that Na⁺ content inside the *ApNa⁺-ATPase*-expressing *E. coli* DK8 cells decreased when the cells were transferred to a new Na⁺-free medium, but no change in the Na⁺ content was observed inside the empty vector transformants (Figure 41). These results suggest that the *E. coli* DK8 expressing *ApNa⁺-ATPase* can extrude Na⁺ from inside the cells to the external medium.

(A) *E. coli* DK8 transformants grown on M13 minimal agar containing 35 mM glucose



(B) *E. coli* DK8 transformants grown on M13 minimal agar containing 35 mM succinate

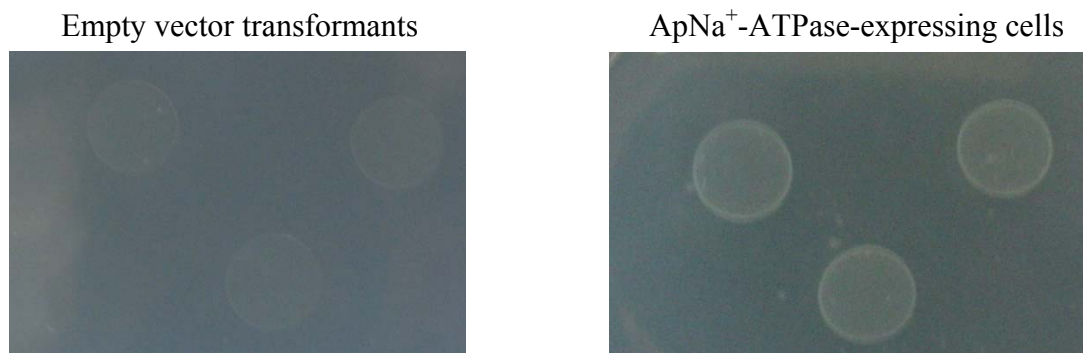


Figure 40 Complementation test of *ApNa⁺-atp* operon in *E. coli* mutant DK8 (Δatp) grown on M13 minimal agar containing 35 mM glucose (A) or succinate (B) for 2 days.

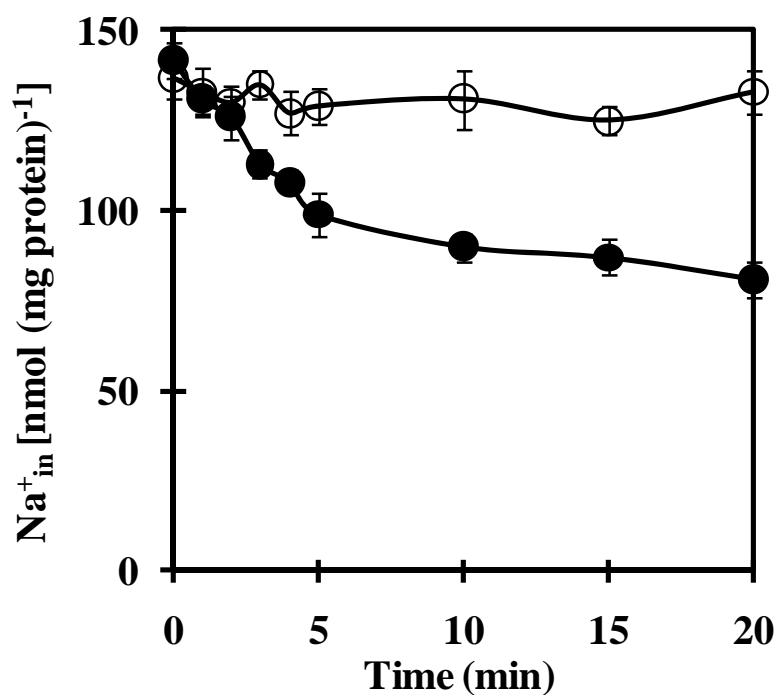


Figure 41 Extrusion of Na⁺ from Na⁺-loaded *E. coli* DK8 transformants. The transformants were grown in LB medium containing 100 $\mu\text{g ml}^{-1}$ ampicillin at 37 °C until the optical density at 620 nm reached 0.6 and then were transferred to medium containing 0.15 M NaCl. After incubation for 1 hr, the cells were collected and transferred to Na⁺-free medium in the presence of 1 mM IPTG. Ten mM of glucose was added for 10 min prior to start the extrusion of Na⁺. Symbol (○) represents the empty vector transformants, whereas (●) represents the ApNa⁺-ATPase-expressing cells. Each value shows the average of three independent measurements.

4.9.5 The effect of NaCl, ATP, Mg²⁺ and pH on ATP hydrolysis activity of inverted membrane vesicles from *E. coli* DK8 transformants

The ATP hydrolysis activity of inverted membrane vesicles from *E. coli* DK8 cells transformed with pTrcHis2C (empty vector transformants) and pTrcHis2C-*ApNa⁺-atp* (*ApNa⁺-ATPase*-expressing cells) was examined. The result showed that the ATP hydrolysis activity of inverted membrane vesicles from *ApNa⁺-ATPase*-expressing cells increased with increasing NaCl concentrations (Figure 42). The apparent K_m value for Na⁺ as determined from the Lineweaver-Burk plot was 3.0 mM (Figure 42, inset). The ATP hydrolysis activity of control cells (the empty vector transformants) was very low and did not increase upon the increase of NaCl concentrations. Figure 43A showed that the ATP hydrolysis activity from *ApNa⁺-ATPase*-expressing cells was increased when increasing ATP concentrations were done in the experiment. The apparent K_m value for ATP was determined to be 2.8 mM (Figure 43A, inset).

The dependence of *ATPase* on Mg²⁺ was also tested. Figure 43B shows that maximal ATP hydrolysis activity was observed at 5 mM Mg²⁺. The enzyme activity was decreased when the Mg²⁺ concentration was higher than 5 mM. The pH of the assay medium also influenced on the enzyme activity. When the pH was increased from pH 6.0 to pH 8.0, the enzyme activity was increased progressively (Figure 43C). The optimum pH for this enzyme was pH 8.0. Increasing the pH further to pH 11.0 resulted in a decline of enzyme activity.

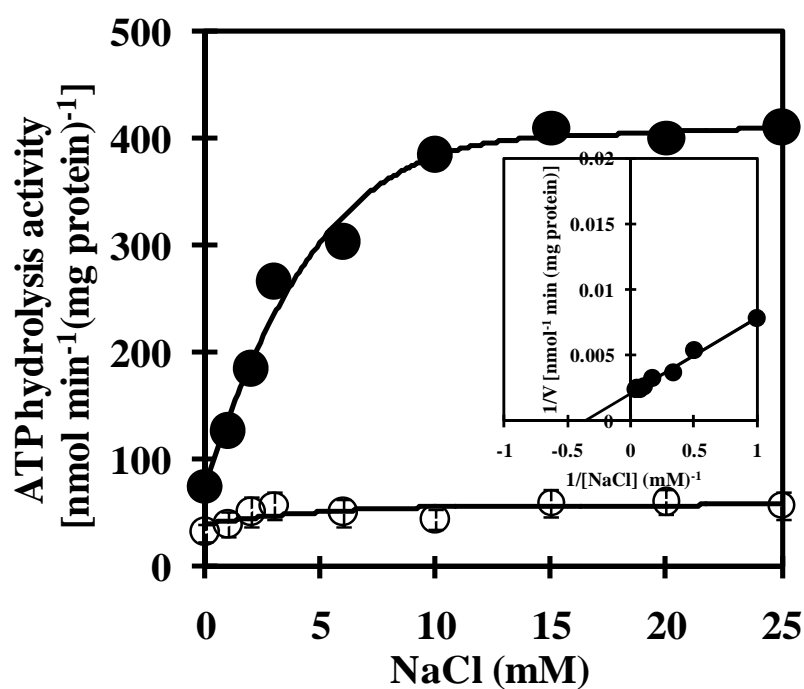


Figure 42 Effect of NaCl on ATP hydrolysis activity of inverted membrane vesicles from *E. coli* DK8 transformants. The enzyme activity was measured in the presence of various concentrations of NaCl. Inset shows a double-reciprocal plot of activity versus NaCl concentration. Symbol (○) represents the empty vector transformants, whereas (●) represents the ApNa⁺-ATPase-expressing cells. Each value shows the average of three independent measurements.

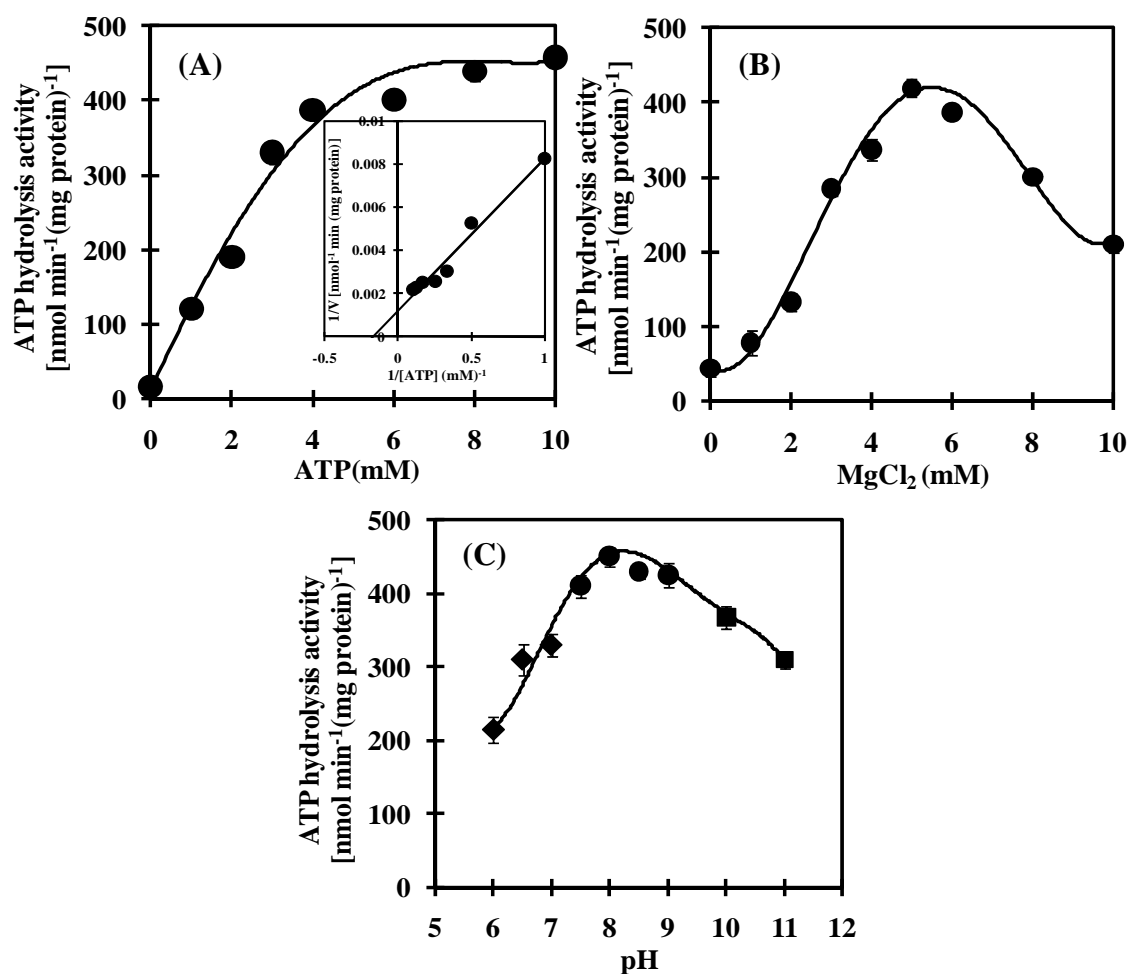


Figure 43 Effect of ATP, Mg²⁺ and pH on ATP hydrolysis activity of inverted membrane vesicles from ApNa⁺-ATPase-expressing *E. coli* DK8 cells. In (A) and (B), the enzyme activity was measured in the presence of various concentrations of ATP and MgCl₂, respectively. Inset in (A) shows a double-reciprocal plot of activity versus ATP concentration. In (C), the enzyme activity was measured at various pH values using 20 mM Mes-KOH for pH 6.0-7.0 (◆), 20 mM Tris-HCl for pH 7.5-9.0 (●) and 20 mM Glycine-KOH for pH 10.0-11.0 (■). Each value shows the average of three independent measurements.

4.9.6 The effect of inhibitors on ATP hydrolysis activity of inverted membrane vesicles from ApNa⁺-ATPase-expressing *E. coli* DK8 cells

The ATP hydrolysis activity of inverted membrane vesicles from *E. coli* DK8 cells transformed with pTrcHis2C-*ApNa⁺-atp* (ApNa⁺-ATPase-expressing cells) was inhibited by azide (F₁ inhibitor) of 55%, DCCD (F₀ inhibitor) of 70%, tributyltin chloride (F₀ inhibitor) of 80% and monensin (Na⁺-gradient dissipator) of 70% but not by CCCP (a protonophore) and KNO₃ (a permeant anion) (Figure 44). Moreover, Na⁺ provided protection against inhibition by DCCD in a pH-dependent manner. At pH 7.6, when 1, 10 and 50 mM NaCl were composed in the individual reaction medium, the inhibition of ATP hydrolysis activity by DCCD was about 70% while in the absence of NaCl, ATP hydrolysis activity was inhibited approximately 85% (Figure 45A). At pH 9.0, ATP hydrolysis activity was inhibited about 70% in the absence of NaCl. In the presence of 1 and 10 mM NaCl, ATP hydrolysis activity was inhibited by about 40% while 50 mM NaCl inhibited ATP hydrolysis activity of approximately 30% (Figure 45B).

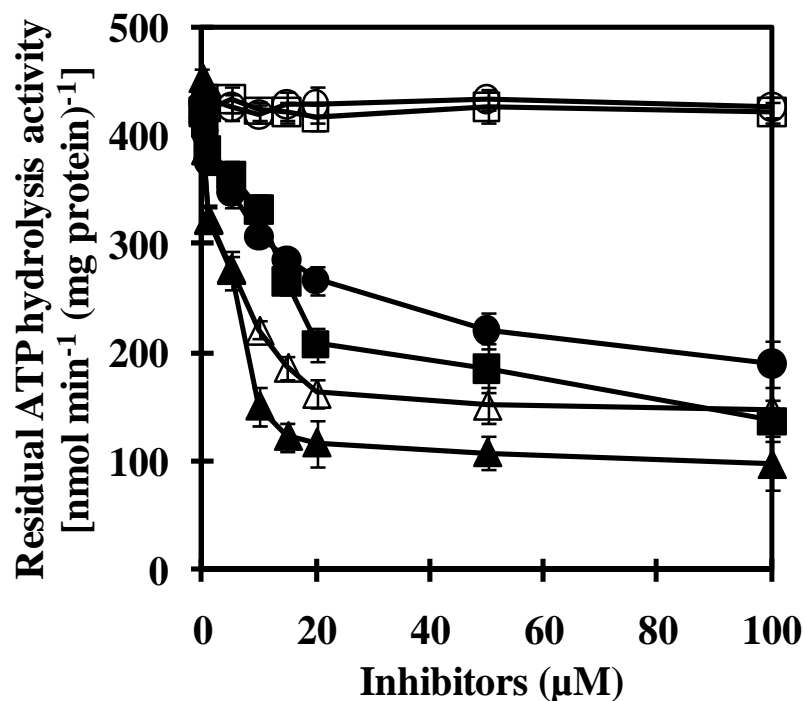


Figure 44 Effect of inhibitors on ATP hydrolysis activity of inverted membrane vesicles from ApNa⁺-ATPase-expressing *E. coli* DK8 cells. The residual ATP hydrolysis activity of ATPase in inverted membrane vesicles (30 ug protein) was determined in the reaction mixture containing 20 mM Tris-HCl pH 7.6, 5 mM MgCl₂ and 10 mM NaCl. The reaction was started by adding of 4 mM ATP (Tris salt) into the reaction mixture. Each inhibitor was added to the reaction mixture 10 min before the start of the reaction: CCCP (○), KNO₃ (□), azide (●), DCCD (■), tributyltin chloride (▲), monensin (△). Each value shows the average of three independent measurements.

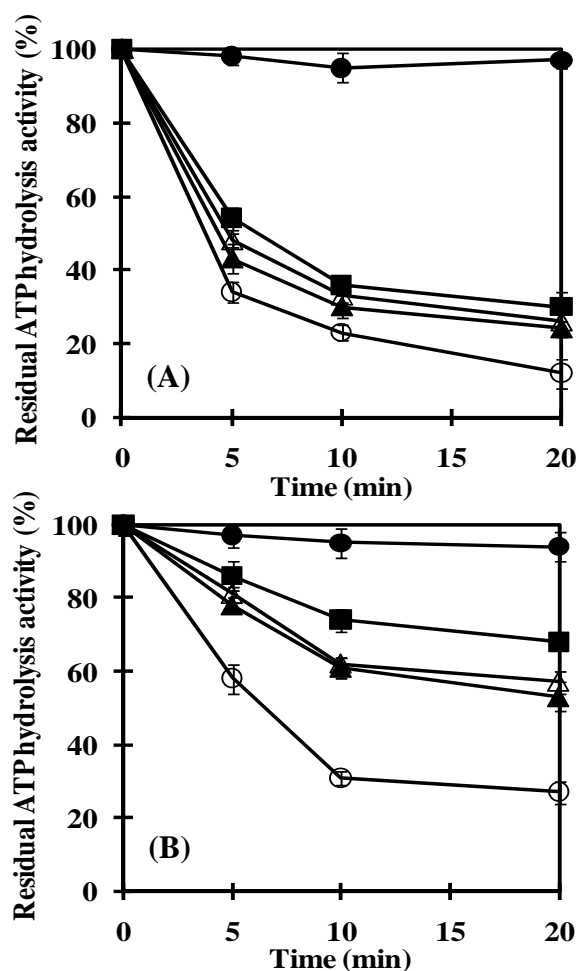


Figure 45 Protection of ATPase of inverted membrane vesicles from ApNa^+ -ATPase-expressing *E. coli* DK8 cells from DCCD inhibition by Na^+ at pH 7.6 and pH 9.0. The inverted membrane vesicles was incubated with 200 μM DCCD in either 20 mM Tris-HCl, pH 7.6 (A) or 20 mM Tricine-KOH, pH 9.0 (B). The individual mixtures contained the following additions of NaCl: 0 mM NaCl (○), 1 mM NaCl (▲), 10 mM NaCl (△) and 50 mM NaCl (■). The residual ATP hydrolysis activity of ATPase in inverted membrane vesicles (30 μg protein) taken at the indicated times was determined in the reaction mixture containing 20 mM Tris-HCl pH 7.6, 5 mM MgCl_2 . The reaction was started by addition of 4 mM ATP (Tris salt). One hundred percent activity corresponded to 423 $\text{nmol min}^{-1} (\text{mg protein})^{-1}$. Control without DCCD (●). Each value shows the average of three independent measurements.

4.9.7 ATP synthesis by Na⁺-loaded inverted membrane vesicles from *E. coli* DK8 transformants

To know whether the expressed ApNa⁺-ATPase in *E. coli* DK8 cells transformed with pTrcHis2C (empty vector transformants) and pTrcHis2C-*ApNa⁺-atp* (ApNa⁺-ATPase-expressing cells) has ATP synthesis activity, the ATP synthesis activity was assayed using the luciferin/luciferase reaction. As shown in Figure 46, ATP synthesis by Na⁺-loaded inverted membrane vesicles from ApNa⁺-ATPase-expressing *E. coli* DK8 cells was higher than empty vector transformants approximately 3 fold in the presence of ΔpNa^+ and $\Delta\psi$. To examine the requirement of $\Delta\psi$ on ATP synthesis, inhibitors and ionophores were added to the reaction medium. The results showed that membrane potential-generated K⁺/valinomycin and protonophore CCCP stimulated ATP synthesis (Figure 47A), implying that ATP synthesis required $\Delta\psi$ but not ΔpH . In contrast, Na⁺ gradient dissipator monensin and F₀ inhibitor DCCD inhibited ATP synthesis, suggesting that ATP synthesis by F-type ATPase required ΔpNa^+ . Furthermore, the application of external Na⁺ (20 and 50 mM NaCl) into the reaction medium decreased ATP synthesis (Figure 47B). This means the decrease in ΔpNa^+ due to external Na⁺ causes the decrease in the ATP synthesis.

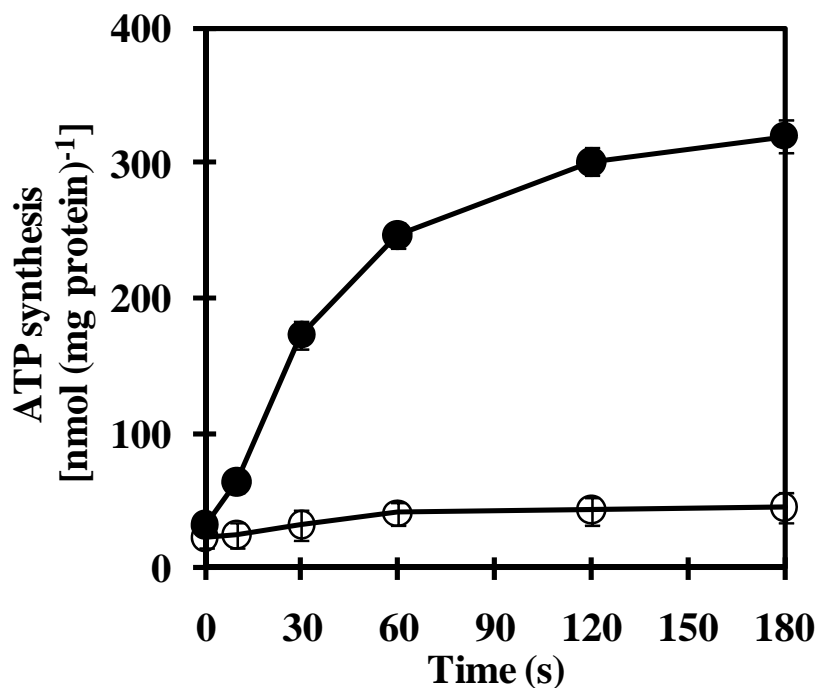


Figure 46 ATP synthesis by Na⁺-loaded inverted membrane vesicles from *E. coli* DK8 transformants was measured in the reaction medium (0.5 ml) containing 5 mM potassium phosphate pH 7.5, 5 mM MgCl₂, 0.2 M KCl, 0.1 mM ADP, 1 μM valinomycin and Na⁺-loaded inverted membrane vesicles (30 μg protein). Symbol (○) represents the Na⁺-loaded inverted membrane vesicles from the empty vector transformants, whereas (●) represents the Na⁺-loaded inverted membrane vesicles from the ApNa⁺-ATPase-expressing cells. Each value shows the average of three independent measurements.

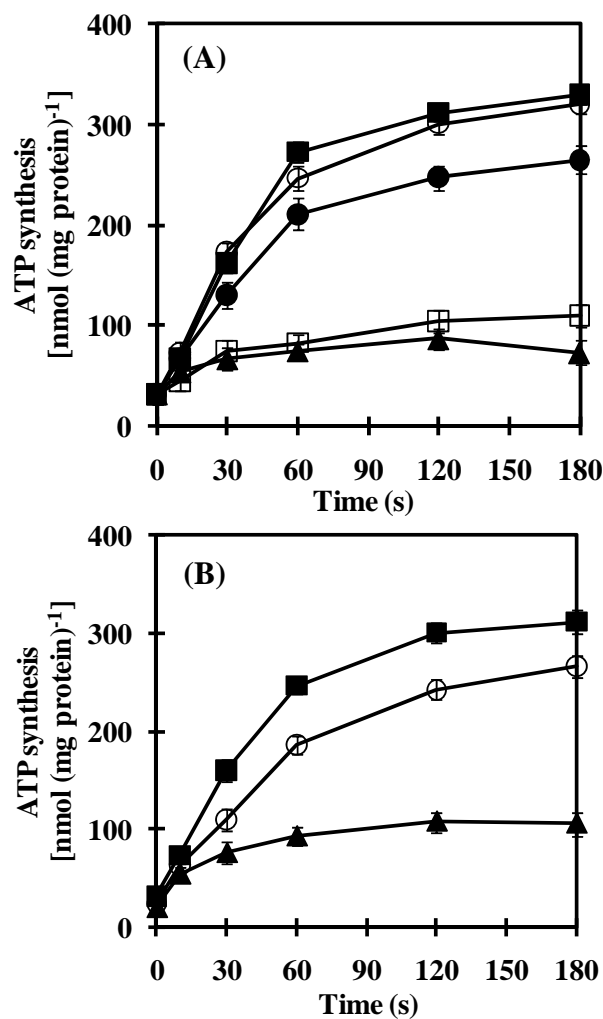


Figure 47 Dependence of ΔpNa^+ and $\Delta\Psi$ on ATP synthesis by Na^+ -loaded inverted membrane vesicles from $ApNa^+$ -ATPase-expressing *E. coli* DK8 cells. (A) Effect of CCCP, DCCD, monensin and valinomycin on ATP synthesis. ATP synthesis was measured in the reaction medium (0.5 ml) containing 5 mM potassium phosphate pH 7.5, 5 mM $MgCl_2$, 0.2 M KCl, 0.1 mM ADP, Na^+ -loaded inverted membrane vesicles (30 μg protein) with or without addition of chemicals. Without chemical (●), 1 M CCCP (■), 100 μM DCCD (▲), 10 μM monensin (□) and 1 μM valinomycin (○) in individual reaction. (B) Effect of external Na^+ on ATP synthesis. ATP synthesis was measured in the presence of 0 mM NaCl (■), 20 mM NaCl (○) and 50 mM NaCl (▲) in individual reaction. Each value shows the average of three independent measurements.

4.10 Western blot analysis of ApNa⁺-ATPase expressed in *E. coli* DK8 cells

4.10.1 Effect of induction time on the expression of ApNa⁺-ATPase in *E. coli* DK8 transformants

The individual expression plasmid pTrcHis2C and pTrcHis2C-*ApNa⁺-atp* containing IPTG-inducible *trc* promoter were introduced into *E. coli* mutant DK8 (Δatp). The expression of γ subunit of ApNa⁺-ATPase with the calculated molecular masses of 35 kDa was detected in *E. coli* DK8 cells transformed with pTrcHis2C-*ApNa⁺-atp* (ApNa⁺-ATPase-expressing cells) at all induction times but not in *E. coli* DK8 cells transformed with pTrcHis2C (empty vector transformants) (Figure 48).

4.10.2 Effect of NaCl in the growth medium on ATP hydrolysis activity of inverted membrane vesicles from *E. coli* DK8 transformants

E. coli DK8 cells transformed with pTrcHis2C (empty vector transformants) and pTrcHis2C-*ApNa⁺-atp* (ApNa⁺-ATPase-expressing cells) were grown in the growth medium containing various NaCl concentrations. Then IPTG was added to final conc. of 1 mM. After induction for 2 hrs, inverted membrane vesicles were prepared and ATP hydrolysis activity was tested. The results showed that ATP hydrolysis activity of inverted membranes vesicles of the ApNa⁺-ATPase-expressing cells was stimulated after the cells were stressed with NaCl while the empty vector transformants did not (Figure 49).

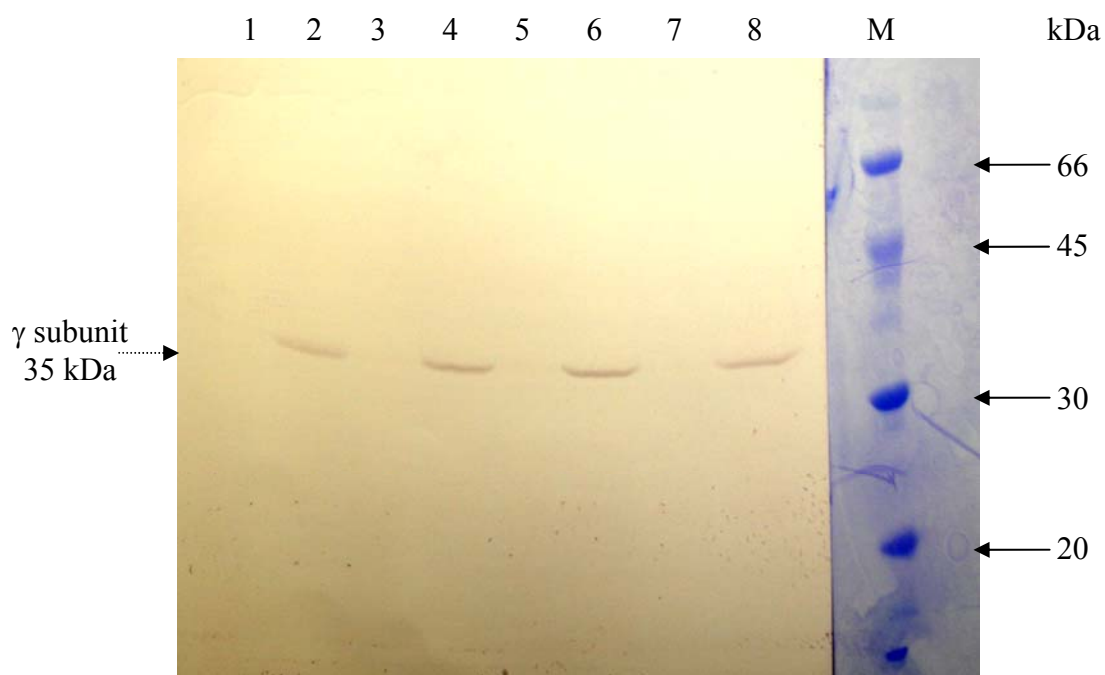


Figure 48 Effect of induction time on the expression of ApNa⁺-ATPase in *E. coli* DK8 cells by 1 mM IPTG. The induction time was 0, 2, 5 and 16 hrs. Inverted membrane vesicles (50 μg protein) were separated on 12% SDS-PAGE and transferred onto PVDF membrane. His tag-containing γ subunit (*ApNa⁺-atpG*) was detected by immunoblotting. Lane 1, 3, 5, 7 are lanes loaded empty vector transformants. Lane 2, 4, 6, 8 are lanes loaded ApNa⁺-ATPase-expressing cells. Lane M is molecular weight marker.

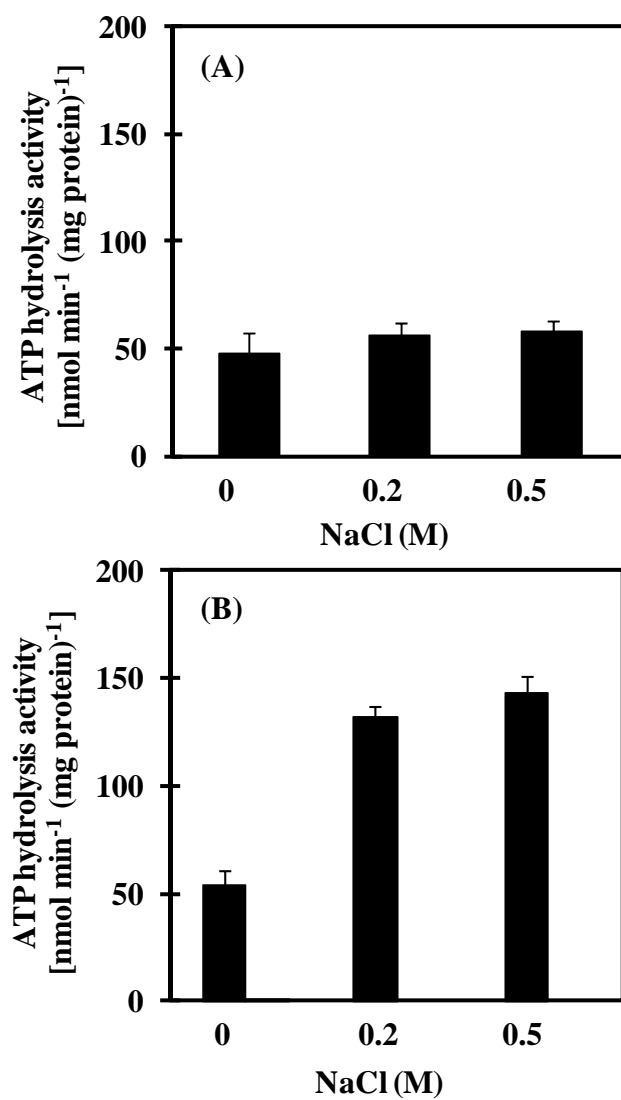


Figure 49 Effect of NaCl in the growth medium on ATP hydrolysis activity of inverted membrane vesicles from *E. coli* DK8 transformants. (A) and (B) are the empty vector transformants and ApNa⁺-ATPase-expressing cells, respectively.

4.10.3 Effect of NaCl in the growth medium on the expression of ApNa⁺-ATPase in inverted membrane vesicles from ApNa⁺-ATPase-expressing *E. coli* DK8 cells

E. coli DK8 cells transformed with pTrcHis2C-*ApNa⁺-atp* (ApNa⁺-ATPase-expressing cells) were grown in the growth medium containing various NaCl concentrations and then IPTG was added to final conc. of 1 mM. After induction for 2 hrs, inverted membrane vesicles were prepared and immunoblot analysis was done. The results showed that the expression level of ApNa⁺-ATPase increased with the increase of NaCl in the growth medium (Figure 50).

4.10.4 Localization of ApNa⁺-ATPase in ApNa⁺-ATPase-expressing *E. coli* DK8 cells

To examine the localization of γ subunit in *E. coli* mutant DK8 (Δatp), *E. coli* DK8 cells transformed with pTrcHis2C-*ApNa⁺-atp* (ApNa⁺-ATPase-expressing cells) were fractionated into the periplasmic, cytoplasmic and membrane fractions, followed by SDS-PAGE and immunoblot analyses. The γ subunit was detected in the membrane fraction (Figure 51). These results suggest that the γ subunit and whole complex are assembled into the cytoplasmic membranes of *E. coli* DK8 cells.

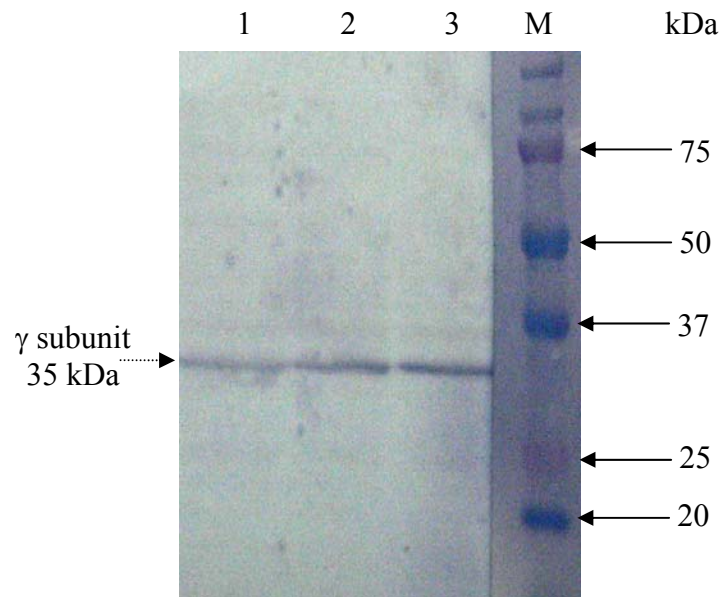


Figure 50 Effect of NaCl in the growth medium on the expression of $ApNa^+$ -ATPase in inverted membrane vesicles from $ApNa^+$ -ATPase-expressing *E. coli* DK8 cells. The cells were grown in LB medium containing 0.0 M NaCl (lane 1), 0.2 M NaCl (lane 2) and 0.5 M NaCl (lane 3). Inverted membrane vesicles (50 μ g protein) were separated on 12% SDS-PAGE and transferred onto PVDF membrane. His tag-containing γ subunit (*ApNa⁺-atpG*) was detected by immunoblotting. Lane M is molecular weight marker.

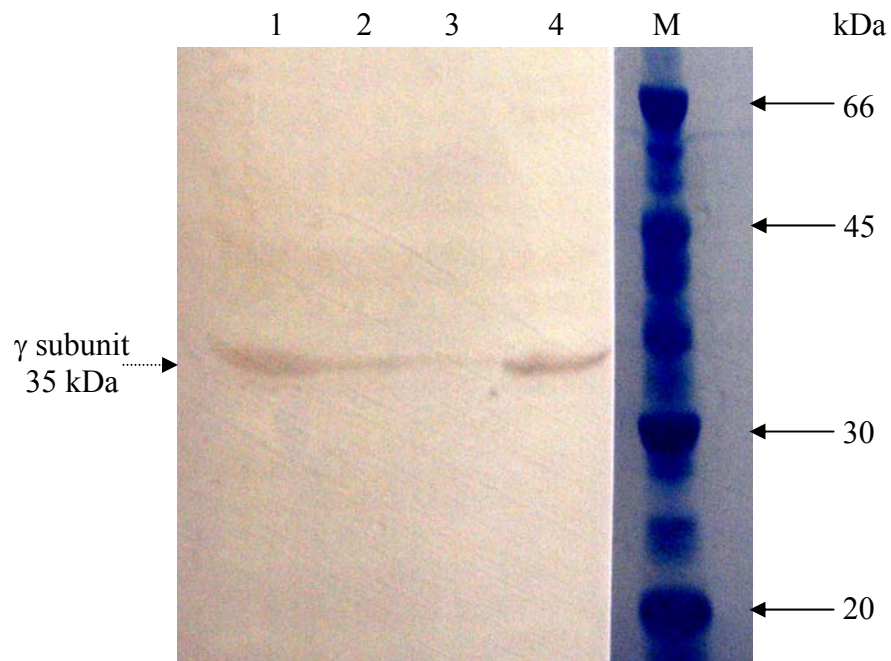


Figure 51 Localization of ApNa^+ -ATPase in ApNa^+ -ATPase-expressing *E. coli* DK8 cells. Samples (50 μg protein) were separated on 12% SDS-PAGE and transferred onto PVDF membrane. His tag-containing γ subunit (*ApNa*⁺-*atpG*) was detected by immunoblotting. Lane 1, Whole cells; lane 2, periplasmic fraction; lane 3, cytoplasmic fraction; lane 4, membrane fraction; lane M, molecular weight marker.

4.11 Construction of pUC303-*ApNa*⁺-*atp* plasmid for the expression of *ApNa*⁺-ATPase in a freshwater cyanobacterium *Synechococcus* sp. PCC 7942

The expression plasmid designated as pUC303-*ApNa*⁺-*atp* was constructed under the control of the IPTG-inducible *trc* promoter (Figure 52). The plasmid, pUC303, which containing chloramphenicol and streptomycin sulfate resistant gene was used as control plasmid. Each plasmid was transformed first into *E. coli* DH5 α cells and the positive transformants were selected on LB agar containing 100 $\mu\text{g ml}^{-1}$ streptomycin and 10 $\mu\text{g ml}^{-1}$ chloramphenicol. After the positive clones were picked up, the plasmids were extracted and transformed into *Synechococcus* sp. PCC 7942 cells. The transformants were selected on BG11 agar containing 50 $\mu\text{g ml}^{-1}$ streptomycin. The positive clones were picked up and then transferred to a new BG11 liquid medium containing 50 $\mu\text{g ml}^{-1}$ streptomycin. After cultivation for 2 weeks, the plasmids were extracted and amplified by PCR technique with the chloramphenicol-specific primers and specific primers for *atpG* encoding γ subunit of *ApNa*⁺-*atp* operon. Figure 53A shows the band patterns of the 800-bp PCR products amplified and checked by chloramphenicol-specific primers. The result showed that both of plasmid pUC303 and pUC303-*ApNa*⁺-*atp* could be amplified with chloramphenicol-specific primers. Figure 53B shows the band patterns of the 520-bp PCR products amplified with specific primers for *atpG* encoding γ subunit of *ApNa*⁺-*atp* operon. As expected, only plasmid pUC303-*ApNa*⁺-*atp* could be amplified with *atpG* specific primers.

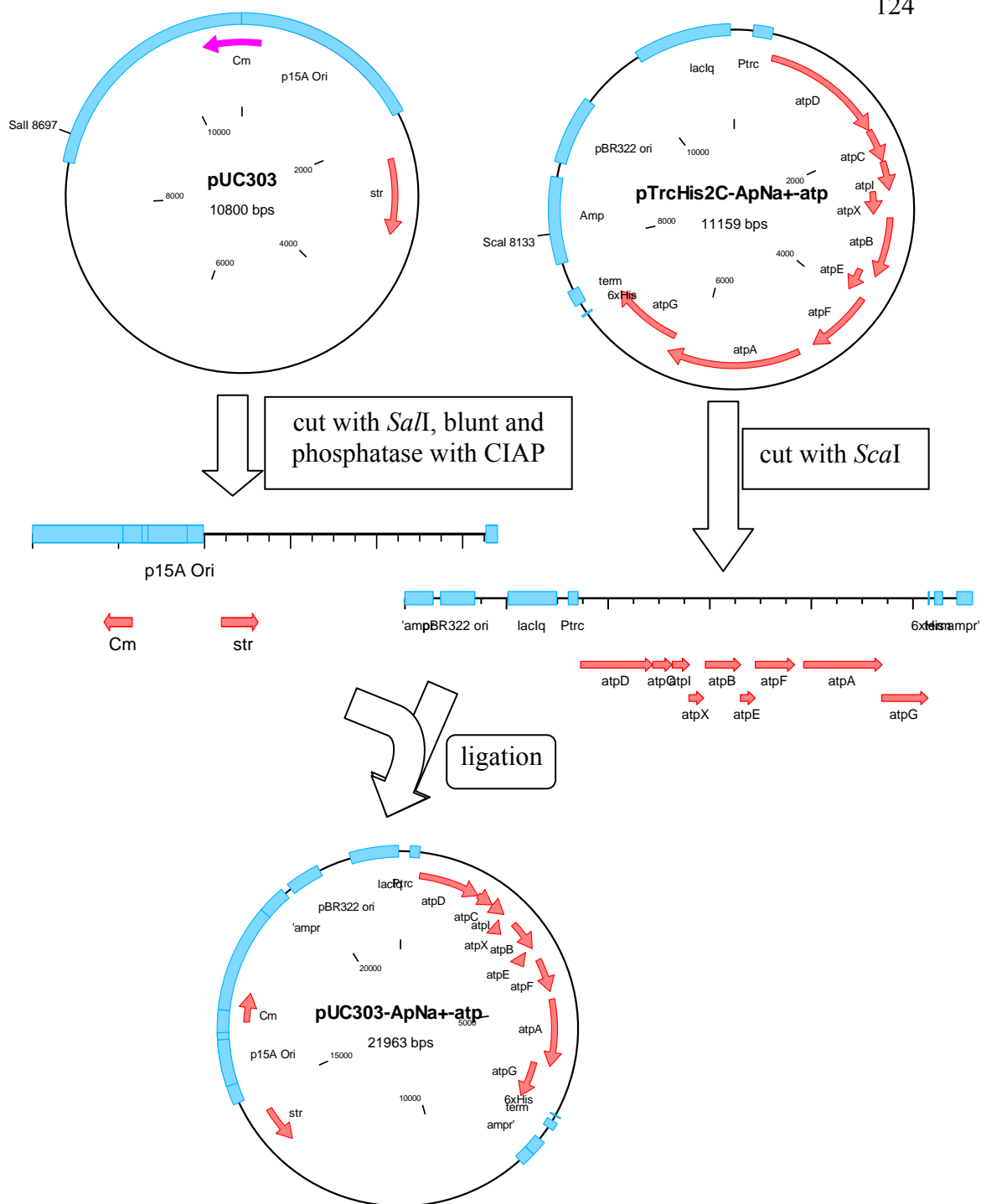


Figure 52 Schematics of the construction of recombinant plasmid *pUC303-ApNa⁺-atp*. The recombinant plasmid *pTrcHis2C-ApNa⁺-atp* was digested with *ScaI* and then ligated into *pUC303* at *SalI*-digested and blunt-ended site. After that recombinant plasmid *pUC303-ApNa⁺-atp* was transformed into *E. coli* DH5 α and a freshwater cyanobacterium *Synechococcus* sp. PCC 7942.

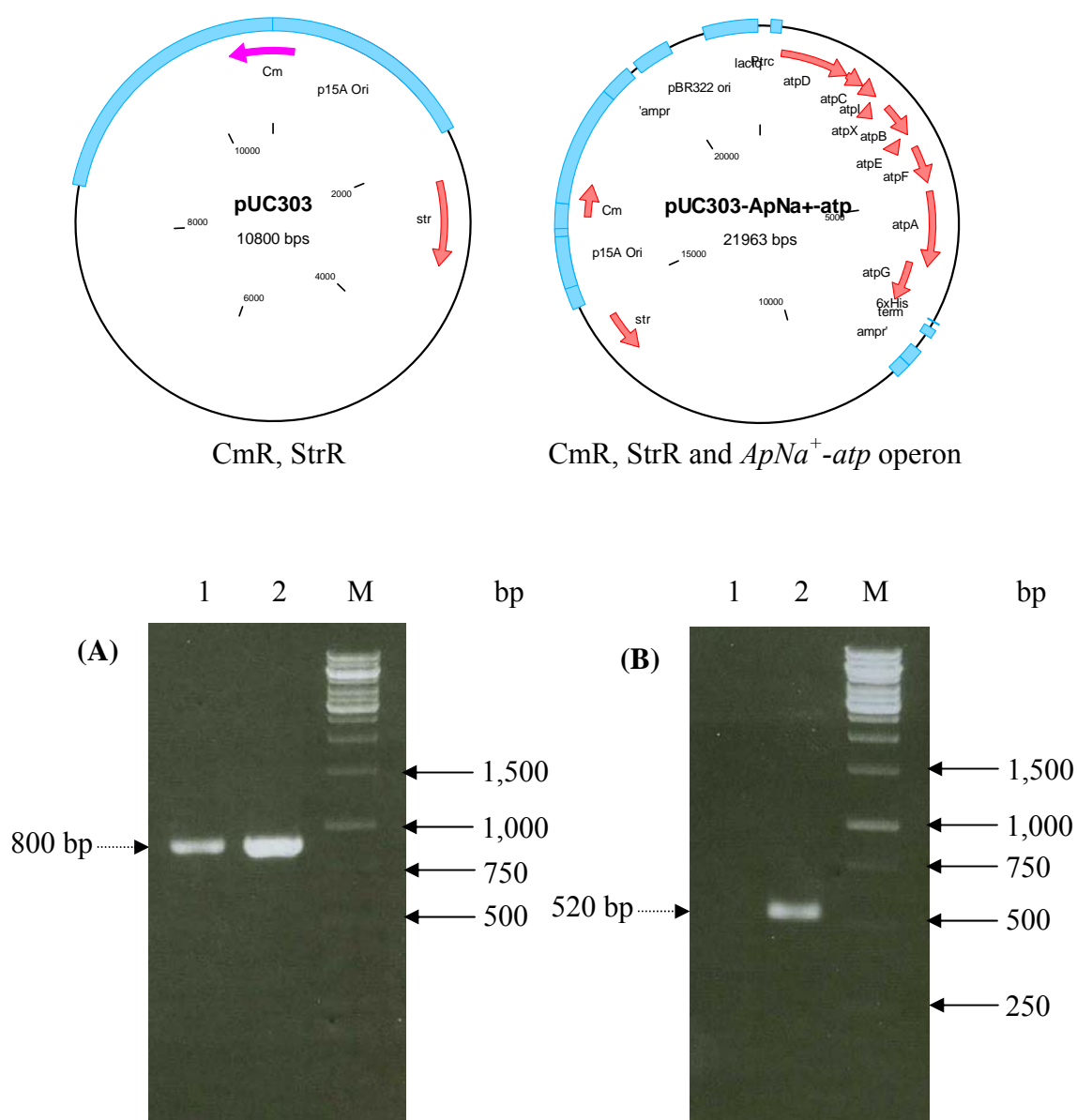


Figure 53 The map of pUC303 and pUC303-*ApNa⁺-atp* (upper) and the band of PCR products (lower). The pUC303 and pUC303-*ApNa⁺-atp* were amplified with chloramphenicol-specific primers (product size 800 bp) (A) and *atpG* encoding γ subunit of *ApNa⁺-atp*-specific primers (product size 520 bp) (B). Lane 1, 2 and M are plasmid pUC303, pUC303-*ApNa⁺-atp* and molecular weight marker, respectively.

4.12 Characterization of ApNa⁺-ATPase expressed in *Synechococcus* sp. PCC 7942 cells

4.12.1 Effect of NaCl in the growth medium on the growth of *Synechococcus* sp. PCC 7942 transformants

The NaCl-stress tolerance in *Synechococcus* sp. PCC 7942 transformants was investigated. It was shown that both of *Synechococcus* sp. PCC 7942 cells transformed with pUC303 (empty vector transformants) and pUC303-*ApNa⁺-atp* (*ApNa⁺-ATPase*-expressing cells) could grow at almost the same rate in BG11 medium (Figure 54A). At 0.3 M NaCl condition, the growth rate of both empty vector transformants and *ApNa⁺-ATPase*-expressing cells decreased but the growth rate of *ApNa⁺-ATPase*-expressing cells was higher than the growth rate of empty vector transformants (Figure 54B). At 0.5 M NaCl condition, empty vector transformants could not grow whereas *ApNa⁺-ATPase*-expressing cells could grow slowly (Figure 54C), indicating that the transformation of *ApNa⁺-atp* operon into *Synechococcus* sp. PCC 7942 could confer salt tolerance. Moreover, we tested whether *ApNa⁺-ATPase*-expressing cells could grow in seawater. Seawater was taken from the Mikawa area of Aichi Prefecture in Japan and its salinity was 30.4 psu, ~0.41 M sodium. It was found that the *ApNa⁺-ATPase*-expressing cells could grow in seawater while the empty vector transformants could not (Figure 54D).

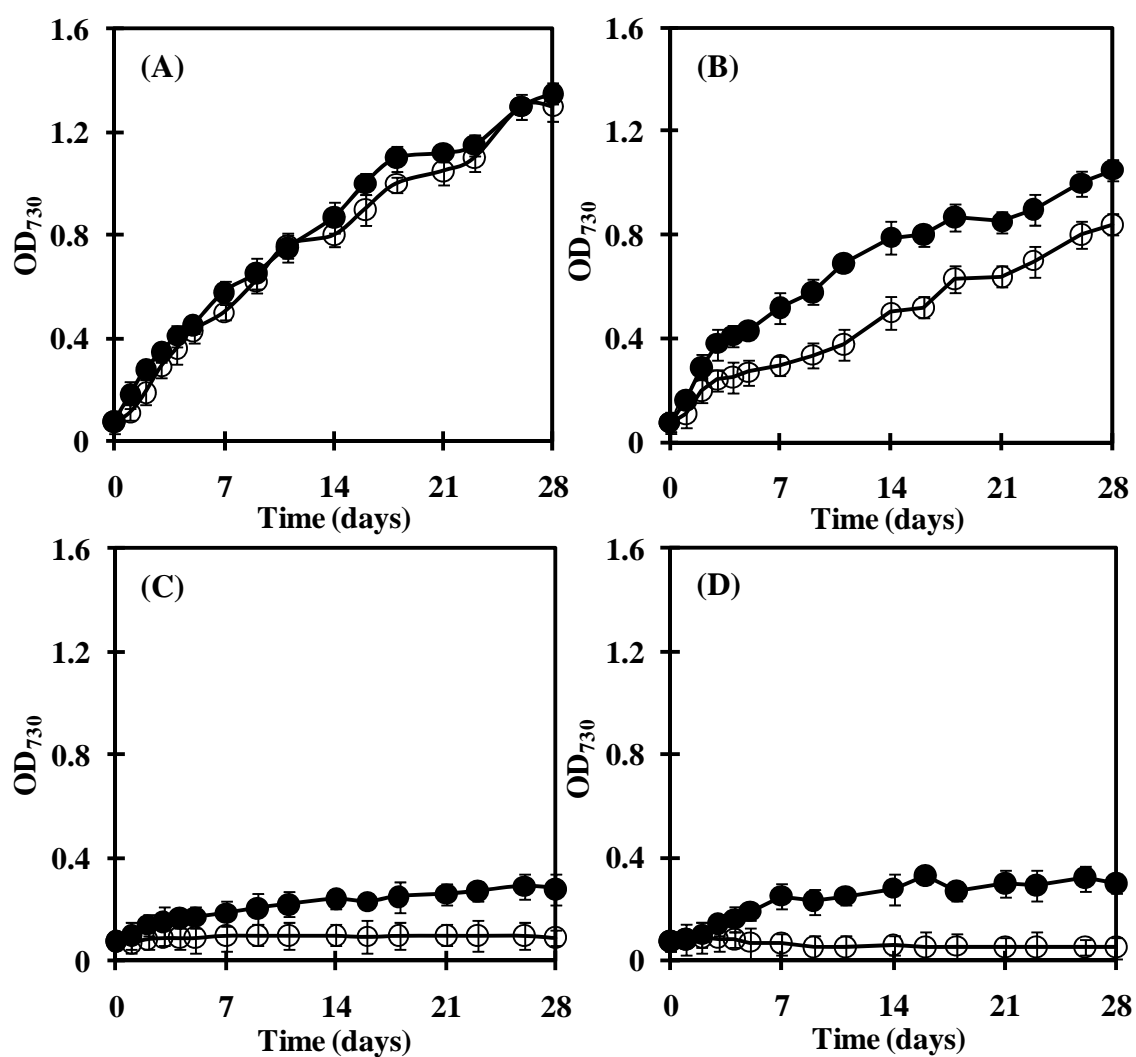


Figure 54 Effect of NaCl on the growth of *Synechococcus* sp. PCC 7942 transformants. *Synechococcus* sp. PCC 7942 transformants were grown in BG11 medium containing 0.0 M NaCl (A), 0.3 M NaCl (B), 0.5 M NaCl (C) or seawater (D). Symbol (○) represents the empty vector transformants, whereas (●) represents the ApNa⁺-ATPase-expressing cells. Each value shows the average of three independent measurements.

4.12.2 Na⁺ content inside the cells of Na⁺-loaded *Synechococcus* sp. PCC 7942 transformants

To determine whether Na⁺-loaded *Synechococcus* sp. PCC 7942 transformants could extrude Na⁺ from inside to outside the cells, the Na⁺ content inside the cells of Na⁺-loaded *Synechococcus* sp. PCC 7942 transformed with pUC303 (empty vector transformants) and pUC303-*ApNa⁺-atp* (*ApNa⁺-ATPase*-expressing cells) was measured. It was found that Na⁺ content inside the *ApNa⁺-ATPase*-expressing *Synechococcus* sp. PCC 7942 cells decreased when the cells were transferred to a new Na⁺-free medium, but no change in the Na⁺ content was observed inside the empty vector transformants (Figure 55). These results suggest that the *ApNa⁺-ATPase*-expressing *Synechococcus* sp. PCC 7942 cells can extrude Na⁺ from inside the cells to the external medium via *ApNa⁺-ATPase*.

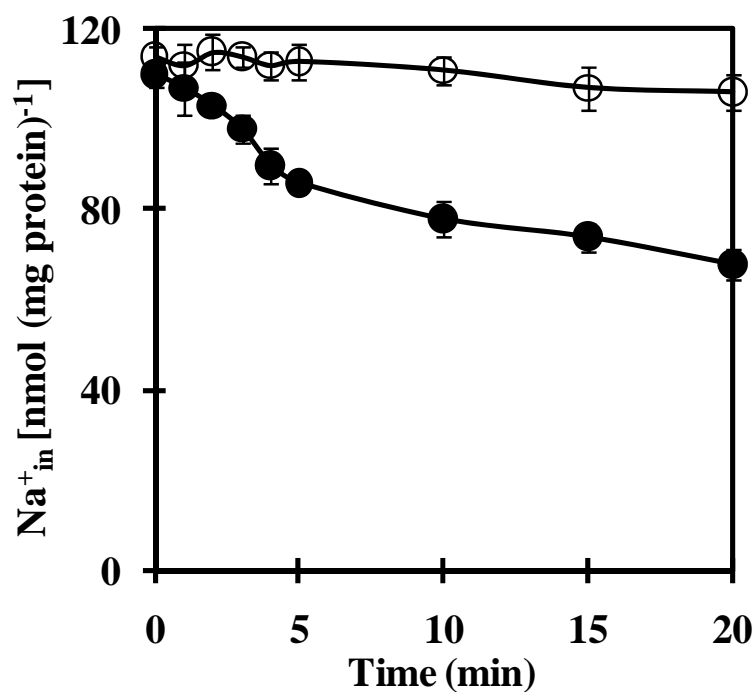


Figure 55 Extrusion of Na^+ from Na^+ -loaded *Synechococcus* sp. PCC 7942 transformants. The transformants were grown in BG11 medium at 30 °C for 7 days and then were transferred to medium containing 0.15 M NaCl. After incubation for 1 day, the cells were collected and transferred to Na^+ -free medium in the presence of 0.5 mM IPTG. Ten mM of glucose was added for 10 min prior to start the extrusion of Na^+ . Symbol (○) represents the membrane vesicles of the empty vector transformants, whereas (●) represents the membrane vesicles of the ApNa^+ -ATPase-expressing cells. Each value shows the average of three independent measurements.

4.12.3 The effect of NaCl, ATP, Mg²⁺ and pH on ATP hydrolysis activity of inverted membrane vesicles from *Synechococcus* sp. PCC 7942 transformants

The ATP hydrolysis activity of inverted membrane vesicles from *Synechococcus* sp. PCC 7942 cells transformed with pUC303 (empty vector transformants) and pUC303-*ApNa⁺-atp* (*ApNa⁺-ATPase*-expressing cells) was examined. The result showed that the ATP hydrolysis activity of inverted membrane vesicles from *ApNa⁺-ATPase*-expressing cells increased when the NaCl concentrations were increased (Figure 56). The apparent K_m value for Na^+ as determined from the Lineweaver-Burk plot was 1.75 mM (Figure 56, inset). The ATP hydrolysis activity of the control (the empty vector transformants) was very low and did not increase upon the increase of NaCl concentrations. Figure 57A showed that ATP hydrolysis activity from *ApNa⁺-ATPase*-expressing cells increased corresponding to the increase of ATP concentrations. The apparent K_m value for ATP was 1.56 mM (Figure 57A, inset).

The dependence of *ATPase* on Mg^{2+} was also tested. Figure 57B shows that maximal ATP hydrolysis activity was observed at 5 mM Mg^{2+} . The enzyme activity was decreased when the Mg^{2+} concentration was higher than 5 mM. The pH of the assay medium also influenced on the enzyme activity. When the pH was increased from pH 6.0 to pH 8.0, the enzyme activity was increased progressively (Figure 57C). The optimum pH for enzyme activity was pH 8.0. Increasing the pH further to pH 11.0 resulted in a slightly declined enzyme activity.

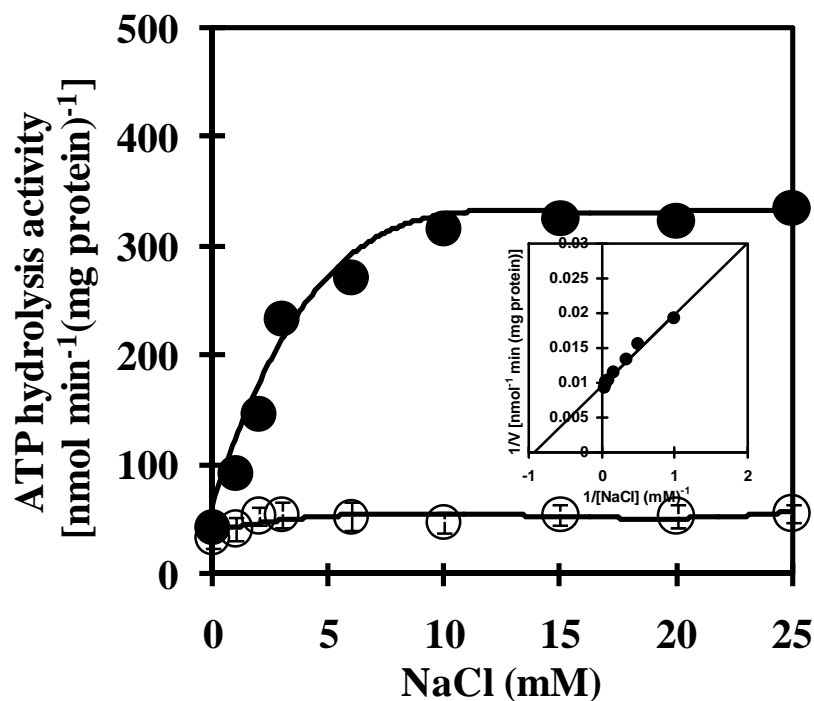


Figure 56 Effect of NaCl on ATP hydrolysis activity of inverted membrane vesicles from *Synechococcus* sp. PCC 7942 transformants. The enzyme activity was measured in the presence of various concentrations of NaCl. Inset shows a double-reciprocal plot of activity versus NaCl concentration. Symbol (○) represents the membrane vesicles of the empty vector transformants, whereas (●) represents the membrane vesicles of the ApNa⁺-ATPase-expressing cells. Each value shows the average of three independent measurements.

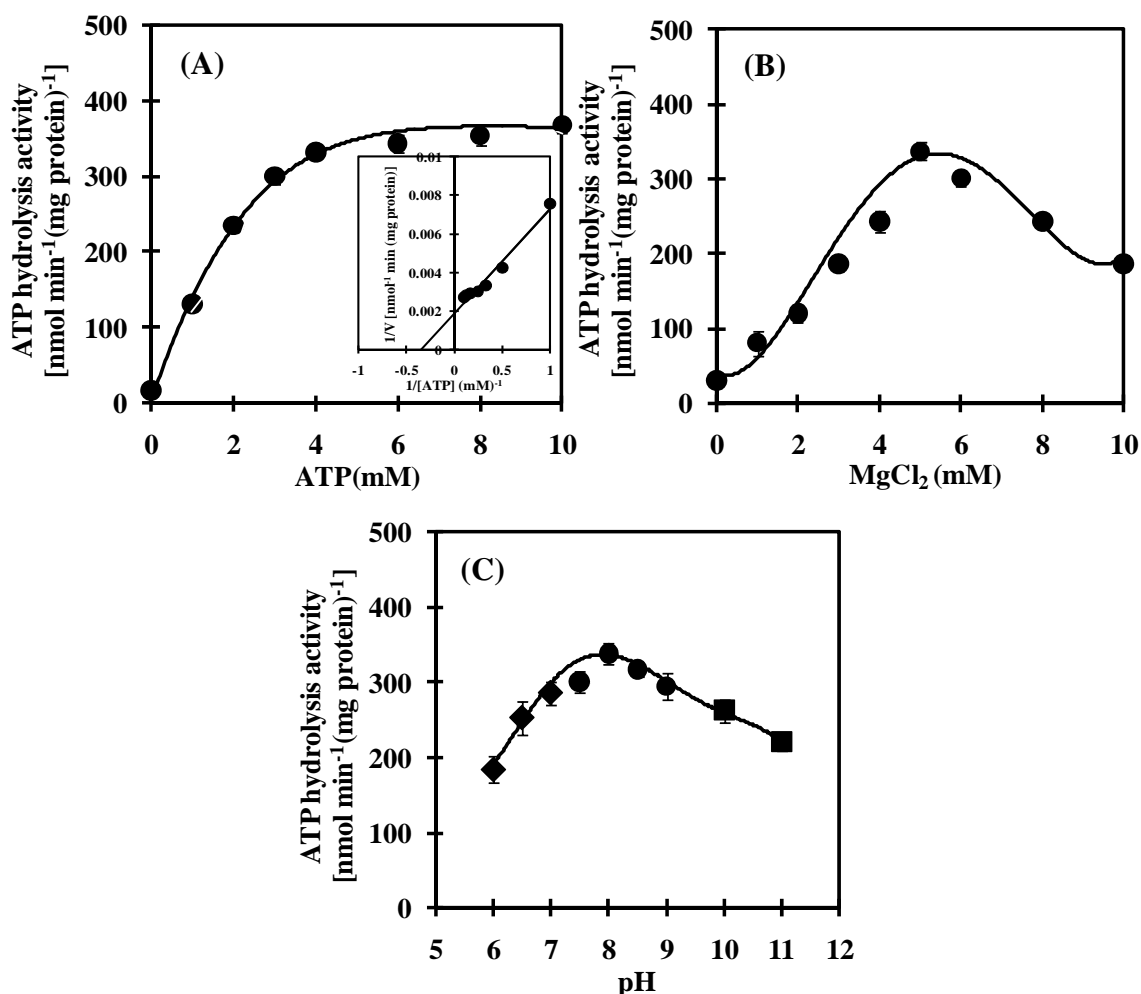


Figure 57 Effect of ATP, MgCl_2 and pH on ATP hydrolysis activity of inverted membrane vesicles from ApNa^+ -ATPase-expressing *Synechococcus* sp. PCC 7942 cells. In (A) and (B), the enzyme activity was measured in the presence of various concentrations of ATP and MgCl_2 , respectively. Inset in (A) shows a double-reciprocal plot of activity versus ATP concentration. In (C), the enzyme activity was measured at various pH values using 20 mM Mes-KOH for pH 6.0-7.0 (\blacklozenge), 20 mM Tris-HCl for pH 7.5-9.0 (\bullet) and 20 mM Glycine-KOH for pH 10.0-11.0 (\blacksquare). Each value shows the average of three independent measurements.

4.12.4 The effect of inhibitors on ATP hydrolysis activity of inverted membrane vesicles from ApNa⁺-ATPase-expressing *Synechococcus* sp. PCC 7942 cells

The ATP hydrolysis activity of inverted membrane vesicles from *Synechococcus* sp. PCC 7942 cells transformed with pUC303-*ApNa⁺-atp* (*ApNa⁺-ATPase*-expressing cells) was inhibited by azide (F_1 inhibitor) of 50%, DCCD (F_0 inhibitor) of 67%, tributyltin chloride (F_0 inhibitor) of 71% and monensin (Na^+ -gradient dissipator) 60% but not inhibited by CCCP (a protonophore) and KNO_3 (a permeant anion) (Figure 58). Moreover, Na^+ provided protection against the inhibition of DCCD in a pH-dependent manner. At pH 7.6, when NaCl at 1, 10 and 50 mM concentrations was added into the individual reaction medium, the inhibition of DCCD on ATP hydrolysis activity was about 70, 60, 55%, respectively while ATP hydrolysis activity in the absence of NaCl was inhibited for approximately 80% (Figure 59A). At pH 9.0, in the absence of NaCl, ATP hydrolysis activity was inhibited about 67%. ATP hydrolysis activity was inhibited by about 40% in the presence of 1 and 10 mM NaCl while 50 mM NaCl inhibited ATP hydrolysis activity for approximately 30% (Figure 59B).

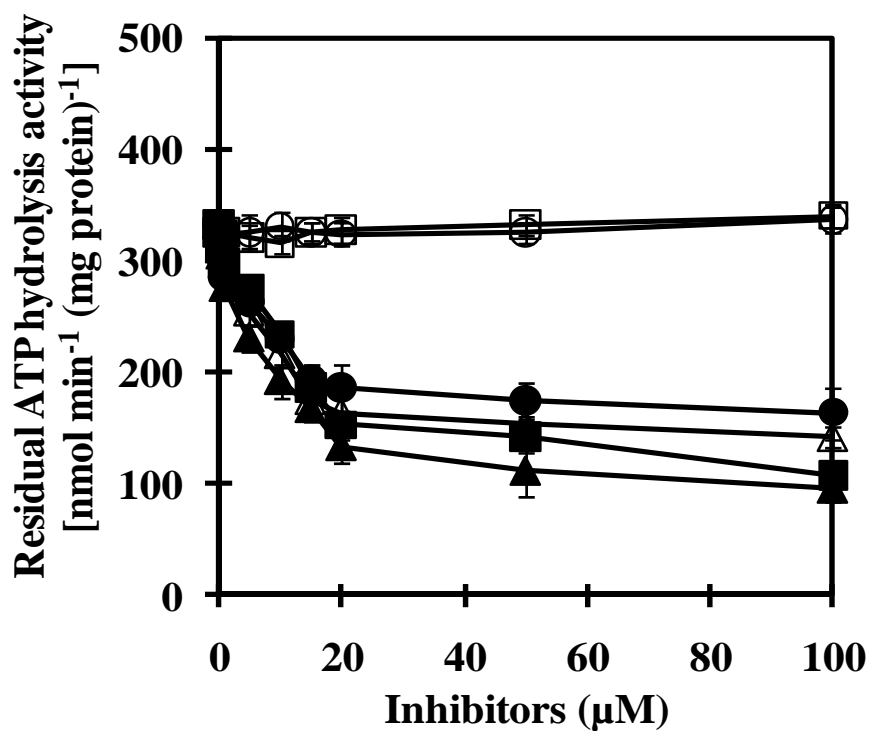


Figure 58 Effect of inhibitors on ATP hydrolysis activity of inverted membrane vesicles from ApNa⁺-ATPase-expressing *Synechococcus* sp. PCC 7942 cells. The residual ATP hydrolysis activity of ATPase in inverted membrane vesicles (30 ug protein) was determined in the reaction mixture containing 20 mM Tris-HCl pH 7.6, 5 mM MgCl₂ and 10 mM NaCl. The reaction was started by adding of 4 mM ATP (Tris salt). Each inhibitor was added to the reaction mixture for 10 min before the start of the reaction. All inhibitors are CCCP (○), KNO₃ (□), azide (●), DCCD (■), tributyltin chloride (▲), and monensin (△). Each value shows the average of three independent measurements.

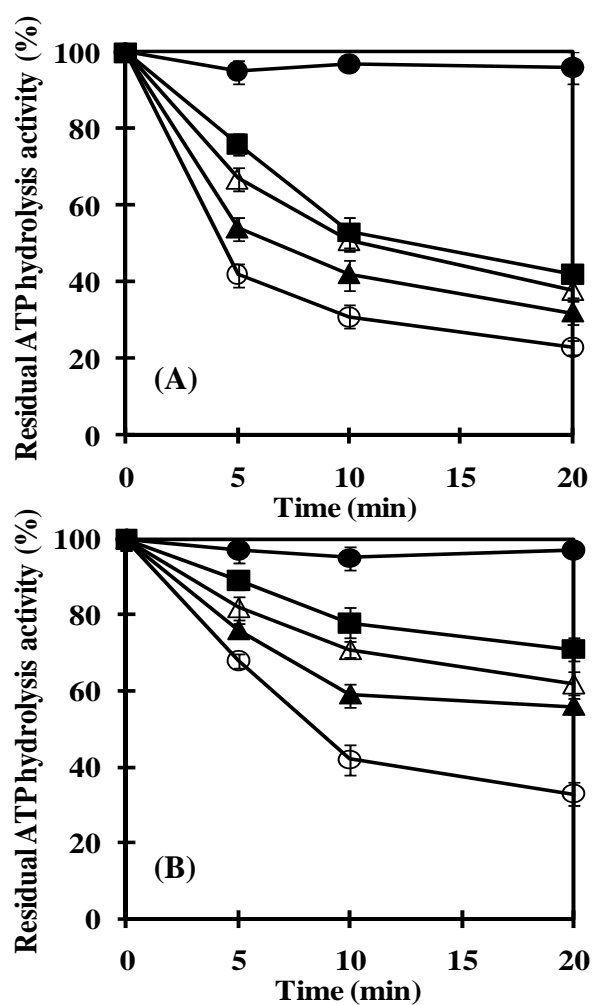


Figure 59 Protection of ATPase in inverted membrane vesicles from ApNa⁺-ATPase-expressing *Synechococcus* sp. PCC 7942 cells from DCCD inhibition by Na⁺ at pH 7.6 and pH 9.0. The inverted membrane vesicles was incubated with 200 μ M DCCD in either 20 mM Tris-HCl, pH 7.6 (A) or 20 mM Tricine-KOH, pH 9.0 (B). The individual mixtures contained the following additions: 0 mM (○), 1 mM NaCl (▲), 10 mM NaCl (△) and 50 mM NaCl (■). The residual ATP hydrolysis activity of ATPase in inverted membrane vesicles (30 μ g protein) taken at the indicated times was determined in the reaction mixture containing 20 mM Tris-HCl pH 7.6, 5 mM MgCl₂. The reaction was started by addition of 4 mM ATP (Tris salt). One hundred percent activity corresponded to 343 nmol min⁻¹ (mg protein)⁻¹. The control without DCCD represents as symbol (●). Each value shows the average of three independent measurements.

4.12.5 ATP synthesis by Na⁺-loaded inverted membrane vesicles from *Synechococcus* sp. PCC 7942 transformants

To know whether the expressed ApNa⁺-ATPase in *Synechococcus* sp. PCC 7942 cells transformed with pUC303 (empty vector transformants) and pUC303-*ApNa⁺-atp* (ApNa⁺-ATPase-expressing cells) has ATP synthesis activity, the ATP synthesis activity was assayed using the luciferin/luciferase reaction. It was shown that ATP synthesis by Na⁺-loaded inverted membrane vesicles of ApNa⁺-ATPase-expressing *Synechococcus* sp. PCC 7942 cells was higher than empty vector transformants for approximately 4 fold in the presence of ΔpNa^+ and $\Delta\psi$ (Figure 60). To examine the requirement of $\Delta\psi$ on ATP synthesis, inhibitors and ionophores were added to the reaction medium. The results showed that membrane potential-generated K⁺/valinomycin and protonophore CCCP stimulated the ATP synthesis (Figure 61A). This means ATP synthesis required $\Delta\psi$ but not ΔpH . In contrast, Na⁺ gradient dissipator monensin and F₀ inhibitor DCCD inhibited ATP synthesis, suggesting that ATP synthesis by F-type ATPase required ΔpNa^+ . Furthermore, the application of external Na⁺ (20 and 50 mM NaCl) into the reaction medium decreased ATP synthesis (Figure 61B). This means the decrease in ΔpNa^+ due to external Na⁺ causes the decrease in the ATP synthesis.

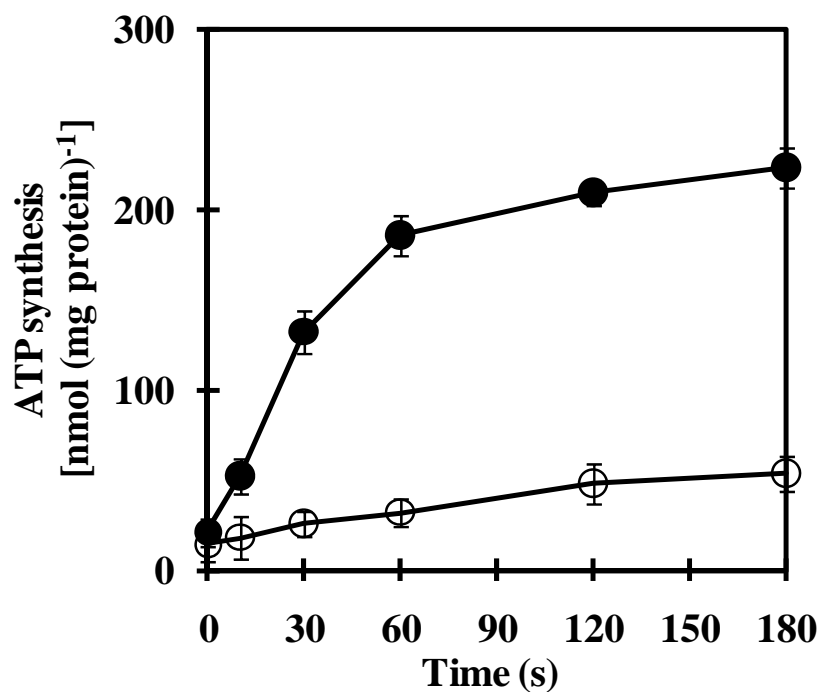


Figure 60 ATP synthesis by Na⁺-loaded inverted membrane vesicles from *Synechococcus* sp. PCC 7942 transformants was measured in the reaction medium (0.5 ml) containing 5 mM potassium phosphate pH 7.5, 5 mM MgCl₂, 0.2 M KCl, 0.1 mM ADP, 1 μM valinomycin and Na⁺-loaded inverted membrane vesicles (30 μg protein). Symbol (○) represents the Na⁺-loaded inverted membrane vesicles from the empty vector transformants, whereas (●) represents the Na⁺-loaded inverted membrane vesicles from the ApNa⁺-ATPase-expressing cells. Each value shows the average of three independent measurements.

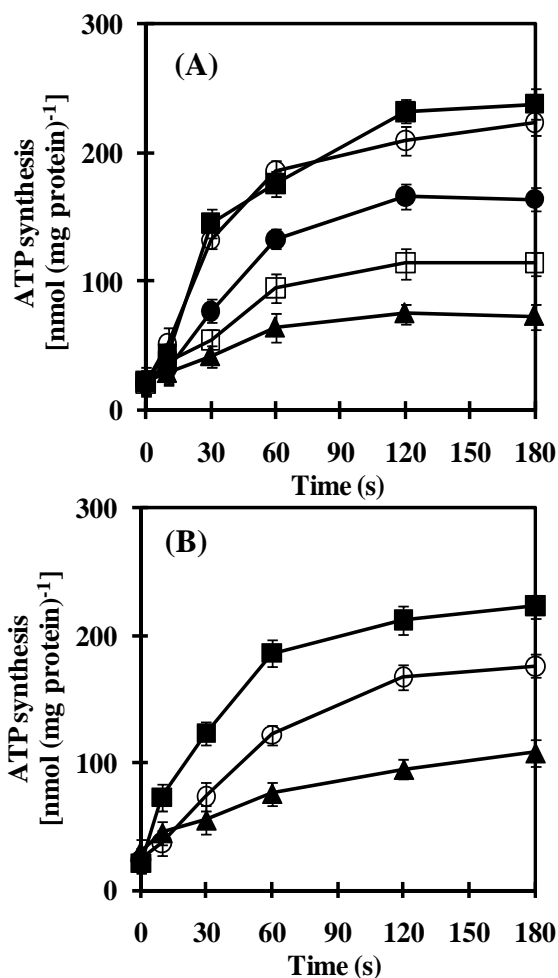


Figure 61 Dependence of ΔpNa^+ and $\Delta\Psi$ on ATP synthesis by Na^+ -loaded inverted membrane vesicles from $ApNa^+$ -ATPase-expressing *Synechococcus* sp. PCC 7942 cells. (A) Effect of CCCP, DCCD, monensin and valinomycin on ATP synthesis. ATP synthesis was measured in the reaction medium (0.5 ml) containing 5 mM potassium phosphate pH 7.5, 5 mM $MgCl_2$, 0.2 M KCl, 0.1 mM ADP, Na^+ -loaded inverted membrane vesicles (30 μg protein) with or without chemicals. Without chemical (●), 1 M CCCP (■), 100 μM DCCD (▲), 10 μM monensin (□) and 1 μM valinomycin (○) in individual reaction. (B) Effect of external Na^+ on ATP synthesis. ATP synthesis was measured in the presence of 0 mM NaCl (■), 20 mM NaCl (○) and 50 mM NaCl (▲) in individual reaction. Each value shows the average of three independent measurements.

4.13 Western blot analysis of ApNa⁺-ATPase expressed in *Synechococcus* sp. PCC 7942 cells

4.13.1 Expression and localization of ApNa⁺-ATPase in *Synechococcus* sp. PCC 7942 cells

The individual expression plasmid pUC303 and pUC303-*ApNa⁺-atp* containing IPTG-inducible *trc* promoter were introduced into *Synechococcus* sp. PCC 7942. The expression of γ subunit of ApNa⁺-ATPase with the calculated molecular mass of 35 kDa was detected in membrane vesicles from *Synechococcus* sp. PCC 7942 cells transformed with pUC303-*ApNa⁺-atp* (ApNa⁺-ATPase-expressing cells) but not in *Synechococcus* sp. PCC 7942 cells transformed with pUC303 (empty vector transformants) (Figure 62).

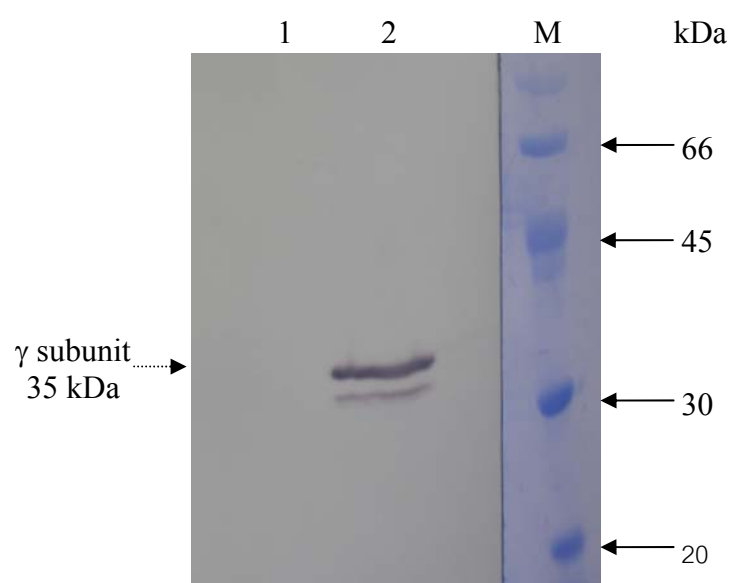


Figure 62 Immunoblot analysis of ApNa⁺-ATPase in cyanobacterium *Synechococcus* sp. PCC 7942 cells. *Synechococcus* sp. PCC 7942 cells were transformed with plasmid pUC303 (Lane 1), pUC303-*ApNa⁺-atp* operon (Lane 2) and molecular weight marker (Lane M).

To examine the localization of ApNa^+ -ATPase, the membrane vesicles (total membrane fractions) from *Synechococcus* sp. PCC 7942 transformed with pUC303-*ApNa}^+-atp* (ApNa^+ -ATPase-expressing cells) were applied on the sucrose density gradient. Thylakoid membranes remained at the 58% sucrose interphase, while cytoplasmic membranes moved into the 30% sucrose layer (Figure 63). Thylakoid membranes contained about 4.1 μg chlorophyll per mg protein, while cytoplasmic membranes contained 0.063 μg chlorophyll per mg protein. Moreover, data presented in Figure 64 revealed that a single protein band of the corresponding molecular mass of γ subunit of ApNa^+ -ATPase was found in cytoplasmic membrane fraction. In order to test whether the thylakoid membrane fraction is free from contaminated cytoplasmic membrane, we have tested the cross-reactivity of the thylakoid membrane fraction to the antibody against NrtA, which is a protein involved in nitrate transport and is localized only in the cytoplasmic membrane of *Synechococcus* sp. PCC 7942 (Omata, 1995). The results showed that the antibody against NrtA strongly cross-reacted with the cytoplasmic membrane fraction fractionated from ApNa^+ -ATPase-expressing cells. This indicated that ApNa^+ -ATPase localized in cytoplasmic membrane of ApNa^+ -ATPase-expressing *Synechococcus* sp. PCC 7942 cells.

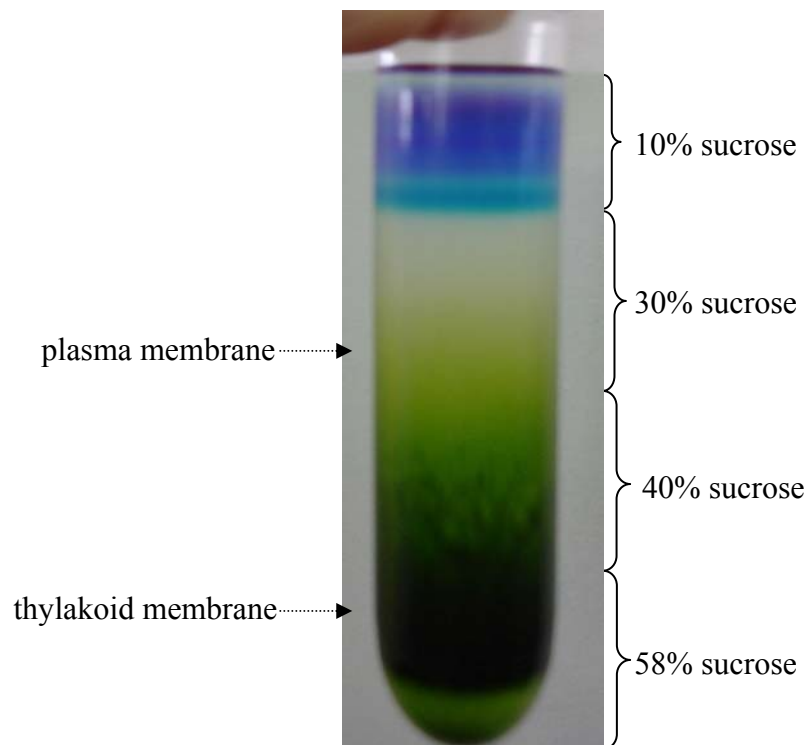


Figure 63 Separation of plasma membrane and thylakoid membrane fractions on a sucrose gradient centrifugation.

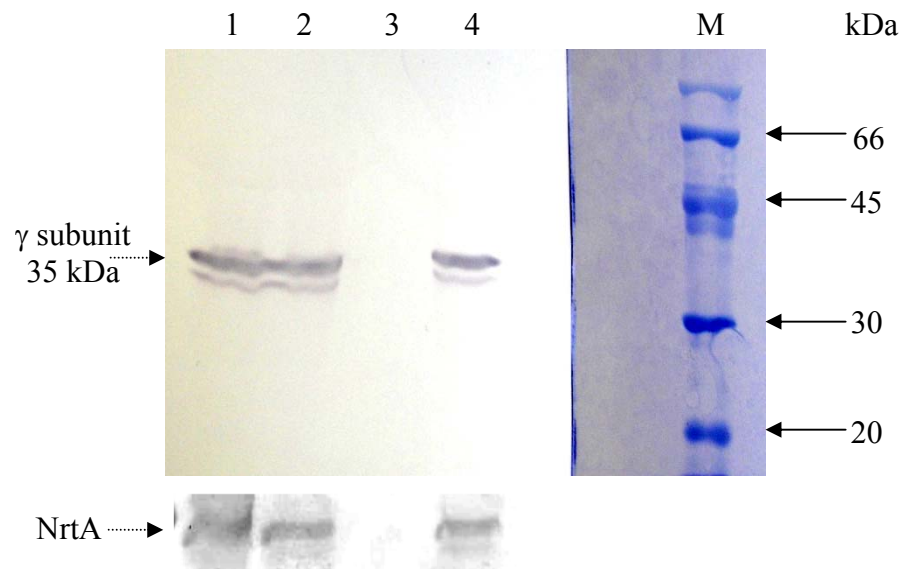


Figure 64 The localization of ApNa^+ -ATPase in ApNa^+ -ATPase-expressing *Synechococcus* sp. PCC 7942 cells. The ApNa^+ -ATPase-expressing cells were prepared as whole cells (Lane 1) and fractionated as membrane vesicles (Lane 2), thylakoid membranes (Lane 3), cytoplasmic membrane (Lane 4). Samples (50 μg protein) were separated on 12% SDS-PAGE and transferred onto PVDF membrane. His tag-containing γ subunit (*ApNa⁺-atpG*) was detected by immunoblotting. Lane M is molecular weight marker.

4.13.2 Effect of NaCl in the growth medium on ATP hydrolysis activity of inverted membrane vesicles from *Synechococcus* sp. PCC7942 transformants

Synechococcus sp. PCC7942 cells transformed with pUC303 (empty vector transformants) and pUC303-*ApNa⁺-atp* (*ApNa⁺-ATPase*-expressing cells) were grown in the growth medium containing various NaCl concentrations and then IPTG was added to final conc. of 0.5 mM. After induction for 3 days, inverted membrane vesicles were prepared and ATP hydrolysis activity was tested. The results showed that ATP hydrolysis activity of inverted membranes vesicles from the *ApNa⁺-ATPase*-expressing cells was stimulated after the cells were stressed with NaCl while the empty vector transformants did not (Figure 65).

4.13.3 Effect of NaCl in the growth medium on the expression of *ApNa⁺-ATPase* in inverted membrane vesicles from *ApNa⁺-ATPase*-expressing *Synechococcus* sp. PCC 7942 cells

Synechococcus sp. PCC 7942 cells transformed with pUC303-*ApNa⁺-atp* (*ApNa⁺-ATPase*-expressing cells) were grown in the growth medium containing various NaCl concentrations and then IPTG was added to final conc. of 0.5 mM. After induction for 3 days, inverted membrane vesicles were prepared and immunoblot analysis was done. The results showed that the expression level of *ApNa⁺-ATPase* increased with the increase of NaCl in the growth medium (Figure 66).

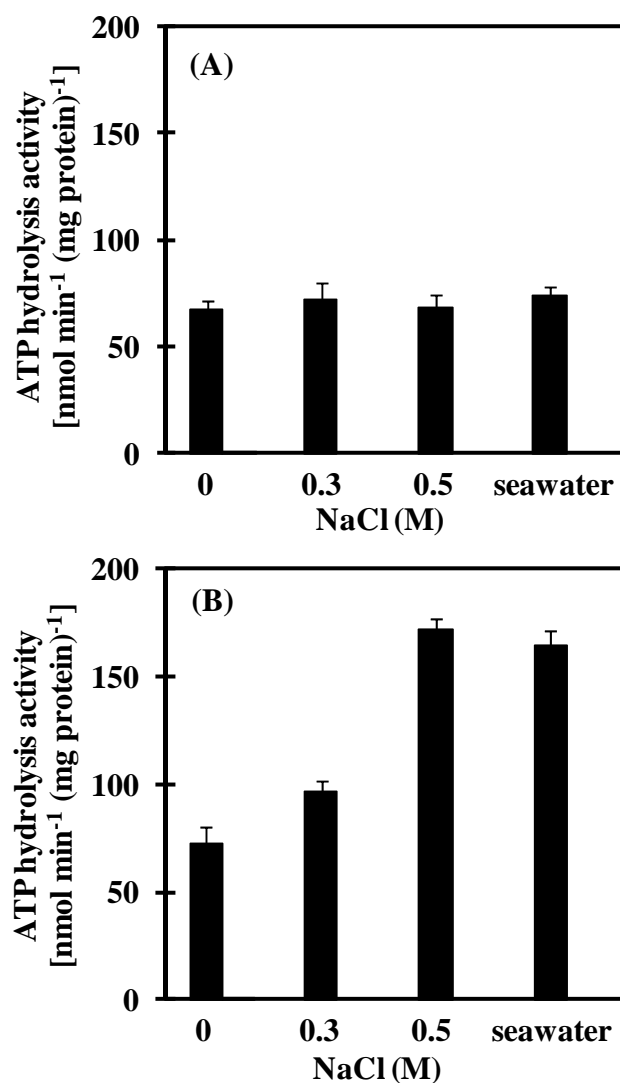


Figure 65 Effect of NaCl in the growth medium on ATP hydrolysis activity of inverted membrane vesicles from *Synechococcus* sp. PCC 7942 transformants. (A) and (B) are the empty vector transformants and ApNa⁺-ATPase-expressing cells, respectively.

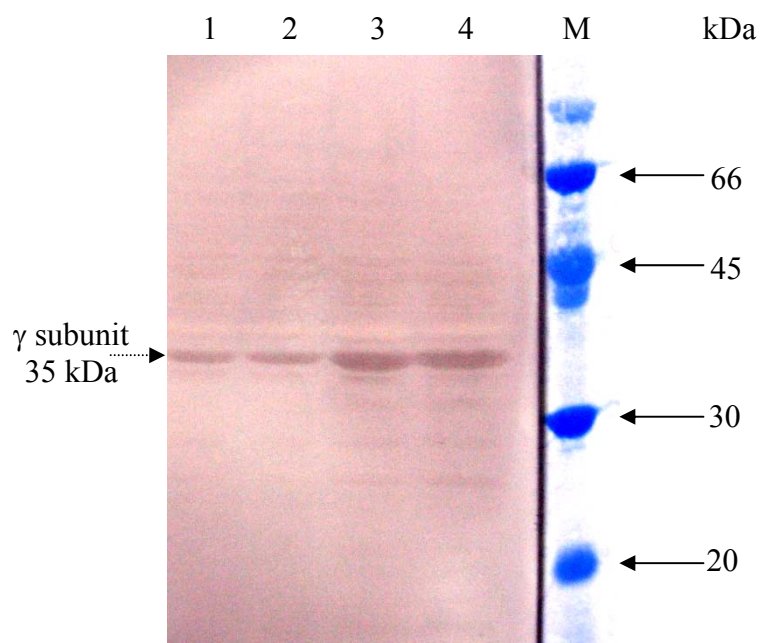


Figure 66 Effect of NaCl in the growth medium on ApNa^+ -ATPase expression in ApNa^+ -ATPase-expressing *synechococcus* sp. PCC 7942 cells. The cells were grown in BG11 medium containing 0.0 M NaCl (lane 1), 0.3 M NaCl (lane 2), 0.5 M NaCl (lane 3), seawater (lane 4). Inverted membrane vesicles (50 μg protein) were separated on 12% SDS-PAGE and transferred onto PVDF membrane. His tag-containing γ subunit (*ApNa⁺-atpG*) was detected by immunoblotting. Lane M is molecular weight marker.

CHAPTER V

DISCUSSION

ATPases associated with various cations such as Ca^{2+} , Cu^{2+} , K^+ and Mg^{2+} in a number of cyanobacteria have been studied (Reed *et al.*, 1981; Lerma and Gómez-Lojero, 1987; Kanamaru *et al.*, 1994; Geisler *et al.*, 1998). However, ATPase involved in Na^+ transport in cyanobacteria has not been demonstrated experimentally. In this study, we focused on the involvement of ATPase in Na^+ homeostasis in the alkaliphilic halotolerant cyanobacterium *A. halophytica*. From the experiment, we also found that *A. halophytica* requires Na^+ for its growth and K^+ could not replace Na^+ (Figure 10A). Furthermore, high ATP hydrolysis activity detected in inverted membrane vesicles from cells grown under high salinity and high pH conditions (Figure 11A, B) suggested that ATPase from *A. halophytica* plays a role in the response of cells against an increase in salinity and pH. Similar observations were found in *Streptococcus faecalis*, *Tetraselmis viridis*, and *Heterosigma akashiwo* (Kinoshita *et al.*, 1984; Gimmler, 2000). The presence of gramicidin D, an ionophore that dissipates Na^+ -gradients, in the growth medium resulted in the cessation of cell growth (Figure 12A). These results are in agreement with those previously reported in a facultative anaerobic alkaliphile M-12 (*Amphibacillus* sp.) which utilized sodium motive force ($\Delta\mu\text{Na}^+$) generated by a sodium pump for active transport of solutes while other alkaliphiles produced $\Delta\mu\text{Na}^+$ by a Na^+/H^+ antiporter which is a secondary transport system for Na^+ (Krulwich, 1986; Koyama, 1993; Kaieda *et al.*, 1998).

To investigate Na^+ transport in relation to ATPase activity in *A. halophytica*, the ATPase was purified and tentatively classified as an F-type ATPase. This is based

on the results that its activity was inhibited by azide and DCCD, which are inhibitors of F-type ATPase but not by orthovanadate and nitrate which are inhibitors of P-type and V-type ATPases, respectively (Table 6). DCCD is believed to inhibit F-type ATPase due to the binding of DCCD to a highly conserved carboxyl residue in the c subunit of the F_0 portion (Linnett and Beechey, 1979). The band pattern of the purified enzyme analyzed by SDS-PAGE as shown in Figure 18 was comparable to the typical mobilities and band pattern of F-type ATPase subunits from both *Ilyobacter tartaricus* (Neumann *et al.*, 1998) and a thermoalkaliphilic *Bacillus* sp. strain TA2.A1 (Cook *et al.*, 2003). The polypeptide bands could tentatively be identified as ATPase subunits of an F-type ATPase, namely: α (56 kDa), β (52 kDa), γ (35 kDa), a (25 kDa), b (22 kDa), δ (22 kDa), ϵ (16.5 kDa) and c (6.5 kDa). The molecular weight of the ATPase complex (suggested to be $\alpha_3\beta_3\gamma\delta\epsilon abc_{8-9}$) determined by SDS-PAGE (Figure 19) was about 500 kDa which is close to the molecular weight of ATPase complex determined by gel filtration (528 kDa) (Figure 17). Moreover, the band tentatively identified as F-type ATPase subunit c of *A. halophytica* was confirmed by LC-MS/MS analysis. One of the obtained sequences after trypsin digestion namely “ISSGAEGIAR” was found to be highly identical to the partial sequence of F-type ATPase subunit c of at least four strains of cyanobacteria, namely *Synechococcus* sp. WH 8102, *Synechococcus* sp. PCC 9902, *Synechococcus* sp. PCC 7002 and *Gloeobacter violaceus*. Overall, the results from the inhibitor effects, and the typical subunits band pattern as well as the protection by Na^+ against DCCD inhibition of ATP hydrolysis activity (Table 6 and Figure 24A, B), suggest that the ATPase from *A. halophytica* is likely a member of the F-type ATPases.

The purified ATPase from *A. halophytica* was reconstituted into liposomes to investigate the possible role of Na^+ -stimulated ATPase on the transport of Na^+ . The

reconstituted proteoliposomes showed catalytic properties, namely K_m 's of Na^+ and ATP identical to those of the purified ATPase. Moreover, an increase in the concentration of NaCl and ATP led to an increase in Na^+ uptake by the proteoliposomes (Figure 27A, B). These results suggest the presence of an ATP-dependent Na^+ pump in the proteoliposomes. The substrate ATP was hydrolyzed by ATPase to provide a driving force for Na^+ uptake. A previous report demonstrated the function of Na^+ -ATPase as a Na^+ pump in the plasma membrane of the marine alga *Heterosigma akashiwo* based on the similarity of the kinetic properties of Na^+ transport and Na^+ -ATPase activity (Shono *et al.*, 1996). In *A. halophytica*, the apparent K_m value of Na^+ transport for Na^+ and ATP were 3.3 and 0.5 mM, respectively. These values are close to the apparent K_m values of Na^+ -stimulated ATPase activity for Na^+ (2 mM) and ATP (1.2 mM). This indicates that the purified ATPase from *A. halophytica* is indeed a Na^+ pump. The uptake of Na^+ into proteoliposomes was abolished by Na^+ gradient dissipators gramicidin D and monensin whereas a protonophore CCCP and the permeant anion nitrate had a stimulatory effect on Na^+ uptake (Figure 28), suggesting that the operation of electrogenic Na^+ transport by Na^+ -stimulated ATPase in *A. halophytica*. Moreover, ATP-dependent Na^+ uptake by proteoliposomes was a primary and not a secondary event, i.e. the transport was not catalyzed by a Na^+/H^+ antiporter or other secondary events driven by proton potential.

As observed in Figure 29A, Na^+ uptake by ATPase is associated with H^+ efflux in *A. halophytica*. Previously, the marine alga *Tetraselmis viridis* was shown to contain Na^+ -ATPase capable of translocating Na^+ into plasma membrane vesicles which was accompanied by H^+ efflux with the consequence of the alkalization of the vesicle lumen (Balnokin *et al.*, 1999). In this study, we attempted to elucidate the

mechanism of Na^+ - and H^+ -transport by Na^+ -stimulated ATPase reconstituted into liposomes. Two possible mechanisms of Na^+ -transport can be hypothesized (Balnokin *et al.*, 2004). Mechanism 1 proposes that the Na^+ -stimulated ATPase operates as a uniporter catalyzing only Na^+ transport across proteoliposomes, subsequently, H^+ transport is driven by the membrane potential generated by Na^+ -stimulated ATPase. Mechanism 2 proposes that the Na^+ -stimulated ATPase operates as an antiporter catalyzing an exchange of Na^+ for H^+ .

To distinguish between these two mechanisms, we studied the role of membrane potential in ATP-dependent H^+ translocation. The dissipation of membrane potential would result in complete suppression of H^+ efflux, if the membrane potential across the proteoliposome generated by Na^+ -stimulated ATPase were the only driving force for H^+ extrusion. On the other hand, if H^+ efflux occurred directly via the Na^+ -stimulated ATPase as an antiporter by exchanging Na^+ for H^+ , the dissipation of the membrane potential would not suppress H^+ efflux (Balnokin *et al.*, 1999). A permeant anion, nitrate, that generally penetrates easily across biological membranes down its electrochemical gradient is often used as a charge-compensating anion to abolish membrane potential (positive inside) across proteoliposomes during the measurements of ATP-driven H^+ translocation. If nitrate inhibits the ATP-dependent alkalization of the proteoliposome lumen and promotes both dissipation of membrane potential and ATP-dependent Na^+ uptake, it can be concluded that ATP- and Na^+ -dependent H^+ efflux from proteoliposomes is driven by the membrane potential generated by Na^+ -ATPase. Hence, Na^+ -ATPase operates as a uniporter carrying only Na^+ , and H^+ is not involved in the catalytic cycle of this enzyme. On the contrary, if nitrate increases both ATP-dependent alkalization of the proteoliposome lumen and Na^+ uptake while

membrane potential is dissipated, it can be concluded that Na⁺-stimulated ATPase operates as an antiporter catalyzing Na⁺/H⁺ exchange.

Our results are consistent with mechanism 1 by which the purified Na⁺-stimulated ATPase operates as a uniporter. The ATP-dependent Na⁺ uptake in proteoliposomes was accelerated in the presence of CCCP and nitrate (Figure 28) and both agents dissipated membrane potential generated by Na⁺-stimulated ATPase (Figure 30A). CCCP stimulated ATP-dependent alkalization of proteoliposomes while nitrate inhibited this alkalization (Figure 29A). Only Na⁺ but not K⁺, Li⁺ and Ca²⁺ promoted H⁺ efflux (Figure 29B). The results indicate that H⁺ efflux from proteoliposomes is driven by the membrane potential generated by Na⁺-stimulated ATPase and is specific for Na⁺. Moreover, this dependence of lumen alkalization on Na⁺ coincided with the requirement of Na⁺ but not K⁺, Li⁺ and Ca²⁺ on ATPase activity (Figure 21A). Therefore, we can conclude that 1) Na⁺-stimulated ATPase from *A. halophytica* operates as a uniporter which takes up only Na⁺ while H⁺ is counterion and 2) ATP-dependent lumen alkalization occurred as a result of the operation of the Na⁺-stimulated ATPase. H⁺ efflux does not occur directly via Na⁺-stimulated ATPase but is driven by the membrane potential generated during Na⁺-stimulated ATPase operation. The operation of Na⁺-stimulated ATPase as a Na⁺ uniporter has been previously reported in the halotolerant microalga *Dunaliella maritima* (Popova *et al.*, 2005) while Na⁺-translocating ATPase in the marine microalga *Tetraselmis viridis* operates as an Na⁺/H⁺ exchanger (Balnokin *et al.*, 2004).

Despite the fact that several potential Na⁺-ATPases have been implicated in cyanobacteria, the existence of a Na⁺-ATPase responsible for Na⁺ movement has not been experimentally demonstrated. Recent studies in the genome of *Synechocystis* sp.

PCC 6803 showed that the disruption of a gene cluster encoding a putative Na⁺-ATPase subunit led to high NaCl sensitivity of the mutant suggesting the role of Na⁺-ATPase in salt resistance (Wang *et al.*, 2002). Brown *et al.* (1990) reported that NaCl could stimulate light-supported generation of membrane potential in the marine cyanobacterium *Oscillatoria brevis*. They further suggested that *O. brevis* might possess a light-dependent primary Na⁺ pump in the cytoplasmic membrane but it is not clear what kind of a primary Na⁺ pump operates in the cytoplasmic membrane of *O. brevis*. *Synechococcus* R-2 PCC 7942 was postulated to have a primary Na⁺ pump extruding Na⁺ in the light and dark utilizing Na⁺ motive force (Ritchie, 1992). Our study in *A. halophytica* is the first report that experimentally demonstrates the involvement of Na⁺-stimulated ATPase in Na⁺ transport in cyanobacteria using a purified protein incorporated into liposomes.

In molecular biology aspect, the sequence of *ApNa⁺-atp* operon was obtained from the shotgun genome sequencing of *A. halophytica*. Nine ORFs were organized in the order *atpD* (β), *atpC* (ε), *atpI* (I), hypothetical gene (hypothetical protein), *atpB* (a), *atpE* (c), *atpF* (b), *atpA* (α), and *atpG* (γ) (Figure 31), which is different from other bacteria. In *Clostridium paradoxum*, *Escherichia coli*, *Ilyobacter tartaricus*, and *Propionigenium modestum*, the *atp* operon consists of nine structural genes, *atpI* (I), *atpB* (a), *atpE* (c), *atpF* (b), *atpH* (δ), *atpA* (α), *atpG* (γ), *atpD* (β), and *atpC* (ε), which are grouped together to form a single transcriptional unit (Walker *et al.*, 1982; Miki *et al.*, 1988; Kaim *et al.*, 1992; Meier *et al.*, 2003; Ferguson *et al.*, 2006). The *atp* operon in a strictly anaerobic *Acetobacterium woodii* consists of 11 genes including 9 genes found in the bacterial *atp* operons and additional 2 copies of *atpE* (c) (Rahlf *et al.*, 1999). In addition, the structural genes in cyanobacteria *Anabaena* sp. PCC 7210, *Synechococcus* sp. PCC 6301, and *Synechocystis* sp. PCC 6803 are

organized in two separate domains, one containing *atpB* (a), *atpE* (c), *atpF* (b), *atpH* (δ), *atpA* (α), and *atpG* (γ), whereas the other containing *atpD* (β) and *atpC* (ε) (Cozens and Walker, 1987; Curtis, 1987; Lill and Nelson, 1991). Although, the deduced protein sequences of nine ApNa⁺-ATPase subunits showed low percent identity compared with the corresponding sequences of F-type ATPase subunits from different species, the conserved amino acid S68 and T69 at the Na⁺ binding site of the ApNa⁺-ATPase subunit c were found (Figure 33). The Na⁺-binding site of the *I. tartaricus* ATPase and H⁺-binding site of the spinach chloroplast ATPase subunit c were compared by Vollmar *et al.* (2009). The results showed that alanine was present at position 62 of H⁺-translocating ATPase, whereas a polar serine or threonine was observed in the equivalent position of Na⁺-translocating ATPase. Likewise, the hydrophobic side chain leucine was found in H⁺-translocating ATPase at position 63 but threonine was found at the equivalent position of Na⁺-translocating ATPase. The data presented above clearly indicate that F-type Na⁺-ATPase from *A. halophytica* is a Na⁺-translocating ATPase.

Furthermore, this study examined the biochemical properties and physiological functions of ApNa⁺-ATPase. The expression of ApNa⁺-ATPase in ApNa⁺-ATPase-expressing *E. coli* DK8 and *E. coli* TO114 cells could enable the cells to grow better than the control cells under high salinity (Figure 38, 39). As per above data, we thought that the introduction of *ApNa⁺-atp* operon into a freshwater cyanobacterium, *Synechococcus* sp. PCC 7942 will confer salt tolerance to this organism. As expected, the ApNa⁺-ATPase-expressing *Synechococcus* sp. PCC 7942 cells could grow in the BG11 medium containing 0.5 M NaCl and seawater while the empty vector transformants could not (Figure 54). From these results, *ApNa⁺-atp* operon transformation could improve salt tolerance in the freshwater cyanobacterium

Synechococcus sp. PCC 7942 as well as *E. coli* DK8 mutant (Δatp) and salt-sensitive mutant *E. coli* TO114.

The ATP hydrolysis activity of inverted membrane vesicles from ApNa⁺-ATPase-expressing *E. coli* DK8 and *Synechococcus* sp. PCC 7942 cells were dependent on NaCl and ATP concentration in the reaction medium (Figure 42, 43A, 56, 57A). Moreover, the Na⁺ extrusion from Na⁺-loaded ApNa⁺-ATPase-expressing *E. coli* DK8 and *Synechococcus* sp. PCC 7942 cells was observed after the cells were energized with glucose (Figure 41, 55), suggesting that the Na⁺ extrusion is likely due to the contribution by ApNa⁺-ATPase because glucose can yield ATP during its metabolism. ApNa⁺-ATPase was confirmed as a member of F-type Na⁺-ATPase by using appropriate inhibitors. The ATP hydrolysis activity was inhibited by azide (F₁ inhibitor), DCCD (F₀ inhibitor) or tributyltin chloride (F₀ inhibitor). In addition, it was found that monensin (Na⁺-gradient dissipator) inhibited ATP hydrolysis activity, whereas CCCP (a protonophore) and KNO₃ (a permeant anion) did not inhibit (Figure 44, 58). These data indicate the involvement of ΔpNa^+ but not ΔpH on ATP hydrolysis. Moreover, it was found that Na⁺ could protect ATPase from DCCD inhibition in a pH-dependent manner (Figure 45, 59).

Using another approach, ATP synthesis was observed in the Na⁺-loaded inverted membrane vesicles from ApNa⁺-ATPase-expressing *E. coli* DK8 and *Synechococcus* sp. PCC 7942 cells in the presence of ΔpNa^+ and $\Delta \psi$ (Figure 46, 60). Our data revealed that ATP synthesis was stimulated in the presence of K⁺/valinomycin and CCCP (a protonophore). ATP synthesis decreased when external Na⁺ and monensin (Na⁺ gradient dissipator) were added because both of them reduced ΔpNa^+ (Figure 47, 61). Based on these results, it can be concluded that ATP synthesis catalyzed by ApNa⁺-ATPase requires ΔpNa^+ and $\Delta \psi$.

ATP hydrolysis activity assay and Western blot analysis revealed that ATP hydrolysis activity of inverted membrane vesicles and the expression level of γ subunit of ApNa^+ -ATPase expressed in *E. coli* DK8 and *Synechococcus* sp. PCC 7942 cells increased with increasing NaCl concentration in the growth medium (Figure 49, 50, 65, 66). Taken together, our results strongly suggest a role for ApNa^+ -ATPase in the salt-stress tolerance of this photosynthetic organism.

In this work, only ApNa^+ -ATPase enzyme activity and protein expression were studied. To in dept understand the regulation of ApNa^+ -ATPase gene expression in response to salt stress, the mRNA expression level and promoter analysis of F-type *ApNa⁺-atp* operon should be studied.

CHAPTER VI

CONCLUSIONS

The present study on Na⁺-ATPase in *Aphanothece halophytica* has revealed the following findings:

1. High ATP hydrolysis activity was detected in inverted membrane vesicles from *A. halophytica* grown under high salinity and high pH conditions.
2. The effect of inhibitors, the typical subunits band pattern, LC-MS/MS analysis as well as the protection by Na⁺ against DCCD inhibition of ATP hydrolysis activity suggest that the ATPase from *A. halophytica* is a member of the F-type ATPases.
3. An increase in the concentration of NaCl and ATP led to an increase in ATP hydrolysis activity and Na⁺ uptake into proteoliposomes. These results suggest that the uptake of Na⁺ into proteoliposomes is mediated by this enzyme upon ATP hydrolysis.
4. The transport of Na⁺ in *A. halophytica* is electrogenic and operates via a uniport mechanism with H⁺ countertransport as a secondary event energized by the membrane potential generated by the operation of Na⁺-stimulated ATPase.
5. From the short gun cloning of *A. halophytica*, the sequence of *ApNa⁺-atp* operon encoding F-type Na⁺-ATPase was obtained. A single transcription unit containing nine open reading frames (ORFs) were organized in the order *atpD* (β), *atpC* (ϵ), *atpI* (Γ), hypothetical gene (hypothetical protein), *atpB* (α), *atpE* (δ), *atpF* (θ), *atpA* (α), and *atpG* (γ).

6. The alignment of the c subunit ATPase from *A. halophytica* to those from different species presented the conserved Na⁺-motif consisting of E³⁴, E⁶⁷, S⁶⁸ T⁶⁹ and Y⁷² in the c subunit of *A. halophytica*. These data clearly indicate that the isolated F-type *atp* operon from *A. halophytica* is Na⁺-*atp* operon.
7. The expression of ApNa⁺-ATPase in ApNa⁺-ATPase-expressing *E. coli* DK8 and TO114 cells could enabled the cells to grow better than the control cells. Moreover, it was found that the introduction of *ApNa⁺-atp* operon into a freshwater cyanobacterium, *Synechococcus* sp. PCC 7942 could confer salt tolerance to this organism.
8. ATP hydrolysis activity of inverted membrane vesicles from ApNa⁺-ATPase-expressing *E. coli* DK8 and *Synechococcus* sp. PCC 7942 cells increased with increasing concentration of NaCl and ATP.
9. The Na⁺ extrusion from Na⁺-loaded ApNa⁺-ATPase-expressing *E. coli* DK8 and *Synechococcus* sp. PCC 7942 cells was observed after the cells were energized with glucose, suggesting that the Na⁺ extrusion is likely due to the contribution by ApNa⁺-ATPase because glucose can yield ATP during its metabolism.
10. ATP synthesis was observed in Na⁺-loaded inverted membrane vesicles from ApNa⁺-ATPase-expressing *E. coli* DK8 and *Synechococcus* sp. PCC 7942 cells in the presence of ΔpNa^+ and $\Delta\psi$.
11. Western blot analysis revealed that the expression level of ApNa⁺-ATPase in ApNa⁺-ATPase-expressing *E. coli* DK8 and *Synechococcus* sp. PCC 7942 cells depended on NaCl concentration in the growth medium.
12. ApNa⁺-ATPase localized in the cytoplasmic membrane of *Synechococcus* sp. PCC 7942.

REFERENCES

- Allakhverdiev, S.I., Sakamoto, A., Nishiyama, Y., Inaba, M., and Murata, N. 2000. Ionic and osmotic effects of NaCl-induced inactivation of photosystems I and II in *Synechococcus* sp. Plant Physiol. 123: 1047-1056.
- Apse, M.P., and Blumwald, E. 2002. Engineering of salt tolerance in plants. Curr. Opin. Biotechnol. 13: 146-150.
- Apte, S.K., Reddy, B.R., and Thomas, J. 1987. Relationship between sodium influx and salt tolerance of nitrogen-fixing cyanobacteria. Appl. Environ. Microbiol. 53: 1934-1939.
- Apte, S.K., and Thomas, J. 1980. Sodium is required for nitrogenase activity in cyanobacteria. Curr. Microbiol. 3: 291-293.
- Apte, S.K., and Thomas, J. 1983a. Impairment of photosynthesis by sodium deficiency and its relationship to nitrogen fixation in the cyanobacterium *Anabaena torulosa*. FEMS Microbiol. Lett. 16: 153-157.
- Apte, S.K., and Thomas, J. 1984. Effect of sodium on nitrogen fixation in *Anabaena torulosa* and *Plectonema boryanum*. J. Gen. Microbiol. 130: 1161-1168.
- Apte, S.K., and Thomas, J. 1985. Effect of sodium on membrane potential, uptake of phosphate, nucleoside phosphate pool and synthesis and expression of nitrogenase in *Anabaena torulosa*. Indian J. Exp. Biol. 23: 518-522.
- Balnokin, Y.V., and Popova, L.G. 1994. The ATP-driven Na⁺-pump in the plasma membrane of the marine unicellular alga, *Platymonas viridis*. FEBS Lett. 343: 61-64.
- Balnokin, Y.V., Popova, L.G., and Andreev, I.M. 1999. Electrogenicity of the Na⁺-

- ATPase from the marine microalga *Tetraselmis (Platymonas) viridis* and associated H⁺ countertransport. FEBS Lett. 462: 402-406.
- Balnokin, Y.V., Popova, L.G., Pagis, L.Y., and Andreev, I.M. 2004. The Na⁺-transporting ATPase in the plasma membrane of the marine microalga *Tetraselmis viridis* catalyzes Na⁺/H⁺ exchange. Planta. 219: 332-337.
- Becher, B., Muller, V., and Gottschalk, G. 1992a. The methyltetrahydromethanopterin:coenzyme M methyltransferase of *Methanosarcina mazi* strain Go1 is a primary sodium pump. FEMS Microbiol. Lett. 91: 239-244.
- Becher, B., Müller, V., and Gottschalk, G. 1992b. N⁵-Methyltetrahydromethanopterin:coenzyme M methyltransferase of *Methanosarcina mazi* strain Go1 is a Na⁺-translocating membrane enzyme. J. Bacteriol. 174: 7656-7660.
- Benito, B., Quiñero, F.J., and Rodríguez-Navarro, A. 1997. Overexpression of the sodium ATPase of *Saccharomyces cerevisiae*. Conditions for phosphorylation from ATP and Pi. Biochim. Biophys. Acta. 1328: 214-226.
- Berg, J.M., Tymoczko, J.L., and Stryer, L. 2002. Biochemistry. 5 th ed. New York: W.H. Freeman.
- Berger, S., Ellersiek, U., and Steinmüller, K. 1991. Cyanobacteria contain a mitochondrial complex I-homologous NADH-dehydrogenase. FEBS Lett. 286: 129-132.
- Blumwald, E., Wolosin, J.M., and Parker, L. 1984. Na⁺/H⁺ exchange in the cyanobacterium *Synechocystis* 6311. Biochem. Biophys. Res. Commun. 122: 452-459.
- Bott, M., Pfister, K., Burda, P., Kalbermatter, O., Woehlke, G., and Dimroth, P. 1997. Methylmalonyl-CoA decarboxylase from *Propionigenium modestum*: cloning

- and sequencing of the structural genes and purification of the enzyme complex. Eur. J. Biochem. 250: 590–599.
- Bradford, M. 1976. A rapid and sensitive method for the determination of microgram quantities of protein utilizing the principle of protein-dye binding. Anal. Biochem. 72: 248-254.
- Brown, I.I., Fadeyev, S.I., Kirik, I.I., Severina, I.I., and Skulachev, V.P. 1990. Light-dependent $\Delta\mu\text{Na}$ -generation and utilization in the marine cyanobacterium *Oscillatoria brevis*. FEBS Lett. 270: 203-206.
- Brownell, P.F., and Nicholas, D.J.D. 1967. Some effects of sodium on nitrate assimilation and N_2 fixation in *Anabaena cylindrica*. Plant Physiol. 42: 915-921.
- Buckel, W., and Liedtke, H. 1986. The sodium pump glutacoyl-CoA decarboxylase from *A. fermentans*. Specific cleavage by n-alkanols. Eur. J. Biochem. 156: 251–257.
- Buckel, W., and Semmler, R. 1982. A biotin-dependent sodium pump: glutacoyl-CoA decarboxylase from *Acidaminococcus fermentans*. FEBS Lett. 148: 35–38.
- Casamayor, E.O., Massana, R., Benlloch, S., Øvreås, L., Díez, B., Goddard, V.J., Gasol, J.M., Joint, I., Rodríguez-Valera, F., and Pedrós-Alió, C. 2002. Changes in archaeal, bacterial and eukaryal assemblages along a salinity gradient by comparison of genetic fingerprinting methods in a multipond solar saltern. Environ. Microbiol. 4: 338-348.
- Cayley, S., Lewis, B.A., Guttman, H.J., and Record, M.T. Jr. 1991. Characterization of the cytoplasm of *Escherichia coli* K-12 as a function of external osmolarity. Implications for protein-DNA interactions in vivo. J. Mol. Biol. 222: 281–300.

- Cayley, S., Lewis, B.A., and Record, M.T. Jr. 1992. Origins of the osmoprotective properties of betaine and proline in *Escherichia coli* K-12. J. Bacteriol. 174: 1586–1595.
- Cohen, Y., Jørgensen, B.B., Revsbech, N.P., and Poplawski, R. 1986. Adaptation to hydrogen sulfide of oxygenic and anoxygenic photosynthesis among cyanobacteria. Appl. Environ. Microbiol. 51: 398–407.
- Cook, G.M., Keis, S., Morgan, H.W., von Ballmoos, C., Matthey, U., Kaim, G., and Dimroth, P. 2003. Purification and biochemical characterization of the F₁F₀-ATP synthase from thermoalkaliphilic *Bacillus* sp. strain TA2.A1. J. Bacteriol. 185: 4442-4449.
- Cozens, A.L., and Walker, J.E. 1987. The organization and the sequence of the genes for ATP synthase subunits in the cyanobacterium *Synechococcus* 6301: support for an endosymbiotic origin of chloroplasts. J. Mol. Biol. 194: 359-383.
- Curtis, S.E. 1987. Genes encoding the beta and epsilon subunits of the proton translocating ATPase from *Anabaena* sp. strain PCC 7120. J. Bacteriol. 169: 80-86.
- Dimroth, P. 1992. Structure and function of the Na(+)-translocating ATPase of *Propionigenium modestum*. Acta. Physiol. Scand. Suppl. 607: 97-103.
- Dimroth, P., Jockel, P., and Schmid, M. 2001. Coupling mechanism of the oxaloacetate decarboxylase Na⁺ pump. Biochim. Biophys. Acta. 1505: 1-14.
- Dimroth, P., and Thomer, A. 1993. On the mechanism of sodium ion translocation by oxaloacetate decarboxylase from *Klebsiella pneumoniae*. Biochemistry. 32: 1734–1739.
- Dover, N., and Padan, E. 2001. Transcription of *nhaA*, the main Na⁺/H⁺ antiporter of

- Escherichia coli*, is regulated by Na⁺- and growth phase. J. Bacteriol. 183: 644-653.
- Duggan, P.S., Gottardello, P., and Adams, D.G. 2007. Molecular analysis of genes in *Nostoc punctiforme* involved in pilus biogenesis and plant infection. J. Bacteriol. 198: 4547-4551.
- Echlin, P. 1966. The blue-green algae. Sci. Am. 214(6): 74-81.
- Edgley, M., and Brown, A.D. 1983. Yeast water relations : physiological changes induced by solute stress in *Saccharomyces cerevisiae* and *Saccharomyces rouxii*. J. Gen. Microbiol. 129: 3453-3463.
- Ferguson, S.A., Keis, S., and Cook, G.M. 2006. Biochemical and molecular characterization of a Na⁺-translocating F₁F₀-ATPase from the thermoalkaliphilic bacterium *Clostridium paradoxum*. J. Bacteriol. 188: 5045-5054.
- Fernandes, T.A., Iyer, V., and Apte, S.K. 1993. Differential responses of nitrogen-fixing cyanobacteria to salinity and osmotic stresses. Appl. Env. Microbiol. 59: 899-904.
- Garcia-Gonzalez, M., Sanchez-Maeso, E., Quesada, A., and Fernandez-Valiente, E. 1987. Sodium requirement for photosynthesis and nitrate assimilation in a mutant of *Nostoc muscorum*. J. Plant. Physiol. 127: 423-429.
- Gartner, P., Ecker, A., Fischer, R., Linder, D., Fuchs, G., and Thauer, R.K. 1993. Purification and properties of N⁵-methyltetrahydromethanopterin:coenzyme M methyltransferase from *Methanobacterium thermoautotrophicum*. Eur. J. Biochem. 213: 537- 545.
- Geitler, L. 1932. Cyanophyceae. In R. Kolkwitz (ed.), Rabenhorst Kryptogamen-Flora von Deutschland, osterreich und der Schweiz, vol. 14, pp. 1-1196. Leipzig:

Akademische Verlagsgesellschaft.

- Geisler, M., Koenen, W., Richter, J., and Schumann, J. 1998. Expression and characterization of a *Synechocystis* PCC 6803 P-type ATPase in *E. coli* plasma membranes. Biochim. Biophys. Acta. 1368: 267-275.
- Gimmler, H. 2000. Primary sodium plasma membrane ATPase in salt-tolerant algae: facts and fictions. J. Exp. Bot. 51: 1171-1178.
- Glynn, I.M., and Karlsh, S. 1975. The sodium pump. Annu. Rev. Physiol. 37: 13-55.
- Hagemann, M., and Erdmann, N. 1994. Activation and pathway of glucosylglycerol synthesis in the cyanobacterium *Synechocystis* sp. PCC 6803. Microbiology. 140: 1427-1431.
- Hansmann, S., and Martin, W. 2000. Phylogeny of 33 ribosomal and six other proteins encoded in an ancient gene cluster that is conserved across prokaryotic genomes: influence of excluding poorly alignable sites from analysis. Int. J. Syst. Evol. Microbiol. 50: 1655-1663.
- Haro, R., Garciadeblas, B., and Rodriguez-Navarro, A. 1991. A novel P-type ATPase from yeast involved in sodium transport. FEBS Lett. 291: 189-191.
- Heefner, D.L., and Harold, F.M. 1982. ATP-driven sodium pump in *Streptococcus faecalis*. Proc. Natl. Acad. Sci. USA. 79: 2798-2802.
- Hilbi, H., Dehning, I., Schink, B., and Dimroth, P. 1992. Malonate decarboxylase of *Malonomonas rubra*, a novel type of biotin-containing acetyl enzyme, Eur. J. Biochem. 207: 117-123.
- Hilbi, H., and Dimroth, P. 1994. Purification and characterization of a cytoplasmic enzyme component of the Na⁺-activated malonate decarboxylase system of *Malonomonus rubra*: acetyl-S-acyl carrier protein:malonate acyl carrier protein-SH transferase. Arch. Microbiol. 164: 48-56.

- Hilbi, H., Hermann, R., and Dimroth, P. 1993. The malonate decarboxylase enzyme system of *Malonomonas rubra*: evidence for the cytoplasmic location of the biotin-containing component. Arch. Microbiol. 160: 126-131.
- Hilpert, W., and Dimroth, P. 1983. Purification and characterization of a new sodium-transport decarboxylase. Methylmalonyl-CoA decarboxylase from *Veillonella alcalescens*. Eur. J. Biochem. 132: 579–587.
- Hilpert, W., and Dimroth, P. 1984. Reconstitution of Na⁺ transport from purified methylmalonyl-CoA decarboxylase and phospholipid vesicles. Eur. J. Biochem. 138: 579–583.
- Hilpert, W., Schink, B., and Dimroth, P. 1984. Life by a new decarboxylation-dependent energy conservation mechanism with Na⁺ as coupling ion. EMBO J. 3: 1665–1670.
- Hirota, N., and Imae, Y. 1983. Na⁺-driven flagellar motors of an alkalophilic *Bacillus* strain YN-1. J. Biol. Chem. 258: 10577–10581.
- Hoffmann, A., Hilpert, W., and Dimroth, P. 1989. The carboxytransferase activity of the sodium-ion-translocating methylmalonyl-CoA decarboxylase of *Veillonella alcalescens*. Eur. J. Biochem. 179: 645-650.
- Hoiczky, E., and Baumeister, W. 1998. The junctional pore complex, a prokaryotic secretion organelle, is the molecular motor underlying gliding motility in cyanobacteria. Curr. Biol. 8: 1161-1168.
- Incharoensakdi, A., and Waditee, R. 2000. Degradation of glycine betaine by betaine homocysteine methyltransferase in *Aphanothece halophytica* : effect of salt downshock and starvation. Curr. Microbiol. 41: 227-231.
- Incharoensakdi, A., and Wutipraditkul, N. 1999. Accumulation of glycine betaine and its synthesis from radioactive precursors under salt-stress in the

- cyanobacterium *Aphanothece halophytica*. J. Appl. Phycol. 11: 515-523.
- Joset, F., Jeanjean, R., and Hagemann, M. 1996. Dynamics of response of cyanobacteria to salt stress : deciphering the molecular events. Physiol. Plant. 96: 738-744.
- Kaieda, N., Wakagi, T., and Koyama, N. 1998. Presence of Na⁺-stimulated V-type ATPase in the membrane of a facultatively anaerobic and halophilic alkaliphile. FEMS Microbiol. Lett. 167: 57-61.
- Kaim, G., Ludwig, W., Dimroth, P., and Schleifer, K.H. 1992. Cloning, sequencing and *in vivo* expression of genes encoding the F₀ part of the sodium-ion-dependent ATP synthase of *Propionigenium modestum* in *Escherichia coli*. Eur. J. Biochem. 207: 463-470.
- Kakinuma, Y. 1987. Sodium/proton antiporter in *Streptococcus faecalis*. J. Bacteriol. 169: 3886-3890.
- Kakinuma, Y., and Unemoto, T. 1985. Sucrose uptake is driven by the Na⁺ electrochemical potential in the marine bacterium *Vibrio alginolyticus*. J. Bacteriol. 163: 1293-1295.
- Kanamaru, K., Kashiwagi, S., and Mizuno, T. 1994. A copper-transporting P-type ATPase found in the thylakoid membrane of the cyanobacterium *Synechococcus* species PCC 7942. Mol. Microbiol. 13: 369-377.
- Kemp, B., and Bremer, E. 1998. Uptake and synthesis of compatible solutes as microbial stress responses to high-osmolarity environments. Arch. Microbiol. 170: 319-330.
- Kengen, S.W.M., Mosterd, J.J., Nelissen, R.L.H., Keltjens, J.T., van der Drift, C., and Vogels, G.D. 1988. Reductive activation of the methyl-tetrahydromethanopterin:coenzyme M methyltransferase from

- Methanobacterium thermoautotrophicum* strain Δ H, Arch. Microbiol. 150: 405-412.
- Kengen, S.W.M., Daas, P.J.H., Duits, E.F.G., Keltjens, J.T., van der Drift, C., and Vogels, G.D. 1992. Isolation of a 5-hydroxybenzimidazolylcobamide-containing enzyme involved in the methyltetrahydromethanopterin:coenzyme M methyltransferase reaction in *Methanobacterium thermoautotrophicum*. Biochim. Biophys. Acta. 1118: 249-260.
- Kinoshita, N., Unemoto, T., and Kobayashi, H. 1984. Sodium-stimulated ATPase in *Streptococcus faecalis*. J. Bacteriol. 158: 844-848.
- Kobayashi, H., Murakami, N., and Unemoto, T. 1982. Regulation of the cytoplasmic pH in *Streptococcus faecalis*. J. Biol. Chem. 257: 13246-13252.
- Koyama, N. 1993. Stimulatory effect of NH_4^+ on the transport of leucine and glucose in an anaerobic alkaliphile. Eur. J. Biochem. 217: 435-439.
- Krulwich, T.A. 1986. Bioenergetics of alkalophilic bacteria. J. Membr. Biol. 89: 113-124.
- Laemmli, U.K. 1970. Cleavage of structural proteins during the assembly of the head of bacteriophage T₄. Nature. 227: 680-685.
- Lanyi, J.K. 1979. The role of Na^+ in transport processes of bacterial membranes. Biochim. Biophys. Acta. 559: 377-97.
- Laubinger, W., and Dimroth, P. 1987. Characterization of the Na^+ -stimulated ATPase of *Propionigenium modestum* as an enzyme of the F₁F₀ type. Eur. J. Biochem. 168: 475-480.
- Lebel, D., Poirier, G.G., and Beaudoin, A.R. 1978. A convenient method for the ATPase assay. Anal. Biochem. 85: 86-89.
- Lerma, C., and Gómez-Lojero, C. 1987. Preparation of a highly active ATPase of the

- mesophilic cyanobacterium *Spirulina maxima*. Photosynth. Res. 11: 265-277.
- Lienard, T., Becher, B., Marschall, M., Bowien, S., and Gottschalk, G. 1996. Sodium ion translocation by *N*⁵-methyltetrahydromethanopterin:coenzyme M methyltransferase from *Methanosarcina mazei* Go1 reconstituted in ether lipid liposomes. Eur. J. Biochem. 239: 857-864.
- Lill, H., and Nelson, N. 1991. The *atp1* and *atp2* operons of the cyanobacterium *Synechocystis* sp. PCC 6803. Plant Mol. Biol. 17: 641-652.
- Linnett, P.E., and Beechey, R.B. 1979. Inhibitors of the ATP synthase system. Meth. Enzymol. 55: 472-518.
- McCue, K.F., and Hanson, A.D. 1990. Drought and salt tolerance : towards understanding and application. Trends Biotechnol. 8: 358-362.
- Meeks, J.C., Campbell, E.L., Summers, M.L., and Wong, F.C. 2002. Cellular differentiation in the cyanobacterium *Nostoc punctiforme*. Arch. Microbiol. 178: 395-403.
- Meeks, J.C., and Elhai, J. 2002. Regulation of cellular differentiation in filamentous cyanobacteria in free-living and plant-associated symbiotic growth states. Microbiol. Mol. Biol. Rev. 66: 94-121.
- Meier, T., Ballmoos, C.V., Neumann, S., and Kaim, G. 2003. Complete DNA sequence of the *atp* operon of the sodium-dependent F₁F₀ ATP synthase from *Ilyobacter tartaricus* and identification of the encoded subunits. Biochim. Biophys. Acta. 1625: 221-226.
- Miki, J., Maeda, M., Mukohata, Y., and Futai, M. 1988. The γ -subunit of ATP synthase from spinach chloroplast. Primary structure deduced from the cloned cDNA sequence. FEBS Lett. 232: 221-226.
- Moriyama, Y., Iwamoto, A., Hanada, H., Maeda, M., and Futai, M. 1991. One-step

- purification of *Escherichia coli* H⁺-ATPase (F₀F₁) and its reconstitution into liposomes with neurotransmitter transporter. J. Biol. Chem. 266: 22141–22146.
- Mulkiđjanian, A.Y., Galperin, M.Y., Makarova, K.S., Wolf, Y.I., and Koonin, E.V. 2008. Evolutionary primacy of sodium bioenergetics. Biol. Direct. 3:13.
- Murata, T., Kawano, M., Igarashi, K., Yamato, I., and Kakinuma, Y. 2001. Catalytic properties of Na⁺-translocating V-ATPase in *Enterococcus hirae*. Biochim. Biophys. Acta. 1505: 75–81.
- Neisser, A., Fromwald, S., Schmatzberger, A., and Paschek, G.A. 1994. Immunological and functional localization of both F-type and P-type ATPase in cyanobacterial plasma membranes. Biochem. Biophys. Res. Commun. 200: 884-892.
- Nelson, D.L., and Cox, M.M. 2000. Lehninger Principles of Biochemistry. 3 rd ed. New York: Worth Publishers.
- Neumann, S., Matthey, U., Kaim, G., and Dimroth, P. 1998. Purification and properties of F₁F₀ ATPase of *Ilyobacter tartaricus*, a sodium ion pump. J. Bacteriol. 180: 3312-3316.
- Nieto, J.J., Fernández-Castillo, R., Márquez, M.C., Ventosa, A., Quesada, E., and Ruiz-Berraquero, F. 1989. Survey of metal tolerance in moderately halophilic eubacteria. Appl. Environ. Microbiol. 55: 2385-2390.
- Nishi, T., and Forgac, M. 2002. The vacuolar H⁺-ATPases : Nature's most versatile proton pumps. Nat. Rev. Mol. Cell. Biol. 3: 94-103.
- Omata, T. 1995. Structure, function and regulation of the nitrate transport system of the cyanobacterium *Synechococcus* sp. PCC 7942. Plant cell physiol. 36: 207-213.

- Padan, E. 1998. The molecular mechanisms of regulation of the Na⁺/H⁺ antiporters. In A. Oren (Ed.), Microbiology and Biochemistry of Hypersaline Environments, pp. 163-175. Boca Raton, FL: CRC Press.
- Padan, E., and Krulwich, T. 2000. Sodium stress. In G. Storz and R. Hengge-Aronis (eds.), Bacterial Stress Responses, pp. 117-130. Washington DC: ASM Press.
- Padan, E., and Schuldiner, S. 1992. Na⁺ transport systems in prokaryotes. In E. Bakker (Ed.), Alkali Cation Transport Systems in Prokaryotes, pp. 3-24. Boca Raton, FL: CRC Press.
- Padan, E., and Schuldiner, S. 1993. Na⁺/H⁺ antiporters, molecular devices that couple the Na⁺ and H⁺ circulation in cells. J. Bioenerg. Biomembr. 25: 647-669.
- Padan, E., and Schuldiner, S. 1994. Molecular physiology of Na⁺/H⁺ antiporters, key transporters in circulation of Na⁺ and H⁺ in cells. Biochim. Biophys. Acta. 1185: 129-151.
- Padan, E., and Schuldiner, S. 1996. Bacterial Na⁺/H⁺ antiporters : molecular biology, biochemistry and physiology. In W.N. Konings, H.R. Kaback and J.S. Lolkema (eds.), Handbook of biological physics, vol. 2, pp. 501-531. Amsterdam: Elsevier Science.
- Padan, E., Venturi, M., Gerchman, Y., and Dover, N. 2001. Na⁺/H⁺ antiporters. Biochim. Biophys. Acta. 1505: 144–157.
- Pfenninger-Li, X.D., Albracht, S.P.J., van Belzen, R., and Dimroth, P. 1996. NADH:ubiquinone oxidoreductase of *Vibrio alginolyticus*: purification, properties, and reconstitution of the Na⁺ Pump. Biochemistry. 35: 6233-6242.
- Popova, L.G., Balnokin, Y.V., Dietz, K.J., and Gimmler, H. 1998. Na⁺-ATPase from the plasma membrane of the marine alga *Tetraselmis (Platymonas) viridis* forms a phosphorylated intermediate. FEBS Lett. 426: 161–164.

- Popova, L.G., Shumkova, G.A., Andreev, I.M., and Balnokin, Y.V. 2005. Functional identification of electrogenic Na⁺-translocating ATPase in the plasma membrane of the halotolerant microalga *Dunaliella maritima*. FEBS Lett. 579: 5002-5006.
- Rahlf, S., Aufurth, S., and Müller, V. 1999. The Na⁺-F₁F₀-ATPase operon from *Acetobacterium woodii*. J. Biol. Chem. 274: 33999-34004.
- Reed, R.H., Rowell, P., and Stewart, W.D.P. 1981. Characterization of the transport of potassium ions in the cyanobacterium *Anabaena variabilis* KütZ. Eur. J. Biochem. 116: 323-330.
- Regev, R., Peri, I., Gilboa, H., and Avi-Dor, Y. 1990. ¹³C NMR study of the interrelation between synthesis and uptake of compatible solutes in two moderately halophilic eubacteria, Bacterium Ba1 and *Vibrio costicola*. Arch. Biochem. Biophys. 278: 106-112.
- Reidlinger, J., and Muller, V. 1994. Purification of ATP synthase from *Acetobacterium woodii* and identification as a Na⁺-translocating F₁F₀-type enzyme. Eur. J. Biochem. 223: 275-283.
- Reinhold, L., Volokita, M., Zenvirth, D., and Kaplan, A. 1984. Is HCO₃⁻ transport in *Anabaena* a Na⁺ symport? Plant Physiol. 76: 1090-1092.
- Ritchie, R.J. 1992. Sodium transport and the origin of the membrane potential in the cyanobacterium *Synechococcus* R-2 (*Anacystis nidulans*) PCC 7942. J. Plant Physiol. 139: 320-330.
- Sanchez-Maeso, E., Fernandez-Pinas, F., Garcia-Gonzalez, M., and Fernandez-Valiente, E. 1987. Sodium requirement for photosynthesis and its relationship with dinitrogen fixation and the external CO₂ concentration in cyanobacteria. Plant Physiol. 85: 585-587.

- Schwarz, E., Oesterhelt, D., Reinke, H., Beyreuther, K., and Dimroth, P. 1988. The sodium translocating oxaloacetate decarboxylase of *Klebsiella pneumoniae*. Sequence of the biotin-containing α -subunit and relationship to other biotin-containing enzymes. J. Biol. Chem. 263: 9640–9645.
- Serrano, R. 1996. Salt tolerance in plants and microorganisms: toxicity targets and defence responses. Int. Rev. Cytol. 165: 1-52.
- Shi, H.Z., Lee, B.H., Wu, S.J., and Zhu, J.K. 2003. Overexpression of a plasma membrane Na^+/H^+ antiporter gene improves salt tolerance in *Arabidopsis thaliana*. Nature Biotechnol. 21: 81-85.
- Shono, M., Hara, Y., Wada, M., and Fujii, T. 1996. A sodium pump in the plasma membrane of the marine alga *Heterosigma akashiwo*. Plant Cell Physiol. 37: 385-388.
- Soong, T.W., Yong, T.F., Ramanan, N., and Wang, Y. 2000. The *Candida albicans* antiporter gene CNH1 has a role in Na^+ and H^+ transport, salt tolerance, and morphogenesis. Microbiology. 146: 1035-1044.
- Stanier, R.Y., Kunisawa, R., Mandel, M., and Cohen-Bazire, G. 1971. Purification and properties of unicellular blue-green algae (order Chroococcales). Bacteriol. Rev. 35: 171-205.
- Takabe, T., Incharoensakdi, A., Arakawa, K., and Yokota, S. 1988. CO_2 fixation rate and RuBisCO content increase in the halotolerant cyanobacterium, *Aphanothece halophytica*. Plant Physiol. 88: 1120-1124.
- Thomas, J., and Apte, S.K. 1984. Sodium requirement and metabolism in nitrogen-fixing cyanobacteria. J. Biosci. 6: 771-794.
- Thomas, J., Apte, S.K., and Reddy, B.R. 1988. Sodium metabolism in cyanobacterial nitrogen fixation and salt tolerance. In H. Bothe, F.J. deBruijn and W.E.

- Newton (eds.), Nitrogen Fixation : Hundred Years After, pp. 195-201. Stuttgart: Gustav Fischer-Verlag.
- Ubbink-Kok, T., Boekema, E.J., van Breemen, J.F.L., Brisson, A., Konings, W.N., and Lolkema, J.S. 2000. Stator structure and subunit composition of the V_1/V_0 Na^+ -ATPase of the thermophilic bacterium *Caloramator fervidus*. J. Mol. Biol. 296: 311-321.
- Ueda, A., Kanechi, M., Uno, Y., and Inagaki, N. 2003. Photosynthetic limitations of a halophyte sea aster (*Aster tripolium* L.) under water stress and NaCl stress. J. Plant Res. 116: 65-70.
- Ueno, S., Kaieda, N., and Koyama, N. 2000. Characterization of a P-type Na^+ -ATPase of a facultatively anaerobic alkaliphilic, *Exiguobacterium aurantiacum*. J. Biol. Chem. 275: 14537-14540.
- Vimont, S., and Berche, P. 2000. NhaA, an Na^+/H^+ antiporter involved in environmental survival of *Vibrio cholerae*. J. Bact. 182: 2937-2944.
- Vollmar, M., Schlieper, D., Winn, M., Büchner, C., and Groth, G. 2009. Structure of the c_{14} rotor ring of the proton translocating chloroplast ATP synthase. J. Biol. Chem. 284: 18228-18235.
- von Ballmoos, C., Wiedenmann, A., and Dimroth, P. 2009. Essentials for ATP synthesis by F1F0 ATP synthases. Annu. Rev. Biochem. 78: 649-672.
- Wada, M., Satoh, S., and Fujii, T. 1989. Presence of a Na^+ -activated ATPase in the plasma membrane of the marine raphidophycean *Heterosigma akashiwo*. Plant Cell Physiol. 30: 923-928.
- Waditee, R., Hibino, T., Nakamura, T., Incharoensakdi, A., and Takabe, T. 2002. Overexpression of a Na^+/H^+ antiporter confers salt tolerance on a freshwater cyanobacterium, making it capable of growth in sea water. Proc. Natl. Acad.

Sci. USA. 99: 4109-4114.

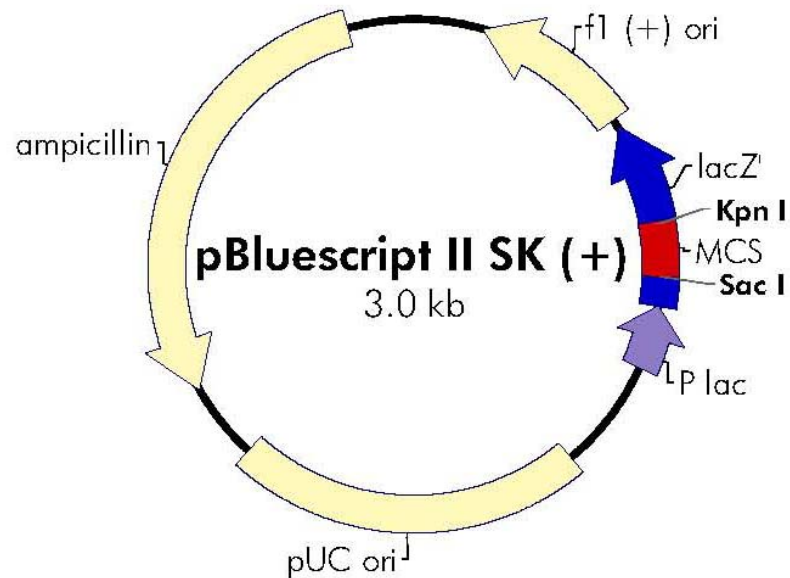
- Waditee, R., Hibino, T., Tanaka, Y., Nakamura, T., Incharoensakdi, A., and Takabe, T. 2001. Halotolerant cyanobacterium *Aphanothece halophytica* contains an Na⁺/H⁺ antiporter, homologous to eukaryotic ones, with novel ion specificity affected by C terminal tail. J. Biol. Chem. 276: 36931-36938.
- Waditee, R., et al. 2003. Isolation and functional characterization of N-methyltransferases that catalyze betaine synthesis from glycine in a halotolerant photosynthetic organism *Aphanothece halophytica*. J. Biol. Chem. 278: 4932-4942.
- Walker, J.E., Saraste, M., Runswick, M.J., and Gay, N.J. 1982. Distantly related sequences in the α - and β -subunits of ATP synthase, myosin, kinases and other ATP-requiring enzymes and a common nucleotide binding fold. EMBO J. 1: 945-951.
- Wang, H.L., Postier, B.L., and Burnap, R.L. 2002. Polymerase chain reaction-based mutageneses identify key transporters belonging to multigene families involved in Na⁺ and pH homeostasis of *Synechocystis* sp. PCC 6803. Mol. Microbiol. 44: 1493-1506.
- Welsh, D.T., Lindsay, Y.E., Caumette, P., Herbert, R.A., and Hannan, J. 1996. Identification of trehalose and glycine betaine as compatible solutes in the moderately halophilic sulfate reducing bacterium, *Desulfovibrio halophilus*. FEMS Microbiol. Lett. 140: 203-207.
- Wifling, K., and Dimroth, P. 1989. Isolation and characterization of oxaloacetate decarboxylase of *Salmonella typhimurium*, a sodium ion pump. Arch. Microbiol. 152: 584-588.
- Wilmotte, A. 1994. Molecular evolution and taxonomy of the cyanobacteria. In D.A.

- Bryant (ed.), The Molecular Biology of Cyanobacteria, pp. 1-25. Dordrecht: Kluwer Academic Publishers.
- Woehlke, G., and Dimroth, P. 1994. Anaerobic growth of *Salmonella typhimurium* on L(+)- and D(-)-tartrate involves an oxaloacetate decarboxylase Na⁺ pump. Arch. Microbiol. 162: 233-237.
- Woodcock, D.M., et al. 1989. Quantitative evaluation of *Escherichia coli* host strains for tolerance to cytosine methylation in plasmid and phage recombinants. Nucl. Acids. Res. 17: 3469-3478.
- Wyn Jones, R.G., and Pollard, A. 1983. Proteins, enzymes and inorganic ions. In A. Lauchi and R.L. Bielecki (eds.), Encyclopaedia of plant physiology, New series. Inorganic plant nutrition, vol. 15, pp. 528-562. Heidelberg: Springer-Verlag.
- Xiong, J., Fischer, W.M., Inoue, K., Nakahara, M., and Bauer, C.E. 2000. Molecular evidence for the early evolution of photosynthesis. Science. 289: 1724-1730.
- Yancey, P.H., Clark, M.E., Hand, S.C., Bowlus, R.D., and Somero, G.N. 1982. Living with water stress : evolution of osmolyte systems. Science. 217: 1214-1222.

APPENDICES

APPENDIX A

pBluescript II SK (+)



**pBluescript II SK (+/-) Multiple Cloning Site Region
(sequence shown 598–826)**

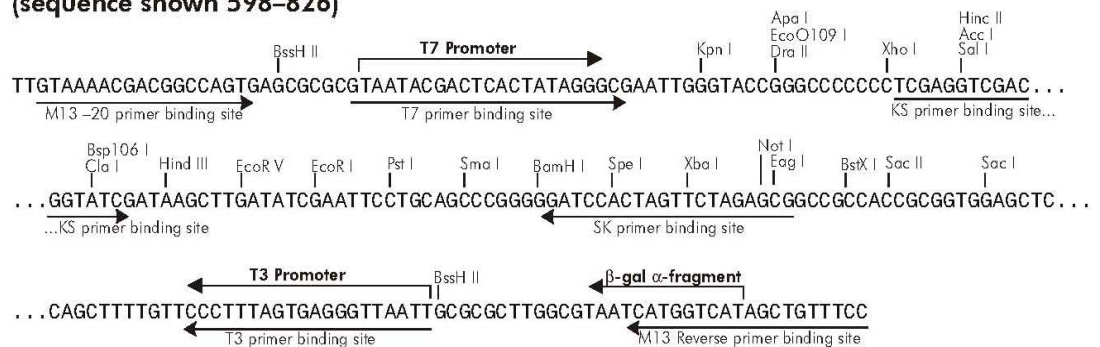
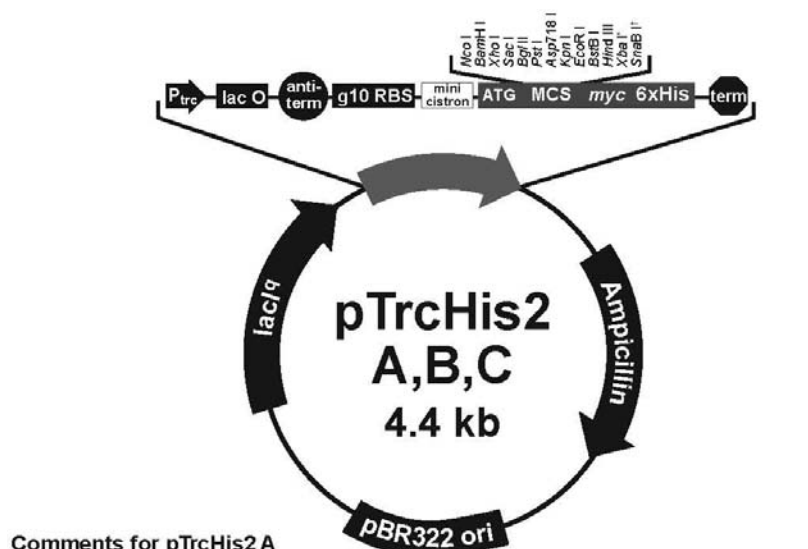


Figure A.1 Map of pBluescript II SK (+) vector and cloning region

APPENDIX B

pTrcHis2C



Comments for pTrcHis2 A
4406 nucleotides

trc promoter region: bases 190-382
 -35 region: bases 193-198
 -10 region: bases 216-221
 lac operator (*lacO*): bases 228-248
rrnB antitermination signal: bases 264-333
 gene 10 region: bases 346-354
 Ribosome binding site: bases 369-373
 pTrcHis forward priming site: bases 370-390
 Minicistron ORF: bases 383-409
 Reinitiation RBS: bases 398-403
 Expression ATG: bases 413-415
 Multiple cloning site: bases 411-464
myc epitope: bases 471-503
 Polyhistidine tag: bases 516-533
mycHis reverse priming site: bases 508-527
rrnB T1 and T2 transcriptional terminators: bases 639-796
 Ampicillin resistance ORF: bases 1076-1936
 pBR322 origin: bases 2081-2754
 Lac Repressor (*lacI^q*) ORF: bases 3285-4367

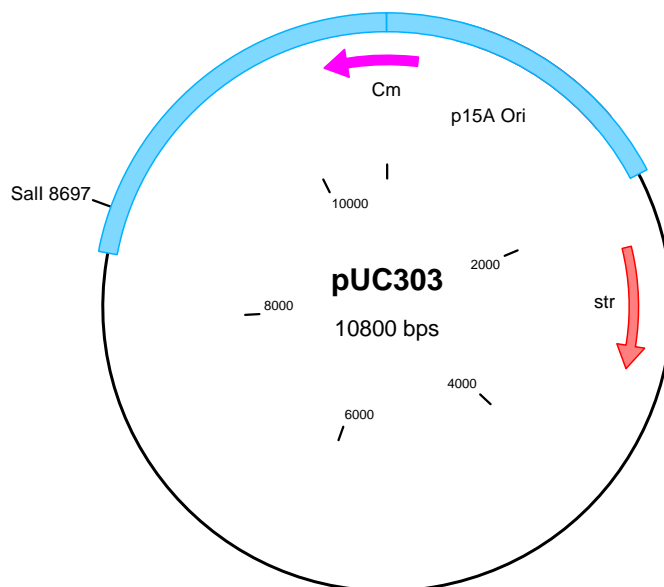
* *Xba* I is only found
in pTrcHis2 B

† *SnaB* I is only found in
pTrcHis2 C

```

      pTrcHis forward priming site           Mini cistron           RBS           Nco
      |-----|                               |-----|           |-----|           |
361  AAAATTTAAAG AGG TATATAT TA  ATG TAT CGA TTA AAT AAG GAG GAA TAA ACC
      Met Tyr Arg Leu Asn Lys Glu Glu ***
      BamH I       Xho I Sac I Bgl II       Pst I Asp718 I Kpn I       EcoR I BstB I Hind III SnaB I
413  ATG GATCCGAGCT CGAGATCTGC AGCTGGTACC ATATGGGAAT TCGAAGCT TA CGTA
      Met
      myc epitope tag                               Sal I
461  GAA CAA AAA CTC ATC TCA GAA GAG GAT CTG AAT AGC GCC GTC GAC CAT
      Glu Gln Lys Leu Ile Ser Glu Glu Asp Leu Asn Ser Ala Val Asp His
      ProBond™ binding domain
510  CAT CAT CAT CAT CAT TGA GTTTA
      His His His His His ***
  
```

Figure A.2 Map of pTrcHis2C vector and cloning/expression region

APPENDIX C**pUC303****Figure A.3** Map of pUC303 vector

APPENDIX D

BG11 and BG11 plus Turk Island Salt Solution

Stock solution preparation

Solution I (100 ml): K ₂ HPO ₄	3.135 g	Solution VI (500 ml):	
Solution II (100 ml): MgSO ₄ ·7H ₂ O	7.5 g	H ₃ BO ₃	1.43 g
Solution III (100 ml): CaCl ₂ ·2H ₂ O	3.6 g	ZnSO ₄ ·7H ₂ O	110 mg
Solution IV (100 ml): Na ₂ CO ₃	2.0 g	Na ₂ MoO ₄ ·2H ₂ O	195 mg
Solution V (100 ml):		MnCl ₂ ·4H ₂ O	0.905 g
EDTA	0.1 g	CuSO ₄ ·5H ₂ O	39.5 mg
Citric acid	0.1 g	Co(NO ₃) ₂ ·6H ₂ O	24.5 mg
Sterile filtrate, store at 4 °C		Sterile filtrate, store at 4 °C	

BG11 medium (1,000 ml)

Chemical	Solid medium	Liquid medium
Bacto-agar	15 g	-
NaNO ₃	1.5 g	1.5 g
Solution I	1 ml	1 ml
Solution II	1 ml	1 ml
Solution III	1 ml	1 ml
Solution IV	1 ml	1 ml
Solution V	1 ml	1 ml
Solution VI	1 ml	1 ml
H ₂ O added up to	1,000 ml	1,000 ml

BG11 medium + Turk Island Salt Solution (1,000 ml)

Chemical	Solid medium	Liquid medium
Bacto-agar	15 g	-
NaNO ₃	1.5 g	1.5 g
KCl	0.67 g	0.67 g
MgSO ₄ .7H ₂ O	6.92 g	6.92 g
MgCl ₂ .6H ₂ O	5.5 g	5.5 g
CaCl ₂ .2H ₂ O	1.47 g	1.47 g
Solution I	1 ml	1 ml
Solution II	1 ml	1 ml
Solution III	1 ml	1 ml
Solution IV	1 ml	1 ml
Solution V	1 ml	1 ml
Solution VI	1 ml	1 ml
NaCl (0.5M)	29.22 g	29.22 g
H ₂ O added up to	1,000 ml	1,000 ml

Remark: The culture medium was mixed and then the mixture was adjusted pH to 7.6 with 2 M NaOH. The total volume was adjusted to 1 litre with distilled water. The medium was sterilized by autoclaving at 15 lb/in² for 15 minute.

APPENDIX E

ATP hydrolysis activity assay

Assay

1. The reaction mixture (1 ml) was prepared as the following components.

Chemical	Final conc.	Volume
1 M Tris-HCl pH 7.6	20 mM	20 μ l
1 M MgCl ₂	5 mM	5 μ l
5 M NaCl	100 mM	20 μ l
100 mM ATP	2 mM	20 μ l
Sample	30 μ g protein	X μ l
H ₂ O added up to		1 ml

2. The reaction mixture was incubated at 37 °C for 15 min.

3. Proteins were precipitated with 5% TCA and centrifuged 3,800 g for 10 min.

4. The supernatant was used for determination of inorganic phosphate.

Remark: Blank is assayed as describe above except that no sample is added.

APPENDIX F

Determination of inorganic phosphate (Pi)

Reagents:

Solution A = copper acetate pH 4.0

0.25 % copper sulfate

4.6% sodium acetate.3H₂O

Solution B = 5% ammonium molybdate in H₂SO₄

Solution C = 10% ascorbic acid

Method:

1. To 1.0 ml of the supernatant, 3.0 ml of solution A, 0.1 ml of solution B and 0.01 ml of solution C were added and mixed.
2. Twenty minutes later, the absorbance was read at 850 nm using a spectrophotometer Beckman DU 800 and the Pi content was calculated by comparison to the standard curve of Pi.

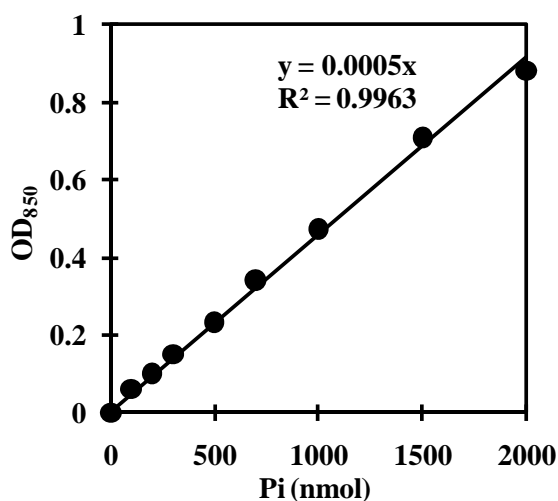


Figure A.4 Standard curve of Pi

APPENDIX G

Determination of protein by Bradford's method

Bradford stock solution

100 ml 95% ethanol
200 ml 88% phosphoric acid
350 mg Serva Blue G
Stable indefinitely at room temperature

Bradford working buffer

425 ml distilled water
15 ml 95% ethanol
30 ml 88% phosphoric acid
30 ml Bradford stock solution
Filter through Whatman No. 1 paper

Assay

1. The protein solution (10 μ l) was added into tube.
2. 1 ml of Bradford working buffer was added and then the mixture was vortex.
3. After incubation for 10 min, OD₅₉₅ was read and the protein content was calculated by comparison to the standard curve of BSA.

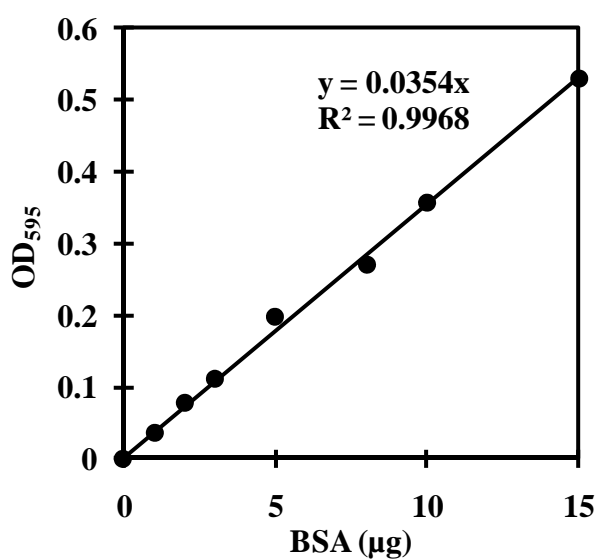


Figure A.5 Standard curve of BSA

APPENDIX H

Preparation for polyacrylamide gel electrophoresis

1) Stock reagents

30% (w/v) Acrylamide and 0.8% (w/v) N,N'-methylene-bis-acrylamide (100 ml)

Acrylamide	29.2 g
N,N'-methylene-bis-acrylamide	0.8 g

The volume of mixture was adjusted to 100 ml with distilled water and then the mixture was stirred until completely dissolved.

1.5 M Tris-HCl pH 8.8 (100 ml)

Tris (hydroxymethyl) aminomethane	18.17 g
-----------------------------------	---------

The mixture was adjusted pH to 8.8 with 1 N HCl and adjusted volume to 100 ml with distilled water.

2 M Tris-HCl pH 8.8 (100 ml)

Tris (hydroxymethyl) aminomethane	24.2g
-----------------------------------	-------

The mixture was adjusted pH to 8.8 with 1 N HCl and adjusted volume to 100 ml with distilled water.

0.5 M Tris-HCl pH 6.8 (100 ml)

Tris (hydroxymethyl) aminomethane	6.06 g
-----------------------------------	--------

The mixture was adjusted pH to 6.8 with 1 N HCl and adjusted volume to 100 ml with distilled water.

1 M Tris-HCl pH 6.8 (100 ml)

Tris (hydroxymethyl) aminomethane	12.1 g
-----------------------------------	--------

The mixture was adjusted pH to 6.8 with 1 N HCl and adjusted volume to 100 ml with distilled water.

10% (w/v) Ammonium persulfate (1 ml)

Ammonium persulfate	0.1 g
---------------------	-------

The volume of mixture was adjusted to 1 ml with distilled water.

10% (w/v) SDS (100 ml)

SDS	10 g
-----	------

The volume of mixture was adjusted to 100 ml with distilled water.

0.5% (w/v) Bromophenol blue (10 ml)

Bromophenol blue	0.05 g
------------------	--------

The volume of mixture was adjusted to 10 ml with distilled water.

Solution B (SDS-PAGE)

2 M Tris-HCl pH 8.8	75 ml
---------------------	-------

10% SDS	4 ml
---------	------

Distilled water	21 ml
-----------------	-------

Solution C (SDS-PAGE)

1 M Tris-HCl pH 6.8	50 ml
---------------------	-------

10% SDS	4 ml
---------	------

Distilled water	46 ml
-----------------	-------

2) SDS-PAGE

12% separating gel

30% acrylamide solution	4.17 ml
-------------------------	---------

Solution B	2.5 ml
Distilled water	3.33 ml
10% ammonium persulfate	50 μ l
TEMED	5 μ l

5% stacking gel

30% acrylamide solution	1.67 ml
Solution C	2.5 ml
Distilled water	5.8 ml
10% ammonium persulfate	50 μ l
TEMED	5 μ l

Sample buffer

1 M Tris-HCl pH 6.8	0.6 ml
Glycerol	0.8 ml
10% SDS	2 ml
β -mercaptoethanol	0.5 ml
0.5% bromophenol blue	0.5 ml
distilled water	5.8 ml

The ratio of sample and sample buffer is 4:1. The mixture was heated for 5 minutes in boiling water before loading to the gel.

Electrophoresis buffer (1000 ml)

Tris (hydroxymethyl) aminomethane	3 g
Glycine	14.4 g
SDS	1 g

The volume of mixture was adjusted to 1000 ml with distilled water (pH should be approximately 8.3). Do not adjust pH with acid or base.

Staining solution (1000 ml)

Coomassie Blue R-250	10 g
Methanol	450 ml
Glacial acetic acid	100 ml

Destaining solution (1000 ml)

Methanol	100 ml
Glacial acetic acid	100 ml

APPENDIX I

In-gel tryptic digestion

The protein band was cut with clean scalpel and washed with 200 μ l of washing solution for 30 min, repeat until the gel was no longer blue color and then removed solution. Acetonitrile (200 μ l) was added for 10 min and removed. The gel was dried by speedvac for 10 min, after that 10 mM DTT was added for 10 min at 37 °C and removed. Wash the gel twice with washing solution. Iodoacetamide (55 mM) was added for 10 min in the dark and discarded. Wash the gel with 200 μ l of washing solution twice and acetonitrile was added for 10 min and removed. After the gel was dried, add 0.1 mg ml⁻¹ trypsin solution until the gel was submerged and then incubate at 37 °C for 2 hrs. The reaction was stopped by adding 1 ml of formic acid. The solution was collected and the peptide was extracted from the gel by incubating the gel in ultrapure water : acetonitrile (50 : 50) for 30 min.

Remark: Washing solution composed of 10 ml of 25 mM NH₄HCO₃ and 10 ml of acetonitrile.

APPENDIX J

Sodium-22 and scintillation fluid preparation

Specification:

Chemical form	Sodium chloride in aqueous solution
Specific activity	> 3.7 GBq/mg sodium > 100 mCi/mg protein
Radioactive concentration:	Refer to vial/plot table
Chemical purity:	< 10 µg/ml of any cation impurity < 50 µg/ml of total cation impurities
Radionuclidic purity:	No γ impurities detected
pH:	3.0-8.0

Nuclear Data:

Production process:	$^{24}\text{Mg} (d,\alpha) ^{22}\text{Na}$
Half-life	2.6 years
Type of decay:	β^+ , electron capture
β^+ energy (maximum)	1.83 MeV
γ energy (maximum)	1.28 MeV (0.51 MeV from β^+)

Scintillation fluid (1,000 ml) was prepared as follows:

5.5 g PPO (2, 5-diphenyloxazole) and 0.1 g POPOP [1, 4-bis (5-phenyloxazole-2-yl) benzene] in 1,000 ml of a solution composed of 667 ml Toluene and 333 ml of Triton X-100 were mixed. The contents are completely dissolved before the solution is used. The solution should be stored in a brown bottle in a cool dark place.

APPENDIX K

PCR amplification protocol for *ApNa⁺-atp* operon

PCR amplification mixture

Chemical	Volume
10x PCR buffer for KOD plus *	5.0 μ l
25 mM MgCl ₂	2.5 μ l
2 mM dNTPs each	5.0 μ l
Primer ApNa ⁺ -ATPaseBamHI-F (5 pmol/ μ l)	4.0 μ l
Primer ApNa ⁺ -ATPaseSalI-R (5 pmol/ μ l)	4.0 μ l
DNA	X μ l
DMSO	2.5 μ l
KOD plus DNA polymerase (1unit/ μ l)	1.0 μ l
MQ-water	26-X μ l
Total	50.0 μ l

Program running PCR (35 cycles)

94 °C 2 min (Pre denaturation time)

94 °C 30 sec (Denaturation time)

52 °C 30 sec (Annealing time)

68 °C 7 min (Extension time)

68 °C 8 min (Final Extension cycle)

4 °C for overnight

Remark: *10x PCR buffer for KOD plus = 1.2 M Tris-HCl, 100 mM KCl, 60 mM (NH₄)₂SO₄, 1% Triton X-100, 0.01% BSA, pH8.0.

APPENDIX L

E. coli transformation by heat shock method

1. Preparation of competent cells

200 µl overnight culture of *E. coli* DH5α was inoculated into 100 ml sterile LB medium, then grown at 37 °C, 250 rpm until OD₆₂₀ reached 0.3-0.4. The culture was incubated on ice for 30 minutes. The cells were collected by centrifugation at 5,000 g, 4 °C for 10 minutes. The pellet was resuspended with 100 ml of cold 0.1 M MgCl₂ and centrifuged at 5,000 g, 4 °C for 10 minutes. A supernatant was discarded then the pellet was resuspended with 100 ml of cold 0.1 M CaCl₂ and incubated on ice for 30-60 minutes. After incubation, the cell suspension was centrifuge at 5,000 g, 4 °C, for 10 minutes. A supernatant was discarded then the pellet was resuspended with 3 ml of cold 0.1 M CaCl₂ containing 15% glycerol. The cell suspension was aliquoted 100 µl/tube on ice prior to immediate drop into liquid nitrogen. The competent cells were stored at -80 °C until use.

2. Transformation

The plasmid was mixed with cold cell suspension in microtube and place on ice for 45 min. The mixture was incubated at 42 °C for 90 sec and placed on ice for 5 minutes. The cell suspension was transferred into a new sterile tube containing 1 ml of LB broth. The transformed cells were incubated at 37 °C, 200 rpm for 1 hr and spreaded onto the LB agar plate containing appropriate antibiotic. The plate was incubated at 37 °C overnight.

APPENDIX M**LB medium****LB medium (1,000 ml)**

Chemical	Liquid medium	Solid medium
Bacto tryptone	10 g	10 g
Yeast extract	5 g	5 g
NaCl	10 g	10 g
Agar	-	15 g

All compositions were dissolved together with 1 liter of distilled water. The medium was sterilized by autoclaving at 15 lb/in² for 15 minute.

APPENDIX N

Preparation of *E. coli* plasmid by alkaline lysis method

Reagents:

Solution I (100 ml)

5.0 ml 1.0 M Glucose

2.5 ml 1.0 M Tris-HCl, pH 8.0

2.0 ml 0.5 M EDTA, pH 8.0

After autoclave 20 µg/ml of RNase was added and stored at 4°C.

Solution II (25 ml)

0.5 ml 10 M NaOH

1.25 ml 20% SDS

Solution III (500 ml)

147 g potassium acetate

57.5 ml glacial acetate

Autoclave and store at 4°C.

Method:

A single colony of *E. coli* harboring recombinant plasmid was grown in 1.5 ml of LB solution containing appropriate antibiotic at 37 °C for overnight with shaking. The cells were harvested by centrifugation at 4,000 g for 10 min at 4 °C and suspended in 100 µl of solution I by vigorous vortexing. After 5 minutes incubation at room temperature, the cells were lysed by the addition of 200 µl of freshly prepare solution II, mixed by gently inversion and incubated on ice for 5 min. The cell lysate was neutralized by gently mixing with 150 µl of solution III followed by 5 minutes incubation on ice. The mixture was centrifuged at 12,000 g for 5 min at 4 °C. The clear lysate was collected, extracted once with phenol:chloroform:isoamylalcohol (25:24:1). Subsequently, the plasmid was precipitated by adding 2 volumes of ice-cold absolute ethanol, mixed by inversion several times before incubated at -20 °C for 10 minutes and then centrifuged for 10 min at 12,000 g at 4 °C. The plasmid was washed with 70% ethanol and recollected by centrifugation for 3 min. Finally, the air-dried pellet was dissolved in 20 µl of TE buffer (10 mM Tris-HCl and 1 mM EDTA pH 8.0) and stored at -20 °C.

APPENDIX O

Agarose gel electrophoresis for DNA

TBE buffer:

- Concentrated stock solution (per liter)

5X: 54 g Tris base

27.5 g Boric acid

20 ml 0.5 M EDTA (pH 8.0)

- Working solution

0.5X: 0.045 M Tris-borate

0.001 M EDTA

Preparation of agarose gel:

1. The edges of a clean, dry, glass was sealed plate and then molded on a horizontal section of the bench.
2. TBE electrophoresis buffer (100 ml) was prepared.
3. 1 g of agarose was weighed and put into the TBE buffer.
4. The mixture was boiled for 2-3 minute with microwave.
5. Ethidium bromide (a stock solution of 1 mg/ml) was added into the gel solution by adjusting final concentration to $0.5 \mu\text{g ml}^{-1}$ and then mixed.
6. The comb was placed in suitable position.
7. Agarose solution was poured onto the tray.
8. After gel was completely set (30-45 min at room temperature), the comb was removed carefully and then gel was placed into the electrophoresis tank.

Method for running DNA on agarose gel:

To measure the size and the amount of DNA in the sample, 1.0% agarose gel (consist of 0.5 mg/ml ethidium bromide) in 1x TBE buffer (89 mM Tris-HCl, 89 mM boric acid and 2.5 mM EDTA pH 8.3) consisting 0.5 mg/ml ethidium bromide was used. The DNA sample was mixed with 1/5 volume of loading dyd (0.25% bromphenol blue, 0.25% xylene cyanol FF and 30% glycerol in water) before loading into the well of gel with submerged in the 1x TBE buffer in an electrophoretic chamber. An appropriate amount of 100 bp or 1 kb GeneRuler™ (Fermentas, USA) was also load to the gel to serve as a DNA marker. Generally, the gel was run at 100 volts until bromphenol blue migrated to the other egde. The DNA band was visualized under UV light and photograph. The concentration and molecular weight of DNAs sample were estimated by comparing with the intensity and relative mobility of 100 bp or 1 kb GeneRuler™ (Fermentas, USA).

APPENDIX P**LBK medium****LBK medium (1,000 ml)**

Chemical	Liquid medium	Solid medium
Bacto tryptone	10 g	10 g
Yeast extract	5 g	5 g
KCl	10 g	10 g
Agar	-	15 g

All compositions were dissolved together with 1 liter of distilled water. The medium was sterilized by autoclaving at 15 lb/in² for 15 minute.

APPENDIX Q

ATP calibration curve

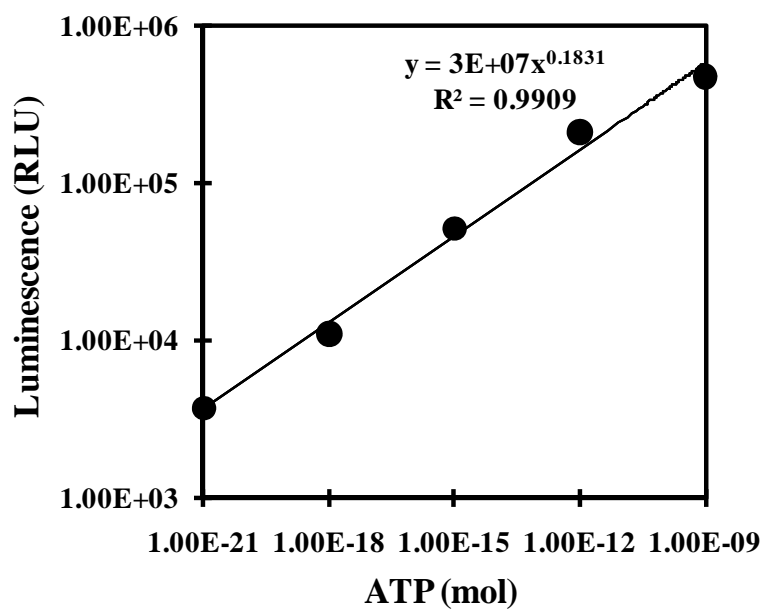


Figure A.6 Standard curve of ATP

APPENDIX R

Buffers for Western blotting

Blotting transfer buffer

Final concentration per litre

39 mM glycine

48 mM Tris-base

0.037% SDS

20% methanol

PBS buffer (Phosphate Buffered Saline)

Final concentration per litre

10 mM sodium phosphate pH 7.4

150 mM NaCl

Blocking buffer

5% (w/v) skim milk and 0.01% Tween 20 in PBS buffer

APPENDIX S

Detection reagents for Western blotting

Reagents:

18 ml of 150 mM Barbitol pH 9.6

2 ml of 0.1% NTB (Nitro Blue Tetrazolium)

80 μ l of 1 M $MgCl_2$

200 μ l of 0.5% BCIP (5-bromo-4-chloro-3-indolyl phosphate)

Method:

Detection reagent for Western blotting should be freshly prepared and used within 30 minutes. When the bands are of the desired intensity, wash the nitrocellulose membrane with deionized water 2-3 times and take photograph.

APPENDIX T

Plasmid transformation into *Synechococcus* sp. PCC 7942

1. Preparation of competent cells

The cells grown in 100 ml of BG11 medium for 7 days were collected by centrifugation at 5,000 g, 4 °C for 10 minutes. The pellet was resuspended with 10 ml of new BG11 medium and the cell suspension was aliquot 1 ml per tube for immediately transformation.

2. Transformation

The plasmid was mixed with 1 ml of the cell suspension in microtube and incubated on a rotary shaker at 30 °C, 160 rpm under continuous illumination by cool white fluorescence tubes of 25 $\mu\text{mol photon m}^{-2} \text{s}^{-1}$ for overnight. The transformed cells were spreaded onto the BG11 agar plate containing appropriate antibiotic. The plate was incubated at 30 °C until the green colonies appear and then subcultured into BG11 liquid medium containing the same antibiotic as in the plate.

APPENDIX U

Preparation of *Synechococcus* sp. PCC 7942 plasmid by alkaline lysis method

Reagents:

Solution I (100 ml)

5.0 ml 1.0 M Glucose

2.5 ml 1.0 M Tris-HCl, pH 8.0

2.0 ml 0.5 M EDTA, pH 8.0

After autoclave, 20 $\mu\text{g ml}^{-1}$ of RNase was added and stored at 4°C.

Solution II (25 ml)

0.5 ml 10 M NaOH

1.25 ml 20% SDS

Solution III (500 ml)

147 g potassium acetate

57.5 ml glacial acetate

Autoclave and store at 4°C.

Method:

A 5-ml cell culture was harvested by centrifugation at 8,000 g for 10 min at 4 °C and suspended in 100 µl of solution I by vigorous vortexing. The cell suspension was incubated with lysozyme (5 mg ml⁻¹) for 30 min at 37 °C. After that the cells were lysed by the addition of 200 µl of freshly prepare solution II, mixed by gently inversion and incubated on ice for 5 min. The cell lysate was neutralized by gently mixing with 150 µl of solution III followed by 5 minutes incubation on ice. The mixture was centrifuged at 12,000 g for 5 min at 4 °C. The clear lysate was collected, extracted once with phenol/chloroform/isoamylalcohol (25 : 24 : 1). Subsequently, the plasmid was precipitated by adding 2 volumes of ice-cold absolute ethanol, mixed by inversion several times before incubated at -20 °C for 10 minutes and then centrifuged for 10 min at 12,000 g at 4 °C. The plasmid was washed with 70% ethanol and recollected by centrifugation for 3 min. Finally, the air-dried pellet was dissolved in 20 µl of TE buffer (10 mM Tris-HCl and 1mM EDTA pH 8.0) and stored at -20 °C.

APPENDIX V

PCR amplification protocol for chloramphenicol resistant gene

PCR amplification mixture

Chemical	Volume
10x GeneAmp PCR Gold buffer *	5.0 μ l
25 mM MgCl ₂	2.5 μ l
2 mM dNTPs each	5.0 μ l
Primer pACYCcm1-F (5 pmol/ μ l)	4.0 μ l
Primer pACYCcm1-R (5 pmol/ μ l)	4.0 μ l
DNA	X μ l
AmpliTaq Gold DNA polymerase (1 unit/ μ l)	1.0 μ l
MQ-water	28.5-X μ l
Total	50.0 μ l

Program running PCR (35 cycles)

94 °C 5 min (Pre denaturation time)

94 °C 30 sec (Denaturation time)

55 °C 30 sec (Annealing time)

72 °C 40 sec (Extension time)

72 °C 7 min (Final Extension cycle)

4 °C for overnight

Remark: *10x GeneAmp PCR Gold buffer = 100 mM Tris-HCl and 500 mM KCl, pH8.0.

APPENDIX W

PCR amplification protocol for *atpG* encoding γ subunit of ApNa⁺-ATPase

PCR amplification mixture

Chemical	Volume
10x GeneAmp PCR Gold buffer *	5.0 μ l
25 mM MgCl ₂	2.5 μ l
2 mM dNTPs each	5.0 μ l
Primer gammaXbaI-F (5 pmol/ μ l)	4.0 μ l
Primer gammaSall-R (5 pmol/ μ l)	4.0 μ l
DNA	X μ l
AmpliTaq Gold DNA polymerase (1 unit/ μ l)	1.0 μ l
MQ-water	28.5-X μ l
Total	50.0 μ l

Program running PCR (35 cycles)

94 °C 5 min (Pre denaturation time)

94 °C 30 sec (Denaturation time)

55 °C 30 sec (Annealing time)

72 °C 40 sec (Extension time)

72 °C 7 min (Final Extension cycle)

4 °C for overnight

Remark: *10x GeneAmp PCR Gold buffer = 100 mM Tris-HCl and 500 mM KCl, pH8.0.

BIOGRAPHY

Miss Kanteera Soontharapirakkul was born on April 27th, 1983 in Bangkok province, Thailand. She graduated with a Bachelor of Science degree in Biochemistry with first Class Honours, Faculty of Science, Kasetsart University in 2005. After graduating with Bachelor's Degree of Science, She enrolled in the Doctor of Philosophy Program (Ph.D.) in Biochemistry, Faculty of Science, Chulalongkorn University during May 2005 – April 2011. During her study, the output of her research work can be summarized as follows:

1. Bualuang, A., **Soontharapirakkul, K.**, and Incharoensakdi, A. 2010. Na⁺/H⁺ exchange activity in the alkaliphile halotolerant cyanobacterium *Aphanothece halophytica*. J. Appl. Phycol. 22: 123-129.

2. **Soontharapirakkul, K.**, and Incharoensakdi, A. 2010. Na⁺-stimulated ATPase of alkaliphilic halotolerant cyanobacterium *Aphanothece halophytica* translocates Na⁺ into proteoliposomes via Na⁺ uniport mechanism. BMC Biochem. 11:30. doi:10.1186/1471-2091-11-30.

3. **Soontharapirakkul, K.**, Promden, W., Yamada, N., Kageyama, H., Incharoensakdi, A., Iwamoto-Kihara, A., and Takabe, T. 2011. Halotolerant cyanobacterium *Aphanothece halophytica* contains a Na⁺-dependent F₁F₀-ATP synthase with potential role in salt tolerance. J. Biol. Chem. 286: 10169-10176.

4. **Soontharapirakkul, K.**, Takabe, T., and Incharoensakdi, A. 2008. Oral presentation, Effect of sodium chloride concentrations and pH of growth medium on the Na⁺-stimulated ATPase activity in cyanobacterium *Aphanothece halophytica*. The 13th Biological Sciences Graduate Congress 2008, Department of Biological Sciences, National University of Singapore, Singapore. December, 15-17.

Grants:

2007-2011: Royal Golden Jubilee Ph.D. program, The Thailand Research Fund, Bangkok, Thailand. Grant No. PHD/0012/2550

2009-2011: The 90th Anniversary of Chulalongkorn University Fund (Ratchadaphiseksomphote Endowment Fund), Bangkok, Thailand